HYBRID TRACKING CONTROLLER WITH ATTACHED TMD

by

Ali Bozer

B.S. in C.E., Yıldız Technical University, 1999

M.S. in C.E., Boğaziçi University, 2002

Submitted to the Institute for Graduate Studies in
Science and Engineering in partial fulfillment of
the requirements for the degree of
Doctor of Philosophy

Graduate Program in Civil Engineering

Boğaziçi University

2009

to,

my father, Ertuğrul Ömer BOZER

my mother, Seval BOZER

my sister, F. Tuba BOZER

ACKNOWLEDGEMENTS

"Whenever there is restraint there is stress". This principle of mechanics of materials holds for human psychology as well. It is my feeling that whenever one tries to expand in knowledge, he is faced with the restraints of unknown. Some choose the comfort of ignorance and some force the restraints in order to expand the boundaries of knowledge. In the second case stress is evident, and endurance is the key to achievement.

I would like to express my most sincere thanks to my advisor Prof. Dr. Gulay ALTAY for she ignites the hunger of knowledge inside me. If not her I might have chosen the pseudo comfort of ignorance. I am also grateful for her invaluable guidance and belief in me at times when I feel the restraints are unyielding.

This gratitude also extends to Asst. Prof. Hilmi Luş and Assoc. Prof. Unal Aldemir for their active participation and never ending support when I reach to yield critical point.

I would like to thank also Prof. Dr. Cengiz Dökmeci for his introduction and direction of how a scientist should be and Asst. Prof. Kutay Orakçal for serving in my committee and reviewing this thesis.

Last but not least, I have my deepest thanks to my family for they weave the very fabric of me with necessary endurance, and friends, who are with me acting as stress relieving agents in all the stages of this thesis.

ABSTRACT

HYBRID TRACKING CONTROLLER WITH ATTACHED TMD

Supplemental damping systems can be substitute for hysteretic or kinetic damping and eliminate the need for additional strength and stiffness for desired performance levels. Supplemental dampers dissipate the energy mechanically and activated through movements of main structural system. Tuned Mass Dampers are examples of motion-activated devices in which flow of energy in the structure is disturbed through the vibration of a secondary system. In the essence tuned-mass dampers (TMDs) or vibration absorbers are mass-spring-dashpot systems that are tuned to a particular vibration mode of the structure on which they are installed. Under a dynamic excitation, the TMD resonates at the same frequency as the main structure but out-of-phase from it, thereby diverting the input energy from the main structure into itself.

The environmental loads, such as wind and earthquake loads, possess many frequency components. Therefore, tuned mass dampers are optimized to render them effective for such large bandwidth inputs. To broaden the operational range of a TMD some damping is introduced in the optimization procedure. Although this added damping term smoothens the sharp peaks of frequency response function out of the operating range it also considerably decreases the effectiveness of TMD in the operating range. Thus, in this study it is aimed to constraint the response of the structure in the boundaries of the operating range of TMD, then the requirement for additive damping will be eliminated and TMD can be used in full efficiency.

As a consequence a hybrid system is proposed in which the combined plant/non-optimal TMD structure is equipped with an active controller such that the closed-loop system tracks the response of an oscillator with natural frequency set to the operating frequency of TMD unit. In the proposed system closed-loop states are not regulated to zero. Instead controller tries to help TMD to suppress vibration effectively thus lesser control effort is needed. This is further verified by numerical simulations which show the performance of the proposed approach under wind and earthquake loads.

ÖZET

TMD EKLİ HİBRİT İZLEMCİ DENETİMCİ

Harici sönümlendirme sistemleri histerezis ve kinetik sönümün yerini alarak arzu edilen performans seviyelerindeki gerekli ek dayanım ve rijitlik ihtiyacını ortadan kaldırır. Harici sönümleyiciler enerjiyi mekanik olarak yutar ve ana taşıyıcı sistemin hareketi ile etkinleşirler. Hareket-etkin cihazlarin bir örneği olarak Ayarlı Kütle Sönümleyici yapıdaki enerji akışını ikincil sistemin titreşimi ile engeller. Özünde, ayarlı kütle sönümleyiciler (TMD) veya titreşim soğurucular kütle-yay-amortisör sistemleridir ve monte edildikleri yapının belirli bir titreşim moduna ayarlanırlar. Dinamik etkiler altında TMD ana yapı ile aynı titreşim frekansında fakat farklı fazda hareket ederek girdi enerjisini ana yapıdan kendi üzerine yönlendirir.

Rüzgar ve deprem yükleri gibi çevresel yüklerin frekans içeriği çok çeşitli olduğundan ayarlı kütle sönümleyiciler geniş frekans aralıklı yükler için de etkin kılınmak üzere optimize edilmektedir. TMD'nin faaliyet menzilini artırabilmek için yapılan optimizasyon işlemi sırasında harici sönümleyici eklenmesi gerekmektedir. Bu ek sönüm, frekans cevabındaki keskin pik noktalarını yumuşatmakla beraber TMD'nin operasyon aralığındaki etkinliğini de oldukça azaltmaktadır. Bu sebeple bu çalışma kapsamında yapının frekans cevabını TMD'nin çalışma aralığı içinde sınırlandırmak böylece ek sönüm ihtiyacını ortadan kaldırarak TMD'yi en etkin biçimde çalıştırmak hedeflenmektedir.

Sonuç olarak bütünleşik yapı/optimum olmayan TMD sistemini aktif denetimci ile birleştiren hibrit bir sistem önerilmektedir. Bu sistemde hibrit denetimci kapalı-çevrim sistemin cevabının doğal titreşim frekansı TMD ünitesinin işletim frekansına ayarlanmış osilatörün cevabını izleyecek şekilde kontrol etmektedir. Önerilen sistemde kapalı-çevrim durumları sıfırlanmamaktadır. Bunun yerine kontrolcü TMD'nin yapı titreşimini etkin olarak sönümlendirmesine yardımcı olmaktadır, bu sebeple daha az kontrol gayreti gereklidir. Bu önerilen yaklaşım nümerik simülasyonlar ile doğrulanmış ve sistemin performansı rüzgar ve deprem yükleri altında gösterilmiştir.

TABLE OF CONTENTS

LIST OF FIGURES

LIST OF TABLES

LIST OF SYMBOLS/ABBREVIATIONS

A	State matrix of the plant
$\hat{A}$	State matrix of the augmented plant
A_c	State matrix of the controller
A_{cl}	State matrix of the closed loop system
B	Input matrix of the plant
$\hat{B}$	Input matrix of the augmented plant
B_{cl}	Input matrix of the closed loop system
B_u	Control input mapping matrix
B_w	Disturbance input mapping matrix
C	Output matrix of the plant
C_{cl}	Output matrix of the closed loop system
C_m	Measured output mapping matrix
C_y	Output mapping matrix
D	input-to-output coupling matrix
E(s)	Laplace transform of error signal
F	State matrix of the reference model
G(s)	Transfer function of the system
$G(i\omega)$	Frequency response of the system
H	Output matrix of the reference model
I	Identity matrix
J	Quadratic performance index
K(s)	Transfer function of the controller
L(s)	Loop transfer function
$L(i\omega)$	Frequency response of loop transfer function
P(s)	Generalized plant
P(t)	Riccati matrix
Q	State weighting matrix for LQR control design
$\hat{Q}$	State weighting matrix for the augmented plant
R(s)	Laplace transform of reference signal

R	Control weighting matrix for LQR control design
S(s)	Sensitivity function
T(s)	Complementary sensitivity function
U(s)	Laplace transform of input signal
Y(s)	Laplace transform of output signal
W(s)	Laplace transform of the disturbance signal
$W(i\omega)$	Frequency weighting matrix
c_s	damping constant of the structure
c_{TMD}	damping constant of the TMD unit
e(t)	error signal vector
k_s	stiffness of the structure
k_{TMD}	stiffness of the TMD unit
m(t)	measured output vector
m_s	mass of the structure
m_{TMD}	mass of the TMD unit
p	Langrange multiplier
r(t)	reference signal vector
t_r	rise time
t_s	settling time
u(t)	control input signal
w(t)	disturbance input signal
x(t)	state vector of the plant
$\hat{x}(t)$	state vector of the augmented plant
x_{st}	static displacement of the primary structure
$\ddot{x}_g(t)$	ground motion acceleration input
y(t)	output signal vector
$\tilde{y}(t)$	trajectory signal
z(t)	state vector of reference model
z(s)	Output signals to be minimized/penalized

β	forced frequency ratio
γ	mistuning factor
λ	frequency ratio of TMD to primary structure
μ	mass ratio of TMD to structural system
ω	frequency of the input excitation
ω_a^2	squared natural frequency of the TMD
ω_n^2	squared natural frequency of the primary structure
ς_a	damping ratio of TMD
$\|\|\cdot\|\|_2$	2 norm
$\|\|\cdot\|\|_\infty$	Infinity norm

AMD	Active mass driver
ATMD	Active tuned mass damper
DAF	Dynamic Amplification Factor
DMF	Dynamic Magnification Factor
DTMD	Double Tuned Mass Damper
GM	Gain margin
H_2	H_2 Controller Design
H_∞	H_∞ Controller Design
LQR	Linear Quadratic Regulator
MDOF	Multi Degree of Freedom
MTMD	Multiple Tuned Mass Damper
P	Proportional feedback compensation
PI	Proportional-Integral compensation
PID	Proportional-Integral-Derivative compensation
PM	Phase margin
SDOF	Single Degree of Freedom
TLD	Tuned Liquid Damper
TMD	Tuned Mass Damper

1. INTRODUCTION

1.1. Control of Civil Structures

The conventional approach for earthquake resistant design is a strength-base one where the load-bearing components are designed to resist earthquake demands with sufficient strength and ability to absorb and dissipate seismic energy through a large number of hysteretic cycles. This has a direct effect of increased energy dissipation through inelastic deformations and it also has an indirect effect of structural softening so that the amount of input energy transmitted to the structure is decreased.

On the other hand, the challenge to find better means of new designs or strengthening existing ones leads to development of some innovative concepts. One of the innovative systems for structural protection is passive energy dissipation where input seismic energy is dissipated not only by the structure itself but also with some type of damping devices. In these systems dampers are incorporated in the structure and dissipate energy throughout the height of the structure. Metallic dampers, friction dampers, viscoelastic dampers, viscous dampers, tuned mass dampers and tuned liquid dampers are some examples of passive energy dissipation.

Last but not least innovative system for structural protection is the active control in which the motion of the structure is controlled or modified by means of a control system through some external energy supply. In comparison with passive energy dissipation, active structural control systems have a more recent origin.

An active structural control system consists of sensors to measure external excitations or/and structural response; a controller device to process the measured information and to compute the necessary control forces; and actuators to produce the required forces. If the control forces are computed on the basis of structural response measurements it is called as *closed-loop control*.

Among structural control strategies are mass dampers (MDs), in their passive, active and hybrid versions. The passive MD is the tuned mass damper (TMD), in which the auxiliary mass is connected to the main structure through a spring and a damping device. The active version of the MD is the active mass driver (AMD), in which the mass is connected to the structure through an actuator. Finally, the hybrid MD is an active tuned mass damper (ATMD), in which the auxiliary mass is connected to the structure through an actuator, a spring and, eventually, a damping device.

1.2. Tuned Mass Damper

In the essence tuned-mass dampers (TMDs) or vibration absorbers are mass-spring-dashpot systems that are tuned to a particular vibration mode of the structure on which they are installed. The objective of a tuned-mass damper is to transfer some of the vibration energy to the auxiliary mass thus to reduce the energy demand on the primary structural members under the action of external forces. In its simplest form, a tuned-mass damper only requires the assembly of a mass, a spring, and a viscous damper at a structure therefore it is relatively inexpensive and easy to implement. On the other hand, although the required mass is a small fraction of the structural mass, it is relatively large hence; a large space is needed for their installation.

The concept of mass damper is first invented by Frahm in 1909 which is called dynamic vibration absorber [1]. This vibration device did not have any inherent damping and it was effective only when absorber's natural frequency was very close to excitation frequency. Also its effectiveness sharply degraded if excitation frequency deviated from absorber's natural frequency. Therefore, its operating range was very limited and could be used when the excitation frequency was known. The modern concept of tuned-mass dampers emerged from the early studies of Den Hartog [1] about the theory of undamped and damped dynamic vibration absorbers when there is no damping in the main structure. Then he developed the basic principles and the procedure for proper selection of the absorber parameters. McNamara [2] extended the work of Den Hartog and investigated the effectiveness of TMD under wind excitations when there is damping in the main structure. The normalized root-mean-square response versus frequency ratio for various mass ratios and damper damping was presented in his work. In line with Den Hartog's studies he

found that the maximum response reduction occurs when the TMD is tuned close to the building frequency. Warburton and Ayorinde [3] showed that the optimum absorber parameters given for one degree-of-freedom damped systems can be utilized for distributed parameter systems such as beams and plates when their response is represented by a single fundamental mode. However it was also reported that for more complex elastic bodies such as cylindrical shells, for which the natural frequencies are more closely spaced, this simplified procedure loose accuracy in predicting optimum absorber parameters. Warburton [4] extended his early study to cover multi-degree of freedom systems and searched the effect of higher vibration modes on optimum absorber parameters. He convinced that if the natural frequencies of the structure in not closely spaced than the optimum parameters of TMD is close to findings of Den Hartog. Furthermore if mass ratio gets larger the deviation from Den Hartog's optimal parameters is more pronounced. Warburton [5] realized that optimum absorber parameters are derived to minimize the displacement response when the excitation was a harmonic force. Thus in his extensive paper he derived absorber parameters for undamped single-degree-of-freedom systems for harmonic and white noise random excitations with force and acceleration as input. He also selected the optimization criteria as minimizing various response parameters. Warburton further provided single-degree-of-freedom analogies to multi-degree-of-freedom systems so that the optimal values can be used for MDOF systems by replacing a MDOF system by an equivalent SDOF system. Abe and Igusa [6] advanced studies on the effects of TMD for structures with closely spaced natural frequencies. They investigated the response under the variation of the ratios of TMD and structural model masses, the damping of the system, and the differences between the structural natural frequencies and the loading frequency. Then writers convinced that if a structure has an n closely space natural frequency then at least n TMDs should be attached to the structure to control the response. Also TMD locations should be such that the response of the system is decoupled into n SDOF structure/TMD systems. Consequently, Tsai and Lin [7] determined the optimum parameters of a damped primary system excited by an external force by a numerical search procedure. Then through a curve-fitting procedure they developed an explicit formula for these optimum parameters. Sadek et. al. [8] offered a different approach in obtaining optimal parameters. In their method they selected the optimization criteria as to provide equal and large damping ratios in the vibration modes of structure-TMD system. Then they formulated the closed-form optimum parameters in terms of mass ratio of the TMD, the

damping ratio and modes shape of the structure. Up to Hoang et. al. [9] exact formulas for optimal TMD parameters had been extensively derived for two theoretical forms: harmonic excitation and random excitation with white-noise spectral density, either on the structure or at the base. In their study they modified the closed form formulas given by Warburton [5] to cover site-specific earthquake excitations. First they used a numerical search procedure to obtain optimal parameters for variations in TMD mass ratio and characteristic ground properties. Then they derived the closed form optimal formulas for TMD frequency and TMD damping ratio by a curve fitting procedure.

Rüdinger investigated the effectiveness of tuned mass dampers when they are equipped with viscoelastic damper [10] or non-linear viscous damper [11]. In both damper configurations he observed the same reduction in the structural vibration as a conventional tuned mass damper. However he reported that the nonlinear tuned mass damper must be tuned to a specific amplitude and excitation intensity in contrast to conventional linear tuned mass damper. Almazan et. al. [12] proposed a tuned mass damper in which a pendular mass is supported by cables and linked to a unidirectional friction damper. This device can be tuned in each principal direction independently and allows control of vibrations in both principal directions. Writers reported that level of response reduction with the proposed devise is similar to that obtained form an ideal linear viscous TMD. Unlike the traditional TMD which is attached to a primary mass by a spring and damper Wong and Cheung [13] attached the auxiliary mass by a spring to primary mass and by a damper to ground. The damping of the primary mass was assumed to be zero so the optimum parameters were derived based on the fixed point theory of Den Hartog [1]. Writers reported that although the damping requirement of the TMD is greater the proposed model shows a better performance.

Yang et al. [14] proposed a hybrid use of a base isolation system with tuned-mass damper. The base isolation system is used to decouple horizontal ground motion from the building and tuned-mass damper is used to limit the lateral displacement. The authors reported a better performance than an active mass damper alone. The hybrid base isolation tuned-mass damper system was further enhanced by Tsai [15] in which tuned-mass damper unit is accelerated to reduce the lateral deformation at the early stages of an earthquake. Later on effect of tuned mass damper on displacement demand of base isolated buildings is

further studied by Taniguchi et. al. [16] They performed a stochastic dynamic analysis based on a white-noise model of ground motion and reported a 15%-25% reduction in the displacement demand of the base isolated structure. This is also verified by far-field ground motions, however for near-field records the effectiveness was reduced by %10.

Rana and Soong [17] investigated the detuning effect in TMDs and observed that detuning in frequency ratio is more severe than detuning in damping ratio, with increasing damping of the main mass also with increasing mass ratio the effect of detuning become less severe. They also used multiple tuned mass dampers to control the multiple vibration modes of the main mass. In their study they utilized TMD to control a single mode of a MDOF structure by using readily available design procedure of TMD for SDOF structures and observed that the presence of higher mode TMDs causes some deterioration in the first mode response. Marano et. al. [18] considered the probability of failure of a TMD in the optimization problem. They related the failure of TMD to threshold crossing probability by its maximum displacement over an admissible value. Their criterion for optimization was the minimization of the dimensionless peak of the maximum displacement when the structure is subjected to base acceleration which is modeled as a stationary stochastic process. They found out that optimum solutions to the progressively decreased admissible TMD displacement are obtained by increasing TMD damping. Whereas depending on the mass ratio of the TMD unit the change in optimal frequency varied from small to negligible. As a consequence of decreased lateral displacement of TMD writers reported a reduction in vibration control efficiency. Later on Marano et. al. [19] worked on the uncertainties in system parameters and introduced a robust optimization procedure for a TMD attached to a SDOF system. The problem is treated by characterizing all uncertain parameters, including not only mechanical properties of main structure and TMD but also input spectral contents, by a nominal mean value and variance. Robustness is than formulated as a multiobjective optimization problem, in which both the mean and standard deviation of the deterministic objective functions are minimized.

All the researchers agree on that if TMD is tuned properly it is very effective on mitigating the vibration response on the other hand if it is mistuned due to errors in identifying natural frequencies of the structure or due to some fabrication errors of TMD; the effectiveness of TMD is greatly reduced. To increase the effectiveness of TMD the use

of multiple tuned mass dampers (MTMD) with the distributed natural frequencies was proposed by Xu and Igusa [20]. They investigated the displacement response of an oscillator supporting n sub-oscillators where the natural frequencies of the sub-oscillators are equally spaced over a frequency range. Writers showed that multiple sub-oscillators can have better vibration control properties than a single sub-oscillator of equal mass. The most striking conclusion was the sub-oscillators are more effective at low damping values which render them more appropriate for the cases where the damping of the oscillators is limited to low values such as liquid tuned dampers (LTDs). Further Yamaguchi and Harnpornchai [21] investigated the effect of frequency range, damping ratio and total number of TMD units on the performance of MTMD. They assumed that the mass and damping ratio of each TMD are the same; the natural frequencies of MTMD's are equally distributed. They reported that the controlled structural response is transformed from a two-peak characteristic to a one-peak characteristic with the increase in frequency range of a MTMD. Therefore there is an optimum value of the frequency range of TMD which makes the frequency response curve flat for a wide range of frequency. When it comes to damping ratio they concluded that the role of damping in a MTMD is basically the same as that in a single TMD that is the excessive damping increases the structural resonance peak in the frequency response curve. It was also reported that increasing the total number of TMDs is identical to increasing the frequency range when the frequency spacing is fixed. On the other hand when frequency range is kept constant the effect of total number of TMDs is similar to the effect of the TMDs damping. Further writers compared robustness of MTMD with TMD under harmonically forced oscillations and reported that optimum MTMD is not very robust but by compromising effectiveness certain robustness could be achieved. Yamaguchi and Harnpornchai's [21] results were based on numerical simulations whereas Abe and Fujino [22] derived closed-form solutions for the modal properties of the MTMD-structure system. They formulated the optimal damping and critical bandwidth for MTMD systems. Further Kareem and Kline [23] investigated the effectiveness of MTMD under narrow and wide band wind loads, and under stationary earthquake excitation. They also investigated the effects of variable mass or variable frequency distribution as opposed to uniform distribution of mass or frequency. However, they reported no distinct advantage or disadvantage between two approaches. Joshi and Jangid [24] investigated optimum parameters of MTMD for damped systems under base excitation by a numerical search technique. They modeled the base excitation as a white

noise stationary random process and searched the optimum parameters under different damping ratios of the main system and mass ratios of the MTMD. Apart from well known conclusions they reported that the damping in the main system does not influence the optimum damping ratio of both the single TMD and the MTMD system. Thus in the companion paper Jangid [25] derived an explicit formula using curve fitting scheme for the optimum parameters of MTMDs for undamped systems. In his work the main system was excited by harmonic-base acceleration and optimization criteria was to minimize the steady-state displacement response of the main system. Furthermore, Li [26] investigated the optimum parameters of MTMDs under ground acceleration excitation and the criteria selected for the optimization was the minimization of the maximum value of dynamic magnification factor. He conducted the numerical searching in two directions, first by keeping the stiffness constant and varying the mass and damping coefficient, second by keeping the mass constant and varying the stiffness and damping coefficient. However analyses showed nearly same optimal parameters and performance between two approaches. Park and Reed [27] compared the effectiveness and robustness of MTMDs when the mass is uniformly or linearly distributed. They also considered the effects of redundancy and assessed the reliability when an individual damper fails. They found out that the uniformly distributed system is more effective in reducing peak dynamic magnification factor and it is slightly reliable, on the other hand the linearly distributed system is more robust under mistuning. Gu et. al. [28] performed a parametric study on buffeting control of a bridge with MTMD system. They found out that the control efficiency is sensitive to central frequency ratio and frequency bandwidth ratio however is less affected by damping ratio of TMD units. Consequently Li [29] evaluated the performance of various MTMD systems in the case of seismic excitation by both considering the minimization of displacement dynamic magnification factor and acceleration dynamic magnification factor of the structure. He eventually reported that MTMD damper constructed with each TMD having identical stiffness and damping coefficient, but unequal mass and damping ratio provides better effectiveness and robustness. Li and Liu [30] further extended the work of Li and they provided suggestion on selecting the total mass ratio and total number of the MTMD units with the identical stiffness and damping coefficient but unequal mass and damping ratio. Furthermore, Li and Liu [31] uniformly distributed the system parameters i.e. mass, stiffness and damping coefficients instead of uniform distribution of natural frequencies. They concluded that

better performance is obtained if the stiffness is uniformly distributed around the mean stiffness yet, there was no significant advantage observed when compared with uniform natural frequency distribution. Chen and Wu [32] applied shake table tests on a three-storey model structure to validate the effectiveness of TMD and MTMD under white noise input and scaled earthquake records. A single TMD is tuned either to first or second mode of the structure and MTMD is the simultaneous use of TMDs placed to various floors. They reported that under white noise input the theoretical optimum TMD give rise to best performance on the other hand when the test structure is subjected to real earthquake excitations optimal parameters do not lead to minimal structural response. Also MTMD was found significantly superior to conventional single mode TMD. Zuo and Nayfeh [33] realized the optimization problem by formulating the TMD as a feedback controller by treating the springs and dashpots as local position and velocity feedback elements. In their paper they defined the optimization problem as to maximize the minimum damping and compared the performance under minimax, H_2 and H_∞ optimization. Yau and Yang [34] proposed a wideband MTMD system composed of several MTMD subsystems to account for multi-mode vibration problem. Each sub-system was composed of one set of TMD units covering a frequency bandwidth with its central frequency tuned to frequency of the vibrational mode considered. The optimization criterion was to minimize the maximum peak amplitude. For the first two modes of a continuous truss bridge they reported a great reduction for both the resonant peaks, in addition for mistuning case if the half bandwidth of the MTMD subsystem is selected as twice the deviation of target frequency the proposed system exhibited a higher level of robustness. Hoang and Warnitchai [35] proposed an optimization algorithm by using a non-linear programming technique in which TMD parameters to be optimized is viewed as design variables. Then a performance function J is defined. To evaluate performance function physical structural response is represented by the state coordinates so that J can be expressed in terms of the state covariance matrix which is obtainable by solving the Lyapunov equation. Then numerical optimization was defined as an iterative search for design variables which yields minimum performance function J. It is evident that if the number of TMD units in MTMD is large enough the optimization process becomes very tedious due to the abundance of control parameters. To overcome this Du et. al.[36] investigated the performance of MTMD and proposed a method which is very time efficient if the number of TMD units goes to infinity (IMTMD). In the case of infinite TMD units the natural frequencies of infinitesimal TMDs

cover a continuous frequency range. The force applied to the main structure by infinitesimal TMD is calculated then TMD units are expressed as feedback components which receive the base acceleration and primary structures displacement as inputs and produces applied force to the main structure as output. Once this is solved transfer functions are obtained and corresponding dynamic magnifications are derived. Then design parameters which minimize the max dynamic magnification factor are calculated using H∞ optimization. With the proposed methodology writers found the same optimization parameters of the conventional methods and analysis duration was greatly reduced. Unlike the previous studies on MTMDs Li and Ni [37] applied not certain constraints such as identical damping ratio, uniformly distributed frequency spacing, uniform mass distribution or uniform stiffness to simplify the optimization process. Instead they used a gradient based method for optimizing non-uniformly distributed parameters of MTMD. It is concluded that non-uniform MTMD gives better performance and more robust than uniform MTMD.

Most researchers working on the MTMD have assumed that the total number of the TMD units consisting of the MTMD is an odd number and the frequency range is distributed over a central frequency. Li and Zhang [38] abandoned the central frequency hypothesis and proposed the arbitrary integer based MTMD which provided less restriction concerning the number of TMD units. Consequently Li [39] introduced the dual-layer multiple tuned mass dampers, referred to as DL-MTMD, consisting of one large TMD and several smaller TMD units attached to large TMD unit. Small TMD units were arbitrary integer based with the uniform distribution of natural frequencies. He reported that DL-MTMD can yield better effectiveness and higher robustness in comparison with both the arbitrary integer based multiple tuned mass dampers and odd number based multiple tuned mass dampers. Furthermore optimum damping of the large mass is reported to be zero rendering DL-MTMD more easily to manufacture. In their paper they approximately achieved the same control performance when compared to odd number based multiple tuned mass dampers. In fact when the total number of smaller TMD units in the DL-MTMD is set to unity it was referred as double tuned mass damper (DTMD). Investigations of Li further revealed that DL-MTMD has a little better effectiveness with respect to DTMD but they reach the same level of robustness therefore Li and Zhu [40]

carried on investigations on the double tuned mass dampers (DTMD). They also introduced a novel optimization criterion in which a weighted dynamic magnification factor (DMF) is calculated for each mistuning case. Then minimum sum of these weighted DMFs are searched for optimization. They demonstrated that DTMD can provide higher effectiveness with respect to MTMD and TMD and it is very close to MTMD in term of robustness whereas if novel optimization criterion is used than effectiveness is reduced but robustness is significantly increased. Ok et al. [41] investigated the effectiveness of a system termed as bi-tuned mass damper in which two small mass dampers are attached to a primary structure. In order to achieve satisfactory performance of a bi-tuned mass dampers system, they first introduced two performance measures to quantify the effectiveness and robustness of the bi-tuned mass dampers in the original and off-tuning conditions, respectively. First, the "nominal" performance index was defined in terms of the peak response of the original structure subject to harmonic excitations. Second, the "robust" performance index was defined in terms of the peak response when the structure experiences perturbation in its dynamic properties due to normal wear or damage, or incomplete description of a real structure by a numerical model. A conventional optimization method to find parameters that reduce the peak responses both in original and perturbed conditions is to use weighting factors to combine the multiple objectives into a single objective function. However, the single-objective optimization approach based on arbitrary weights does not guarantee a compromising solution for these multiple objectives thus, writers adopted a genetic-algorithm based multi-objective optimization approach to maximize the nominal and robust performances simultaneously without prescribing the weighting factors arbitrarily. Once the optimal parameters are obtained corresponding to a selected mass ratio, the multi-objective optimization process was repeated as the mass ratio of the bi-tuned mass dampers is varied. Finally writers obtained a set of reasonable optimal solutions for the given range of mass ratios and they utilized a nonlinear curve fitting scheme to derive a closed-form optimal design formula of bi-tuned mass dampers as a function of the mass ratio. For a MDOF structure equipped with bi-tuned mass damper and tuned mass damper writers reported that the nominal performance of the bi-tuned mass damper was slightly improved when compared to tuned mass damper performance but when it comes to robust performance bi-tuned mass damper system showed a significant improvement.

Evidently, much progress has been extended in recent years in terms of the studies on TMD and MTMD to mitigate vibration of structures. However, in most studies it was assumed that a structure vibrates in only one direction or in multiple directions independently. In real structures this assumption is not always appropriate due to coupled vibration modes. Furthermore there exist not only transverse vibrations but also torsional vibrations in real structures. To address this problem Jangid and Datta [42] investigated the effectiveness of multiple tuned mass dampers when they are attached to asymmetric structures. They found that effectiveness of MTMDs in controlling the translational response is less for asymmetric system than the corresponding symmetric system. Also optimum frequency bandwidth of MTMDs changes with the change in the eccentricity of the asymmetric system. Later on Lin et. al. [43] found out that control effectiveness of a TMD depends not only the controlled modal parameters of a structure but also on the installed location and moving direction of TMD as well as the earthquake direction. They suggested that the moving direction of TMD should be the same as the controlled degree of freedom and they found that the greater the distance between TMD and mass center of the installed floor the more vibration reduction is achieved. Lin et. al. [44] introduced a tuned mass damper which simultaneously suppresses both the vertical and torsional buffeting responses of a bridge deck. The proposed tuned mass damper has two frequencies tuned to the effective frequencies of the first flexural and torsional modes of the bridge. These frequencies are adjusted by changing the ratio of the torsional mass inertia and the total mass of the damper which is achieved by modifying the mass distribution of TMD. Singh et. al. [45] studied on a multistory building subjected to bi-directional earthquake induced ground motion. In order to control the coupled lateral and torsional response they placed four tuned mass dampers along two orthogonal directions in pairs. In optimization they used drift based and acceleration based performance functions and utilized a genetic algorithm to obtain optimal parameters which were defined as mass ratio, tuning frequency ratio, damping ratio and position from center of mass. Later Ahlawat and Ramaswamy [46] used the similar tuned mass damper placement as used by Singh et. al. [45] however, they utilized a multiobjective optimization approach with genetic algorithm. As an objective function they considered the acceleration, displacement and torsional response of the building to an excitation that has been applied at different angles varying from 0-90^{o}. In the extensive paper of Li and Qu [47] multiple tuned mass dampers with identical stiffness and damping coefficient but different mass for mitigating the translational and torsional

vibration was discussed. The optimization criterion was to minimize the dynamic magnification factor of both the translational and torsional responses of the two-degree-of-freedom asymmetric structure. Writers gave special emphasis on the effects of the normalized eccentricity ratio (NER) on the performance of MTMDs. They found out that NER affects significantly the performance of the MTMD for both torsionally flexible and torsionally intermediate stiff structures. On the other hand for torsionally stiff structures the effects of NER is found to be negligible.

1.3. Active Structural Control

The idea of using active control to limit the response of civil engineering structures is first clearly formulated by Yao [48] in 1972. In his pioneer paper a feedback structural control system is proposed where control forces are provided by thruster engines mounted on the top of a tall building. Following the concept of Yao, Roorda [49] introduced a more realistic control method in tall structures. He considered a uniform cantilever beam representing a tall structure to be controlled. Then he fastened a pair of eccentric tendons by a rigid bar at some point near the top of the cantilever. These tendons were also attached to a hydraulic servo rams at base thus push-pull effect provided by hydraulic rams created a torque on the cantilever beam. A significant reduction in the response is reported when the system is subjected to a sinusoidally varying force however, formalized control law was not optimal. Yang [50] first utilized the optimal control scheme namely linear quadratic regulator (LQR) in which the effectiveness of the control system is measured by a performance index. External load was formulated by a stochastic process thus performance index was consisted of the covariances of the responses and the covariances of the control forces. As a control device he utilized active damper in which an auxiliary mass is accelerated by a servo-mechanism. For an idealized two-story building a considerable reduction in response covariance was noted, it was also reported that control effectiveness is affected by the installation locations of the controllers. The determination of optimal control involves the solution of the Ricatti equation which's order increases with the square of the order of the system equation. Therefore control design procedure for large and complex structures becomes cumbersome. Martin and Soong [51] acknowledged this problem and offered a modal control concept in which selected structural modes are controlled. The proposed control law is merely a linear state feedback control which

changes the eigenvalues of the system matrix to achieve the desired control objective. Although this method is very effective in suppressing the vibration of a single mode it does not allow for the examination of the controlled responses in the entire frequency domain. Yang and Giannopoulos [52] demonstrated that modal control may magnify uncontrolled vibrational modes simultaneously. In their study they utilized the transfer matrix technique in which frequency response function of the structure with an active feedback control can be obtained in closed form and all the vibrational modes can be viewed in frequency domain. Authors further improved the active tendon control introduced formerly by Roorda [49] by inclined tendons to flexible cantilever beam. As opposed to Roorda's configuration, in the inclined configuration active tendons apply force but not moment to structure which they are attached. Authors reported that force tendon alone is more effective in suppressing the structural responses than the application of either the moment tendon alone or both. Rohman and Leipholz [53] offered the use of pole assignment method for control of flexible structures. The offered method shares the similar concept with modal control method but provides a more general design procedure for a system of any order and any number of measurements. Rohman et. al. [54] further investigated the control of flexible structures and they implemented close-loop and open-close loop optimal control schemes to reduce deflection of a simple beam subjected to moving loop. They reported that open-close loop control scheme requires the pre-knowledge of forcing function and provides better effectiveness when compared to close-loop optimal control on the other hand, required control forces tend to be higher in the former one.

Sae-Ung and Yao [55] formulated a control law considering tenants' comfort when the building structure is subjected to wind excited vibration. The comfort criterion was based on acceleration peaks causing human perception threshold therefore control law was formulated to produce impulse forces which causes an instantaneous change in acceleration but no instantaneous changes in velocity and displacement. However their method yielded highly nonlinear stochastic differential equations causing them to resort to Monte Carlo simulations. Udwadia and Tabale [56] further investigated the feasibility of pulse control using an open loop control law. The determination of the optimum pulse magnitude was based on the minimization of the root mean square response of the system. Authors simply formulated a closed form solution for the pulse magnitude that minimizes a cost function. Then system states were continuously monitored to determine if a specified threshold

displacement is exceeded. Then predetermined magnitude of pulse was applied to the system. In the companion paper Udwadia and Tabale [57] extended the pulse control scheme for multi degree of freedom systems. This time the determination of the optimum pulse magnitude was based on the minimization of the sum of the weighted norms of the velocity and displacement vectors.

Yang [58] proposed a semi-active control algorithm for control of tall buildings under earthquake excitation with active mass damper and active tendon system. In the proposed control law the control parameters are predetermined so no on-line computation is required to regulate the controllers. However the control law was not optimal. Consequently Yang and Lin [59] investigated optimal control cases when applied to tall buildings. In view of the fact that the optimal close-loop control system requires the solution of a matrix Ricatti equation which is cumbersome for many degrees of freedom, such as a tall building, authors introduced an optimal open-loop control algorithm to reduce on-line computational effort. The optimal open-loop control requires the solution of 4n first order differential equations for an n degrees of freedom structure thus computational effort was still cumbersome when n is large. Therefore authors modified open-loop control algorithm to control not all the vibration modes but few critical modes governing the structural response, thus, reducing the on-line computations. It was reported that the optimal critical-mode control is as effective as the optimal global control, since the response of a tall building under earthquake excitations is usually dominated by a few lowest modes. When compared to control algorithm presented by Yang [58] optimal open-loop critical-mode control is found to be more effective. Further a sensitivity study had been carried out by Yang and Lin [60] to determine the effects of uncertainties involved in estimating structural characteristics on the results of the open-loop optimal control. It was reported that the active tendon control system is not sensitive to estimation errors for the damping and stiffness, on the other hand the active mass damper system is moderately sensitive to the stiffness uncertainty. Samali et. al. [61] investigated the effectiveness of active tendon and active mass damper control systems under coupled lateral-torsional motions of buildings. The problem was formulated using the transfer matrices approach and a closed-loop control law. Both systems were reported to be effective in reducing top floor rotations and top floor displacements, however tendon control forces tend to be higher than mass damper control forces when building is subjected to ground excitation.

Reinhorn et. al. [62] proposed a closed loop, nonoptimal algorithm based on the Newmark beta numerical integration algorithm in conjunction with the Newton-Raphson method. The control algorithm requires the estimation of system response at the end of a time interval. If the system response vector exceeds a tolerance, then a corrective force or a pulse is computed and applied to the structure at the beginning of a time interval.

The optimal closed-loop control requires the solution of Ricatti matrix and optimal only if the earthquake excitation is either zero or a white noise random process. For the optimal open-loop control, the control vector depends only on the earthquake excitation and independent of the response state vector. It does not require the solution of Ricatti matrix thus it is cost effective. When the control vector is expressed in terms of the system state vector and external excitation, the control law is referred to as the optimal closed-open-loop control. Unlike the Ricatti closed-loop control, in which the gain matrix is obtained by disregarding the earthquake excitation, the optimal closed-open-loop control utilizes the information of earthquake excitation and hence it is superior. However, optimal open-loop control and optimal open-closed loop control algorithms are not applicable to earthquake excited-structures, because these control algorithms need the entire ground acceleration history to be known a priori. Acknowledging this problem Yang et. al. [63] developed an optimal algorithm in which at any time instant t, the earthquake record which is available up to time t through measurement is used. This new algorithm was referred as instantaneous optimal control and it was applicable to closed-loop control, open-loop control and open-closed-loop control for the earthquake-excited structures. Authors reported that the control efficiencies for the three instantaneous control algorithms are identical and slightly more efficient than the Ricatti closed-loop control. The superiority of this new algorithm is that the gain matrix for the instantaneous optimal open-loop control is independent of structural characteristics and parameters since the measurement of the building response quantities are not necessary. Instantaneous control algorithm was further developed by Yang et. al. [64,65] to cover the nonlinear and hysteretic structures. This was accomplished by including the hysteretic component explicitly in the equations of motion, which were in turn used as constraints for the determination of optimal control vector. In instantaneous optimal control algorithm the optimal control vector depends only on the measured response however, for nonlinear and hysteretic structures since hysteretic component is included in the state equations, the control vector depended not only on

measured response but also on the hysteretic component of the structural response. In the presented methodology hysteretic component of the total deformation was estimated from an observer using the measured structural response and the specific hysteretic model. By utilizing the response measurements the necessity of tracking a history dependent system matrix was eliminated. In the analyses Yang et. al. used state weighting matrix Q as a diagonal matrix, however this does not guarantee stability of the controlled structure when the number of controllers is small when compared to number of degrees of freedom of the building. Therefore, Yang et. al. [66] proposed methods for determining the weighting matrix Q to guarantee the stability of the controlled structure using Lyapunov direct method. Stable weighting matrix was searched for instantaneous optimal control of linear, nonlinear and hysteretic structural systems. During the earthquakes both the ground and the building are moving, so there is no absolute reference for the determination of the displacement response. Thus the displacement response was obtained by numerically integrating the measured velocity response which leaded to serious error accumulations. In order to address the problem Yang et. al. [67] further improved the instantaneous optimal algorithm by using velocity and acceleration feedbacks instead of displacement feedback for nonlinear or hysteretic structural systems. It was shown that the performance of the acceleration feedback algorithm is as good as that of the displacement feedback algorithm. Although superior to closed-loop optimal control, the optimal open-closed-loop control requires the backward solution of Ricatti matrix which in turn requires the pre-knowledge of the earthquake excitation in the whole control interval. Aldemir et. al. [68] formulated an approximately optimal open-closed-loop control algorithm that utilizes the few step ahead predictions of the earthquake acceleration values. It was reported that proposed algorithm is better when compared to optimal closed-loop control algorithm and its performance will approach to optimal as the more distant future of the earthquake excitation is predicted more precisely. Consequently Aldemir et. al [69] defined a performance index as sum of the response and control energies and tried to minimize that multipoint performance index. The resulting closed-loop control depends on not only current states but also future states that should be predicted. Authors reported a significant reduction in terms of real time response and base shear forces of the structure when predicted states are taken into account. Mei et. al. [70] formulated a similar open-closed-loop optimal control law. First they utilized an earthquake model as an input and designed the feedforward term accordingly. Then they formulated an autoregressive model for

ground motion which is constantly updated using real-time online measurements. Authors reported that if the prediction horizon becomes longer the performance of the proposed control law approaches to that of H_2 control law. Pang and Wong [71] proposed a new predictive instantaneous control algorithm in which earthquake ground velocity is predicted to design feedforward term in the controller. Authors suggested that since the ground velocity is not of such high frequency as the ground acceleration, it can be predicted with higher accuracy leading to more distant future predictions. Ho and Ma [72] combined the standard LQG regulator and input estimation approaches. Estimation method consisted of a cooperative use of a Kalman filter and a recursive least-square estimator. The response reduction was better with the proposed control method however control forces tended to be higher when compared to standard LQG regulator.

It is evident that a delay exists between measuring the response and applying the control action due to the processing of response measurements and reaction time for the actuator. This time-delay results in a worse performance of the control system than theoretical predictions. To alleviate the problem introduction of delay factors are needed but it usually renders system analysis much more complicated. Therefore, much work has concentrated on the analysis of time-delay systems. Rohman [73] investigated the time-delay effect on the distributed parameters structures that are controlled using direct velocity feedback. He showed that for small time delay and using control moments as control actions, the higher order modes become unstable. For time-delay compensation he further suggested either to modify the gain matrix to account for time delay or to remain higher modes uncontrolled by filtering the frequency components corresponding to higher modes in the velocity measurements. Chen et. al. [74] worked on stabilization of time-delay systems containing saturator actuators. They treated both continuous and discrete feedback and derived sufficient conditions to guarantee the stability of both control laws. Since the effect of time delay vary with respect to control algorithm used Yang et. al. [75] examined the performances of linear quadratic optimal control algorithm, instantaneous optimal open-loop control algorithm, instantaneous optimal closed-loop control algorithm and instantaneous optimal open-closed-loop control algorithm under system time delay. They considered both the active tendon and active mass damper for the control of a multi story seismic excited building. Authors demonstrated degradation in the efficiency of the four control system but instantaneous optimal open-loop and instantaneous optimal open-

closed-loop algorithms were found more sensitive to time delay. Also active mass damper was reported to be slightly less sensitive when compared to active tendon control system. Time-delay compensation was based on the availability of the system's state variables. These variables were obtained by using state estimators (observers). However estimation accuracy was questionable due to observation spillovers and the noise content. Abdel-Mooty and Roorda [76] utilized a control scheme that uses direct velocity measurements thus that does not need the state variables of system for time-delay compensation. Authors first defined a time function that is chosen to represent the structural response and composed of harmonic terms in the controlled structure's natural frequencies and the excitation frequencies if known. Then the measured response was fitted into the assumed response by least-squares approximation which performs smoothing and filtering of the uncontrolled frequencies and noise. Fitted curve was extrapolated to obtain a response prediction and the error between the actual response and the predicted one was used to generate compensated signal for the actuator. Further Zhang et. al. [77] computed stable and unstable regions for an active-tendon control system when time-delay is present. The control parameters of displacement control gain and velocity control gain were used as the axis of stability plane. Authors demonstrated that as the time-delay increases the stability region decreases. Agrawal et. al. [78] performed a stability analysis of a SDOF system with time-delayed feedback and derived a closed-form solution for the maximum allowable time delay which was defined as the time decay when the system becomes unstable. Time-delay compensation was realized by modeling the time-delay as transportation lag. The process of data acquisition, data processing, force computation and application of the control force was viewed as the process of transporting information signal. Authors constructed a pipeline model in which control signal flow was treated as an inviscid fluid flow and demonstrated a significant response reduction with the proposed technique. Yang et. al. [79] considered augmenting dynamic equation of the actuators to the state equation of motion. In doing so actuator dynamics were taken in to account in the optimization process and the design of controllers. It was concluded that with the inclusion of actuator dynamics in the optimization process, the degradation of control performance becomes insignificant. Even with compensation methods controlled structures might become unstable without considering the actuator dynamics. Lin et. al. [80] examined the stability of MDOF optimal velocity output feedback control systems in the presence of time-delay and found out that control weighting factor has an important role on the

stability of the controlled system. They formulated an explicit formula to determine the maximum delay time and critical delay time that render the system stable. Chung et. al. [81] modified the instantaneous optimal control algorithm to operate in discrete time. Authors showed that instead of current state variables the time-delay state variables should be used for the online calculation of the time-delay control forces. In discrete time authors managed to relate the current state variables with the time-delayed state variables by utilizing time delay state equation. They demonstrated that real control system with time-delay compensation conserves the eigen properties of the ideal control system with no time-delay. Huang and Betti [82] followed a different approach and instead of relating current state variables with time-delayed ones they formulated the control forces by predicting the state variables that are finite number of steps ahead. Authors utilized an autoregressive model to predict the earthquake excitation to be considered in the prediction of the structural response. In the proposed control scheme quadratic cost function that includes control forces and predicted non-linear states, and subjected to a non-linear constraint equation is minimized at every time step. The resulting controller is a predictive instantaneous controller and optimal control gains are optimized at every time step accounting for the actual and predictive non-linear state of the structure. Pu [83] performed the time delay compensation in phase space by pole assignment method. In the phase plane, the delayed velocity and displacement feedback forces are resolved into active stiffness and active damping components. Then feedback gains are modified such that the real system has the same active stiffness and active damping as the ideal one. However, authors reported that in this methodology selecting proper pole locations is very important and stability is not guaranteed. Up to Grigoriu [84] time delay was considered as a deterministic quantity. He worked on developing optimal control strategies for linear systems with deterministic and random time delay subjected to stochastic input. He used Lyapunov exponent method to investigate the stability of time-delay system. However proposed methodology is heavy in terms of computation especially for small time delay and long observation time. Therefore, an approximate solution was offered by Paola and Pirrotta [85] which is based on the Taylor expansion of the control force. It was concluded that for small value of time delay the approximation fit quite well the exact response however for greater values of time delay the deviation from exact response increases. Cai and Huang [86] introduced time-delay explicitly into the system equation of motion as realized previously by Chung et. al. [81]. However, authors introduced an integral

transformation that renders the system dynamics into a standard first order differential equation without any time delay. Then the controller was designed according to the instantaneous optimal control method, except that substituting the integral transformation into the obtained controller, an integral term appeared in the controller, which is not practical for control implementation. Therefore authors devised a numerical algorithm that computes the integral term. In a very similar fashion to Huang and Betti [82] but this time in continuous space, Wong and Yang [87] proposed a predictive instantaneous optimal control algorithm to reduce the degradation of control performance due to time delay. In this predictive algorithm the structural response at time $t+\tau$ is predicted at time t based on the structural response at time t. Then control force at time $t+\tau$ can be computed and applied when time $t+\tau$ arrives. Authors expanded the predictive instantaneous control algorithm to cover inelastic structures [88]. They used force analogy method to perform inelastic analysis. This method uses the concept of inelastic displacement, where the inelastic analysis is performed based on varying the structural displacement field while keeping the original stiffness unchanged. Therefore state transition matrix needs to be computed only once due to the consistent use of initial stiffness.

For seismic hazard mitigations, the earthquake ground acceleration, including both the magnitude and frequency content, involves the biggest uncertainty among the others. It is possible that a controller with a limited capacity, such as an actuator, may be saturated under unexpected strong earthquakes. Actuator saturation may result in a serious consequence to the controlled structure, such as instability. Therefore, it is also desirable to have controllers whose performance is not affected significantly by saturation and plant uncertainties. Sliding mode control or variable structural control deals with parametric uncertainties in the plant and provide a robust control design. A hypersurface, called the sliding surface is defined in the state space. The error between actual and desired response is zero when the state falls on the sliding surface. Initially controls are applied such that an arbitrary initial state will be brought on to the sliding surface. Once on the sliding surface, the system is said to be in the sliding mode, and controls are applied to keep the state in sliding mode and to make the closed-loop system robust with respect to parametric uncertainties. First systematic investigation of sliding mode control SMC was realized by Yang et. al. [89]. It was reported that when each story is equipped with a controller, complete compensation for the earthquake excitation can be achieved both theoretically

and numerically. In the case of saturation the response quantities are still in elastic limit but floor accelerations may increase significantly. It was further demonstrated that the controller for a complete compensation is robust with respect to system uncertainties. In the following paper of Yang et. al. [90] SMC was applied to linear structures as a special case and the results were compared with classical LQR. Authors reported a superior performance of SMC especially when actuator saturation is considered. Modulation of control effort in SMC was made either by adjusting the sliding surface or by specifying the saturation level of the actuators. To accomplish modulation of response quantities and control effort in an easy and systematic manner Yang et. al. [91] introduced a fixed order compensator using the linear quadratic optimal control theory in sliding mode control. Adhikari et. al. [92] combined the modal space control and sliding mode control in which only dominant vibrational modes were controlled through proposed algorithm. The main difference was sliding surface and nonlinear control forces are no longer defined in terms of the physical states but in terms of the modal coordinates which are obtained from the modal analyses of equation of motion. Matheu et. al. [93] developed sliding mode control algorithm for the full state and output feedback cases. Authors also presented a systematic approach for recasting equation of motion to uncouple sliding motion from the control actions such that control actions are only applied to impose sliding constraints. Zhao et. al. [94] extended the use of SMC to base isolated buildings for base isolation systems exhibit a highly nonlinear behavior. In the SMC framework, the control force is given as the sum of a corrective control force and an equivalent control force. The corrective control force makes the response trajectory deviating from the sliding surface back into the sliding surface, while the equivalent control force causes the response to be parallel to the sliding surface or, in special cases, keeps the trajectory within the sliding surface. The effectiveness and robustness of SMC depend on which one of the above two forces is the dominant part of the control force, and the effect is strongly related to the dynamic characteristics of the sliding surface determined by the LQR method. Therefore, by taking into account the dynamic characteristics of the sliding surfaces Lee et. al. [95] presented a systematic design procedure to decide on optimal weighting matrices between corrective control force and an equivalent control force. Lee et. al. [96] further improved the SMC algorithm an introduced a shape function to determine which of the equivalent and corrective control forces is the dominant part.

In the case of parametric uncertainties related with both system and exogenous inputs, an alternative control strategy to sliding control is robust control design. The development of robust control theory was motivated by the inability of the LQG theory to directly accommodate plant uncertainties. The need to address uncertainty in a systematic way led to the development of the H_∞ problem. H_∞ optimal control method generates feedback gains to minimize the infinity norm of the state space system. The infinity norm represents the maximum amplification of the transfer function between a family of disturbance inputs and set of regulated outputs. Investigation of robust control theory for civil engineering applications is first realized by Shimitendorf et. al. [97]. The H_∞ control law was first designed assuming full state feedback. Than based on the control gains obtained in the first step an observer was designed. The resulting controller was reported to be robust with respect to parameter uncertainty on the model. It was capable of recovering the control performance achieved by full state feedback, using only limited number of sensors and observer. Actuator dynamics was also introduced to eliminate time-delay effect resulting from slow response of actuator. Direct measurement of floor accelerations are the most reliable and least expensive measurements for building structures thus, H_∞ control law is further extended by Jabbari et. al [98] to use acceleration measurements as output feedbacks. Authors also investigated the controllability issue when all the floors are not equipped with an actuator. In this control algorithm an observer was used to estimate system states however, observer based controller requires a significant amount of on-line computational effort due to the complexity of the structure, thus resulting in system time-delays. To overcome the problem Kose et. al. [99] implemented and H_∞ control algorithm that uses only the measured information from a limited number of sensors installed at strategic locations of the structure. They presented conditions for the existence of a H_∞ static output feedback control law that guarantees desirable performance. This requires solution of two matrix inequalities simultaneously. Instead, authors designed a full state feedback controller corresponding to the solution of the first inequality alone. Then they obtained a static output feedback controller that has the same performance as the full state feedback controller designed earlier. The performances of static output feedback H_∞ control and sliding mode control were compared by experimental tests conducted by Yang et. al. [94]. It can be concluded from the tests that sliding mode control was slightly better than H_∞ control for the acceleration reduction. On the other hand similar performance was achieved in reducing peak interstory drifts. Chase and Smith [100] considered actuator

saturation in designing H_∞ state feedback controllers. They modeled the actuator saturation effect as nonlinearities in the same fashion as plant uncertainties. Wu et. al. [101] compared the performances of reduced order H_∞ and LQR controllers under wind excitation. Authors conducted both deterministic and stochastic analyses and reported similar control performances between H_∞ and LQR controllers. Instead of including actuator saturation Yang et. al. [102] formulated a H_2 based control strategy in which the peak values of the control forces are constrained. These constraints were based on physical actuator limits thus actuator saturation was prevented. The proposed strategy was applied to a benchmark problem and a better performance was reported in terms of both structural response and control forces than that of the LQG controller. The same approach was formulated for H_∞ controllers by Yang et. al. [103] and similar performance was obtained between the H_2 and H_∞ controllers. Wu and Lin [104] interpreted H_∞ control to minimize the ratio of the sum of the system energy and control energy with respected to the external excitation energy. System energy can be characterized as strain energy or kinetic energy thus two energy control formulation was developed by the authors. Unlike LQR control there exists no unique positive definite solution for H_∞ control. Therefore, iterative numerical procedures are applied to determine a lower bound solution. Based on energy control formulations authors developed an analytical methodology to determine lower bound solution. Under prescribed upper and lower bounds of structured real parameter uncertainties Lim et. al. [105] focused on developing a robust controller that guarantee robust stability of uncertain linear time invariant system when actuator saturation is considered. The resulting controller was a bang bang controller and sufficient conditions were suggested for the existence of such controller. When the design performance is given by a target damping ratio of the fundamental mode there is no explicit form or relationship between the cost function and the required performance criteria. One useful method is to investigate the eigenvalues of the system. Since the eigenvalues or poles of a linear dynamic system represent the damping ratios as well as the natural frequencies of the system modes. Then it is possible to obtain a controller such that the closed-loop system has certain desirable eigenvalues or poles by a pole placement or pole assignment method. Park et. al. [106] proposed a method that combined the desirable features of pole placement and H∞ control method. In the method, performance requirements of the control system were represented as a target damping ratio. By tracing the pole locations through the bilinear transform, a quadratic equation was formulated, which defines the relationship

between the closed-loop poles and the transform parameters. This quadratic equation then was incorporated with the H∞ control framework to include robust control features. In order to determine the control command accurate information of all the states of the entire system is required. For civil engineering structures such requirement becomes difficult due to the complexity of the problem and the limitations of the physical system. Ma et. al. [107] developed a decentralized robust control algorithm in which the structure is decomposed into several subsystems. The controllers located in each subsystem use only the information of the local subsystem to compute control forces. The interactions among subsystems are treated as uncertain disturbances to the individual sub systems. Performance of the proposed control scheme was reported to better and more robust to actuator failure and uncertainties in structural parameters when compared to LQR control. Wang et. al. [108] further studied decentralized controllers and partially decentralized controllers in which the controller also receives sensor data from neighboring subsystems. The performance of the latter case was reported to be better than the former case. When compared to centralized controllers equivalent performance was reported by the authors. Du et. al. [109] formulated a mixed H_2/ H_∞ control optimization problem to incorporate different performance requirements. In their new approach pole placement is used to improve damping characteristics of the modes of interest. The control effort is constrained by minimizing the H_2 norm of the transfer function from the disturbance to control input. Robust stability is maintained by constraining the maximum singular value of the transfer function from the disturbance to control input below a weighting function by H_∞ control.

1.4. Active Tuned Mass Damper

On of the most important limitations of the Tuned Mass Damper is the mass ratio. Larger mass ratios always results in better performance, on the other hand especially for tall buildings required mass ratio results in a huge mass sitting on the top of a building which is undesirable and even impracticable for certain cases. It is natural that if means of increasing the efficiency of Tuned Mass Damper can be found, better performance can be achieved with smaller mass ratios. Chang and Soong [110] introduced an active force to act between the structure and TMD system to enhance the effectiveness of a passive TMD system. Authors demonstrated a further reduction in displacement and acceleration response of building when TMD system was operated in an active mode. Abdel-Rohman

and Leipholz [111] convinced that although the effectiveness of active tuned mass damper, ATMD, is better than the passive TMD, it is still not comparable to active tendon control. This is due to the fact that force applied by the TMD to the building is opposite in direction to the control force. The optimal parameters used in ATMD were the same with passive TMD in which TMD was tuned to the first mode natural frequency of the building. However Abdel-Rohman [112] realized that the active control introduces to both the building and the tuned mass damper an active stiffness and active damping which change the original structural parameters. Thus in formulating optimal design of ATMD, Abdel-Rohman considered not only an optimal control law but also on selecting proper TMD parameters which minimize further the control energy consumption. Further Abdel-Rohman [113] compared the effectiveness of ATMD and active tendon mechanisms for controlling tall buildings against wind forces. He concluded that active tendon mechanism was very efficient in providing the active damping and active stiffness to the building. However this mechanism was sensitive to time-delay. Whereas ATMD was effective only for free vibration control but was not effective for forced vibration control. On the other hand ATMD was not sensitive to time delay effect. To compensate this disadvantages Abdel-Rohman combined the ATMD and active tendon to obtain a feasible mechanism. In his work he also combined the passive TMD with active tendon and passive tendon with ATMD. He reported that using a combined passive tendon with a passive TMD is very economical. On the other hand best performance is obtained by combining active tendon with active TMD. Suhardjo et. al. [114] utilized the frequency-domain-based H2 optimal-control method to formulate the control law for ATMD. H2 optimal-control method enables designer to use frequency-depended weighting functions as opposed to constant weighting functions. Thus by only minimizing building response components at the frequencies at which these response components are large, control effort is not wasted. That is why smaller control forces were reported by authors when H2 optimal-control method is used. Likewise TMD, ATMD reduces the response only in a single mode. By utilizing H2 optimal-control method however, Spencer et. al. [115] proved that through appropriate choice of weighting function the response of both the first and second mode can be significantly influenced. Chang and Yang [116] investigated the efficiency of ATMD when the structure is subjected to stationary Gaussian white noise ground excitation. They considered both velocity feedback and complete feedback cases. Authors found out that velocity feedback ATMD could not reduce the structural response when

TMD parameters are optimal. With optimal parameters, only ATMD with complete feedback was effective on reducing structural response. On the other hand when TMD was non-optimal, that is the damping of TMD unit was set to zero, than velocity feedback ATMD was also effective in reducing structural response but still ATMD control using the optimal TMD with complete feedback was found more efficient than that of nonoptimal ATMD with velocity feedback. Ankireddi and Yang [117] proposed a simple method for the design of an ATMD for suppressing the firstmode response of tall buildings. To minimize the variance of the roof displacement, the optimal frequency ratio and damping ratio for the passive mass damper were first obtained in closed form analytical expressions, by assuming zero structural damping and Gaussian white-noise excitation. Based on the passive damper's optimal characteristics, the optimal controller feedback gains were next derived for the same objective function. Since ATMD reduces the response only in a single mode, Mackriell at. al. [118] utilized critical mode control approach to formulate the control forces. In the critical mode control, control force is calculated using feedback from the critical first mode of vibration, and controls only that mode. Authors did not considered complete feedback in their study; instead they used combinations of first mode displacement and velocity, and first mode acceleration and velocity. In the end pure first mode acceleration feedback algorithm was found to be most efficient among various combinations. Adhikari and Yamaguchi [119] applied sliding mode control theory for the control of a tall building equipped with ATMD. However, authors reported that large response of ATMD prevented then controlled system from reaching the sliding mode. Thus controller needs larger forces to control the system. To filter out the undesirable effects of the ATMD response on control scheme a filter was proposed. Yan et. al. [120] extended the study of Ankireddi and Yang [117] by considering a more realistic power spectral density of wind instead of Gaussian white noise. Authors reported that frequency ratio in the analytic expression is not only sensitive to the type of wind excitation but also to the structural building height. Therefore a modified expression was proposed that takes into consideration the effect of mass ratios and the building fundamental frequency. Wang et. al. [121] worked on composite active-passive TMD system which was first found by Kajima Corporation Research Team. This system was very similar to double tuned mass damper system in which a smaller TMD unit is attached to a large TMD unit. The difference is smaller TMD is equipped with an actuator. Since control forces were exerted on a small mass, the size of the active controller and required control forces were smaller.

Nagashima [122] derived analytical expressions of the linear quadratic regulator feedback gains of the ATMD by solving the Ricatti equation. He than realized that if the stiffness of TMD is calibrated to satisfy a certain condition, then the control law is simplified to be composed of the feedback gains only for the displacement of the structure and the velocity of the auxiliary mass stroke. In the performance index, if only the structure displacement is weighted than the tuning condition coincided with the optimal conditions for a passive TMD developed by Den Hartog [1]. On the other hand if only the structure velocity is weighted than stiffness of the TMD unit should be increased with the increase of feedback gain for the structural displacement. Li and Liu [123] extended the active tuned mass damper concept to multiple tuned mass dampers. The proposed active multiple tuned mass damper, AMTMD, control strategy offered smaller size for an individual ATMD than one massive ATMD. Optimum parameters for AMTMD were searched through the minimization of the minimum values of the maximum dynamic magnification factors. Futher Li [124] extended the composite active-passive TMD (APTMD) system to multiple active-passive TMD (MAPTMD) system in which both active and passive TMDs were subdivided in to smaller masses. It was concluded that MAPTMD has a better effectiveness and can render higher robustness with respect to a single APTMD. Cao and Li [125] proposed a new method on obtaining control gains for ATMD. Instead of LQR method, they derive the optimal control gains from variances of displacement responses. Then they obtained a simplified method to calculate the effective damping of ATMD based on the proposed methodology. Although being much simpler than standard LQR, the proposed methodology considered only the first mode in the design. Collins et. al. [126] used bang-bang control and formulated the control law by minimizing the time derivative of a Lyapunov function of the open-loop system. Bang-bang controller operates only when the controlled response exceeds a predetermined threshold thus active force may not always be necessary. In the case where no control is applied TMD is tuned as a passive device. Therefore authors calculated the optimum TMD parameters by the minimization of the maximum value of frequency response function corresponding to structure-ATMD system. Li and Zhu [127] proposed an open-closed loop control algorithm for multiple active tuned mass dampers by both feeding forward the ground motion acceleration and feeding back the structural velocity and displacement. However authors reported no significant advantage of open-closed loop scheme when compared to closed-loop control. Bani-Hani [128] investigated the potential use of neural-network-based control methods in

wind excited tall buildings using an active tuned mass damper system. This control technique utilizes artificial intelligence and can be thought of as adaptive or self-organizing systems that learn through interaction with their environment. Therefore, the correctness of formulated mathematical model is not of great influence to performance. Guclu and Yazici [129] implemented another type of intelligent control technique, fuzzy logic controller to active tuned mass damper.

1.5. Objectives

It is a well known fact that tuned mass damper (TMD) is most effective when the TMD is tuned to input frequency, however in civil engineering it is not possible to know the input characteristics since building are subjected to environmental loads which are random in nature such as wind and earthquake. Thus, the best course of action taken is usually to tune the TMD to building's natural frequency since the worst case scenario will be a resonance case in which a dominant input frequency coincides with the building's natural frequency. However, operational range of such a system is band-limited i.e a narrow frequency range around the natural frequency and do not cover a broad band frequency range as in the case of earthquake or wind loads. A widely accepted remedy to this situation is to introduce some damping to TMD unit which will broaden the operational range by compromising effectiveness.

The net effect of the added auxiliary mass on the structure, aside from a slight decrease in natural frequency, is the addition of an inertia force that is opposite to the displacement vector of the structure. Since exerted inertia force is related to the mass auxiliary mass, the effectiveness of TMD can be increased by increasing the mass ratio which is the ratio of the auxiliary mass block to the mass of the structure. However in most cases this is not implementable since a huge mass is required to be placed on top of a building. Alternatively, the efficiency of TMD can be improved by the addition of an active force to the mass damper as a substitute to inertia force. This addition of an active force enables achieving the same effectiveness of a large TMD with a small active TMD. Up to date active tuned mass dampers have been extensively studied by many researchers since it allows relatively small mass ratios when compared to passive tuned mass dampers. This is very important especially when the huge mass of a tall building is considered.

In this study an alternative approach is investigated to increase the effectiveness of TMD. When a structure is excited with a single frequency disturbance, it is well known that TMD is most effective when it is tuned to input frequency and no damping is introduced. This is due to the fact that frequency of the steady state response of the structure matches the frequency of the input and that falls in the operating range of TMD unit. However, if the structure is excited with a broadband input such as an earthquake, then the frequency content of the response will fall out of the operating range of TMD unit. Therefore to broaden the operational range of a TMD some damping is introduced to TMD unit. Although this added damping term smoothens the sharp peaks of frequency response function out of the operating range it also considerably decreases the effectiveness of TMD in the operating range. Thus, if we can find a way to constraint the response of the structure in the boundaries of the operating range of TMD, then the requirement for additive damping will be eliminated and TMD can be used in full efficiency. As a consequence in this study we aim to alter the system response of a broad band input as if it was a steady-state response to a single frequency input. This can be achieved if the structure is equipped with an active controller such that controller forces the system to track a single frequency reference input which coincides with the operating frequency of TMD unit. Then the response of the controlled structure will match the desired operating frequency of TMD unit. As a consequence in this study a hybrid system is suggested in which a tracking type controller is used together with a passive undamped TMD unit.

2. LINEAR CONTROL THEORY

2.1. Analytical Modeling

2.1.1. General Assumptions

The overall goal of feedback control is to drive the output variable of a dynamic system to follow a desired reference variable accurately regardless of the reference variable's path and of any external disturbances or any changes in the dynamics of the process. This complex goal is met as the result of a number of simple, distinct steps. The first of these is to develop a mathematical description of the real physical system to be controlled [130]. An ideal mathematical model can be obtained by applying natural laws to the ideal physical model and composed of a set of nonlinear differential equations that describe the physics of the ideal system. In civil engineering discipline ideal physical model is described by decomposing the real physical system into ideal building blocks such as masses, beams, columns and so on. Likewise a reduced mathematical model can be obtained from the ideal mathematical model by linearization, lumping and so on. In that sense no mathematical system can precisely model a real physical system, there are always assumptions. The mathematical models used in this thesis are linear and time-invariant.

A linear system response obeys the principle of superposition which states that the outputs of a linear system to an input consisting of linear combination of two different inputs can be obtained by linearly superposing the outputs to the respective inputs [131]. Thus the response to a general signal can be solved by decomposing the given signal into a sum of elementary components. Then response to general signal is the sum of the responses of the elementary signals. The elementary signals need to be sufficiently "rich" that any reasonable signal can be expressed as a sum of them. In that sense impulse and exponential signals are the best candidates for elementary signals. Given a continuous function f(t) at $t=\tau$, then

$$f(t) = \int_{-\infty}^{\infty} f(\tau)\delta(t-\tau)d\tau \tag{2.1}$$

In other words the function f(t) can be represented as sum of impulses. If we replace f with u, then Eq. (2.1) represents an input u(t) as a sum of impulses of intensity u(t-τ). If we express the impulse response as h(t,τ), the response at t to an impulse applied at τ. The total response is the sum of these with intensity u.

$$y(t) = \int_{-\infty}^{\infty} u(\tau)h(t,\tau)d\tau \tag{2.2}$$

A system with time-varying parameters is called a time-varying system, while a system whose parameters are constant with time is called time-invariant system. If the system is not only linear but also time invariant, then the impulse response is given by h(t-τ) because the response at t to an input applied at τ depends only on the difference between the time the impulse is applied and the time we are observing the response.

$$y(t) = \int_{-\infty}^{\infty} u(\tau)h(t-\tau)d\tau \text{ or } y(t) = \int_{-\infty}^{\infty} u(t-\tau)h(\tau)d\tau \tag{2.3}$$

2.1.2. Frequency Response

Frequency response is related to the steady-state response of a system when a harmonic function is applied as the input. A harmonic input, $u(t)$, can be:

$$u(t) = u_0 \cos(\omega t) \text{ or } u(t) = u_0 \sin(\omega t) \tag{2.4}$$

where, u_0 is the constant amplitude and ω is the frequency of excitation. If we express the harmonic input in the complex space as:

$$u(t) = u_0 e^{i\omega t} \tag{2.5}$$

where $i = \sqrt{-1}$, and

$$e^{i\omega t} = \cos(\omega t) + i\sin(\omega t) \tag{2.6}$$

Equation (2.6) is a complex representation in which $\cos(\omega t)$ is called the real part of $e^{i\omega t}$ and $\sin(\omega t)$ is called the imaginary part of $e^{i\omega t}$. Hence, complex space representation of a harmonic function is a mean of representing both the possibilities of a simple harmonic input, namely $u_0 \cos(\omega t)$ and $u_0 \sin(\omega t)$, respectively in one expression. By obtaining a steady state response to the complex input given by Equation (2.5), we will be obtaining simultaneously the steady state responses of a linear, stable system to $u_0 \cos(\omega t)$ and $u_0 \sin(\omega t)$.

Solution to ordinary differential equations consists of two parts. One is the complimentary solution which depends upon the initial conditions, and the other is the particular solution which depends upon the input. While the transient response of a linear stable system is largely described by the complimentary solution, the steady-state response is the same as the particular solution at large times. The particular solution is of the same form as the input and must by itself satisfy the differential equation. In the complex space, we can write the steady-state response to harmonic input as follows:

$$y_{ss}(t) = y_0(i\omega)e^{i\omega t} \tag{2.7}$$

where y_0 is the steady-state response amplitude and is a complex function of the frequency of excitation, ω.

By applying superposition principle, linear differential equation of a lumped parameter system can be written as:

$$\begin{aligned} &a_n y^{(n)}(t) + a_{n-1} y^{(n-1)}(t) + \ldots + a_1 y^{(1)}(t) + a_0 y(t) \\ &= b_m u^{(m)}(t) + b_{m-1} u^{(m-1)}(t) + \ldots + b_1 u^{(1)} + b_0 u(t) \end{aligned} \tag{2.8}$$

where $y^{(k)}$ denotes the *k*th derivative of *y(t)* with respect to time, t and $u^{(k)}$ denotes the *k*th derivative of *u(t)*. Equation (2.8) can be re-written as follows:

$$D_1\{y_{ss}(t)\} = D_2\{u(t)\} \tag{2.9}$$

In Equation (2.9) $D_1\{.\}$ and $D_2\{.\}$ are differential operators given by:

$$D_1\{.\} = a_n d^n/dt^n + a_{n-1} d^{n-1}/dt^{n-1} + ... + a_1 d/dt + a_0 \tag{2.10}$$

$$D_2\{.\} = b_m d^m/dt^m + b_{m-1} d^{m-1}/dt^{m-1} + ... + b_1 d/dt + b_0 \tag{2.11}$$

Then noting that

$$D_1\{e^{i\omega t}\} = \left[(i\omega)^n a_n d^n/dt^n + (i\omega)^{n-1} a_{n-1} d^{n-1}/dt^{n-1} + ... + (i\omega) a_1 d/dt + a_0\right] e^{i\omega t} \tag{2.12}$$

$$D_2\{e^{i\omega t}\} = \left[(i\omega)^m b_m d^m/dt^m + (i\omega)^{m-1} b_{m-1} d^{m-1}/dt^{m-1} + ... + (i\omega) b_1 d/dt + b_0\right] e^{i\omega t} \tag{2.13}$$

We can write, using Equation (2.9),

$$y_0(i\omega) = G(i\omega) u_0 \tag{2.14}$$

where $G(i\omega)$ is called the frequency response of the system, and is given by

$$\begin{aligned} G(i\omega) &= \left[(i\omega)^m b_m + (i\omega)^{m-1} b_{m-1} + ... + (i\omega) b_1 + b_0\right] \\ &/\left[(i\omega)^n a_n + (i\omega)^{n-1} a_{n-1} + ... + (i\omega) a_1 + a_0\right] \end{aligned} \tag{2.15}$$

Equations (2.14) and (2.15) describe how the steady-state output of a linear system is related to its input through the frequency response $G(i\omega)$ which is also a complex quantity, consisting of both real and imaginary parts. Instead of the real and imaginary parts, an alternative description of a complex quantity is in terms of its magnitude and the

phase which can be thought of a vector's length and direction respectively. Representation of a complex quantity as a vector in the complex space is called a phasor. The magnitude of a phasor represents the amplitude of a harmonic function, while the phase determines the value of the function at t=0. The phasor description of the steady-state output amplitude is given by:

$$y_0(i\omega) = |y_0(i\omega)|e^{i\alpha(\omega)} \tag{2.16}$$

where $|y_0(i\omega)|$ is the magnitude and $\alpha(\omega)$ is the phase of $y_0(i\omega)$. We can also express the frequency response, $G(i\omega)$ in terms of its magnitude, $|G(i\omega)|$, and phase, $\phi(\omega)$, as follows:

$$G(i\omega) = |G(i\omega)|e^{i\phi(\omega)} \tag{2.17}$$

Substituting of Equations (2.16) and (2.17) into Equation (2.14) gives that $|y_0(i\omega)| = |G(i\omega)|u_0$ and $\alpha(\omega) = \phi(\omega)$. Hence Equation (2.7) can be rewritten as:

$$y_{ss}(t) = y_0(i\omega)e^{i\omega t} = |G(i\omega)|u_0 e^{i\phi(\omega)}e^{i\omega t} = |G(i\omega)|u_0 e^{i[\omega t+\phi(\omega)]} \tag{2.18}$$

From Equation (2.18), it is clear that the steady-state response is governed by the amplitude of the harmonic input, u_0 and magnitude and phase of the frequency response, $G(i\omega)$, which represents the characteristics of the system, and are functions of the frequency of excitation.

Since the range of frequencies required to study a linear system is usually very large, it is often useful to plot magnitude, $|G(i\omega)|$ and phase, $\phi(\omega)$ with respect to the frequency, ω on a logarithmic scale of frequency called Bode plots. In Bode plots magnitude is usually converted to gain in decibels (dB) by taking the logarithm of $|G(i\omega)|$ to the base 10, and multiplying the result with 20 as follows:

$$Gain = 20\log_{10}\left|G(i\omega)\right| \tag{2.19}$$

2.1.3. Laplace Transform and Transfer Function

Frequency response function was the transformation of governing differential equations into a complex algebraic expression that defines the steady-state response of a linear system to harmonic inputs. For a general input, a similar complex expression can be obtained by applying Laplace transformation to the input *u(t)*, defined as

$$U(s) = Lu(t) = \int_0^\infty e^{-st}u(t)dt \tag{2.20}$$

where s denotes the Laplace variable and *U(s)* is called the Laplace transform of *u(t).* The Laplace transform of a function *u(t)* is defined only if the infinite integral in Equation (2.20) exists, and converges to a functional form *U(s).* Laplace transform converges only if *u(t)* is piecewise continuous and bounded by an exponential. If the input, *u(t),* and its time derivatives are Laplace transformable, then the differential equation of a linear, time invariant system is Laplace transformable, which implies that the output, *y(t),* is also transformable. The governing equation of the system given by Equation (2.8) can be transformed to the Laplace domain as:

$$(s^n a_n + s^{n-1}a_{n-1} + ... + sa_1 + a_0)Y(s) = (s^m b_m + s^{m-1}b_{m-1} + ... + sb_1 + b_0)U(s) \tag{2.21}$$

The transfer function is then defined as the ratio of the Laplace transform of the output, *Y(s)*, and that of the input, *U(s)*.

$$G(s) = (s^m b_m + s^{m-1}b_{m-1} + ... + sb_1 + b_0)/(s^n a_n + s^{n-1}a_{n-1} + ... + sa_1 + a_0) \tag{2.22}$$

The transfer function, *G(s)*, represents how an input, *U(s)*, is transferred to the output, *Y(s)*. In other words it defines the relationship between the input and the output when the initial conditions are zero.

The roots of the numerator and denominator polynomials of the transfer function, *G(s)*, given by Equation (2.22) represent the characteristics of the linear, time-invariant system. The denominator polynomial of the transfer function, *G(s)*, equated to zero is called the characteristic equation of the system and is given by:

$$s^n a_n + s^{n-1} a_{n-1} + \ldots + s a_1 + a_0 = 0 \tag{2.23}$$

The roots of the characteristic equation are called the poles of the system. The roots of the numerator polynomial of *G(s)* equated to zero are called the zeros of the transfer function given by:

$$s^m b_m + s^{m-1} b_{m-1} + \ldots + s b_1 + b_0 = 0 \tag{2.24}$$

As for the most linear, time-invariant systems if m ≤ n, the system is said to be proper. If m < n then the system is said to be strictly proper.

A special transform, called the Fourier transform, can be defined by substituting $s = i\omega$ in the definition of the Laplace transform given by Equation (2.20)

$$U(i\omega) = \int_0^\infty e^{-i\omega t} u(t) dt \tag{2.25}$$

Fourier transform is widely used as a method of calculating the response of linear systems to arbitrary inputs by transforming an arbitrary input, *u(t)*, to its frequency domain counterpart, *U(iω)*. Then, we can determine the resulting output (assuming zero initial conditions) in the frequency domain as

$$Y(i\omega) = G(i\omega) U(i\omega) \tag{2.26}$$

where *G(iω)* is the predetermined frequency response. The output in the time domain is obtained by applying the inverse Fourier transform as follows:

$$y(t) = 1/(2\pi)\int_{-\infty}^{\infty} e^{i\omega t} Y(i\omega) d\omega \tag{2.27}$$

2.1.4. State Space Representation

The governing higher order differential equation of a system can be described by a set of simultaneous first-order differential equations. The set of first-order differential equations are called the state equations into which the governing equation has been transformed. The order of the system however remains unchanged when we express it in terms of the state variables. The state of the system is defined as any set of quantities which must be specified at a given time in order to completely determine the behavior of the system. The quantities constituting the state are called state variables, and the hypothetical space spanned by the space variables is called the state space [131].

In contrast to classical methods, the state-space methods work directly with the governing differential equations of the system in the time-domain. Representing the governing differential equations by first order state equations makes it possible to directly solve the state equations in time using standard numerical methods. Since the state equations are always of first order irrespective of the system's order or the number of inputs or outputs, the greatest advantage of state-space methods is that they do not formally distinguish between single-input, single-output systems and multivariable systems. This allows efficient design and analysis of multivariable systems with the same ease as for single variable systems [131].

Let's describe a SDOF system exited with a forcing function F. Equation of motion for such a system is given by

$$m\ddot{y}(t) + c\dot{y}(t) + ky(t) = F(t) \tag{2.28}$$

where m, c and k are the mass, damping coefficient and stiffness of the SDOF system respectively and y(t) is the displacement of the mass in the considered degree of freedom. The system is described by a second order differential equation; hence the order of the system is two. Thus we need two linearly independent state-variables to describe the

system. When dealing with a physical system, it is often desirable to select physical quantities as state variables. If we define the state variables as the mass displacement and the velocity of the mass as follows:

$$x_1(t) = y(t) \tag{2.29}$$

$$x_2(t) = \dot{y}(t) \tag{2.30}$$

Differentiating the state variables once gives

$$\dot{x}_1(t) = \dot{y}(t) = x_2(t) \tag{2.31}$$

$$\begin{aligned} \dot{x}_2(t) = \ddot{y}(t) &= -k/m\, y(t) - c/m\, \dot{y}(t) + 1/m\, F(t) \\ &= -k/m\, x_1(t) - c/m\, x_2(t) + 1/m\, F(t) \end{aligned} \tag{2.32}$$

Equations (2.30) and (2.31) can be written in matrix form as:

$$\begin{bmatrix} \dot{x}_1(t) \\ \dot{x}_2(t) \end{bmatrix} = \underbrace{\begin{bmatrix} 0 & 1 \\ -k/m & -c/m \end{bmatrix}}_{\text{A}} \begin{bmatrix} x_1(t) \\ x_2(t) \end{bmatrix} + \underbrace{\begin{bmatrix} 0 \\ 1/m \end{bmatrix}}_{\text{B}} F(t) \tag{2.33}$$

The mathematical model in this standard form is known as the state equation of the model. A state space model is represented as:

$$\dot{x}(t) = Ax(t) + Bu(t) \tag{2.34}$$

$$y(t) = Cx(t) + Du(t) \tag{2.35}$$

The variable x(t) is called the state of the system, u(t) is the input to the system and y(t) is the output of the system. The matrix A is the state matrix, B is the input matrix, C is the output matrix and D is the input-to-output coupling matrix.

The transfer matrix is obtained by taking Laplace transform of the governing equations, for zero initial conditions. Taking the Laplace transform of both sides of the matrix state equation, Equation (2.34) yields:

$$sX(s) = AX(s) + BU(s) \tag{2.36}$$

where *X(s)=L[x(t)]*, and *U(s)=L[u(t)]*. Rearranging Equation (2.36) we can write

$$(sI - A)X(s) = BU(s) \tag{2.37}$$

or,

$$X(s) = (sI - A)^{-1} BU(s) \tag{2.38}$$

Similarly, taking the Laplace transform of the output equation, Equation (2.35) with *Y(s)=L[y(t)]* yields

$$Y(s) = CX(s) + DU(s) \tag{2.39}$$

Substituting Equation (2.38) into Equation (2.39) we get

$$Y(s) = C(sI - A)^{-1} BU(s) + DU(s) = \left[C(sI - A)^{-1} B + D\right]U(s) \tag{2.40}$$

From Equation (2.40), it is clear that the transfer matrix, *G(s)*, defined by *Y(s)=G(s)U(s)*, is the following:

$$G(s) = C(sI - A)^{-1} B + D \tag{2.41}$$

It is seen from Equation (2.41) that the transfer matrix is the sum of the rational matrix $C(sI-A)^{-1}B$ and the matrix D. Thus, D represents direct connection between the input and the output, and is called the direct transmission matrix. Systems having D=0 are called strictly proper.

2.2. The Closed Loop System

In general sense a control problem is to determine a feasible control input u, so that controlled variable y, of a plant P follows a reference signal r, as closely as possible despite the influences of disturbances w, measurement errors n, and variations in the plant. If the controller does not use a measure of the controlled systems output in computing the control forces, the system is called open-loop control. If the controlled output of the system is measured by physical sensors and fed back for use in control computation, the system is called closed-loop or feedback control.

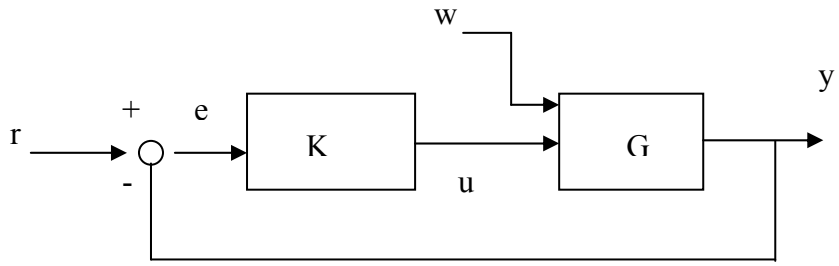

Figure 2.1. Feedback Control System

2.2.5. The Transfer Functions of the Closed Loop System

Figure 2.1 depicts a typical closed-loop system configuration, where G is the plant and K the controller to be designed. r,y,u,e,w are respectively the reference input, output, control signal, error signal and disturbance. Transfer function of the plant can be written in Laplace domain as:

$$Y(s) = G(s)U(s) + G(s)W(s) \tag{2.42}$$

The controller applies an input, *U(s)*, to the plant based upon the error, $E(s) = R(s) - Y(s)$. Thus transfer function of the controller is given by:

$$U(s) = K(s)E(s) = K(s)R(s) - K(s)Y(s) \tag{2.43}$$

Substituting Equation (2.43) into Equation (2.42) we get

$$Y(s) = G(s)K(s)R(s) - G(s)K(s)Y(s) + G(s)W(s) \tag{2.44}$$

Collecting the *Y(s)* terms on the left side of the equation gives:

$$Y(s) = \left[I + G(s)K(s)\right]^{-1} G(s)K(s)R(s) + \left[I + G(s)K(s)\right]^{-1} G(s)W(s) \tag{2.45}$$

By utilizing Equation (2.45), error term, *E(s)*, can be written as:

$$E(s) = R(s) - \left[I + G(s)K(s)\right]^{-1} G(s)K(s)R(s) - \left[I + G(s)K(s)\right]^{-1} G(s)W(s) \tag{2.46}$$

which can be further collected as:

$$E(s) = \left[I - \left[I + G(s)K(s)\right]^{-1} G(s)K(s)\right]R(s) - \left[I + G(s)K(s)\right]^{-1} G(s)W(s) \tag{2.47}$$

where the first term on the right side of Equation (2.47) can be further extended as:

$$I - \frac{G(s)K(s)}{I + G(s)K(s)} = \frac{I}{I + G(s)K(s)} = \left[I + G(s)K(s)\right]^{-1} \tag{2.48}$$

Thus Equation (2.47) becomes:

$$E(s) = \left[I + G(s)K(s)\right]^{-1} R(s) - \left[I + G(s)K(s)\right]^{-1} G(s)W(s) \tag{2.49}$$

then the control signal U(s) is

$$U(s) = K(s)\left[I + G(s)K(s)\right]^{-1} R(s) - K(s)\left[I + G(s)K(s)\right]^{-1} G(s)W(s) \tag{2.50}$$

The following notation and terminology are used:

$L = GK$: loop transfer function

$S = (I + GK)^{-1}$: sensitivity function

$T = (I + GK)^{-1} GK$: complementary sensitivity function

We see from Equation (2.45) that S is the closed loop transfer function from the output disturbances to the outputs, while T is the closed-loop transfer function from the reference signals to the outputs [132]. With feedback the use of high gains in GK results in sensitivity function closer to zero and a complementary sensitivity function closer to unity which in turn enhances the disturbance rejection and reference tracking properties of the closed loop system. On the other hand, high-gain feedback may induce stability, so stability conditions should be carefully checked in design of controllers.

2.2.6. Stability of the Closed Loop System

Two methods are commonly used to determine closed-loop stability [132]:

- The poles of the closed loop system are evaluated. That is, the roots of $1 + L(s) = 0$ are found, where L is the transfer function around the loop. The system is stable if and only if all the closed loop poles are in the open left half s-plane. The poles are also equal to the eigenvalues of the state space A-matrix.
- The frequency response (including negative frequencies) of $L(j\omega)$ is plotted in the complex plane. Such a polar plot is called Nyquist plot. Then the number of anti-clockwise encirclements it makes of the critical point -1 is counted. By Nyquist's stability criterion closed-loop stability is inferred by equating the number of encirclements to the number of open loop poles of the transfer function L.

2.2.7. Performance of the Closed Loop System

Performance can be evaluated on basis on how a control system meets its desired objectives. These objectives can be defined in time domain or in frequency domain. Time domain performance is evaluated by taking into account the step response to a reference input and following characteristics are considered [132]:

- *Rise time (t_r) :* the time it takes for the output to reach 90% of its final value, which is usually required to be small.
- *Settling time (t_s):* the time after which the output remains within ±ε% of its final value (typically ε=5), which is usually required to be small.
- *Overshoot:* the peak value divided by the final value, which should typically be 1.2 (20%) or less.
- *Decay ratio:* the ratio of the second and first peaks, which should typically be 0.3 or less.
- *Steady-state offset:* the difference between the final value and the desired value, which is usually required to be small.

The rise time and settling time are measures of the speed of the response, whereas the overshoot, decay ratio and steady-state offset are related to the quality of the response. The frequency response of the loop transfer function $L(j\omega)$, or of various closed-loop transfer functions, may also be used to characterize closed-loop performance. One advantage of the frequency domain compared to step response analysis is that it considers broader class of signals (sinusoids of any frequency).

In frequency domain, gain margin, GM, and phase margin, PM, provide stability margins for gain and delay uncertainty. More generally, to maintain closed-loop stability, the Nyquist stability condition tells us that the number of encirclements of the critical point -1 by $L(j\omega)$ must not change. Thus the closeness of the frequency response $L(j\omega)$ to the critical point -1 is a good measure of closeness to instability. The GM represents the closeness along the negative real axis, and the PM along the unit circle. The GM is the factor by which the loop gain $|L(j\omega)|$ may be increased before the closed-loop system

becomes unstable. The GM is thus a direct safeguard against steady-state gain uncertainity. Typically GM>2 is required. The PM tells us how much negative phase (phase lag) we can add to *L(s)* at crossover frequency where $|L(j\omega_c)| = 1$, before the phase at this frequency becomes -180° which corresponds to closed loop instability. The PM is a direct safeguard against time delay uncertainty and typically PM larger than 30° or more is required. On a bode plot with a logarithmic axis for $|L(j\omega)|$, we have that GM is the vertical distance (in dB) from the unit magnitude line down to $|L(j\omega_{L180})|$.

2.3. Compensator Design

In a typical single-input, single-output closed loop system dynamic requirements in time domain, as well as gain and phase margins can be effected by changing the controller transfer function, *K(s)*. Since we can use K(s) to compensate for the poor characteristics of plant, G(s), such a controller, K(s), is called the compensator and the procedure for selecting a controller is called closed-loop compensation.

Let's consider a single-degree-of-freedom (SDOF) system with following structural parameters:

$k_s = 1.10^5$ kN/m
$c_s = 3{,}16.10^3$ kN/s (%5 damping)
$m_s = 1.10^4$ tons

If the SDOF system is excited by a forcing function *u(t)* then the governing equation of the above system can be written as:

$$m_s \ddot{y}(t) + c_s \dot{y}(t) + k_s y(t) = u(t) \tag{2.51}$$

The governing equation of the system given by Equation (2.51) can be transformed to the Laplace domain as:

$$(m_s s^2 + c_s + k_s)Y(s) = U(s) \tag{2.52}$$

Solving for the transfer function, G(s), which is defined as the ratio of the Laplace transform of the output, *Y(s)*, and that of the input, *U(s)* and denoting $\zeta_s = c_s / 2m_s\omega_0$, $\omega_0 = \sqrt{k_s / m_s}$ we get:

$$G(s) = \frac{1}{s^2 + 2\zeta_s\omega_0 s + \omega_0^2} \tag{2.53}$$

Step response of the plant is shown in Figure 2.2. The overshoot is %85.3, the rise time is 0.34 seconds and the settling time is 24 seconds. The damping is %5, and hence plant oscillates a lot before coming to a steady state. Let's say that we require the plant to track a step command, and then we have to use a compensator. The simplest compensator would be proportional compensator in which the feedback control signal is made to be linearly proportional to the system error.

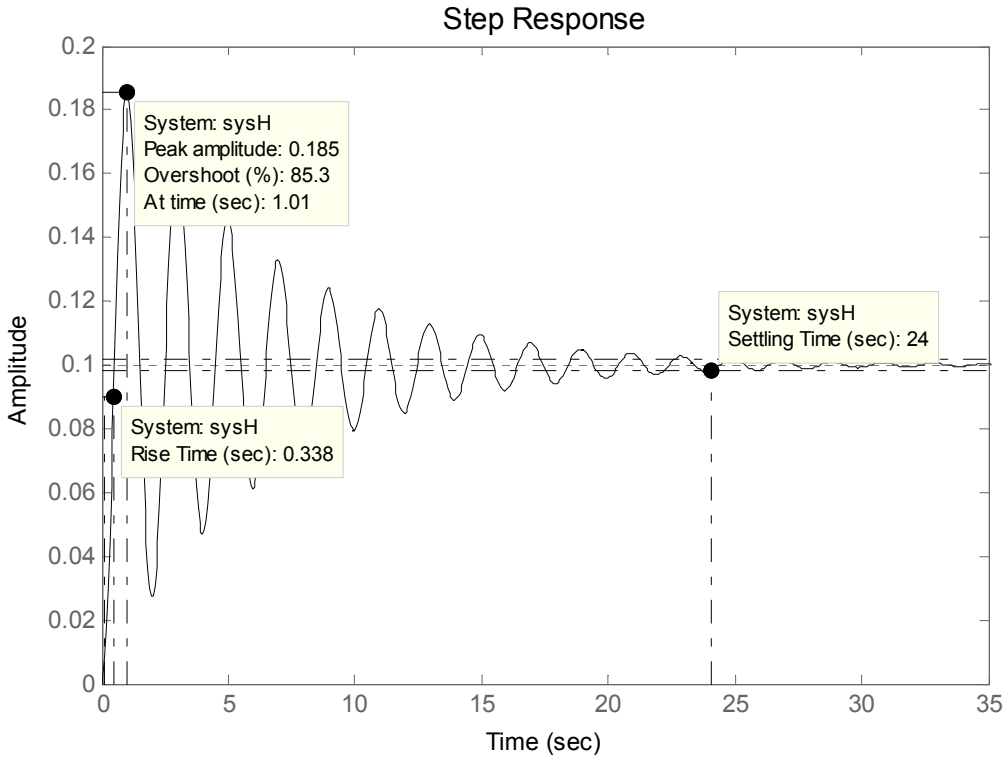

Figure 2.2. Step response of the plant

2.3.8. Proportional feedback compensation (P)

In the general form of proportional compensation the tracking error *e(t)*, is taken as an input to the compensator and the output of the compensator which is also input to the plant is obtained as *u(t)*. The control law is:

$$U(s) = H(s)E(s) = k_p E(s) \tag{2.54}$$

Since $E(s) = R(s) - Y(s)$ and $Y(s) = G(s)U(s)$, the output, Y(s) of the closed loop system can be written as:

$$Y(s) = G(s)k_p(R(s) - Y(s)) \tag{2.55}$$

Collecting the *Y(s)* terms to the left hand side of the equation gives:

$$Y(s)(1 + G(s)k_p) = G(s)k_p R(s) \tag{2.56}$$

So transfer function of the closed loop system from reference command, *R(s)* to output, *Y(s)* can be written as:

$$\frac{Y(s)}{R(s)} = \frac{G(s)k_p}{1 + G(s)k_p} \tag{2.57}$$

If we combine Equation (2.53) with Equation (2.57), what we obtain is:

$$\frac{Y(s)}{R(s)} = \frac{k_p}{s^2 + 2\zeta_s\omega_0 s + (\omega_0^2 + k_p)} \tag{2.58}$$

It is clear from Equation (2.58) that the system with proportional control will usually have a steady-state offset in response to a constant reference input which gets smaller as the gain is increased. Figure 2.3 shows the closed loop response to a reference input when control gain k_p is selected as 50.

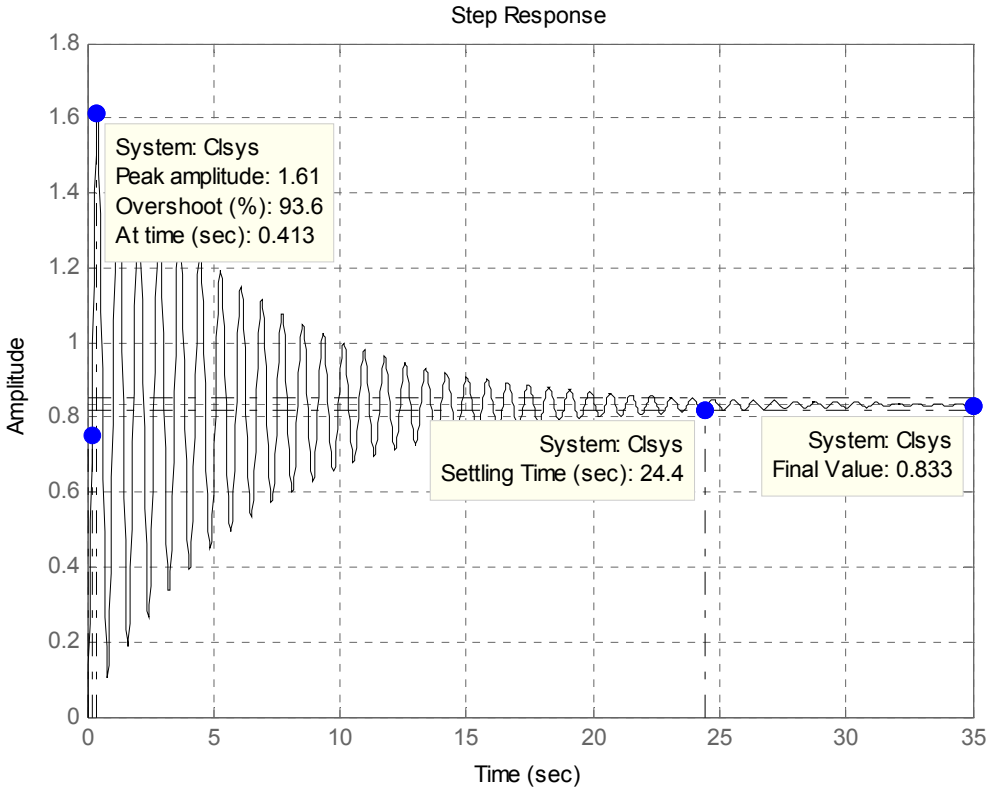

Figure 2.3. Step response of the closed loop system with P compensator

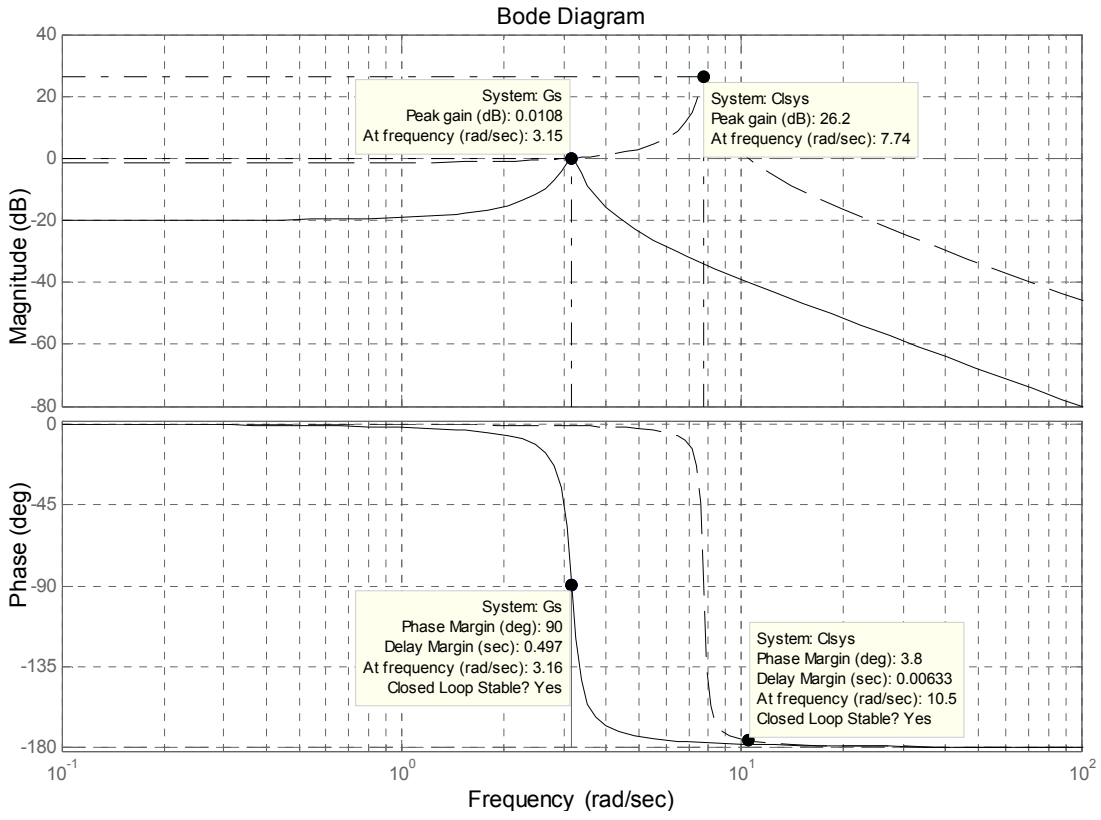

Figure 2.4. Bode plots of the plant and closed loop system with P compensator

It is visible that even for high control gain k_p is there is still a steady-state error present. Furthermore the rigidity and the overshoot of the closed loop system are increased. It is also verified from Figure 2.4 that the frequency of the closed loop system is increased from 3.15 rad/sec to 7.74 rad/sec. The peak gain of the closed loop system is also increased and phase margin in other words tolerance to time delay is very much decreased.

2.3.9. Proportional-Integral compensation (PI)

By adding an integral term in the compensator, the compensator transfer function can be written in Laplace domain as:

$$H(s) = k_p + \frac{k_t}{s} \tag{2.59}$$

Since the integral term in the control signal is a summation of all past values of e(t), the control output can be a nonzero constant even when the error signal is zero. This feature leads to cancellation of a constant disturbance w by the compensator, even while the system error is zero. The control law can be written as:

$$U(s) = H(s)E(s) = k_p E(s) + k_t \frac{E(s)}{s} \tag{2.60}$$

So transfer function of the closed loop system from reference command, *R(s)* to output, *Y(s)* can be written as:

$$\frac{Y(s)}{R(s)} = \frac{G(s)(k_p + k_t / s)}{1 + G(s)(k_p + k_t / s)} \tag{2.61}$$

Combination of Equation (2.53) with Equation (2.61), gives:

$$\frac{y}{r} = \frac{k_p s + k_t}{s(s^2 + 2\zeta_s \omega_0 s + (\omega_0^2 + k_p)) + k_t} \tag{2.62}$$

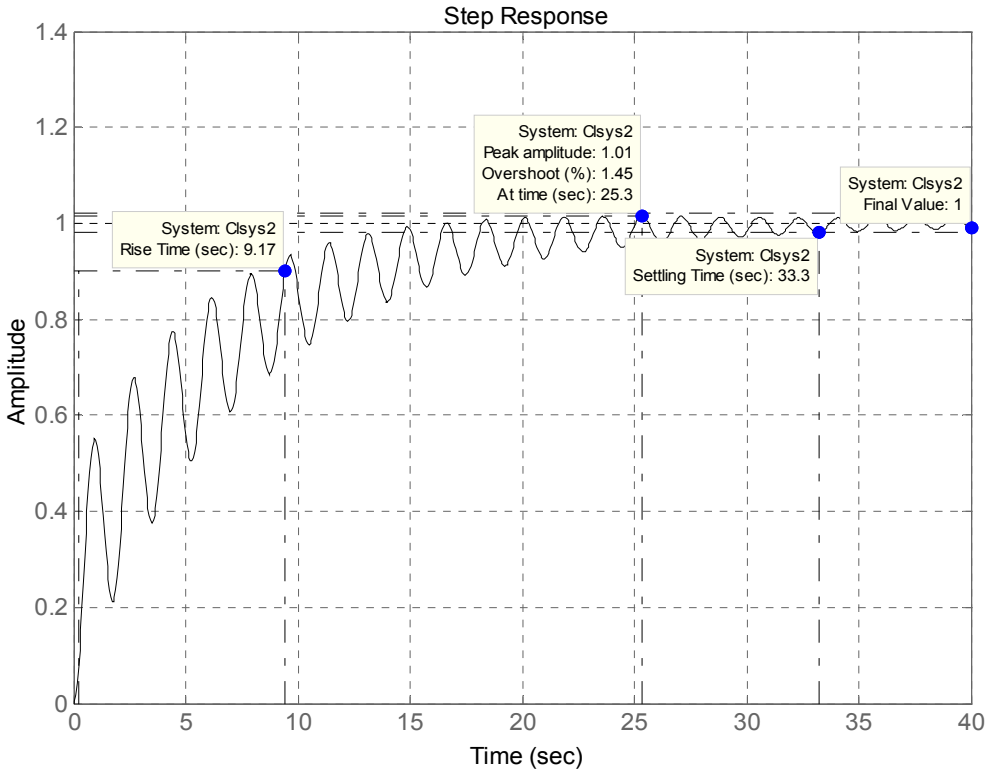

Figure 2.5. Step response of the closed loop system with PI compensator

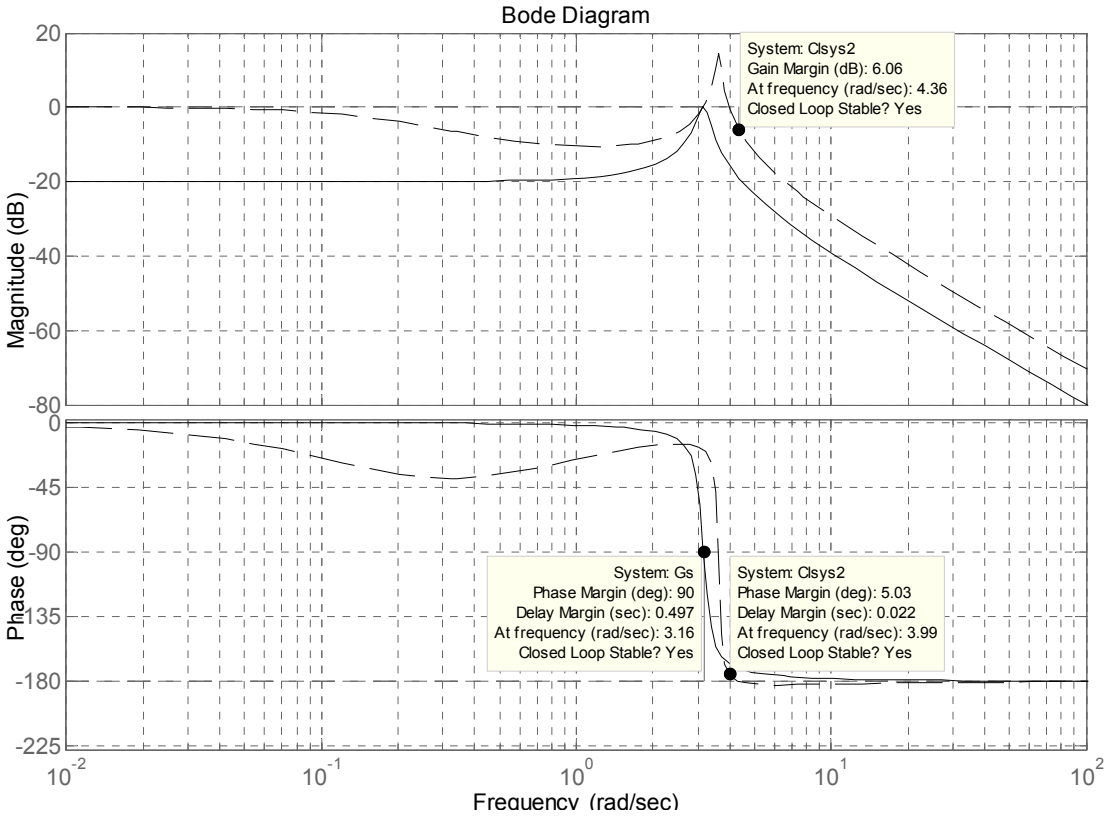

Figure 2.6. Bode plots of the plant and closed loop system with PI compensator

In PI control without changing the rigidity of the structure, i.e using smaller gains for k_p it is possible to track a step response. For k_p=3 and k_t=2, Figure 2.5 shows the response of the example SDOF system to step command. It is evident that although closed-loop steady-state error is brought to zero, the settling time and the large number of oscillations of the plant are unaffected. The overshoot on the hand is reduced to only %1.45. The Bode plots of the plant and the closed-loop system are shown in Figure 2.6. DC gain of the plant which is defined as $\lim_{\omega\to 0} G(iw)$ was -20 dB however; DC gain of the closed-loop system was brought to zero, indicating that step response will have a zero steady-state error. The PI compensator increases the gain, while decreasing the phase. The gain margin of the plant is infinity, whereas the gain margin of the closed-loop system is decreased to 6.06 dB and phase margin to 5.03°. Smaller gain margin indicates that further increasing the gain will cause instability in the closed-loop system. Thus, it can be concluded from the degrees of both phase and gain margins of the closed-loop system with respect to the plant PI compensator not only results in a highly oscillatory response, but also a significant loss in robustness.

2.3.10. Proportional-Integral-Derivative compensation (PID)

By including a derivative term to controller, transfer function of the controller becomes:

$$H(s) = k_p + \frac{k_t}{s} + k_D s \tag{2.63}$$

Transfer function of the closed loop system from reference command, *R(s)* to output, *Y(s)* can be written as:

$$\frac{Y(s)}{R(s)} = \frac{G(s)(k_p + k_t/s + k_D s)}{1 + G(s)(k_p + k_t/s + k_D s)} \tag{2.64}$$

Combination of Equation (2.53) with Equation (2.64), gives:

$$\frac{Y(s)}{R(s)} = \frac{k_D s^2 + k_p s + k_t}{s(s^2 + (2\zeta_s \omega_0 + k_D)s + (\omega_0^2 + k_p)) + k_t} \tag{2.65}$$

It is clear from Equation (2.65) that in PID control the k_D term directly effects the damping of the structure. For k_p=2, k_t=10, and k_D=4 the resulting closed-loop step response is plotted in Figure 2.7. The settling time of 3.79 seconds is very small when compared to 24.4 seconds settling time of the plant. Steady-state error and overshoot is zero and no high frequency oscillations are seen in the step response. The performance is thus greatly improved by the PID compensation.

When we examine the Bode plot of the closed-loop system from Figure 2.8, we see that closed loop gain margin and phase margin are infinite. In short, PID compensated closed-loop system has a good combination of performance and stability robustness. However, due to an increased closed-loop gain at high frequencies, there is an increased sensitivity, thus decreased robustness with respect to high frequency measurement noise, which is undesirable.

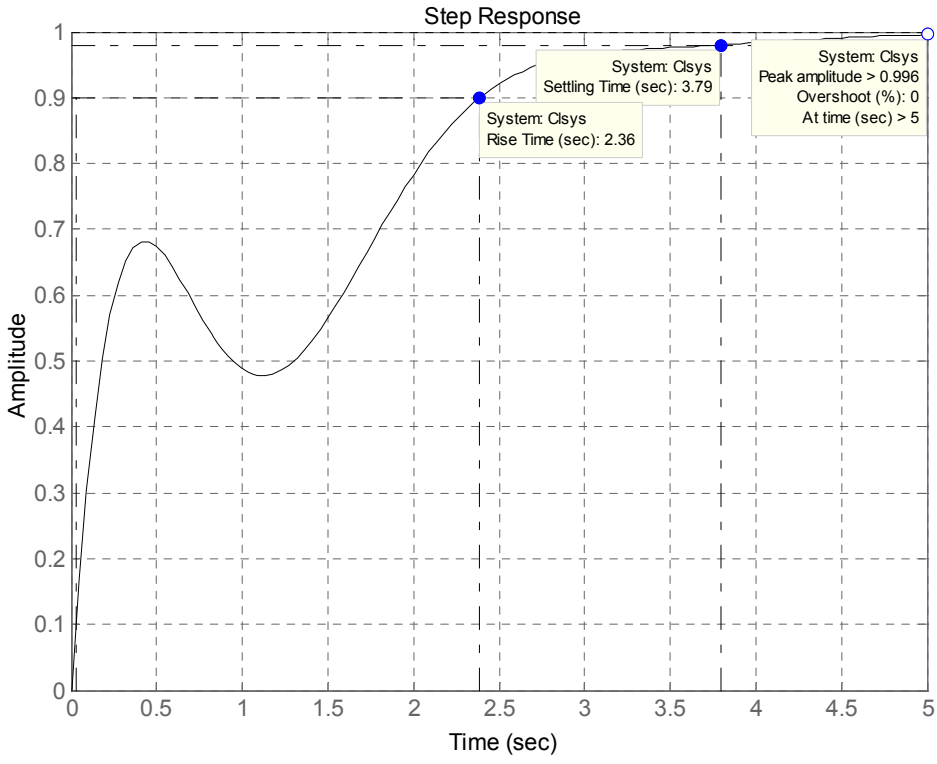

Figure 2.7. Step response of the closed loop system with PID compensator

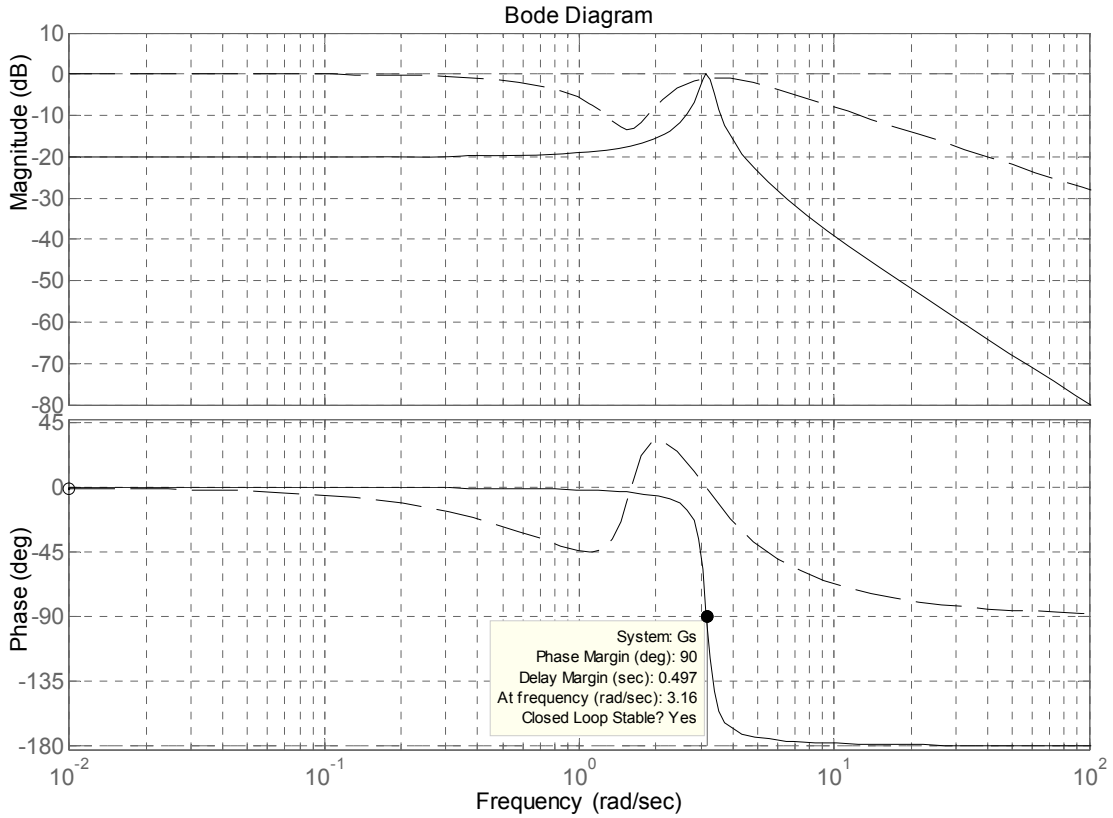

Figure 2.8. Bode plots of the plant and closed loop system with PID compensator

Performance of the closed loop system (controlled system) can be assessed by inspecting the response plots and can be decided if the response characteristics in terms of rise time, max over shoot, settling time and steady state error meet the design requirements. The process of finding suitable PID constants k_D, k_p and k_t is called PID tuning. Often, PID tuning in trying to achieve desirable closed-loop characteristics is an iterative procedure. On the other hand performance of a control system can be quantified by a cost function. A cost function is, in general, a real-valued, non-negative function of the system, or of the time histories of the state, reference output, and control input, subject to a given set of initial conditions and inputs. The cost (the real number resulting from application of the cost function) can be used to evaluate the performance of the system, where superior performance is indicated by a smaller cost [133].

2.3.11. Quadratic Cost Functions

The main objective of a controller is to minimize the output errors which are defined as the errors between the outputs and reference inputs. On the other hand another objective of the controller is to realize this minimization with minimum control effort. In general, there is a one to one correspondence between performance and control effort. Better performance is usually end up with a tighter control. Therefore, a control design is a compromise between performance and control effort. That is why; a cost function should include a measure of both the size of the output errors and the size of the control. A typical cost function is:

$$J = \int_0^{t_f} e^T(t)Z(t)e(t) + u^T(t)R(t)u(t)dt \tag{2.66}$$

Where t_f is the final time, *e(t)* is the output error and *u(t)* is the controller output. The positive definite matrix functions of time *Z(t)* and *R(t)* are the weighting functions. The output error can be written as:

$$e(t) = r(t) - Cx(t) \tag{2.67}$$

where x(t) is the state of the system and C is the output matrix in state space. The contribution of D matrices to output is assumed to be zero. Then the cost function becomes:

$$J = \int_0^{t_f} \{r(t) - Cx(t)\}^T Z(t)\{r(t) - Cx(t)\} + u^T(t)R(t)u(t)dt \tag{2.68}$$

If the reference input is zero, the control system is called regulator in which controller is trying to drive the controlled states to zero. Then setting r(t)=0 the quadratic cost function of a regulator can be written as:

$$J = \int_0^{t_f} x^T(t)Q(t)x(t) + u^T(t)R(t)u(t)dt \tag{2.69}$$

where, Q(t) is a positive semidefinite matrix and defined as,

$$Q(t) = C_e^T Z(t) C_e \tag{2.70}$$

The quadratic cost is dependent on the reference input applied, the disturbance input applied, the initial conditions, the final conditions, and/or constraints on the state and control. Collectively these inputs, conditions, and constraints are known as the test conditions. The test conditions may be simplified to yield information on the effects of one initial condition or the effects of one disturbance input. Performance is also evaluated for simple test conditions, which include step inputs, impulse inputs, and initial conditions and so on. The quadratic cost can be computed by direct integration of the output error and control trajectories that result when the test conditions are applied to the system [133].

For the example SDOF system, if we choose our objectives as

- The output error should be less than 0.1
- The control input should be less than 20

The cost function can be calculated as:

$$J = \frac{1}{20}\int_0^{10} \frac{1}{0.1^2} e^2(t) + \frac{1}{20^2} u^2(t) dt \tag{2.71}$$

The factor 1/10 is used to normalize the cost with respect to the integration time, a factor 1/2 is used to normalize the cost with respect to the number of terms within the integral, factor $1/0.1^2$ is used to normalize the desired size of the error to 1 and factor $1/20^2$ is used to normalize the desired size of the control.

The test conditions consist of a step input and the cost is calculated as J=0.8428. Since the cost is smaller than 1, the design objectives are met with this controller. This is also visible in Figure 2.9 that except for the transient response the response is below the specified values. If we set the final time as 1 second, than the calculated cost is J=5.2896.

That is expected since during transient response design specifications are not met by the controller.

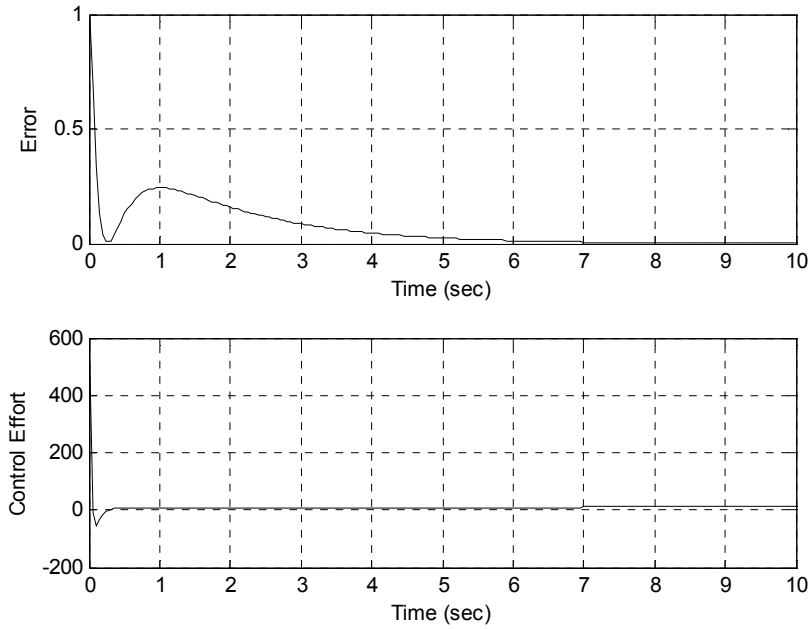

Figure 2.9. The error and control output for example case

Table 2.1. The cost for various controller types and test conditions

Controller Type	Controller Parameters			J	
	k_p	k_t	k_D	Step Input	Sine Input
PI	15	5	0	7,4647	3,1523
PI	25	2	0	7,1650	1,6387
PD	15	0	5	8,1287	1,6216
PD	20	0	10	5,5809	0,8309
PD	30	0	20	3,1527	0,3257
PID	15	10	5	1,3543	1,8254
PID	20	15	10	0,8428	1,0090
PID	25	20	15	0,6204	0,6253
PID	30	25	20	0,5009	0,4219

All in all, the cost function provides a measure of performance depending on the plant, controller and test conditions. In Table 2.1 cost is calculated for various controllers and for two test conditions. If a test condition is a step input the best performance is

obtained with a PID controller and for harmonic inputs best performance is achieved with a PD controller. A control design is to choose best performance controller for a given plant and test conditions. A control law that minimizes a cost function is termed optimal control. In contrast to trial and error based PID control optimal control allows us to directly formulate the performance objectives of a controlled system.

3. OPTIMAL LINEAR CONTROL

3.1. General State Space Model

In Figure 3.1 a general feedback control system is shown where, *w(t)* is the disturbance input vector, *r(t)* is the reference input vector which specifies the desired behavior of some or all plant outputs, *u(t)* is vector of inputs to the plant that are generated by the controller, *y(t)* is the vector of plant outputs and *m(t)* is the vector of plant outputs that are directly measured.

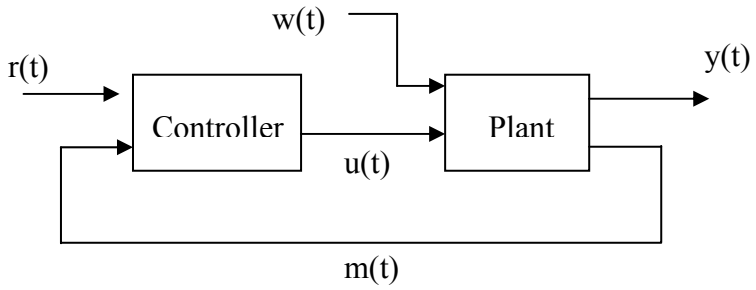

Figure 3.1. A general Closed Loop system

The state model for the plant can be written as:

$$\dot{x}(t) = Ax(t) + \begin{bmatrix} B_u & B_w \end{bmatrix} \begin{bmatrix} u(t) \\ w(t) \end{bmatrix} \tag{3.1}$$

$$\begin{bmatrix} m(t) \\ y(t) \end{bmatrix} = \begin{bmatrix} C_m \\ C_y \end{bmatrix} x(t) + \begin{bmatrix} 0 & D_{mw} \\ D_{yu} & D_{yw} \end{bmatrix} \begin{bmatrix} u(t) \\ w(t) \end{bmatrix} \tag{3.2}$$

Disturbance inputs to the plant are associated with B_w part of the input matrix and the controller output is associated with B_u part of the input matrix. The terms D_{mw} and D_{yw} stands for the measurement errors which can be interpreted as a disturbance input that effect measured output and plant output respectively. The term D_{yu} is used if there is an input-to-output coupling between the control input and the plant output. Similarly the state model of the controller can be written as.

$$\dot{x}_c(t) = A_c x_c(t) + \begin{bmatrix} B_{cr} & B_{cm} \end{bmatrix} \begin{bmatrix} r(t) \\ m(t) \end{bmatrix} \tag{3.3}$$

$$u(t) = C_c x_c(t) + \begin{bmatrix} D_{cr} & D_{cm} \end{bmatrix} \begin{bmatrix} r(t) \\ m(t) \end{bmatrix} \tag{3.4}$$

A state model of the closed loop system is obtained by combining the state model of the plant with the state model of the controller.

$$\begin{bmatrix} \dot{x}(t) \\ \dot{x}_c(t) \end{bmatrix} = \begin{bmatrix} A & 0 \\ 0 & A_c \end{bmatrix} \begin{bmatrix} x(t) \\ x_c(t) \end{bmatrix} + \begin{bmatrix} B_u \\ 0 \end{bmatrix} u(t) + \begin{bmatrix} B_w \\ 0 \end{bmatrix} w(t) + \begin{bmatrix} 0 \\ B_{cr} \end{bmatrix} r(t) + \begin{bmatrix} 0 \\ B_{cm} \end{bmatrix} m(t) \tag{3.5}$$

Since the control input is the output of the controller by appending Equation (3.4) into Equation (3.5) and combining like terms we obtain:

$$\begin{bmatrix} \dot{x}(t) \\ \dot{x}_c(t) \end{bmatrix} = \begin{bmatrix} A & B_u C_c \\ 0 & A_c \end{bmatrix} \begin{bmatrix} x(t) \\ x_c(t) \end{bmatrix} + \begin{bmatrix} B_w \\ 0 \end{bmatrix} w(t) + \begin{bmatrix} B_u D_{cr} \\ B_{cr} \end{bmatrix} r(t) + \begin{bmatrix} B_u D_{cm} \\ B_{cm} \end{bmatrix} m(t) \tag{3.6}$$

The measured output is given by Equation (3.2). Adding into Equation (3.6) and combining like terms yields:

$$\begin{bmatrix} \dot{x}(t) \\ \dot{x}_c(t) \end{bmatrix} = \underbrace{\begin{bmatrix} A + B_u D_{cm} C_m & B_u C_c \\ B_{cm} C_m & A_c \end{bmatrix}}_{A_{cl}} \begin{bmatrix} x(t) \\ x_c(t) \end{bmatrix} + \underbrace{\begin{bmatrix} B_w + B_u D_{cm} D_{mw} \\ B_{cm} D_{mw} \end{bmatrix}}_{B_{clw}} w(t) + \underbrace{\begin{bmatrix} B_u D_{cr} \\ B_{cr} \end{bmatrix}}_{B_{clr}} r(t) \tag{3.7}$$

or in a compact form:

$$\begin{bmatrix} \dot{x}(t) \\ \dot{x}_c(t) \end{bmatrix} = \underbrace{\begin{bmatrix} A + B_u D_{cm} C_m & B_u C_c \\ B_{cm} C_m & A_c \end{bmatrix}}_{A_{cl}} \begin{bmatrix} x(t) \\ x_c(t) \end{bmatrix} + \underbrace{\begin{bmatrix} B_u D_{cr} & B_w + B_u D_{cm} D_{mw} \\ B_{cr} & B_{cm} D_{mw} \end{bmatrix}}_{B_{cl}} \begin{bmatrix} r(t) \\ w(t) \end{bmatrix} \tag{3.8}$$

where A_{cl} is the state matrix and B_{cl} is the input matrix of the closed loop system. The output of the closed loop system is the plant output *y(t),* which can be written from Equation (3.2) as:

$$y(t) = C_y x(t) + D_{yu} u(t) + D_{yw} w(t) \tag{3.9}$$

Since the control input is the output of the controller, Equation (3.9) yields:

$$y(t) = C_y x(t) + D_{yu}\left\{C_c x_c(t) + D_{cr} r(t) + D_{cm} m(t)\right\} + D_{yw} w(t) \tag{3.10}$$

Substituting for m(t) using Equation (3.2) and rearranging the terms gives:

$$y(t) = C_y x(t) + D_{yu} C_c x_c(t) + D_{yu} D_{cr} r(t) + D_{yu} D_{cm}\left\{C_m x(t) + D_{mw} w(t)\right\} + D_{yw} w(t) \tag{3.11}$$

Combining the terms yields:

$$y(t) = \underbrace{\begin{bmatrix} C_y + D_{yu} D_{cm} C_m & D_{yu} C_c \end{bmatrix}}_{C_{cl}} \begin{bmatrix} x(t) \\ x_c(t) \end{bmatrix} + \underbrace{\begin{bmatrix} D_{yw} + D_{yu} D_{cm} D_{mw} \end{bmatrix}}_{D_{clw}} w(t) + \underbrace{\begin{bmatrix} D_{yu} D_{cr} \end{bmatrix}}_{D_{clr}} r(t) \tag{3.12}$$

where for the closed loop system C_{cl} is the output matrix, D_{clw} and D_{clr} are the input-to-output coupling matrices for disturbance and reference input respectively.

3.2. The Linear Quadratic Regulator (LQR)

3.2.1. LQR as a Regulator Problem

In classical linear optimal control, the control vector *u(t)* is to be chosen in such a way that a performance index *J* is minimized. Performance index in quadratic form is written as:

$$J = \frac{1}{2}\int_0^{t_f} x^T(t)Q(t)x(t) + u^T(t)R(t)u(t)dt \tag{3.13}$$

In which the time interval $[0,t_f]$ is defined to be longer than the external excitation, Q is a positive semi-definite matrix, and R is positive definite matrix. The magnitudes of the elements of the weighting matrices Q and R represent the relative importance between the structural response quantities and the control force. If the elements of Q matrix are large structural response will be reduced rapidly but at the expense of large control forces. On the other hand, if the element of R is large, the control force will be small, but the structural response may not be reduced significantly. The designers aim is to find optimum case between structural response and required control force by selecting the relative magnitudes of Q and R.

This optimal control problem is a constrained minimization problem since the state equation given by Equation (3.1) is a constraint on the state and the control. The optimal control problem can be converted to an unconstrained optimization problem of higher dimension by the application of Langrange multipliers.

For a problem of minimizing J(x) which is subjected to the constraint

$$c(x) = 0 \tag{3.14}$$

Equation (3.13) specifies a surface in the space of x. Necessary condition for optimality of J at a point x^* are that x^* satisfies Equation (3.14) and that the directional derivative of J at x^* equals zero in all directions along the surface. This second condition is satisfied if the gradient of J is normal to the surface at x^*. Since the gradient of $c(x)$ is normal to the surface at all points, including x^*, the second condition is satisfied if the gradient of J is parallel to the gradient of $c(x)$ at x^*, or equivalently,

$$\frac{\delta J(x^*)}{\delta x} + p\frac{\delta c(x^*)}{\delta x} = 0 \tag{3.15}$$

For some scalar p, Equations (3.14) and (3.15) form a set of necessary conditions for a solution of the constrained optimization problem. This set of necessary conditions can be generated as the solution to an unconstrained optimization problem with the following cost function:

$$J_a(x,p) = J(x) + pc(x) \tag{3.16}$$

Taking the gradient of J_a with respect to x yields Equation (3.15) and taking the derivative of J_a with respect to p yields Equation (3.14). The parameter p is called the Lagrange multiplier. Similarly, the optimal control problem subjected to constraint given by state equation can be converted to unconstrained optimization problem by writing augmented cost function as:

$$\begin{aligned} &J_a(x(t),u(t),p(t)) \\ &= \int_0^{t_f} \left\{ \frac{1}{2} x^T(t) Q(t) x(t) + \frac{1}{2} u^T(t) R(t) u(t) + p^T(t)\left[Ax(t) + B_u u(t) - \dot{x}(t) \right] \right\} dt \end{aligned} \tag{3.17}$$

The augmented cost function is a function of the state *x(t)*, the control *u(t)*, and the Lagrange multiplier or costate *p(t)*.

The function *J(x)* has a local minimum at x^* if and only if

$$J(x^* + \delta x) \geq J(x^*) \tag{3.18}$$

for all δx sufficiently small. An equivalent statement is that

$$\Delta J(x^*, \delta x) = J(x^* + \delta x) - J(x^*) \geq 0 \tag{3.19}$$

The term $\Delta J(x^*, \delta x)$ is called the increment of J. The optimal control is found by forming the increment of J_a with respect to the state, the control, and the costate. This is formulized as:

$$\begin{aligned}
&\Delta J_a(x,u,p,\delta x,\delta u,\delta p) = J_a(x+\delta x,u+\delta u,p+\delta p) - J_a(x,u,p)\\
&= \int_0^{t_f} \left\{ \begin{aligned} &\frac{1}{2}(x+\delta x)^T Q(x+\delta x) + \frac{1}{2}(u+\delta u)^T R(u+\delta u) \\ &+ (p+\delta p)^T \left[A(x+\delta x) + B_u(u+\delta u) - (\dot{x}+\dot{\delta x})\right] \end{aligned} \right\} dt \\
&- \int_0^{t_f} \left\{ \frac{1}{2} x^T Q x + \frac{1}{2} u^T R u + p^T \left[Ax + B_u u - \dot{x}\right] \right\} dt
\end{aligned} \tag{3.20}$$

Expanding the expression and grouping the terms yields:

$$\begin{aligned}
\Delta J_a &= \int_0^{t_f} \left\{ \frac{1}{2}\delta x^T Q \delta x + \frac{1}{2}\delta u^T R \delta u + \delta p^T \left[A\delta x + B_u \delta u - \dot{\delta x}\right] \right\} dt \\
&+ \int_0^{t_f} \left\{ x^T Q \delta x + u^T R \delta u + \delta p^T \left[Ax + B_u u - \dot{x}\right] + p^T \left[A\delta x + B_u \delta_u - \dot{\delta x}\right] \right\} dt
\end{aligned} \tag{3.21}$$

When dealing with a functional, δx is called the variation of *x*, and the term in the increment that is linear in δx is called the variation of *J* and is denoted $\delta J(x^*, \delta x)$. A necessary condition for x^* to be a local minimum is the variation of *J* is zero at x^* for all δx. Similarly, a necessary condition for the trajectory *x(t)*, *p(t)*, and *u(t)* to be minimum is that the variation of J_a equals zero:

$$\delta J_a(x,u,p,\delta x,\delta u,\delta p) = \int_0^{t_f} \left\{ \begin{aligned} &(x^T Q + p^T A)\delta x + (u^T R + p^T B_u)\delta u \\ &+ \delta p^T \left[Ax + B_u u - \dot{x}\right] - p^T \dot{\delta x} \end{aligned} \right\} dt = 0 \tag{3.22}$$

$\dot{\delta x}(t)$ is a function of $\delta x(t)$, so by integration by parts the last term in the integral can be written as:

$$\int_0^{t_f} p^T(t)\dot{\delta x}(t)dt = p^T(t_f)\delta x(t_f) - p^T(0)\delta x(0) - \int_0^{t_f} \dot{p}^T(t)\delta x(t)dt \tag{3.23}$$

The initial condition on the state is fixed, so $\delta x(0) = 0$. Substituting Equation (3.23) into Equation (2.22) and grouping the terms yields:

$$\delta J_a(x,u,p,\delta x,\delta u,\delta p) = -p^T(t_f)\delta x(t_f) + \int_0^{t_f}\left\{(x^TQ + p^TA + \dot{p}^T)\delta x + (u^TR + p^TB_u)\delta u + \delta p^T\left[Ax + B_u u - \dot{x}\right]\right\}dt = 0 \tag{3.24}$$

Since the variations $\delta x(t_f)$, δx, δu and δp are all arbitrary, Equation (3.20) can be zero if:

$$\dot{p}^T(t) = -x^T(t)Q - p^T(t)A \tag{3.25}$$

$$u(t) = -R^{-1}B_u{}^T p(t) \tag{3.26}$$

where the inverse is guaranteed to exist since *R* is positive definite. Equations (3.1), (3.25) and (3.26) provides the optimal solution for *x(t)*, *u(t)* and *p(t).* The optimal solution is unique since the cost function is quadratic. Quadratic functions have only a single critical point, which is either a global maximum or minimum. The fact that this critical point yields a global minimum results from the positivity requirements on the weighting matrices.

When the control vector is regulated by the state vector, one has:

$$p(t) = P(t)x(t) \tag{3.27}$$

By taking the derivative of *p(t)* we obtain:

$$\dot{p}(t) = \dot{P}(t)x(t) + P(t)\dot{x}(t) \tag{3.28}$$

The unknown matrix *P(t)* can be determined by substituting $\dot{p}(t)$ and $\dot{x}(t)$ from Equation (3.25), and Equation (3.26)

$$\dot{P}(t) = -P(t)A - A^TP(t) - Q + P(t)B_uR^{-1}B_u{}^TP(t),\ P(t_f) = 0 \tag{3.29}$$

Equation (3.29) is the Riccati matrix equation and *P(t)* is the Riccati matrix.

For building structures extensive experience indicates that the Riccati matrix *P(t)* remains constant over the entire duration of earthquake excitation and it drops rapidly to zero near t_f. As a result, the effectiveness of the control system is not affected, when the Riccati matrix is approximated by a constant matrix [134]. Then Riccati equation (3.29) reduces to:

$$PA + A^T P - PB_u R^{-1} B_u{}^T P + Q = 0,\ P(t_f) = 0 \tag{3.30}$$

The control gain *G(t)* is also constant with

$$G = -R^{-1} B_u{}^T P,\ P(t_f) = 0 \tag{3.31}$$

which can be precalculated for a given structure and with prescribed weighting matrices *Q* and *R*.

3.2.2. LQR as a Tracking Problem

Originally the LQR controller is a regulator which aims returning a system to its zero state in some optimal fashion. However LQR controller can be modified to generate tracking systems in which the outputs of a system track a desired trajectory in some optimal sense. When an output y of a control system is desired to track a trajectory $\tilde{y}$, it is clear that there should be a cost term in the performance index involving the error $(y - \tilde{y})$. A performance index in such a manner could be written as:

$$J = \int_0^{t_f} ((y - \tilde{y})^T Z (y - \tilde{y}) + u^T R u) dt \tag{3.32}$$

If we write the state equations for the plant as:

$$\dot{x} = Ax + Bu \tag{3.33}$$

$$y = C_y x \tag{3.34}$$

also defining incoming reference signal $\tilde{y}$ as an output of a known linear reference model such as:

$$\dot{z} = Fz \tag{3.35}$$

$$\tilde{y} = Hz \tag{3.36}$$

If we define a new state as:

$$\hat{x} = \begin{bmatrix} x \\ z \end{bmatrix} \tag{3.37}$$

Then the state matrices for the augmented plant can be written as:

$$\hat{A} = \begin{bmatrix} A & 0 \\ 0 & F \end{bmatrix}, \ \hat{B} = \begin{bmatrix} B \\ 0 \end{bmatrix} \tag{3.38}$$

From Equation (3.32) the performance index can be expanded as:

$$J = \int_0^{t_f} \left(y^T Z y - \tilde{y}^T Z y - y^T Z \tilde{y} + \tilde{y}^T Z \tilde{y} + u^T R u \right) dt \tag{3.39}$$

By combining Equation (3.39) with Equations (3.34) and (3.36) we obtain:

$$J = \int_0^{t_f} \left(x^T C_y^T Z C_y x - z^T H^T Z C_y x - x^T C_y^T Z H z + z^T H^T Z H z + u^T R u \right) dt \tag{3.40}$$

If we define:

$$Q = C_y^T Z C_y$$

$$H^T (C_y^T)^{-1} Q = H^T (C_y^T)^{-1} C_y^T Z C_y = H^T Z C_y$$

$$Q (C_y)^{-1} H = C_y^T Z C_y (C_y)^{-1} H = C_y^T Z H$$

$$H^T (C_y^T)^{-1} Q (C_y)^{-1} H = H^T (C_y^T)^{-1} C_y^T Z C_y (C_y)^{-1} H = H^T Z H$$

By introducing the above definitions the cost function becomes:

$$J = \int_0^{t_f} \begin{pmatrix} x^T Q x - z^T H^T (C_y^T)^{-1} Q x - x^T Q (C_y)^{-1} H z \\ + z^T H^T (C_y^T)^{-1} Q (C_y)^{-1} H z + u^T R u \end{pmatrix} dt \tag{3.41}$$

and in matrix form:

$$\begin{bmatrix} x & z \end{bmatrix} \underbrace{\begin{bmatrix} Q & -Q(C_y)^{-1} H \\ -H^T (C_y^T)^{-1} Q & H^T (C_y^T)^{-1} Q (C_y)^{-1} H \end{bmatrix}}_{\hat{Q}} \begin{bmatrix} x \\ z \end{bmatrix} \tag{3.42}$$

It should be noted that $(C_y)^{-1}$ is not a square matrix, therefore its pseudo inverse is taken which is a matrix of the same dimensions as C_y^T so that, $C_y (C_y)^{-1} C_y = C_y$, $(C_y)^{-1} C_y (C_y)^{-1} = (C_y)^{-1}$ and $C_y (C_y)^{-1}$ and $(C_y)^{-1} C_y$ are Hermitian.

The variables and matrices are constructed in such a fashion that tracking problem converts in a standard regulator problem of minimizing quadratic cost function

$$J = \int_0^{t_f} \left(\hat{x}^T \hat{Q} \hat{x} + u^T R u \right) dt \tag{3.43}$$

subjected to constraint

$$\dot{\hat{x}} = \hat{A} \hat{x} + \hat{B} u \tag{3.44}$$

3.3. Robustness of Multivariable Control Systems

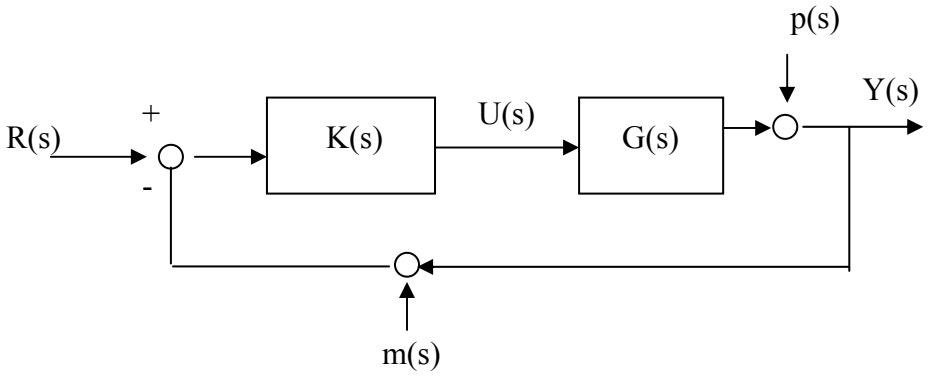

Figure 3.2. A multivariable feedback control system

Block diagram of a linear, time-invariant, multivariable feedback control system is shown in Figure 3.2. The control system consists of a feedback controller with transfer matrix, *K(s)*, and a plant with transfer matrix, *G(s)*, with desired output, *R(s)*. The process noise which is defined as the variations in the mathematical model of the plant, *p(s),* and measurement noise which is defined as the measurement errors, *m(s)* are present in the control system. The output, *Y(s)* can be expressed as [131]:

$$\begin{aligned} Y(s) &= \left[I + G(s)K(s)\right]^{-1} p(s) - \left\{I - \left[I + G(s)K(s)\right]^{-1}\right\} m(s) \\ &+ \left\{I - \left[I + G(s)K(s)\right]^{-1}\right\} R(s) \end{aligned} \tag{3.45}$$

while the control input, *U(s)*, can be expresses as [131]:

$$\begin{aligned} U(s) &= \left[I + K(s)G(s)\right]^{-1} K(s)R(s) - \left[I + K(s)G(s)\right]^{-1} K(s)p(s) \\ &- \left[I + K(s)G(s)\right]^{-1} K(s)m(s) \end{aligned} \tag{3.46}$$

From Equations (3.45) and (3.46), it is clear that the sensitivity of the output with respect to the process and measurement noise depends on the matrix $\left[I + G(s)K(s)\right]^{-1}$, while the sensitivity of the input to process and measurement noise depends upon the matrix $\left[I + K(s)G(s)\right]^{-1}$. The larger the elements of these matrices, the larger will be the sensitivity of the output and input to process and measurement noise. Since robustness is inversely proportional to sensitivity, robustness of the input is measured by the matrix

$[I + G(s)K(s)]$, called the return-difference matrix at the output, and the robustness of the input is measured by the matrix $[I + K(s)G(s)]$, called the return difference matrix at he plant input. Alternatively, we can define the return ratio matrices at the plant's output and input, as $G(s)K(s)$ and $K(s)G(s)$ respectively, and measure robustness properties in terms of return ratios rather than the return differences.

Rather than dealing with the two return ratio matrices, a scalar measure to robustness can be obtained by defining a spectral norm, such as:

$$\|M\|_s = \sigma_{\max} \tag{3.47}$$

where $\sigma_{\max}$ is the positive square-root of the maximum eigenvalue of the matrix $M^H M$. Here M^H denotes the Hermitian of M defined as the transpose of the complex conjugate of M. All positive square-roots of the eigenvalues of $M^H M$ are called the singular values of M.

The singular values help us analyze the properties of multivariable feedback system in a similar manner to a single-input, single-output feedback system. For example, to maximize robustness with respect to the process noise, it is clear from Equation 3.45 that we should minimize the singular values of the sensitivity matrix, $[I + G(s)K(s)]^{-1}$. This implies minimizing the largest singular value, $\sigma_{\max}\{[I + G(s)K(s)]^{-1}\}$, or maximizing the maximum values of the return difference matrix at the output, $\sigma_{\min}[I + G(s)K(s)]$. This is equivalent to maximizing the smallest singular value of the return ratio at the output, $\sigma_{\min}[G(s)K(s)]$. Similarly, the following conditions on the singular values of the return ratio at output result from robustness, optimal control and tracking requirements [131]:

- For robustness with respect to the process noise, $\sigma_{\min}[G(s)K(s)]$ should be maximized.
- For robustness with respect to the measurement noise, $\sigma_{\max}[G(s)K(s)]$ should be minimized.

- For optimal control, $\sigma_{\max}[K(s)]$ should be minimized.
- For tracking a changing desired output, $\sigma_{\min}[G(s)K(s)]$ should be maximized.

Clearly, the second requirement conflicts with the first and the fourth. Also, since $\sigma_{\max}[G(s)K(s)] \le \sigma_{\max}[G(s)]\sigma_{\max}[K(s)]$, the third requirement is in conflict with the first and the fourth. However, since measurement noise usually has predominantly high-frequency content, we achieve a compromise by minimizing $\sigma_{\max}[G(s)K(s)]$and $\sigma_{\max}[K(s)]$ at high frequencies, and maximizing $\sigma_{\min}[G(s)K(s)]$ at low frequencies. In this manner, good robustness properties, optimal control, and tracking system performance can be obtained throughout a given frequency range.

3.4. Signals and System Norms

3.4.3. Norms for Signals

1- Norm The 1-norm of a signal *u(t)* is the integral of its absolute value

$$\|u\|_1 := \int_{-\infty}^{\infty} |u(t)| dt \tag{3.48}$$

2- Norm The square of the 2-norm is called the energy of the signal. The 2-norm of a signal *u(t)* is

$$\|u\|_2 := \left(\int_{-\infty}^{\infty} u(t)^2 \, dt \right)^{1/2} \tag{3.49}$$

∞- Norm The ∞-norm of a signal *u(t)* is the least upper bound of its absolute value or in other words peak value of the signal

$$\|u\|_\infty := \sup_t |u(t)| \tag{3.50}$$

$\sup_{\omega}|.|$ is called the supreme function, and denotes the largest value of the function within the brackets encountered as the frequency, ω, is varied.

3.4.4. Norms for Systems

System norms are actually the input-output gains of the system. If we consider a linear, time-invariant system; the transfer function of such a system, *G(s)*, maps the input signal *U(s)* into the output signal *Y(s)*. We say that *G(s)* is stable if it is analytic in the closed right half plane *(Re s≥0),* proper if *G(j∞)* is finite (degree of denominator ≥ degree of numerator), strictly proper if *G(j∞)* =0 (degree of denominator > degree of numerator), and biproper if G(s) and $G^{-1}(s)$ are both proper (degree of denominator = degree of numerator). The norms for such a transfer function are given:

2- Norm

$$\|G(s)\|_2 := \left(\frac{1}{2\pi}\int_{-\infty}^{\infty}|G(j\omega|^2\, d\omega\right)^{1/2} \tag{3.51}$$

The 2-norm of *G(s)* is finite if and only if *G(s)* is strictly proper and has no poles on the imaginary axis. That is *D*=0 in a state space realization. Minimization of H_2 norm corresponds to minimizing the sum of the squares off all the singular values over all frequencies.

∞- Norm

$$\|G(s)\|_\infty := \sup_{\omega}|G(j\omega|| \tag{3.52}$$

The ∞-norm of *G(s)* equals to the distance in the complex plane from the origin to the farthest point on the Nyquist plot of *G(s)*. It is also the peak value on the Bode magnitude plot of *G(s)*. The 2-norm of *G(s)* is finite if and only if *G(s)* is proper and has no poles on the imaginary axis. That is *D*≠0 is allowed in a state space realization. An important property of the ∞-norm is that it is submultiplicative.

$$\|G(s)H(s)\|_\infty \le \|G(s)\|_\infty \|H(s)\|_\infty \tag{3.53}$$

Minimization of H_∞ norm corresponds to minimizing the peak of the largest singular value.

3.5. H_∞ Optimal Control

By specifying/grouping signals into sets of external inputs, outputs, input to the controller and output from controller, Figure 3.2 can be recast into a standard configuration as in Figure 3.3 in which all the external inputs such as process and measurement noise vectors are denoted by w(s) and output signals to be minimized/penalized are denoted by z(s), Y(s) is the vector of measurements available to the controller K(s) and U(s) is the vector of control signals. P(s) is called the generalized plant or interconnected system.

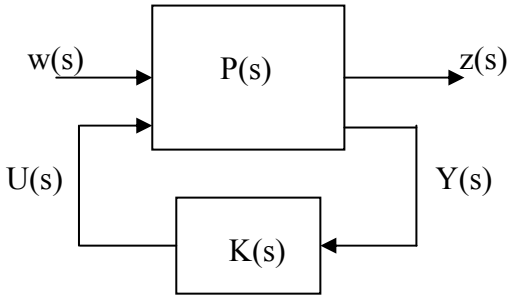

Figure 3.3. The standard H_∞ configuration

The plant's transfer matrix can be partitioned as follows:

$$P(s) = \begin{bmatrix} P_{11}(s) & P_{12}(s) \\ P_{21}(s) & P_{22}(s) \end{bmatrix} \tag{3.53}$$

such that

$$z(s) = P_{11}(s)w(s) + P_{12}(s)U(s) \tag{3.54}$$

and

$$Y(s) = P_{21}(s)w(s) + P_{22}(s)U(s) \tag{3.55}$$

Substituting the control law, $U(s) = K(s)Y(s)$, into Equations (3.54) and (3.55), we can write the following relationship between the error vector and the external inputs vector:

$$z(s) = \left[P_{11}(s) + P_{12}(s)K(s)(I - P_{22}(s)K(s))^{-1}P_{21}(s)\right]w(s) \tag{3.56}$$

The transfer matrix multiplying *w(s)* on the right hand side of Equation (3.56) can be denoted as *F(s)*. Then we can re-write Equation (3.56) as:

$$z(s) = F(s)w(s) \tag{3.57}$$

The H_∞ optimal control synthesis procedure consists of finding a stabilizing controller, *K(s)*, such that the H_∞*-norm* of the closed loop transfer matrix, *F(s)*, is minimized. Obtaining the H_∞*-norm* of a transfer matrix requires calculating the singular values of the transfer matrix with $s=i\omega$ at a range of frequencies, and then obtaining the maximum of the largest singular value over the given frequency range.

In Section 3.3, it was derived that the sensitivity of the output, *Y(s)* with respect to process noise depends upon the matrix $\left[I + K(s)G(s)\right]^{-1}$, which we call the sensitivity matrix of the output, *S(s)*. If a scalar value of this matrix is minimized, we can be assured of the robustness of the closed-loop system with respect to process noise. Such a scalar is the H_∞*-norm*. Thus, robust optimal control problem consists of finding a stabilizing controller, *K(s)* such that the H_∞*-norm* of the sensitivity matrix at the output, $\left\|S(i\omega)\right\|_\infty$ is minimized. In this case *F(s) = S(s)*. However, instead of minimizing $\left\|S(i\omega)\right\|_\infty$ over all frequencies, which will increase sensitivity to high-frequency measurement noise and poor stability margins, $\left\|S(i\omega)\right\|_\infty$ should be minimized over only frequencies where the largest magnitude of process noise occurs. This is practically achieved by defining a frequency

weighting matrix, *W(iω)* such that the largest singular value of *W(iω)* is close to unity in a specified frequency range, $0 \le \omega \le \omega_0$, and rapidly decay to zero for higher frequencies, $\omega > \omega_0$. The frequency, ω_0 is called cut-off frequency below which the sensitivity to process noise is to be minimized. The robust, optimal control problem is then solved by finding a stabilizing controller which minimizes $\|W(i\omega)S(i\omega)\|_\infty$. The H_∞-optimal control problem for a regulator is thus the weighted sensitivity problem.

It can be recalled from Section 3.3 that the requirements of robustness conflict with the requirements of optimal control and tracking performance. While robustness to process noise is obtained by minimizing the largest singular value of weighted sensitivity matrix, *S(s)*, optimal control requires minimizing the largest singular value of *K(s)S(s)*, and good tracking performance to a changing desired output requires maximizing the smallest singular value of the complementary sensitivity matrix, *T(s)=I-S(s)*. However, high-frequency measurement noise rejection requires minimizing the largest singular value of *T(s)* at high frequencies. Such conflicts can be resolved by choosing different frequency ranges for maximizing and minimizing different singular values. The different frequency ranges for the various optimizations can be specified as three frequency weighting matrices, $W_1(i\omega)$, $W_2(i\omega)$, and $W_3(i\omega)$ such that H_∞-norm of the mixed sensitivity matrix, $\|M(i\omega)\|_\infty$ is minimized where [131]

$$M(i\omega) = \begin{bmatrix} W_1(i\omega)S(i\omega) \\ W_2(i\omega)K(i\omega)S(i\omega) \\ W_3(i\omega)T(i\omega) \end{bmatrix} \tag{3.58}$$

Generally there are no analytic formulae for the solution of the mixed sensitivity optimization problem. In practical design, it is usually sufficient to find a stabilizing controller K(s) such that the H_∞-norm of the mixed sensitivity matrix, $\|M(i\omega)\|_\infty$ is less than a given positive number,

$$\|M(i\omega)\|_\infty < \gamma \tag{3.59}$$

where $\gamma > \gamma_0 := \min K_{stabilizing} \|M(i\omega)\|_\infty$. This is called the H_∞ suboptimal problem. An optimal solution is reached by iteratively reducing γ.

The state-state description of the generalized system *P(s)* in Figure3.3 can be given by:

$$\dot{x}(t) = Ax(t) + B_1 w(t) + B_2 u(t) \tag{3.60}$$

$$z(t) = C_1 x(t) + D_{11} w(t) + D_{12} u(t) \tag{3.61}$$

$$y(t) = C_2 x(t) + D_{21} w(t) \tag{3.62}$$

Equation (3.53) can be further denoted in state space as:

$$P = \left[\begin{array}{c|cc} A & B_1 & B_2 \\ \hline C_1 & D_{11} & D_{12} \\ C_2 & D_{21} & 0 \end{array}\right] \tag{3.63}$$

The necessary and sufficient conditions for the existence of an H_∞ suboptimal controller are [135]:

A1 (A,B_2) is stabilizable and (C_2, A) detectable;

A2 $D_{12} = \begin{bmatrix} 0 \\ I \end{bmatrix}$ and $D_{21} = \begin{bmatrix} 0 & I \end{bmatrix}$;

A3 $\begin{bmatrix} A - j\omega I & B_2 \\ C_1 & D_{12} \end{bmatrix}$ has full column rank for all ω;

A4 $\begin{bmatrix} A - j\omega I & B_1 \\ C_2 & D_{21} \end{bmatrix}$ has full row rank for all ω;

For the general control configuration of Figure 3.3, with assumptions (A1) to (A4), there exists a stabilizing controller K(s) such that $\|M(i\omega)\|_\infty < \gamma$ if and only if [132]

i. $X_\infty \geq 0$ is a solution to the algebraic Riccati equation

$$A^T X_\infty + X_\infty A + C_1^T C_1 + X_\infty(\gamma^{-2} B_1 B_1^T - B_2 B_2^T) X_\infty = 0 \tag{3.64}$$

such that Re $\lambda_i\left[A + (\gamma^{-2} B_1 B_1^T - B_2 B_2^T) X_\infty\right] < 0$, for all i, and

ii. $Y_\infty \geq 0$ is a solution to the algebraic Riccati equation

$$A Y_\infty + Y_\infty A^T + B_1 B_1^T + Y_\infty(\gamma^{-2} C_1^T C_1 - B_2^T B_2) Y_\infty = 0 \tag{3.65}$$

such that Re $\lambda_i\left[A + Y_\infty(\gamma^{-2} C_1^T C_1 - C_2^T C_2)\right] < 0$, for all i, and

iii. $\rho(X_\infty Y_\infty) < \gamma^2$

All such controllers are given by $K=F_t(K_c,Q)$ where

$$K_c(s) = \begin{bmatrix} A_\infty & -Z_\infty L_\infty & Z_\infty B_2 \\ F_\infty & 0 & I \\ -C_2 & I & 0 \end{bmatrix} \tag{3.66}$$

$$F_\infty = -B_2^T X_\infty, L_\infty = -Y_\infty C_2^T, Z_\infty = (I - \gamma^{-2} Y_\infty X_\infty)^{-1} \tag{3.67}$$

$$A_\infty = A + \gamma^{-2} B_1 B_1^T X_\infty + B_2 F_\infty + Z_\infty L_\infty C_2 \tag{3.68}$$

and Q(s) is any stable proper transfer function such that $\|Q\|_\infty < \gamma$

3.6. Numerical Illustrations

Let's consider a single-degree-of-freedom (SDOF) system with following structural parameters:

$k_s = 1.10^5$ kN/m
$c_s = 3{,}16.10^3$ kN/s (%5 damping)
$m_s = 1.10^4$ tons

Equation of motion for such a system is given by

$$m_s \ddot{y}(t) + c_s \dot{y}(t) + k_s y(t) = u(t) + w(t) \tag{3.69}$$

The state equations of the plant can be written as

$$\begin{bmatrix} \dot{x}_1 \\ \dot{x}_2 \end{bmatrix} = \begin{bmatrix} 0 & 1 \\ -10 & -0.32 \end{bmatrix} \begin{bmatrix} x_1 \\ x_2 \end{bmatrix} + \begin{bmatrix} 0 & 0 \\ 1 & -1 \end{bmatrix} \begin{bmatrix} w \\ u \end{bmatrix} \tag{3.70}$$

$$\begin{bmatrix} y_1 \\ y_2 \end{bmatrix} = \begin{bmatrix} 1 & 0 \\ 0 & 1 \end{bmatrix} \begin{bmatrix} x_1 \\ x_2 \end{bmatrix} \tag{3.71}$$

It should be noted that the excitation and control forces entered to system is normalized with the mass of the plant. The plant gives two outputs. First output is the first state which is the displacement of the mass and second output is the second state which is the velocity of the mass. In the following sections LQR and H-∞ optimal controllers will be designed for disturbance rejection (regulator problem) and for to track a command signal (tracking problem).

3.6.5. LQR Control of a SDOF System – Regulator Problem

Performance index in quadratic form is written as:

$$J = \frac{1}{2}\int_0^{t_f} x^T(t)Q(t)x(t) + u^T(t)R(t)u(t)dt \tag{3.72}$$

It is desired to regulate the both displacement and velocity states so the state weighting matrix, Q, and the control force weighting matrix, R, are selected as:

$$Q = \begin{bmatrix} 1 & 0 \\ 0 & 1 \end{bmatrix}, R = 0.1 \tag{3.73}$$

The corresponding control gain is calculated to be:

$$K_1 = \begin{bmatrix} 0.4881 & 3.0119 \end{bmatrix} \tag{3.74}$$

The system state vector is multiplied with control gain vector to produce control forces such as:

$$u = \begin{bmatrix} 0.4881 & 3.0119 \end{bmatrix} \begin{bmatrix} x_1 \\ x_2 \end{bmatrix} \tag{3.75}$$

The output of the controller is the input to the plant, so the state equation can be rewritten as:

$$\begin{bmatrix} \dot{x}_1 \\ \dot{x}_2 \end{bmatrix} = \begin{bmatrix} 0 & 1 \\ -10 & -0.32 \end{bmatrix} \begin{bmatrix} x_1 \\ x_2 \end{bmatrix} + \begin{bmatrix} 0 \\ 1 \end{bmatrix} w + \begin{bmatrix} 0 \\ -1 \end{bmatrix} \begin{bmatrix} 0.4881 & 3.0119 \end{bmatrix} \begin{bmatrix} x_1 \\ x_2 \end{bmatrix} \tag{3.76}$$

By collecting the state terms to the left hand side of the Equation (3.76), the closed loop system with negative feedback will be obtained as:

$$\begin{bmatrix} \dot{x}_1 \\ \dot{x}_2 \end{bmatrix} = \begin{bmatrix} 0 & 1 \\ -10.488 & -3.3281 \end{bmatrix} \begin{bmatrix} x_1 \\ x_2 \end{bmatrix} + \begin{bmatrix} 0 \\ 1 \end{bmatrix} w \tag{3.77}$$

Together with the system states we also require to see the control forces, so the output equation becomes:

$$\begin{bmatrix} y_1 \\ y_2 \\ u \end{bmatrix} = \begin{bmatrix} 1 & 0 \\ 0 & 1 \\ 0{,}4881 & 3.0119 \end{bmatrix} \begin{bmatrix} x_1 \\ x_2 \end{bmatrix} \tag{3.78}$$

The natural frequency of the plant is 3.16 rad/sec, damping factor is %5 and overshoot is %85. In the case of controlled plant the frequency is slightly shifted to 3.24 rad/sec and the damping is increased to %51.4. As can be seen from Figure 3.4, the overshoot in the controlled case is %15.2 and settling time is very much reduced to 2.44 sec which was 24 sec in the uncontrolled plant.

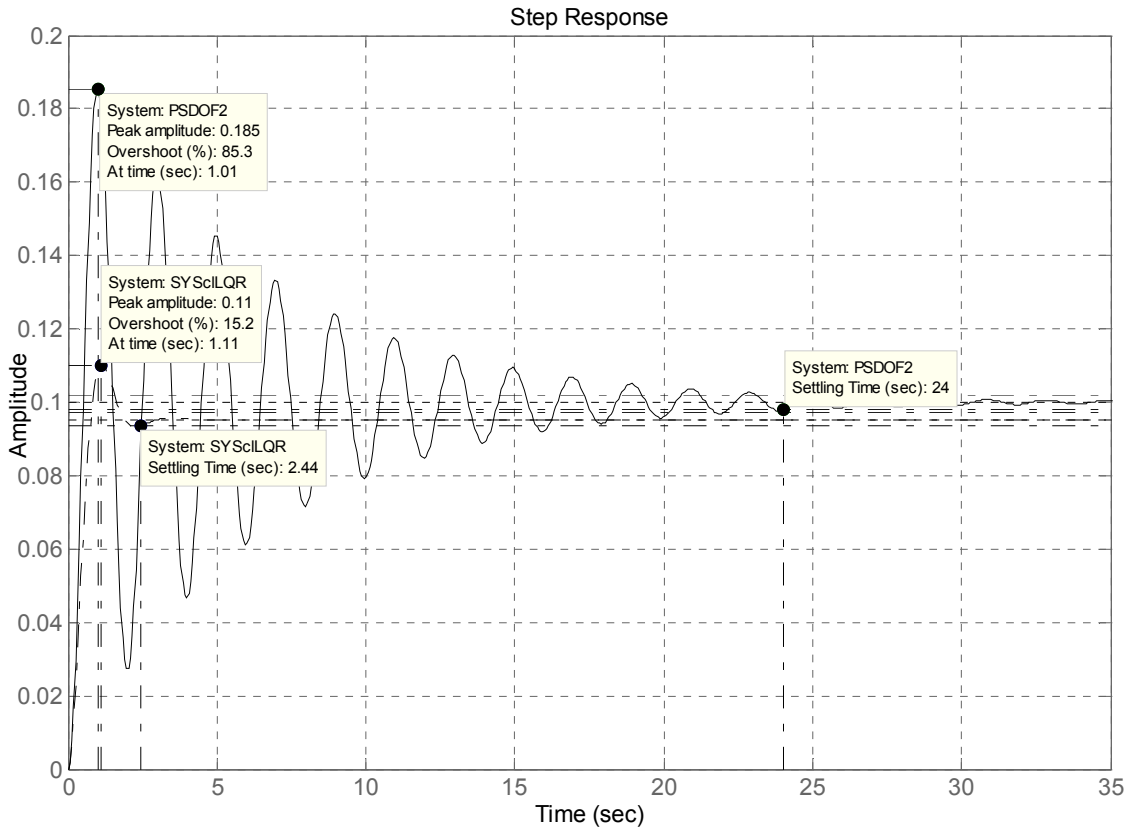

Figure 3.4. Step response of the plant and LQR closed loop system – regulator problem

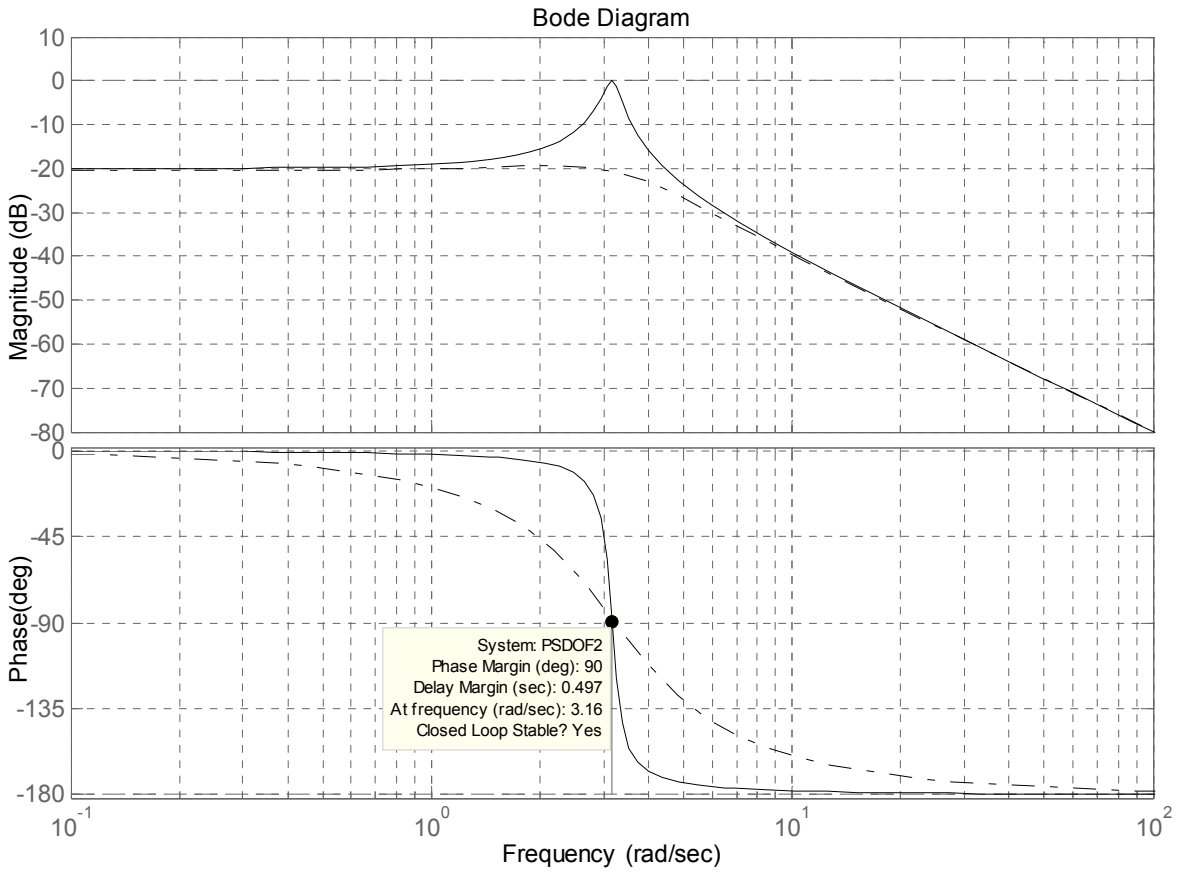

Figure 3.5. Bode plots of the plant and LQR closed loop system – regulator problem

The phase and gain margins are also infinity in the controlled plant which suggests that the LQR controller improves the robustness to time delays. Thus it can be concluded that LQR control is very effective in improving the time response and the robustness of the plant. To see the effect of weighting matrices on the response and control forces the control weighting matrices R_2=0.05 and R_3=0.01 are chosen. The corresponding control gains are calculated as:

$$K_2 = \begin{bmatrix} 0.9545 & 4.3751 \end{bmatrix} \tag{3.79}$$

$$K_3 = \begin{bmatrix} 4.1421 & 10.095 \end{bmatrix} \tag{3.80}$$

As can be viewed from K_1, K_2 and K_3 when the weights on control forces are reduced the elements of the controller gain matrix are increased. The reduction in control

weighting will give emphasis to performance so better time responses will be obtained in the expense of high control forces. This is illustrated in Figure 3.6, where the time responses and control forces are compared. It is seen that for small control weights the response is very much improved but as expected much higher control forces are required.

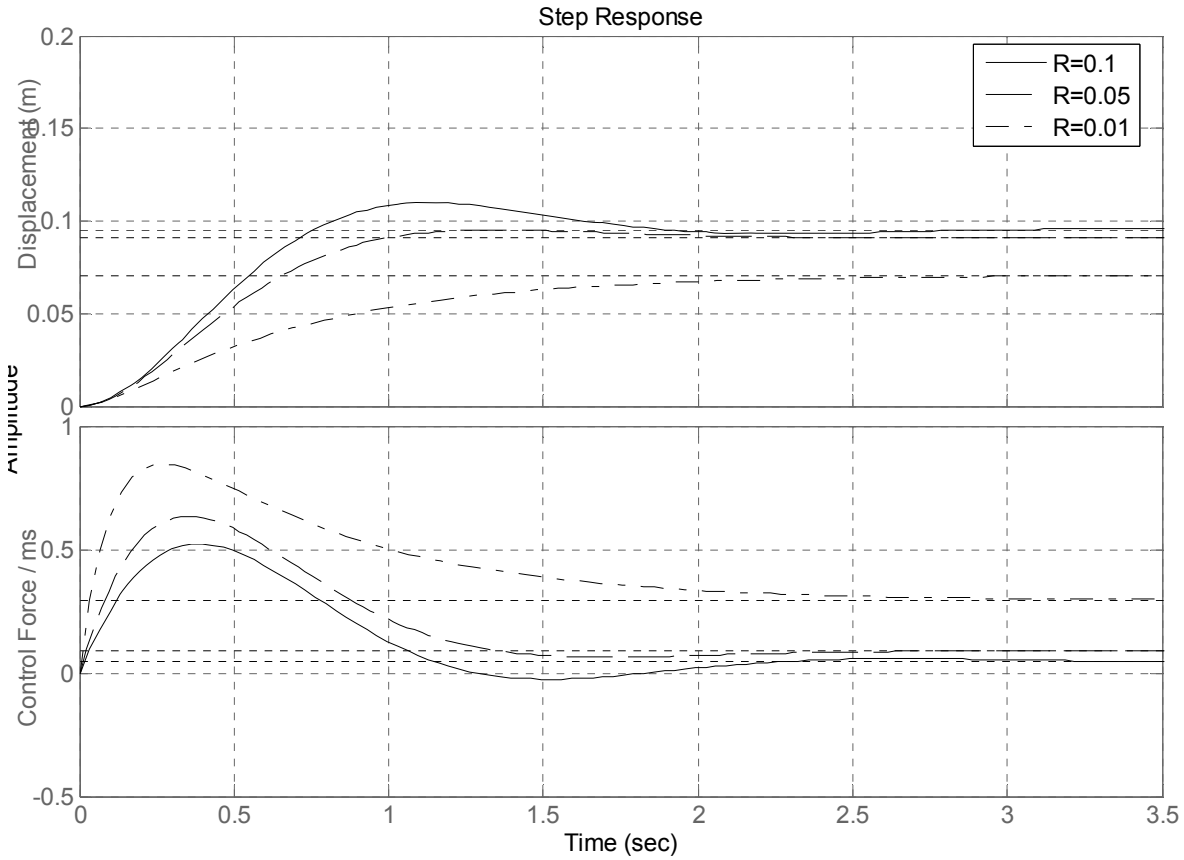

Figure 3.6. Comparison of displacement output and normalized control forces for various LQR control weights – regulator problem

3.6.6. LQR Control of a SDOF System – Tracking Problem

The displacement output of the plant in the example case is desired to track a sinusoidal signal with frequency 2 rad/sec and amplitude of 0.1m. In state space form linear reference model for the sinusoidal signal can be written as:

$$\begin{bmatrix} \dot{z}_1 \\ \dot{z}_2 \end{bmatrix} = \begin{bmatrix} 0 & 1 \\ -4 & 0 \end{bmatrix} \begin{bmatrix} z_1 \\ z_2 \end{bmatrix} \tag{3.81}$$

$$\tilde{y} = \begin{bmatrix} 1 & 0 \end{bmatrix} \tag{3.82}$$

where z and $\tilde{y}$ are the states and the output of the reference model. If we combine the states of the plant and the reference model the augmented plant is then:

$$\begin{bmatrix} \dot{x}_1 \\ \dot{x}_2 \\ \dot{z}_1 \\ \dot{z}_2 \end{bmatrix} = \begin{bmatrix} 0 & 1 & 0 & 0 \\ -10 & -0.316 & 0 & 0 \\ 0 & 0 & 0 & 1 \\ 0 & 0 & -4 & 0 \end{bmatrix} \begin{bmatrix} x_1 \\ x_2 \\ z_1 \\ z_2 \end{bmatrix} + \begin{bmatrix} 0 \\ 1 \\ 0 \\ 0 \end{bmatrix} u(t) \tag{3.83}$$

The state weighting matrix is selected as in the case of LQR regulator problem. Then the state weighting matrix for the augmented plant is calculated according to Equation (3.42) as:

$$\hat{Q} = \begin{bmatrix} 1 & 0 & -1 & 0 \\ 0 & 0 & 0 & 0 \\ -1 & 0 & -1 & 0 \\ 0 & 0 & 0 & 0 \end{bmatrix} \tag{3.84}$$

Utilizing $\hat{Q}$ and by taking R=0.1 the calculated LQR gain is as the following:

$$K = \begin{bmatrix} 0.4881 & 3.0119 & -3.7547 & -1.9260 \end{bmatrix} \tag{3.85}$$

As illustrated in Figure 3.6 the first two terms of the gain matrix K are associated with the states of the plant, and last two terms are associated with the states of the reference model. As can be viewed from the elements of controller gain, K, the feedback component, K_1, is identical with the standard LQR regulator problem and independent of the dynamics of the reference model, whereas feedforward component, K_2, is related to dynamics of the reference model. Thus optimal tracking problem is limited to known class of signals whose dynamics are described by a reference model.

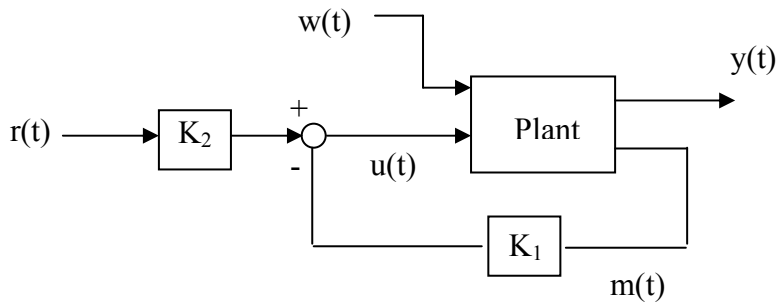

Figure 3.7. Arrangement of tracking system

The control input to the plant can be written as:

$$u(t) = K_1 m(t) + K_2 r(t) \tag{3.86}$$

and in matrix form:

$$u = \begin{bmatrix} 0.4881 & 3.0119 \end{bmatrix} \begin{bmatrix} x_1 \\ x_2 \end{bmatrix} + \begin{bmatrix} -3.7547 & -1.9260 \end{bmatrix} \begin{bmatrix} r_1 \\ r_2 \end{bmatrix} \tag{3.87}$$

The output of the controller is the input to the plant, so the state equation can be rewritten as:

$$\begin{bmatrix} \dot{x}_1 \\ \dot{x}_2 \end{bmatrix} = \begin{bmatrix} 0 & 1 \\ -10 & -0.32 \end{bmatrix} \begin{bmatrix} x_1 \\ x_2 \end{bmatrix} + \begin{bmatrix} 0 \\ 1 \end{bmatrix} w + \begin{bmatrix} 0 \\ -1 \end{bmatrix} \begin{bmatrix} 0.4881 & 3.0119 \end{bmatrix} \begin{bmatrix} x_1 \\ x_2 \end{bmatrix} + \begin{bmatrix} 0 \\ -1 \end{bmatrix} \begin{bmatrix} -3.7547 & -1.9260 \end{bmatrix} \begin{bmatrix} r_1 \\ r_2 \end{bmatrix} \tag{3.88}$$

When we collect the state terms the closed loop system with negative feedback will be:

$$\begin{bmatrix} \dot{x}_1 \\ \dot{x}_2 \end{bmatrix} = \begin{bmatrix} 0 & 1 \\ -10.488 & -3.3281 \end{bmatrix} \begin{bmatrix} x_1 \\ x_2 \end{bmatrix} + \begin{bmatrix} 0 \\ 1 \end{bmatrix} w + \begin{bmatrix} 0 \\ -1 \end{bmatrix} \begin{bmatrix} -3.7547 & -1.9260 \end{bmatrix} \begin{bmatrix} r_1 \\ r_2 \end{bmatrix} \tag{3.89}$$

or in compact form:

$$\begin{bmatrix} \dot{x}_1 \\ \dot{x}_2 \end{bmatrix} = \begin{bmatrix} 0 & 1 \\ -10.488 & -3.3281 \end{bmatrix} \begin{bmatrix} x_1 \\ x_2 \end{bmatrix} + \begin{bmatrix} 0 & 0 & 0 \\ 1 & 3.7547 & 1.9260 \end{bmatrix} \begin{bmatrix} w \\ r_1 \\ r_2 \end{bmatrix} \tag{3.90}$$

As can be seen from Equation (3.90), tracking system is not a single-input-single-output system anymore. Together with the external disturbance, w, the displacement, r_1, and velocity, r_2, information of the reference signal is needed. Thus evaluating performance in terms of step response is meaningless, that is why performance in time domain will be checked in terms of displacement error, $e = y_1 - r_1$. So the output equation in terms of displacement and control forces becomes:

$$\begin{bmatrix} e \\ u \end{bmatrix} = \begin{bmatrix} 1 & 0 \\ 0.4881 & 3.0119 \end{bmatrix} \begin{bmatrix} x_1 \\ x_2 \end{bmatrix} + \begin{bmatrix} 0 & -1 & 0 \\ 0 & -3.7547 & -1.9260 \end{bmatrix} \begin{bmatrix} w \\ r_1 \\ r_2 \end{bmatrix} \tag{3.91}$$

In Figure 3.8 error and normalized control force plots are drawn for control weighting matrices R_1=0.1, R_2=0.05 and R_3=0.01. As in LQR regulating problem when the control weight is decreased the objective of reducing control forces is less emphasized resulting in higher control forces and better performance in minimizing the tracking error. All in all selecting weighting matrices Q and R is a tradeoff between control effort and performance. In the present exercise the closed loop system has one disturbance input and two reference inputs and one error output and one control output. The transfer function matrix of the closed loop system from disturbance to error and transfer function matrix of the closed loop system from disturbance to control output are considered and singular values of the considered closed loop transfer functions are shown in Figure 3.9 and Figure 3.10 respectively again for control weighting matrices R_1=0.1, R_2=0.05 and R_3=0.01. Figures 3.9 and 3.10 suggest that the maximum singular value of the closed loop transfer function from input to error and minimum singular value of the closed loop transfer function from input to control output is obtained for R=0.1 which verifies the time domain performance demonstrated in Figure 3.8.

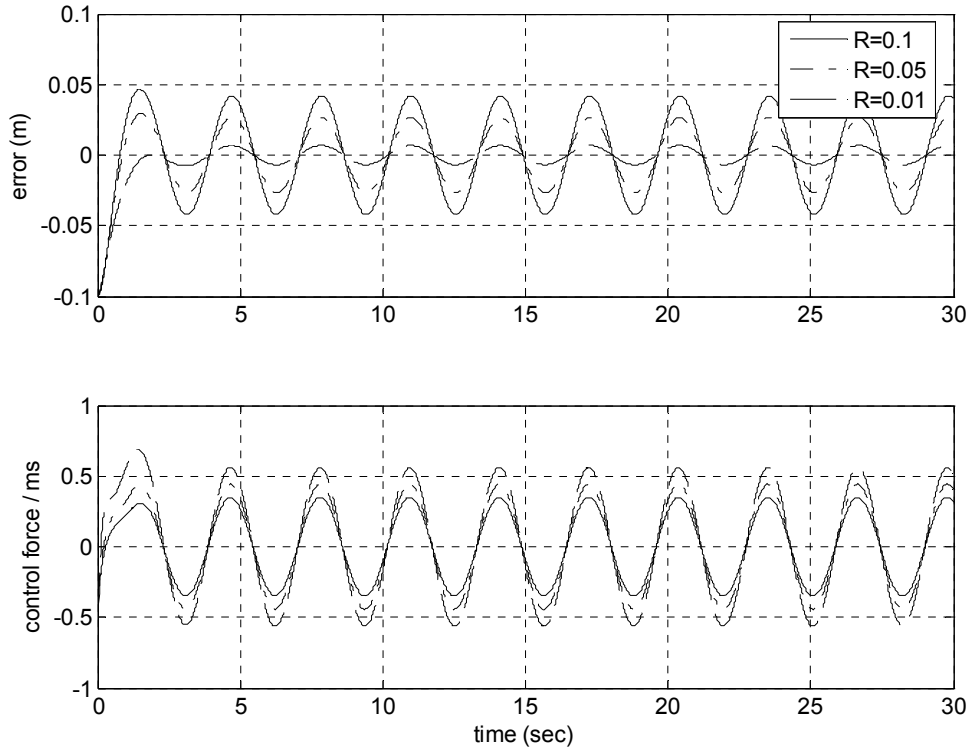

Figure 3.8. Comparison of error and normalized control forces for various LQR control weights – tracking problem

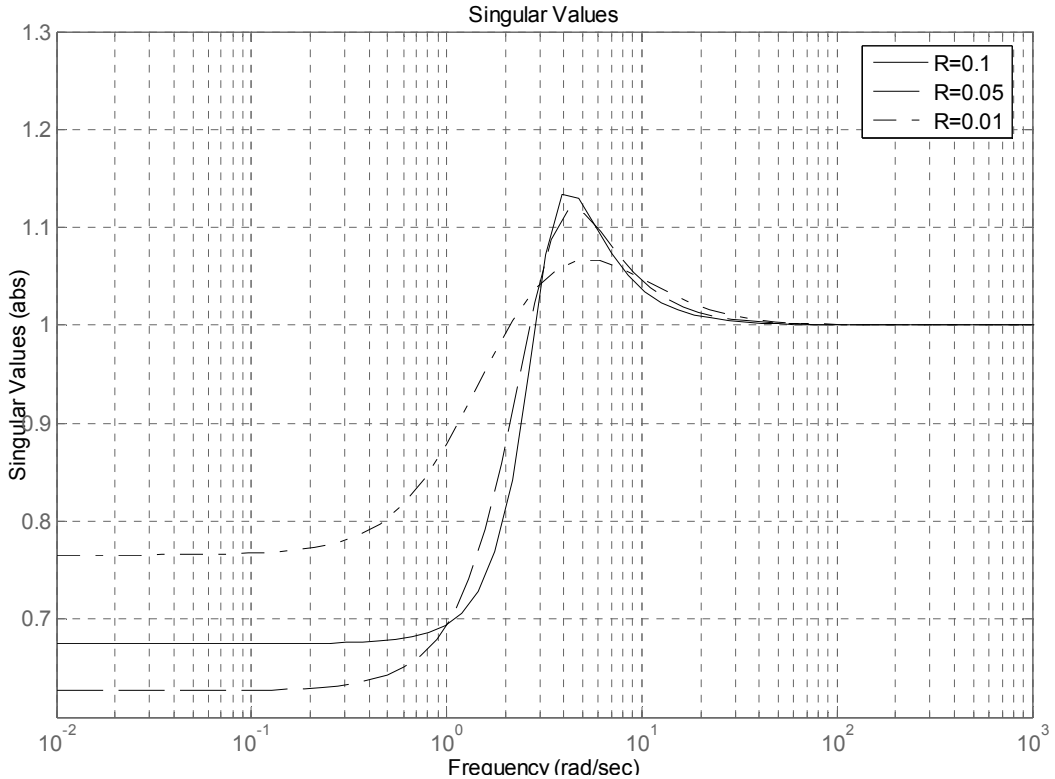

Figure 3.9. Singular values of the LQR closed loop system from input to error

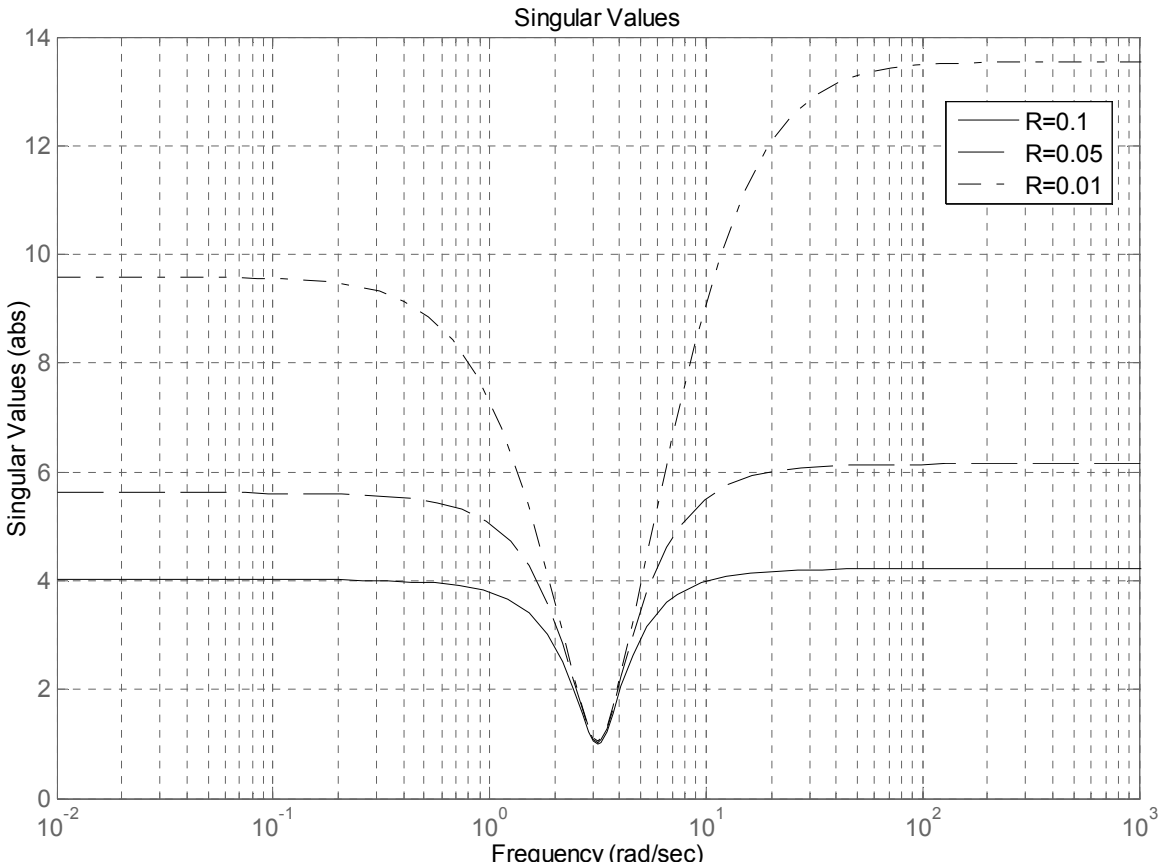

Figure 3.10. Singular values of the LQR closed loop system from input to control force

It is also interesting to note that when the frequency of the reference signal coincides with the frequency of the closed-loop system the error is maximized, on the other hand the control force needed to keep the system in desired trajectory is minimized.

3.6.7. H_∞ Control of a SDOF System – Regulator Problem

The required closed-loop system performance can be achieved for the generalized plant P by satisfying the following performance criterion. Satisfaction of the following norm inequality indicates that the closed-loop system successfully reduces the effect of the disturbance to an acceptable level.

$$\left\| \begin{matrix} W_p S \\ W_u K S \end{matrix} \right\|_\infty < 1 \tag{3.92}$$

where $S=(I+GK)^{-1}$ is the output sensitivity function of the generalized plant, and W_p, W_u are weighting functions used to reflect the relative importance of the performance requirement over different frequency ranges. In the given case performance weighting function is selected as $W_p=1$ and the control weighting function $W_u=2.9*10^{-1}$. The closed loop system is shown in Figure 3.4.

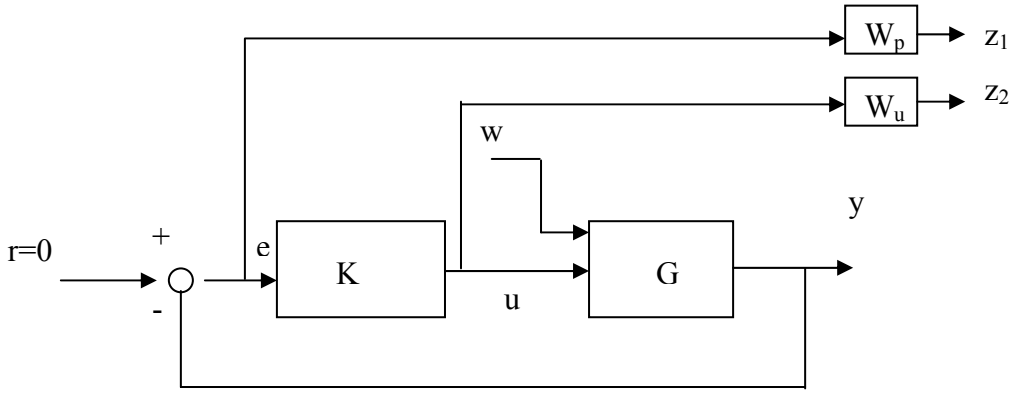

Figure 3.11. Closed-loop system structure with weights on outputs

The problem can be cast as a standard H_∞ optimization in the general control configuration shown in Figure 3.3 by using the command *sysic* in MATLAB.

Table 3.1. MATLAB code for constructing generalized plant – Regulator Case

```
systemnames = 'G Wp Wu';
inputvar = '[dist;control]';
outputvar = '[Wp;Wu;G]';
input_to_G= '[dist+control]';
input_to_Wp= '[G(1)]';
input_to_Wu= '[control]';
sysoutname = 'Ggen';
sysic
```

As can be followed from the command lines, the output of the generalized plant, *Ggen*, includes plant states, weighted control forces and weighted displacement output of the plant since reference signal is zero. The input of the generalized plant is consisted of external disturbance and control forces. The state-space representation of the generalized plant can be written as:

$$\begin{bmatrix} \dot{x}_1 \\ \dot{x}_2 \end{bmatrix} = \begin{bmatrix} 0 & 1 \\ -10 & -0.32 \end{bmatrix} \begin{bmatrix} x_1 \\ x_2 \end{bmatrix} + \begin{bmatrix} 0 & 0 \\ 1 & 1 \end{bmatrix} \begin{bmatrix} w \\ u \end{bmatrix} \tag{3.93}$$

$$\begin{bmatrix} z_1 \\ z_2 \\ y_1 \\ y_2 \end{bmatrix} = \begin{bmatrix} 1 & 0 \\ 0 & 0 \\ 1 & 0 \\ 0 & 1 \end{bmatrix} \begin{bmatrix} x_1 \\ x_2 \end{bmatrix} + \begin{bmatrix} 0 & 0 \\ 0 & 0.29 \\ 0 & 0 \\ 0 & 0 \end{bmatrix} \begin{bmatrix} w \\ u \end{bmatrix} \tag{3.94}$$

The design uses the MATLAB command *hinfsyn* that computes a suboptimal H_∞ controller, based on the generalized plant. The input and output arguments of the *hinfsyn* are

[K1,Scl1,gam1] = hinfsyn(P,nm,nc,`'gmin',0.1,'gmax',10,'tolgam',0.001`*);*

Table 3.2. Arguments of MATLAB command *hinfsyn* – Regulator case

Open-loop interconnection	Ggen
Number of measurements	nm=2
Number of controls	nc=1
initial upper bound on γ	gmin=0.1
initial lower bound on γ	gmax=10
relative error tolerance for γ	tolgam=0.001
K	controller
Scl1	closed-loop system
gam1	H∞ cost

where number of measurements that are procesed by the controller is the displacement and velocity outputs of the plant. The interval for γ iteration is chosen between 0.1 and 10 with tolerance 0.001. When the iteration procedure suceeds, the achievable minimum value of γ is given. In this case the obtained value for γ which is also the H_∞ norm of the closed loop system is 0.2789. This is also verified in Figure 3.12 since H_∞ norm corresponds to the peak of the largest singular value of *Scl1*. The state equations of the controller, *K*, calculated by H_∞ *algorithm* is given by:

$$\begin{bmatrix} \dot{k}_1 \\ \dot{k}_2 \end{bmatrix} = \begin{bmatrix} -0.1 & 0.0113 \\ -11.59 & -1003 \end{bmatrix} \begin{bmatrix} k_1 \\ k_2 \end{bmatrix} + \begin{bmatrix} 14.99 & 14.82 \\ 14.82 & 14990 \end{bmatrix} \begin{bmatrix} x_1 \\ x_2 \end{bmatrix} \tag{3.95}$$

$$[u] = [-0.0399 \quad -0.216] \begin{bmatrix} k_1 \\ k_2 \end{bmatrix} + [0 \quad 0] \begin{bmatrix} x_1 \\ x_2 \end{bmatrix} \tag{3.96}$$

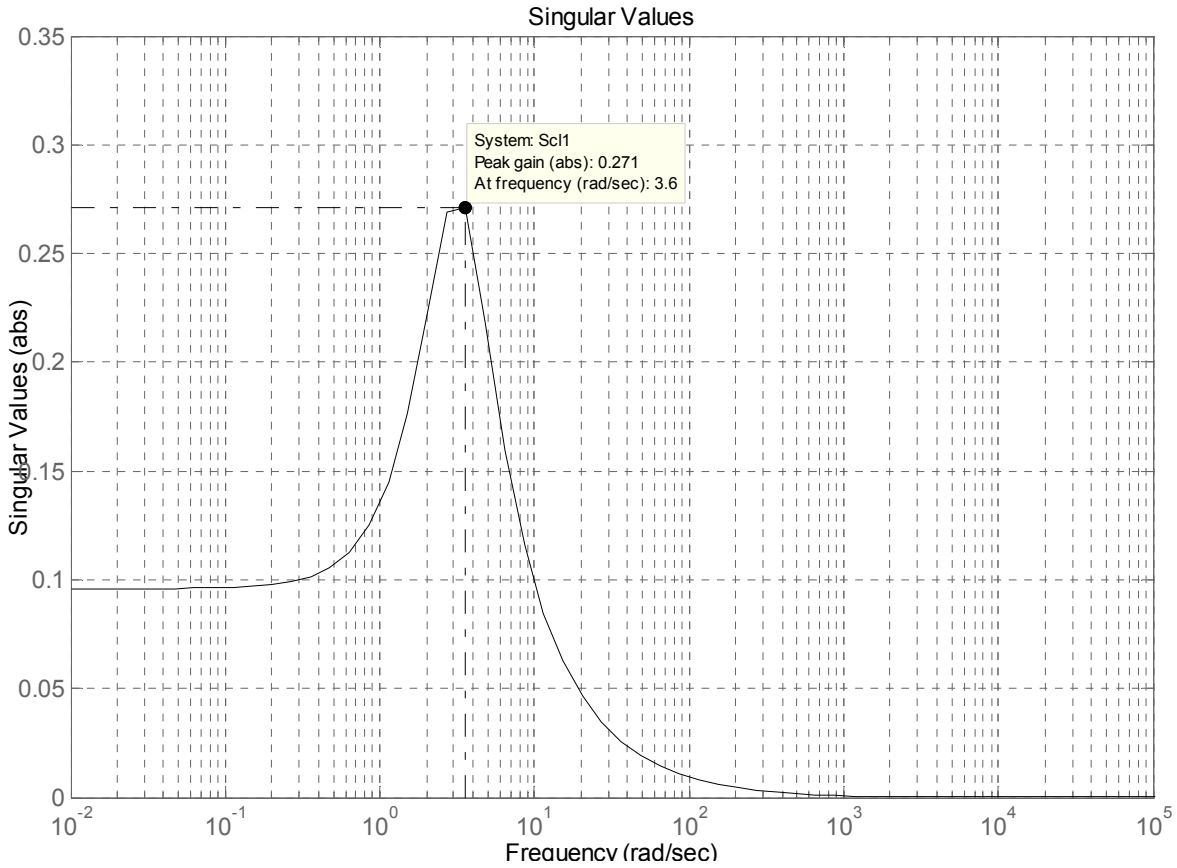

Figure 3.12. Singular values of the closed loop system for Scl1

It should be noted that the closed loop system given in *Scl1* includes the performance weights W_p *and* W_u in its output z_1 and z_2, and the controller, *K*, is formulized on minimizing the maximum singular values of weighted outputs of generalized plant, *Ggen*. However once the controller, K, is obtained the simulated closed loop system should not contain the performance weights anymore. The system interconnection of the plant *G* and the controller *K* is done by MATLAB command sysic.

Table 3.3. MATLAB code for plant and controller interconnection – Regulator Case

```
systemnames = 'G K';
inputvar = '[dist]';
outputvar = '[G(1);K]';
input_to_G= '[dist+K]';
input_to_K= '[G]';
sysoutname = 'CL1';
sysic
```

As can be followed from the command lines, the output of the closed loop system, *CL1*, includes displacement output, and control forces. The input of the generalized plant is the external disturbance. The state-space representation of the generalized plant can be written as:

$$\begin{bmatrix} \dot{x}_1 \\ \dot{x}_2 \\ \dot{k}_1 \\ \dot{k}_2 \end{bmatrix} = \begin{bmatrix} 0 & 1 & 0 & 0 \\ -10 & -0.3162 & -0.0399 & -0.216 \\ 14.99 & 14.82 & -0.1 & 0.0113 \\ 14.82 & 14990 & -11.59 & -1003 \end{bmatrix} \begin{bmatrix} x_1 \\ x_2 \\ k_1 \\ k_2 \end{bmatrix} + \begin{bmatrix} 0 \\ 1 \\ 0 \\ 1 \end{bmatrix} w \tag{3.97}$$

$$\begin{bmatrix} y_1 \\ u \end{bmatrix} = \begin{bmatrix} 1 & 0 & 0 & 0 \\ 0 & 0 & -0.0399 & -0.216 \end{bmatrix} \begin{bmatrix} x_1 \\ x_2 \\ k_1 \\ k_2 \end{bmatrix} \tag{3.98}$$

The performance of the H_∞ closed loop system is compared with the LQR closed loop system obtained in Section 3.6.1. It is visible from Figure 3.13 that time domain performances and corresponding control forces are very close to each other save for a few trials are needed to find the suitable control weights. From singular value plot given in Figure 3.14 it can be concluded that LQR control is slightly better than that of the H_∞ control.

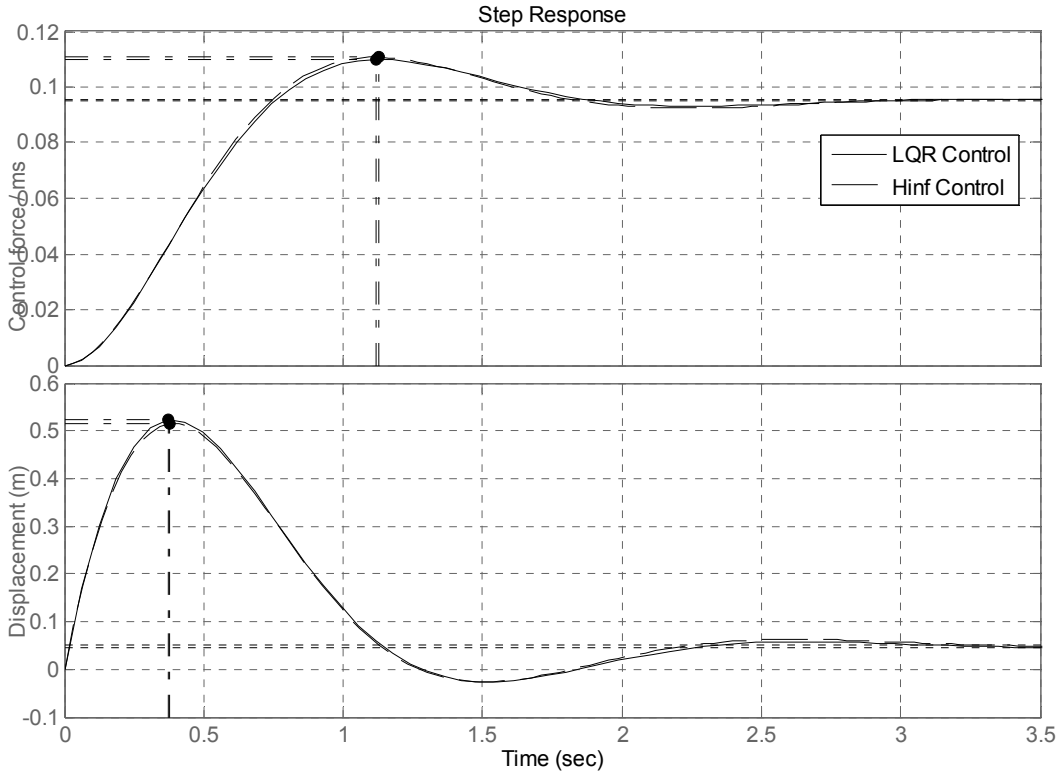

Figure 3.13. LQR and H_∞ closed loop systems response to step command

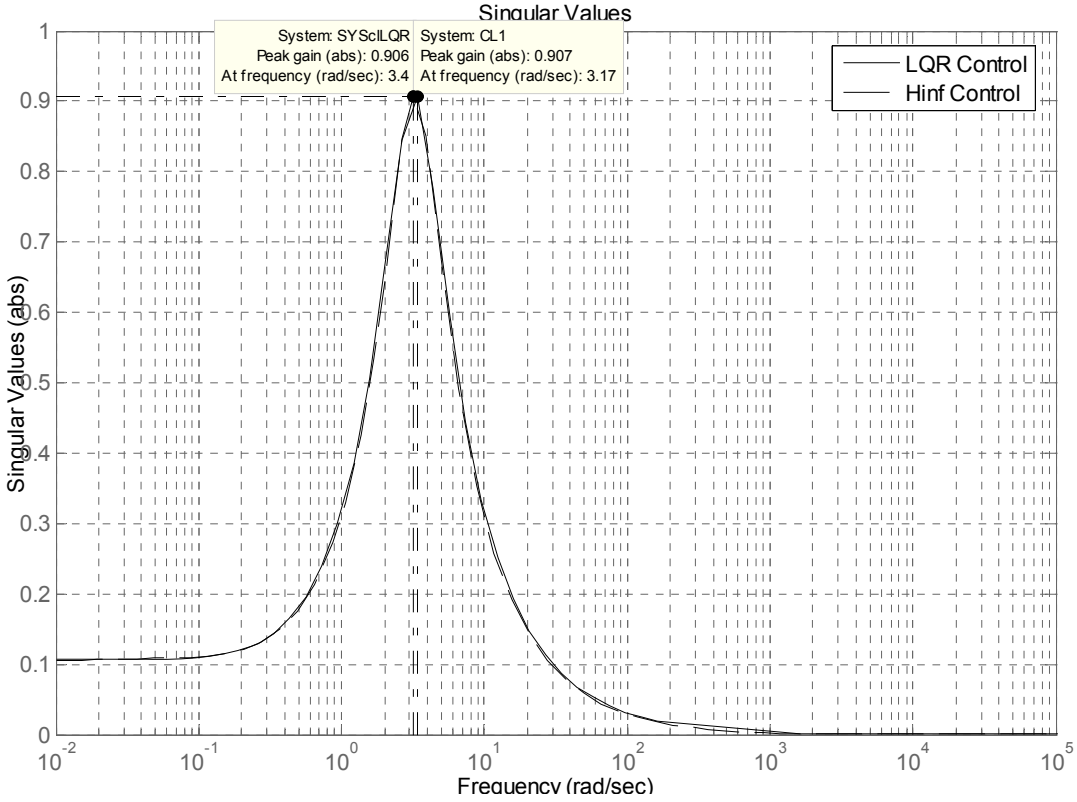

Figure 3.14. Singular value plot for LQR and H_∞ closed loop systems

3.6.8. H_∞ Control of a SDOF System – Tracking Problem

As can be followed from Figure 3.15, in the tracking problem the main difference is that we have a non-zero reference command. Thus the error, *e,* and control force, *u,* are weighted. As in the regulator problem S/KS mixed sensitivity problem is solved that is to find a stabilizing controller which minimizes

$$\left\| \begin{matrix} W_e S \\ W_u KS \end{matrix} \right\|_\infty < 1 \tag{3.99}$$

where $S=(I+GK)^{-1}$ is the output sensitivity function of the generalized plant, and W_p, W_u are weighting functions used to reflect the relative importance of the performance requirement over different frequency ranges. In the given case performance weighting function is selected as $W_p=1$ and the control weighting function $W_u=2.9*10^{-1}$.

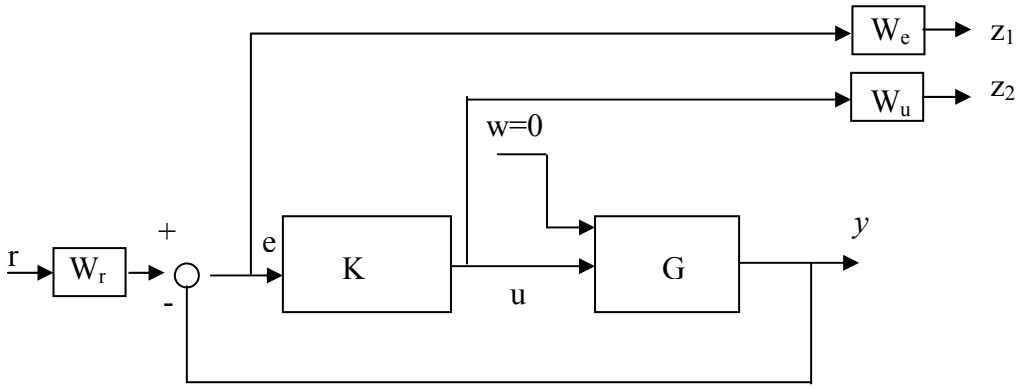

Figure 3.15. S/KS mixed-sensitivity minimization as tracking problem

In Figure 3.15 the weight W_r is used to describe the frequency content of the reference signal. W_r is a transfer function described in laplace domain as:

$$W_r(s) = \frac{2}{s^2 + 0.1s + 4} \tag{3.100}$$

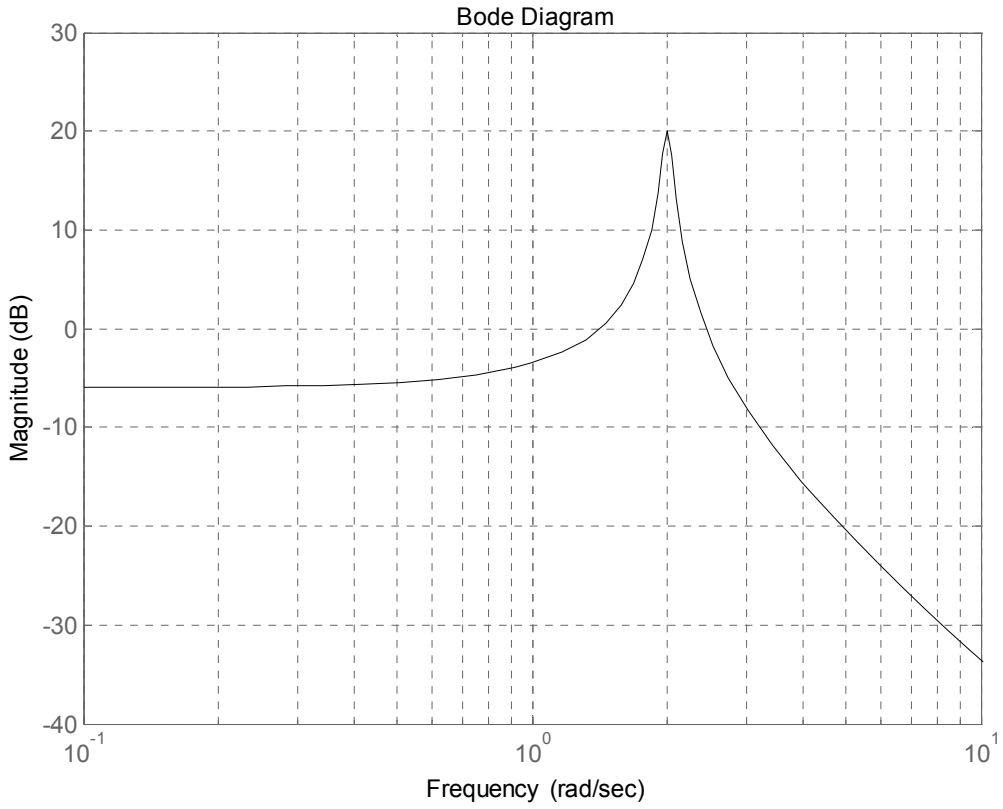

Figure 3.16. Bode magnitude plot of W_r

As can be realized from Figure 3.16, by introducing a weight W_r in to the generalized plant we mathematically say to the optimization algorithm that our reference command is a signal at 2 rad/sec frequency. So, the general control configuration shown in Figure 3.3 can be constructed by executing following MATLAB statements.

Table 3.4. MATLAB code for constructing generalized plant – Tracking Case

```
systemnames = 'G Wr We Wu';
inputvar = '[ref;control]';
outputvar = '[We;Wu;G(1)-Wr]';
input_to_G= '[control]';
input_to_Wr= '[ref]';
input_to_We= '[G(1)-Wr]';
input_to_Wu= '[control]';
sysoutname = 'Ggen';
sysic
```

In the tracking problem the output of the generalized plant, *Ggen*, includes weighted control forces, weighted error and error. Thus we have one error measurement that goes into the controller and output of the controller is the sole input of the generalized plant, *Ggen*. The state-space representation of the generalized plant can be written as:

$$\begin{bmatrix} \dot{x}_1 \\ \dot{x}_2 \\ \dot{r}_1 \\ \dot{r}_2 \end{bmatrix} = \begin{bmatrix} 0 & 1 & 0 & 0 \\ -10 & -0.316 & 0 & 0 \\ 0 & 0 & -0.1 & -2 \\ 0 & 0 & 2 & 0 \end{bmatrix} \begin{bmatrix} x_1 \\ x_2 \\ r_1 \\ r_2 \end{bmatrix} + \begin{bmatrix} 0 & 0 \\ 0 & 1 \\ 1 & 0 \\ 0 & 0 \end{bmatrix} \begin{bmatrix} r \\ u \end{bmatrix} \tag{3.101}$$

$$\begin{bmatrix} z_1 \\ z_2 \\ e \end{bmatrix} = \begin{bmatrix} 1 & 0 & 0 & -1 \\ 0 & 0 & 0 & 0 \\ 1 & 0 & 0 & -1 \end{bmatrix} \begin{bmatrix} x_1 \\ x_2 \\ r_1 \\ r_2 \end{bmatrix} + \begin{bmatrix} 0 & 0 \\ 0 & 0.1 \\ 0 & 0 \end{bmatrix} \begin{bmatrix} r \\ u \end{bmatrix} \tag{3.102}$$

The design uses the MATLAB command *hinfsyn* that computes a suboptimal H_∞ controller, based on the generalized plant. The input and output arguments of the *hinfsyn* are

[K1,Scl1,gam1] = hinfsyn(P,nm,nc,'gmin',0.1,'gmax',10,'tolgam',0.001);

Table 3.5. Arguments of MATLAB command *hinfsyn* – Tracking case

Open-loop interconnection	Ggen
Number of measurements	nm=1
Number of controls	nc=1
initial upper bound on γ	gmin=0.1
initial lower bound on γ	gmax=10
relative error tolerance for γ	tolgam=0.001
K	controller
Scl1	closed-loop system
gam1	H∞ cost

where number of measurements that are procesed by the controller is the error between plant displacement output and reference command. The interval for γ iteration is chosen between 0.1 and 10 with tolerance 0.001. The state equations of the controller, *K*, calculated by H_∞ *algorithm* is given by:

$$\begin{bmatrix} \dot{k}_1 \\ \dot{k}_2 \\ \dot{k}_3 \\ \dot{k}_4 \end{bmatrix} = \begin{bmatrix} 0 & 1 & 0 & 0 \\ -10.58 & -1.121 & 0.553 & 1.619 \\ 994.8 & 0 & -0.1 & -996.8 \\ 63.08 & 0 & 2 & -63.08 \end{bmatrix} \begin{bmatrix} k_1 \\ k_2 \\ k_3 \\ k_4 \end{bmatrix} + \begin{bmatrix} 0 \\ 0 \\ -2396 \\ -1519 \end{bmatrix} [e] \tag{3.103}$$

$$[u] = [-0.024 \quad -0.0334 \quad 0.0230 \quad 0.0672] \begin{bmatrix} k_1 \\ k_2 \\ k_3 \\ k_4 \end{bmatrix} + [0][e] \tag{3.104}$$

As in the case of LQR tracking problem, the H_∞ control has feedback and feedforward terms. The controller is interconnected to the system with following MATLAB statements.

Table 3.6. MATLAB code for plant and controller interconnection – Tracking Case

```
systemnames = 'G K1';
inputvar = '[ref]';
outputvar = '[G(1)-ref;K1]';
input_to_G= '[K1]';
input_to_K1= '[G(1)-ref]';
sysoutname = 'CL1';
sysic
```

It should be noted that weighting functions W_r, W_e and W_u are not included to the closed loop interconnection since they are only used to describe the relative importance and/or frequency content of the outputs and setpoints. In Figure 3.17 the error and normalized control forces of the closed loop system are shown. When we look at the singular value plots from control force to input (Figure 3.19) we see that when the frequency of the reference signal coincides with the frequency of the closed-loop system the control force needed to keep the system in desired trajectory is minimized. This was also seen in LQR controllers. On the other hand in H_∞ synthesis error is also minimized at the coinciding frequency which is contrary to LQR control. This is due to the fact that H_∞ control tries to minimize the maximum singular value of the generalized plant which is naturally occurs in the resonance frequency, in other words the natural frequency of the plant.

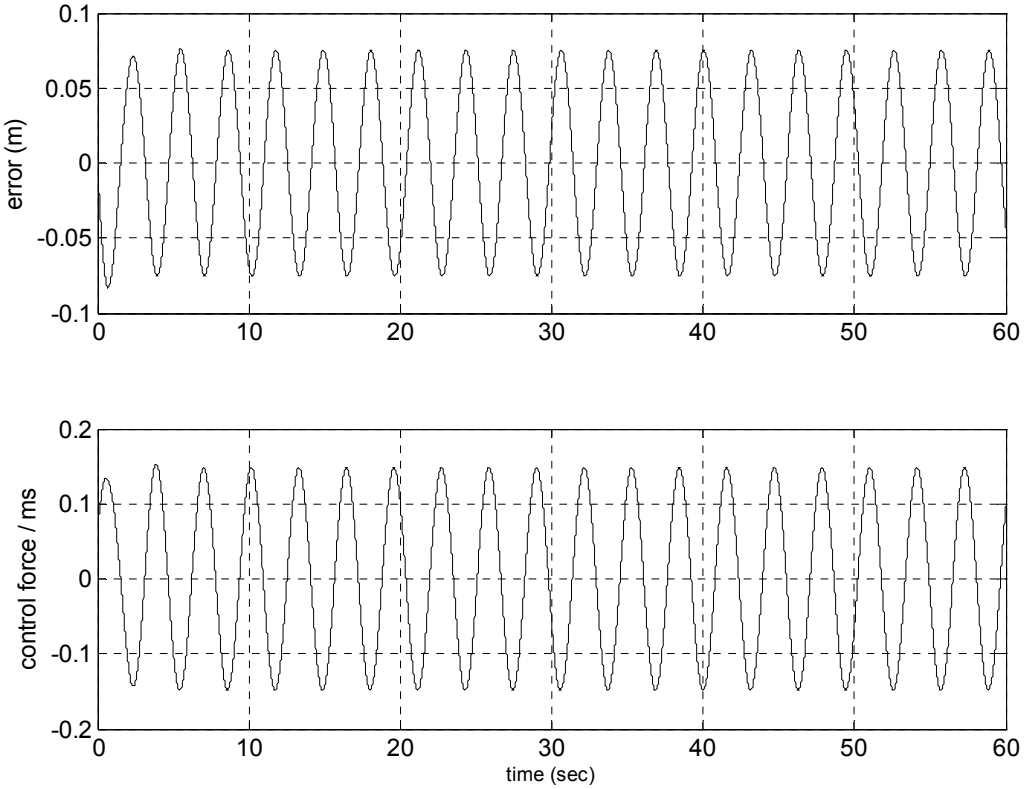

Figure 3.17. Error and control forces of S/KS mixed-sensitivity minimization

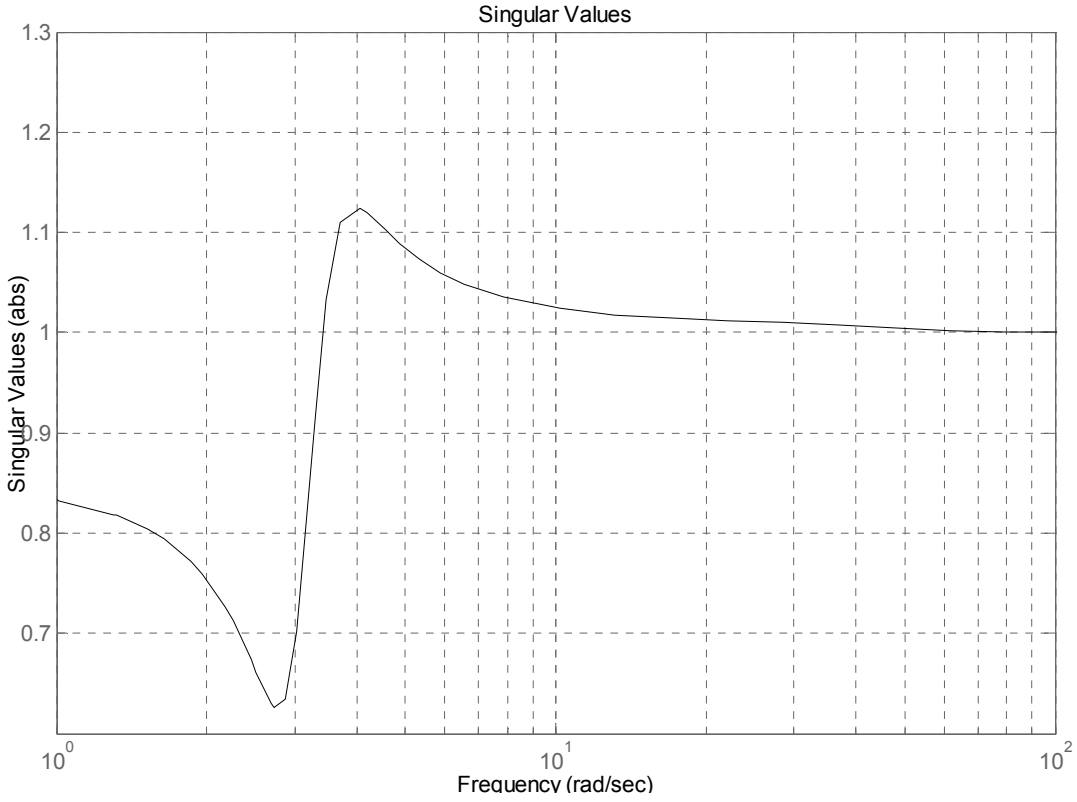

Figure 3.18. Closed loop singular values from input to error - S/KS

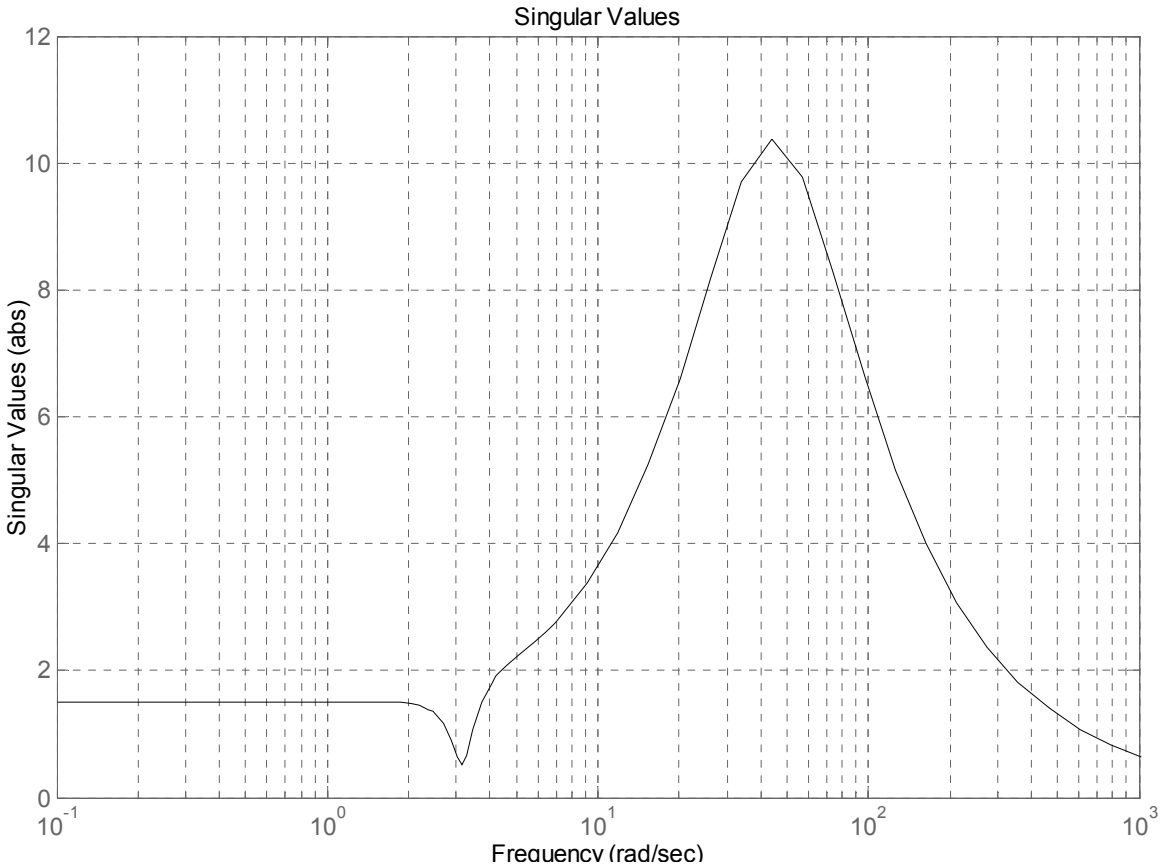

Figure 3.19. Closed loop singular values from input to control force - S/KS

Another mixed sensitivity optimization problem is to find a stabilizing control which minimizes

$$\left\| \begin{matrix} W_e S \\ W_p T \end{matrix} \right\|_\infty < 1 \tag{3.105}$$

where as stated in Section 2.2.5 T is the closed-loop transfer function from the reference signals to the outputs and ability to shape T is desirable for tracking problems and noise attenuation. The S/T mixed-sensitivity optimization problem can be put in to the standard configuration as shown in Figure 3.20.

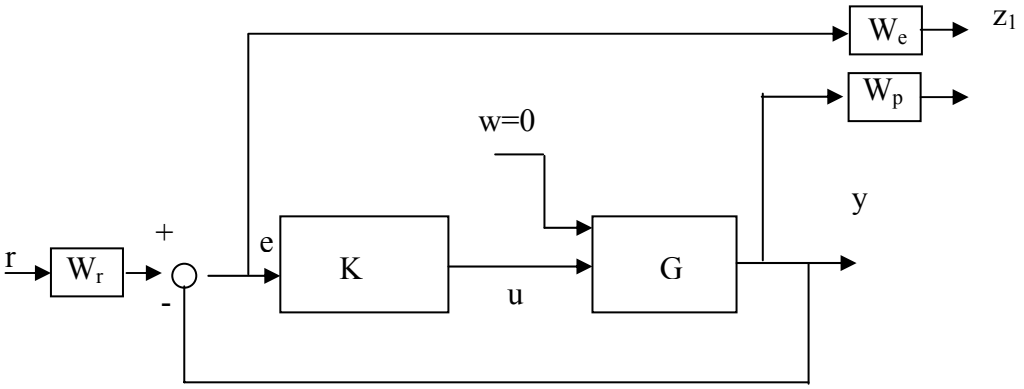

Figure 3.20. S/T mixed-sensitivity minimization as tracking problem

The general control configuration shown in Figure 3.3 can be constructed for S/T mixed sensitivity minimization by executing following MATLAB statements.

Table 3.7. MATLAB code for generalized plant – S/T minimization

```
systemnames = 'G Wr We Wp';
inputvar = '[ref;control]';
outputvar = '[We;Wp;G(1)-Wr]';
input_to_G= '[control]';
input_to_Wr= '[ref]';
input_to_We= '[G(1)-Wr]';
input_to_Wp= '[G(1)]';
sysoutname = 'Ggen';
sysic
```

The state equations of the controller, K, calculated by H_∞ *algorithm* is given by:

$$\begin{bmatrix} \dot{k}_1 \\ \dot{k}_2 \\ \dot{k}_3 \\ \dot{k}_4 \end{bmatrix} = \begin{bmatrix} 0 & 1 & 0 & 0 \\ -80.40 & -126.7 & 251.3 & 7956 \\ 7989 & 0 & -0.1 & -7991 \\ 178.8 & 0 & 2 & -178.8 \end{bmatrix} \begin{bmatrix} k_1 \\ k_2 \\ k_3 \\ k_4 \end{bmatrix} + \begin{bmatrix} 0 \\ 0 \\ -11300 \\ -252.8 \end{bmatrix} [e] \tag{3.106}$$

$$[u] = \begin{bmatrix} -5678 & -89.39 & 117.7 & 5626 \end{bmatrix} \begin{bmatrix} k_1 \\ k_2 \\ k_3 \\ k_4 \end{bmatrix} + [0][e] \tag{3.107}$$

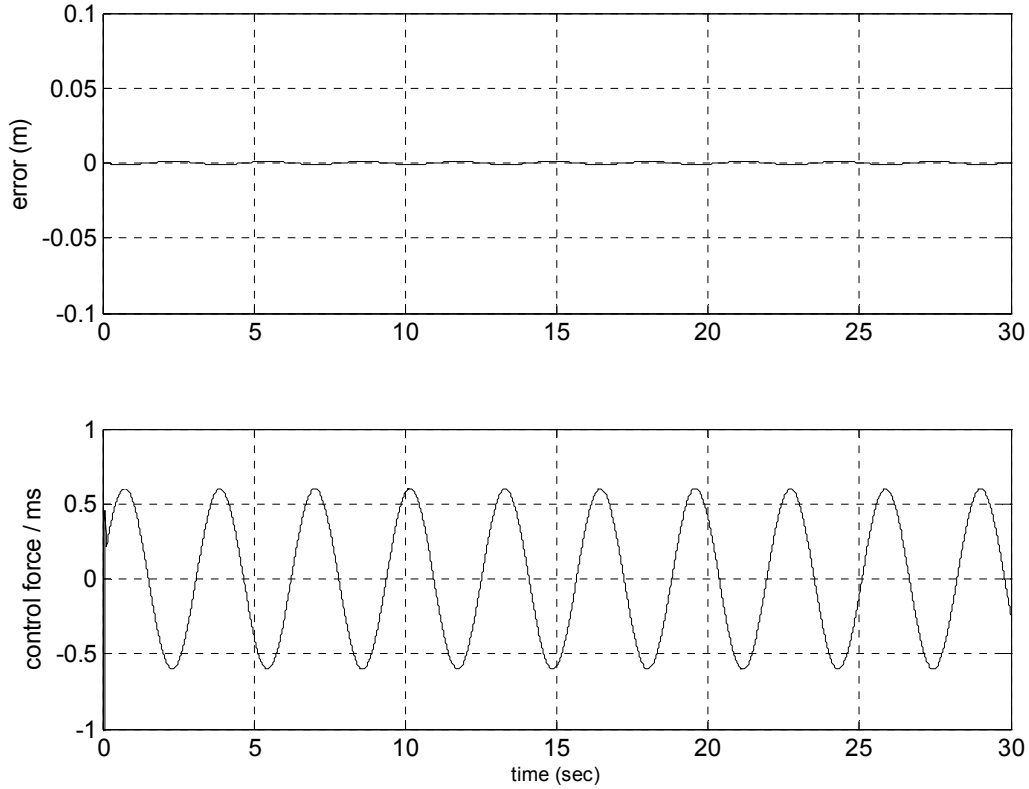

Figure 3.21. Error and normalized control forces of S/T mixed-sensitivity minimization

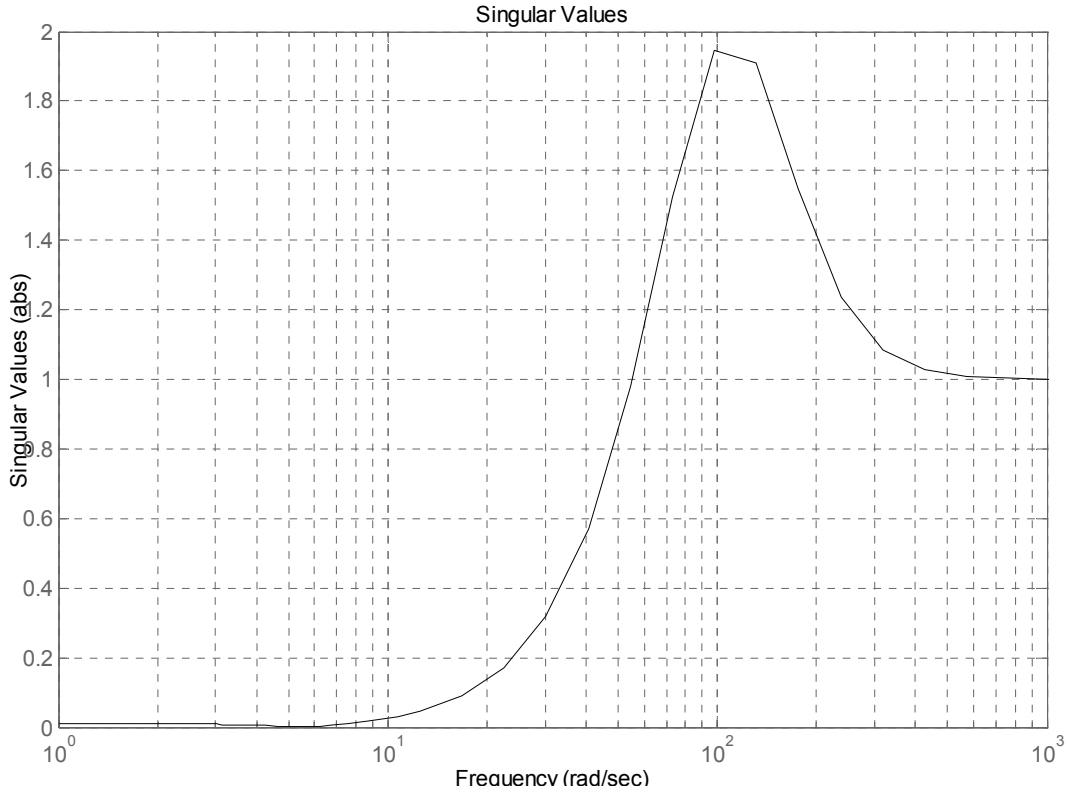

Figure 3.22. Closed loop singular values from input to error - S/T

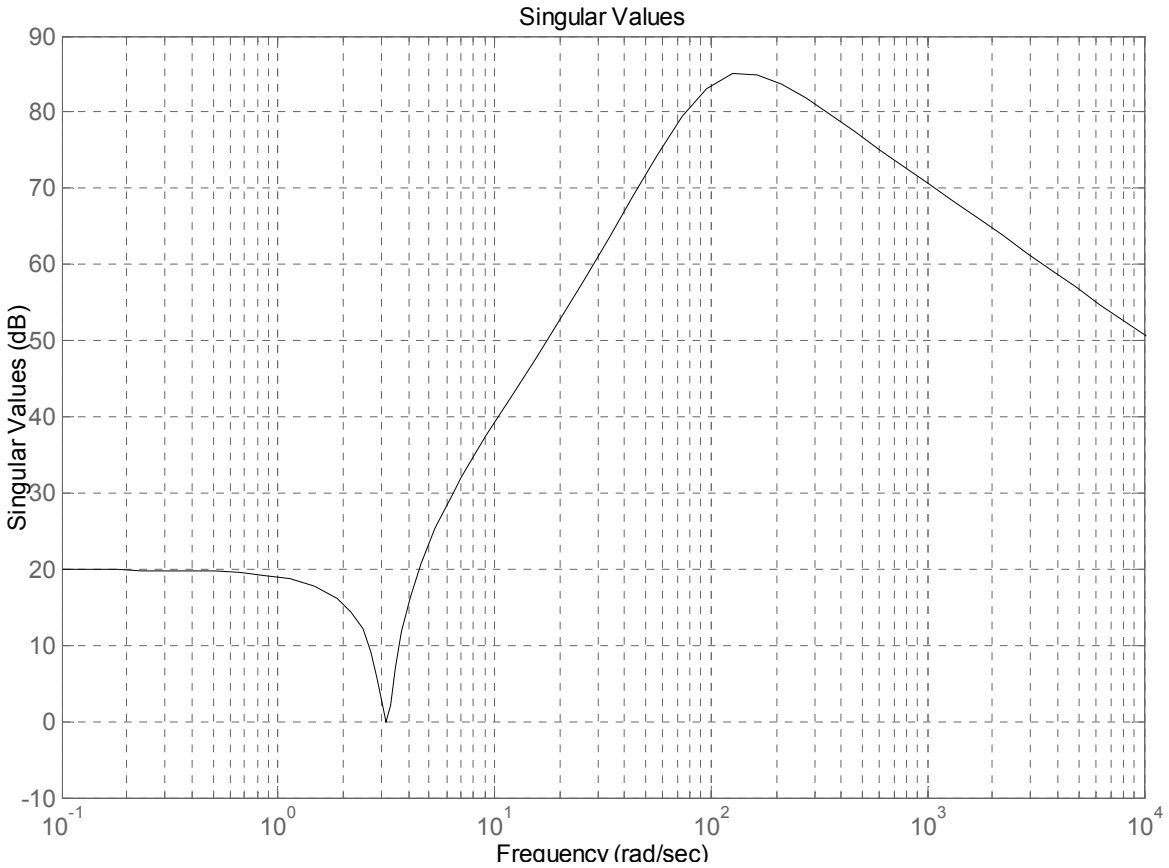

Figure 3.23. Closed loop singular values from input to control force - S/T

In the S/T setting the tracking performance is very much increased as can be seen from Figure 3.21 in time domain and from Figure 3.22 in frequency domain. However sensitivity to high frequency noise is increased when compared to S/KS case. This is expected since S/T synthesis tries to maximize the singular values of the complementary sensitivity function, *T*, on the other hand for noise attenuation singular vales of *T* should be small. The remedy to such conflicting objectives would be to use frequency dependent weights since disturbance rejection and reference tracking is a low-frequency requirement, while noise mitigation is often only relevant for higher frequencies. Moreover since there is no weight on control in S/T configuration the control forces are unbounded especially for high frequency inputs, i.e high frequency noise in command signal.

4. TUNED MASS DAMPERS (TMDS)

4.1. Concept of Tuned Mass Damper

As shown in Figure 4.1, a structural system is modeled as an undamped single-degree-of-freedom system, with mass *M* and elastic stiffness *K*, subjected to an external sinusoidal dynamic force P(t) of amplitude P_0 and of circular frequency ω:

$$P(t) = P_0 \sin \omega t \tag{4.1}$$

The response of the structural system can be reduced by the attachment of a secondary comparatively small vibratory system (TMD), of stiffness *k* and mass *m*. The relative displacement of the primary system and the TMD are denoted $x_1(t)$ and $x_2(t)$ respectively.

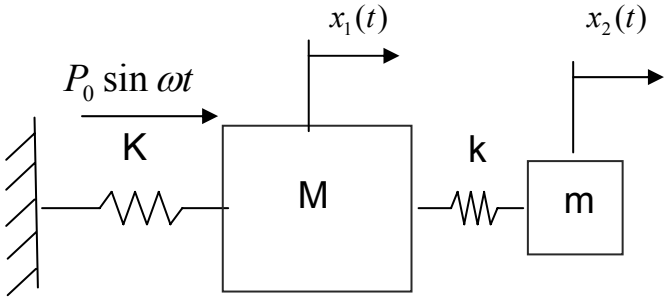

Figure 4.1. Main Structure and TMD

Applying Newton's second law on each mass yields the two equations of motion for this two-degree-of-freedom system:

$$M\ddot{x}_1 + (K + k)x_1 - kx_2 = P_0 \sin \omega t \tag{4.2}$$

$$m\ddot{x}_2 + k(x_2 - x_1) = 0 \tag{4.3}$$

Since the system is undamped, the forced vibration takes a simple form:

$$x_1(t) = a_1 \sin \omega t \tag{4.4}$$

$$x_2(t) = a_2 \sin \omega t \tag{4.5}$$

where a_1 and a_2 are constants representing the amplitude of vibration of the main and the secondary mass respectively. Substituting Equations (4.4) and (4.5) into Equations (4.2) and (4.3) yields:

$$(-Ma_1\omega^2 + (K+k)a_1 - ka_2)\sin \omega t = P_0 \sin \omega t \tag{4.6}$$

$$(-ma_2\omega^2 + k(a_2 - a_1))\sin \omega t = 0 \tag{4.7}$$

Since Equations (4.6) and (4.7) must be satisfied at all times:

$$a_1(-M\omega^2 + K + k) - ka_2 = P_0 \tag{4.8}$$

$$-ka_1 + a_2(-m\omega^2 + k) = 0 \tag{4.9}$$

For simplification, if we introduce the following variables:

$x_{st} = \frac{P_0}{K}$: static displacement of the primary structure

$\omega_n^2 = \frac{K}{M}$: squared natural frequency of the primary structure

$\omega_a^2 = \frac{k}{m}$: squared natural frequency of the TMD

and by dividing Equation (4.8) by K and Equation (4.9) by k, we obtain:

$$a_1\left(1+\frac{k}{K}-\frac{\omega^2}{\omega_n^2}\right)-a_2\frac{k}{K}=x_{st} \tag{4.10}$$

$$a_1=a_2\left(1-\frac{\omega^2}{\omega_a^2}\right) \tag{4.11}$$

Solving for the amplitudes a_1 and a_2 we get:

$$\frac{a_1}{x_{st}}=\frac{\left(1-\frac{\omega^2}{\omega_a^2}\right)}{\left(1-\frac{\omega^2}{\omega_a^2}\right)\left(1+\frac{k}{K}-\frac{\omega^2}{\omega_n^2}\right)-\frac{k}{K}} \tag{4.12}$$

$$\frac{a_2}{x_{st}}=\frac{1}{\left(1-\frac{\omega^2}{\omega_a^2}\right)\left(1+\frac{k}{K}-\frac{\omega^2}{\omega_n^2}\right)-\frac{k}{K}} \tag{4.13}$$

Close inspection of Equation (4.12) reveals that when the natural frequency $\omega_a=\sqrt{k/m}$ of the attached TMD is chosen to be equal to the frequency ω of the disturbing force, a_1 is zero. In other words vibration of the first mass is reduced to zero.

If we examine Equation (4.13) when $\omega_a=\omega$, we see that the first term in denominator is zero, and this equation reduces to:

$$a_2=-\frac{K}{k}x_{st}=-\frac{P_0}{k} \tag{4.14}$$

It can be concluded from Equation (4.14) that TMD exerts a force to the primary structure which is actually equal and opposite of the external force. This is the underlying concept for tuned mass dampers. Although theory necessitates the natural frequency of the attached mass damper to be tuned to the excitation frequency, building structures are

subjected to environmental loads, such as wind and earthquake loads. Since these loads possess many frequency components, the natural frequency of the attached mass is tuned to the fundamental modal frequency of the building in order to avoid resonance case. When we considered the case in which TMD is in resonance with the primary structure, it can be expressed as:

$$\frac{k}{m} = \frac{K}{M} \text{ or } \frac{k}{K} = \frac{m}{M} = \mu \tag{4.15}$$

where μ is defined as the ratio of TMD to the mass of the primary structure. For this case Equations (4.12) and (4.13) becomes:

$$\frac{x_1(t)}{x_{st}} = \frac{\left(1 - \frac{\omega^2}{\omega_a^2}\right)}{\left(1 - \frac{\omega^2}{\omega_a^2}\right)\left(1 + \frac{k}{K} - \frac{\omega^2}{\omega_n^2}\right) - \frac{k}{K}} \sin \omega t \tag{4.16}$$

$$\frac{x_2(t)}{x_{st}} = \frac{1}{\left(1 - \frac{\omega^2}{\omega_a^2}\right)\left(1 + \frac{k}{K} - \frac{\omega^2}{\omega_n^2}\right) - \frac{k}{K}} \sin \omega t \tag{4.17}$$

The denominators of Equation (4.16) and (4.17) are identical and quadratic with two roots in (ω^2 / ω_a^2). Thus for two values of the excitation frequency ω, both denominators become zero, and consequently x_1 and x_2 become infinitely large. This relation can be seen in Figure 3.2. For β = 0, which is forced frequency ratio and defined as ω / ω_n, the term a_1 / x_{st} is 1. In other words dynamic response is equal to static response. However, at the first resonance (ω / ω_n=0.8), a_1 / x_{st} goes to infinity. When the excitation frequency is in resonance with the primary structure and with the TMD, a_1 / x_{st} goes to zero. At the second resonance (ω / ω_n=1.25), a_1 / x_{st} goes to infinity again. The narrow are where $a_1 / x_{st} < 1$ is called the operating range of TMD. Due to the sharp peaks

out of operating range TMD is not useful for broad band frequency inputs as in the case of earthquake or wind loads.

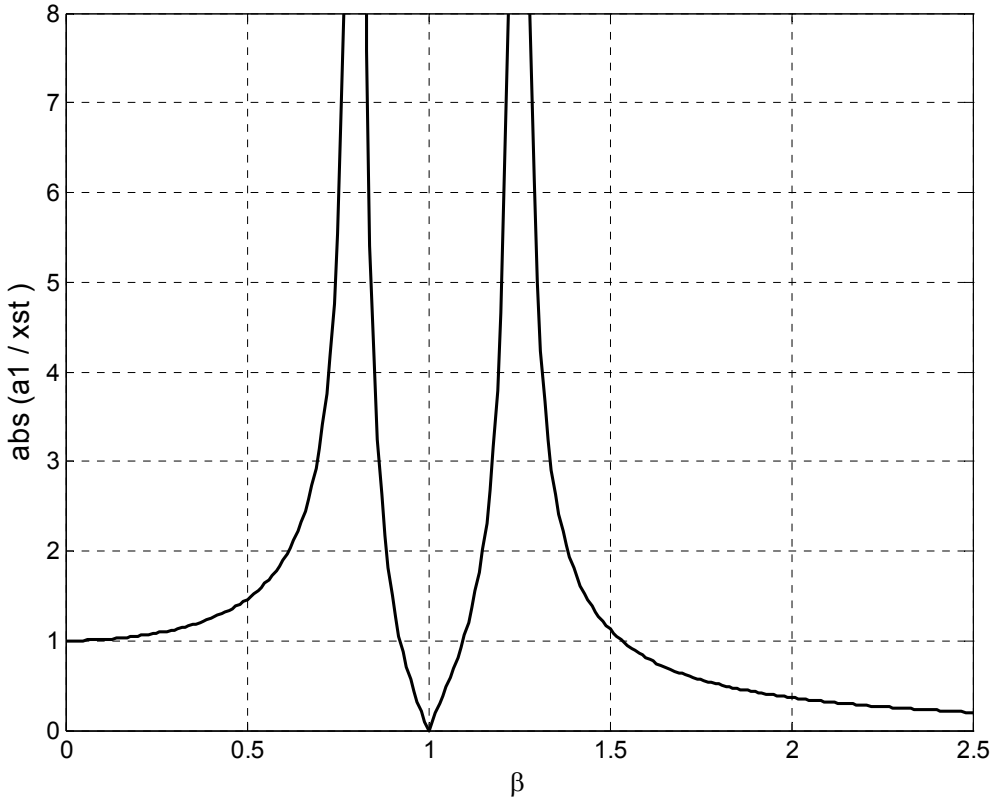

Figure 4.2. Amplitude of primary structure: $\omega_n = \omega_a$, μ=0.2

4.2. Optimization of Tuned Mass Damper

4.2.1. The Case of Undamped Structures

Den Hartog [1] first studied the theory of damped and undamped tuned mass dampers in the absence of damping in the main system. For a sinusoidal excitation with frequency, ω, and amplitude, Po, dynamic amplification factor, DAF, for an undamped structural system is defined as:

$$DAF = \frac{y_{\max}}{y_{st}} = \sqrt{\frac{(\lambda^2 - \beta^2)^2 + (2\varsigma_a \lambda\beta)^2}{\left[(\lambda^2 - \beta^2)(1-\beta^2) - \lambda^2\beta^2\mu\right]^2 + (2\varsigma_a \lambda\beta)^2 (1 - \beta^2 - \beta^2\mu)^2}} \quad (4.18)$$

where,

$x_{st} = \frac{P_0}{K}$: static displacement of the primary structure

$\omega_n^2 = \frac{K}{M}$: squared natural frequency of the primary structure

$\omega_a^2 = \frac{k}{m}$: squared natural frequency of the TMD

$\beta = \omega / \omega_n$: forced frequency ratio

$\lambda = \omega_a / \omega_n$: frequency ratio of TMD to primary structure

$\varsigma_a = c_1 / 2m\omega_a$: damping ratio of TMD

$\mu = m / M$: mass ratio of TMD to structural system

For frequency ratio λ=1 and mass ratio μ=0.05 DAF is plotted for various values of TMD damping ratio ζ_a.

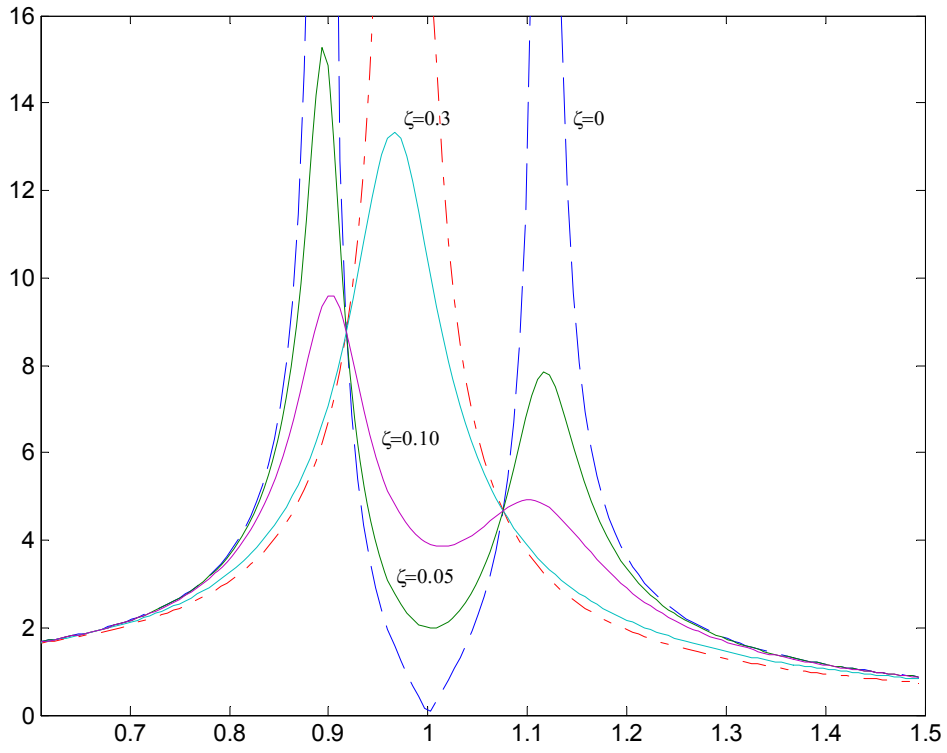

Figure 4.3. Dynamic amplification factor as function of β (λ=1, μ=0.05)

As can be observed from Figure 4.3, there are two infinite resonant peaks of the combined structure/TMD system when the damping ratio of the TMD is zero. On the other hand if the damping ratio of the TMD is infinite then the additional mass is virtually fused to the main structure and one infinite resonant peak is observed. In the case of zero damping ratio of TMD, the lowest value of dynamic amplification factor is obtained between two infinite resonant peaks but in this case the operation range is very limited. It is also visible that if the excitation frequency deviates from resonance frequency the response might be unbounded. Therefore, objective is to obtain a wider frequency bandwidth by introducing some damping to TMD. Also it can be observed that there are two points at which DAF is independent of damping ratio ζ_a. The minimum peak amplitude can be obtained by choosing λ to adjust these two fixed points to reach equal heights. The optimum frequency ratio λ following this procedure is determined by Den Hartog [1] as:

$$\lambda_{opt} = \frac{1}{1+\mu} \tag{4.19}$$

and consequently the optimum damping ratio of the TMD is given by Den Hartog [1] as:

$$\varsigma_{opt} = \sqrt{\frac{3\mu}{8(1+\mu)}} \tag{4.20}$$

Then for mass ratio μ=0.05, λ_{opt} and ζ_{opt} is calculated to be 0.95 and 0.13 respectively. Figure 4.4 shows DAF vs β plot with optimized frequency ratio and with various TMD damping levels. It is evident from Figure 4.4 that for optimum frequency ratio the invariant points are at equal heights and with optimum damping ratio of ζ=0.13 a wider frequency bandwidth is obtained. To validate the time response, the combined structure/TMD system is excited with random white noise input. In Figure 4.5 the response of the primary structure which is idealized as a SDOF system to is compared with ones of the optimized and non-optimized structure/TMD system. The mass ratio of TMD to structural system, μ, is taken as %5. Frequency ratio of the TMD to structural system, λ, is

1 for the non-optimized TMD system and λ is 0.95 for the optimized TMD system. Also, damping ratio of the TMD is 0 and 0.13 for the non-optimized and optimized TMD respectively.

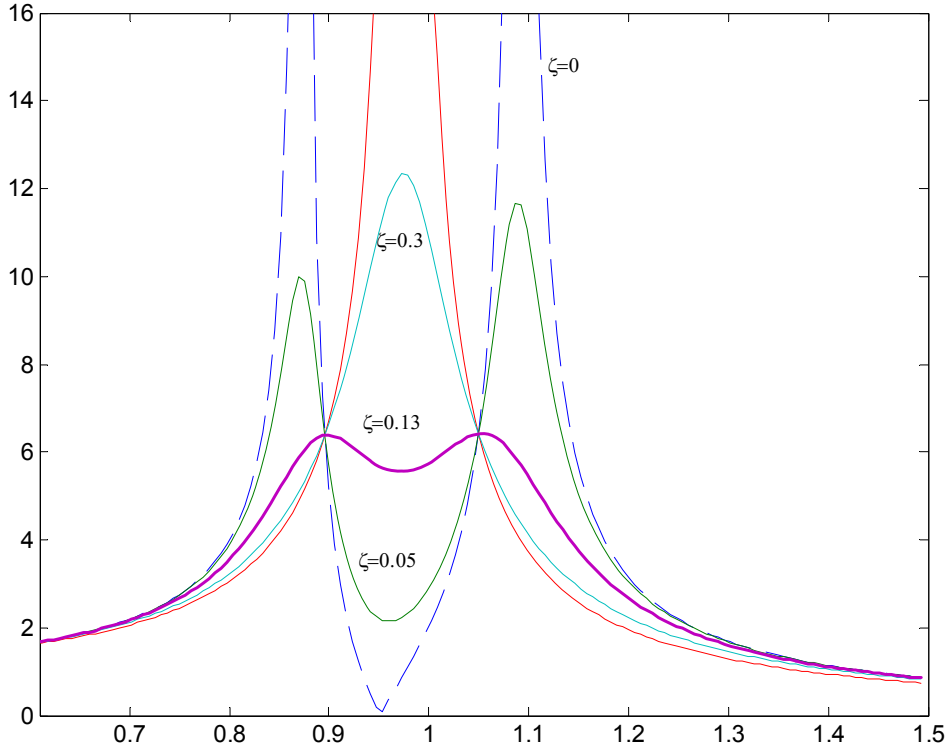

Figure 4.4. Dynamic amplification factor as function of β (λ=0.95, μ=0.05)

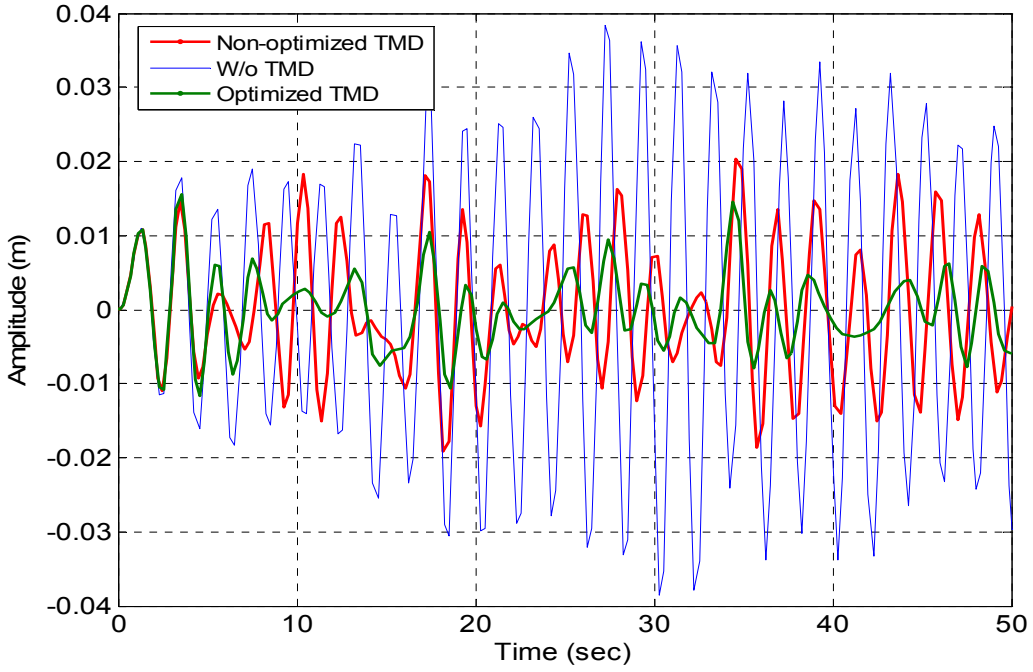

Figure 4.5. Comparison of Responses to white noise excitation

It can be noted from Figure 4.5 that although there is a considerable reduction of the response of the structure with non-optimized TMD, the response is better improved with optimized TMD. The maximum amplitude is reduced by % 47 in the non-optimized TMD case, whereas the reduction is % 60 in the optimized TMD case.

Table 4.1. Optimum Absorber Parameters Attached to Undamped SDOF Structure

Loading Case	Optimization Criteria	Optimum Tuning Conditions	
		λ	ζ
Harmonic Load Applied to Primary Structure	Minimum Relative Displacement Amplitude of Primary Structure	$\frac{1}{1+\mu}$	$\sqrt{\frac{3\mu}{8(1+\mu)}}$
Harmonic Load Applied to Primary Structure	Minimum Relative Acceleration Amplitude of Primary Structure	$\frac{1}{\sqrt{1+\mu}}$	$\sqrt{\frac{3\mu}{8(1+\mu/2)}}$
Harmonic Base Acceleration	Minimum Relative Displacement Amplitude of Primary Structure	$\frac{\sqrt{1-\frac{\mu}{2}}}{1+\mu}$	$\sqrt{\frac{3\mu}{8(1+\mu)(1-\mu/2)}}$
Harmonic Base Acceleration	Minimum Absolute Acceleration Amplitude of Primary Structure	$\frac{1}{1+\mu}$	$\sqrt{\frac{3\mu}{8(1+\mu)}}$
Random Load Applied to Primary Structure	Minimum Root Mean Square Value of Relative Displacement of Primary Structure	$\frac{\sqrt{1+\frac{\mu}{2}}}{1+\mu}$	$\sqrt{\frac{\mu(1+\frac{3\mu}{4})}{4(1+\mu)(1-\mu/2)}}$
Random Base Acceleration	Minimum Root Mean Square Value of Relative Displacement of Primary Structure	$\frac{\sqrt{1-\frac{\mu}{2}}}{1+\mu}$	$\sqrt{\frac{\mu(1-\frac{\mu}{4})}{4(1+\mu)(1-\mu/2)}}$

Den Hartog [1] formulized the optimum parameters for TMD systems for the case where the primary structure is excited with a harmonic force and the optimization criteria was selected to minimize the relative displacement amplitude of primary structure.

However civil engineering structures are subjected to other forms of excitations like random or harmonic base excitation. A detailed analysis was carried out by Warburton [5] to determine the optimum damper parameters for both harmonic and random excitations, with random excitation being applied as a force to the structure (as in the case of wind) or as base acceleration (as in the case of earthquake). Apart from minimization of displacement amplitude he also considered minimization of acceleration amplitude as optimization criteria. Table 4.1 lists optimum tuning conditions, based on various optimization criteria for damped TMDs attached to undamped primary structures.

4.2.2. The Case of Damped Structures

In the previous section, given solutions for TMD systems is valid when there is no damping in the structural system. When damping is present as in the case of civil engineering structures, invariant points no longer exists. Thus, by taking account structural damping, a numerical search technique based on the minimum-maximum amplitude criterion will be utilized to determine the optimum parameters λ_{opt} and $\zeta_{opt.}$ In this procedure maximum amplitude of Dynamic Amplification Factor, DAF_{max}, is tried to minimize through adjustment of two parameters λ_{opt} and ζ_{opt} for the TMD device.

The equation of motion of the TMD structure system can be written as follows:

$$m_s\ddot{x}_s + \left[c_s\dot{x}_s + c_1(\dot{x}_s - \dot{x}_1)\right] + \left[k_s x_s + k_1(x_s - x_1)\right] = F(t) \tag{4.21}$$

$$m_1\ddot{x}_1 + \left[c_1(\dot{x}_1 - \dot{x}_s)\right] + \left[k_1(x_1 - x_s)\right] = 0 \tag{4.22}$$

where, subscript s donates for the main structure and subscript 1 donates for the TMD. F(t) is the input excitation; m, k, c are respectively the mass, stiffness, and damping coefficients; x_s is the displacement of the main structure with respect to the ground and x_1 represents the displacement of the TMD with respect to the ground.

Let's define:

$$\mu = \frac{m_1}{m_s}; \lambda = \frac{\omega_1}{\omega_0}; \zeta_s = \frac{c_s}{2m_s\omega_0}; \zeta_1 = \frac{c_1}{2m_1\omega_1}; \omega_0 = \sqrt{k_s / m_s}; \omega_1 = \sqrt{k_1 / m_1}$$

Transferring Equations (4.21) and (4.22) into frequency domain by Laplace transform which is defined as Z(s) = L[z(t)] and introducing the above parameters gives:

$$X_s s^2 + \left[2\omega_0\zeta_s X_s + 2\lambda\omega_0\zeta_1\mu(X_s - X_1)\right]s + \left[\omega_0^2 X_s + \mu\lambda^2\omega_0^2(X_s - X_1\right] = F / m_s \quad (4.23)$$

$$(\mu X_1)s^2 + \left[2\lambda\omega_0\zeta_1\mu(X_1 - X_s)\right]s + \left[\mu\lambda^2\omega_0^2(X_1 - X_s)\right] = 0 \quad (4.24)$$

In which:

X_s=X_s(s)=L[x_s],
X_1=X_1(s)=L[x_1],
F=F(s)=L[F(t)],

Equations (4.23) and (4.24) can be written in matrix form as follows:

$$\begin{bmatrix} A(s) & B(s) \\ B(s) & G(s) \end{bmatrix}\begin{bmatrix} X_s \\ X_1 \end{bmatrix} = \begin{bmatrix} 1 \\ 0 \end{bmatrix} F / m_s \quad (4.25)$$

In which:

$$A(s) = s^2 + (2\omega_0\zeta_s + 2\lambda\omega_0\zeta_1\mu)s + \omega_0^2 + \mu\lambda^2\omega_0^2$$
$$B(s) = (-2\lambda\omega_0\zeta_1\mu)s - \mu\lambda^2\omega_0^2$$
$$G(s) = \mu s^2 + (2\lambda\omega_0\zeta_1\mu)s + \mu\lambda^2\omega_0^2$$

Transfer Function of the main structure can be found by solving the Eq. (4.25).

$$TF_s(s) = \frac{X_s}{F} = \frac{1}{m_s}\frac{G(s)}{A(s)G(s) - B(s)B(s)} \quad (4.26)$$

Once the Transfer Function is obtained Dynamic Amplification Factor can be calculated through setting s=iω in the Transfer Function and computing $k_s\left|\left[TF_s(i\omega)\right]\right|$. Then optimum values are calculated using the minimum-maximum amplitude procedure. If damping ratio ζ_s of the structure and mass ratio μ of the TMD is known, the procedure can be summarized as follows:

- The damping ratio ζ_1 of the TMD is fixed to zero; within the range of 0.8-1.2 control parameter λ is increased with an increment of 0.001. In each increment maximum amplitude of Dynamic Amplification Factor (DAF_{max}) is determined. The optimum value in this step is the one which minimize the maximum response amplitude, min (DAF_{max}).
- The damping ratio of the TMD is increased by an increment of 0.005 and the rest of the procedure in Step 1 is repeated thus another minimum for the maximum response amplitude is calculated. By comparing all the minimum values that have been computed, the real minimum min [min (DAF_{max})], for the range of $0< \zeta_1 <$ 0.20 is determined.
- The corresponding parameters which make min [min (DAF_{max})] are the optimum parameters for the TMD system.

An equivalent single-degree-of-freedom system with following parameters is considered to be equipped with TMD. The equivalent stiffness, $k_s=1.10^5$ kN/m; the equivalent mass, $m_s=1.10^4$ tons; and damping coefficient, $c_s=3{,}16.10^3$ N/s which corresponds to a %5 structural damping. The mass ratio, μ, of the TMD unit is %5 and following aforementioned procedures the optimum parameters are obtained as 0.935 for frequency ratio of TMD to primary structure, λ, and 0.145 for damping ratio of the TMD unit. As can be seen from Figure 4.6 for various damping ratios of TMD there is no invariant points which Dynamic Amplification Factor (DAF) is independent of damping ratio. In comparison with Den Hartog's solution, it is seen that %5 structural damping has little effect on the optimum frequency ratio, λ_{opt}, however it has some influence on the optimum damping ratio of the TMD, ζ_{opt}.

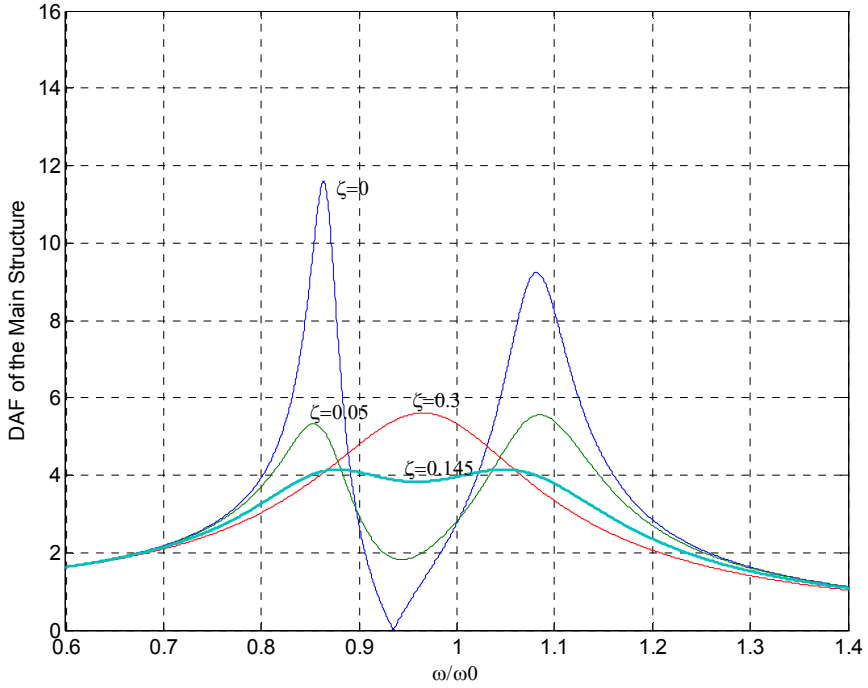

Figure 4.6. DAF for various damping ratios (λ=0.935, μ=0.05)

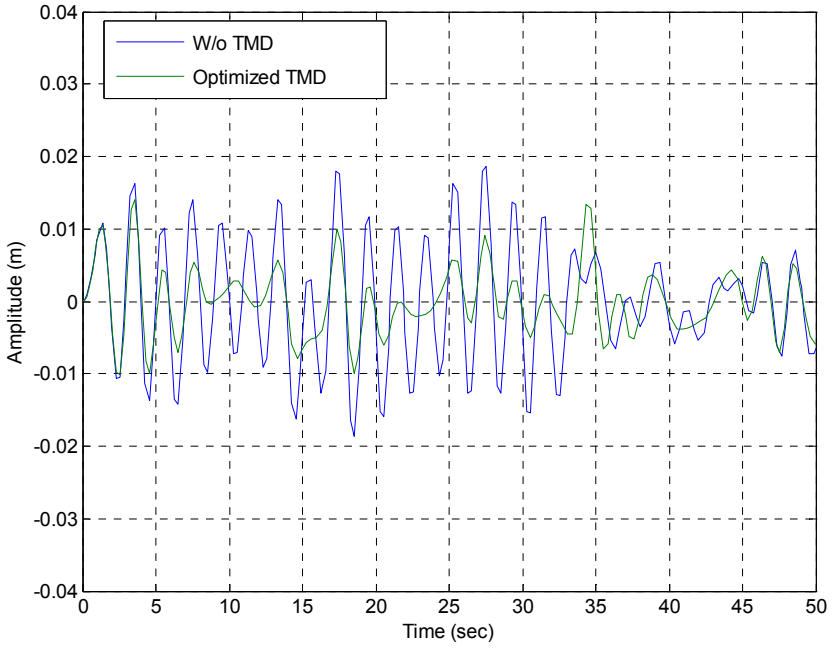

Figure 4.7. Comparison of Responses to white noise excitation

In Figure 4.7 response to white noise excitation is plotted including both combined structure/TMD system and for primary structure alone. It is obvious from the figure that TMD effectiveness is reduced if the main structure is damped, since energy dissipation due to the inherent structural damping causes the contribution of TMD to become a comparatively small portion. The maximum amplitude of the structure is reduced by %24 by use of TMD.

It is a known fact that TMD effectiveness is decreased if the TMD is detuned from the frequency of the main system. Errors in identification the structural frequency and in the damping ratio of TMD may lead to mistuning. Consequently, a single TMD is not a robust system. To validate this we introduce a mistuning factor γ, which is the ratio of the actual frequency of the structure to identified frequency of the structure.

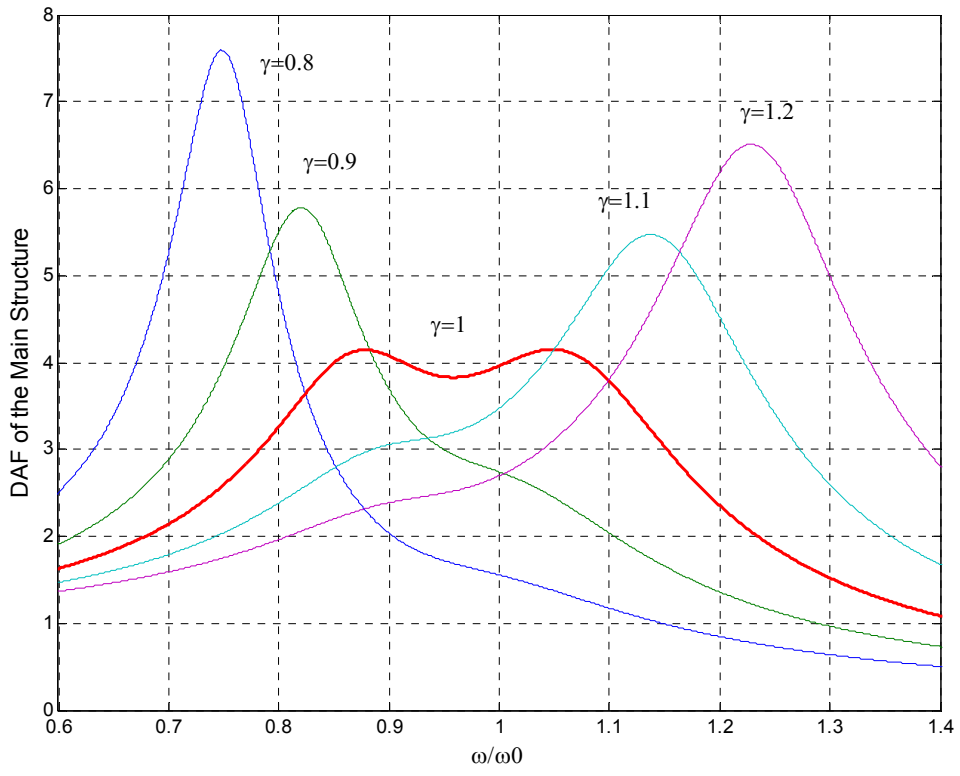

Figure 4.8. DAF for various mistuning factors (λ=0.935, μ=0.05)

It is evident Figure 4.8 that even if there is a %20 mistuning in the TMD, max. DAF is increased by %83. To increase the robustness a double tuned mass damper

(DTMD), consisting of one larger mass block and one smaller mass block connected to larger mass block, can be used.

4.3. Double Tuned Mass Damper (DTMD)

The equation of motion of the DTMD structure system can be written as follows:

$$m_s\ddot{x}_s + \left[c_s\dot{x}_s + c_1(\dot{x}_s - \dot{x}_1)\right] + \left[k_s x_s + k_1(x_s - x_1)\right] = F(t \tag{4.27}$$

$$m_1\ddot{x}_1 + \left[c_1(\dot{x}_1 - \dot{x}_s) + c_2(\dot{x}_1 - \dot{x}_2)\right] + \left[k_1(x_1 - x_s) + k_2(x_1 - x_2)\right] = 0 \tag{4.28}$$

$$m_2\ddot{x}_2 + c_2(\dot{x}_2 - \dot{x}_1) + k_2(x_2 - x_1) = 0 \tag{4.29}$$

Where, subscript s donates for the main structure, subscript 1 donates for the larger mass block and subscript 2 donates for the smaller mass block. F(t) is the input excitation; m, k, c are respectively the mass, stiffness, and damping coefficients; x_s is the displacement of the main structure with respect to the ground, x_1 represents the displacement of the larger mass block with respect to the ground and x_2 represents the displacement of the smaller mass block with respect to the ground. Rest of the procedure is similar to TMD case.

Once we denote:

$$\mu_1 = \frac{m_1}{m_s}; \mu_2 = \frac{m_2}{m_s}; \lambda_1 = \frac{\omega_1}{\omega_0}; \lambda_2 = \frac{\omega_2}{\omega_0}$$

$$\zeta_s = \frac{c_s}{2m_s\omega_0}; \zeta_1 = \frac{c_1}{2m_1\omega_1}; \zeta_2 = \frac{c_2}{2m_2\omega_2}$$

$$\omega_0 = \sqrt{k_s / m_s}; \omega_1 = \sqrt{k_1 / m_1}; \omega_2 = \sqrt{k_2 / m_2}$$

Transferring Equations (4.27), (4.28) and (4.29) into frequency domain by Laplace transform which is defined as Z(s) = L[z(t)] and introducing the above parameters gives:

$$X_s s^2 + \left[2\omega_0 \zeta_s X_s + 2\lambda_1 \omega_0 \zeta_1 \mu_1 (X_s - X_1)\right] s + \left[\omega_0^2 X_s + \mu_1 \lambda_1^2 \omega_0^2 (X_s - X_1)\right] = F / m_s \tag{4.30}$$

$$(\mu_1 X_1) s^2 + \left[2\lambda_1 \omega_0 \zeta_1 \mu_1 (X_1 - X_s) + 2\lambda_2 \omega_0 \zeta_2 \mu_2 (X_1 - X_2)\right] s + \left[\mu_1 \lambda_1^2 \omega_0^2 (X_1 - X_s) + \mu_2 \lambda_2^2 \omega_0^2 (X_1 - X_2)\right] = 0 \tag{4.31}$$

$$(\mu_2 X_2) s^2 + \left[2\lambda_2 \omega_0 \zeta_2 \mu_2 (X_2 - X_1)\right] s + \left[\mu_2 \lambda_2^2 \omega_0^2 (X_2 - X_1)\right] = 0 \tag{4.32}$$

In which:

$X_s = X_s(s) = L[x_s]$,

$X_1 = X_1(s) = L[x_1]$,

$X_2 = X_2(s) = L[x_2]$,

$F = F(s) = L[F(t)]$,

Equations (4.30), (4.31) and (4.32) can be written in matrix form as follows:

$$\begin{bmatrix} A(s) & B(s) & 0 \\ B(s) & F(s) & G(s) \\ 0 & G(s) & I(s) \end{bmatrix} \begin{bmatrix} X_s \\ X_1 \\ X_2 \end{bmatrix} = \begin{bmatrix} 1 \\ 0 \\ 0 \end{bmatrix} F / m_s \tag{4.33}$$

In which:

$$A(s) = s^2 + (2\omega_0 \zeta_s + 2\lambda_1 \omega_0 \zeta_1 \mu_1) s + \omega_0^2 + \mu_1 \lambda_1^2 \omega_0^2$$

$$B(s) = (-2\lambda_1 \omega_0 \zeta_1 \mu_1) s - \mu_1 \lambda_1^2 \omega_0^2$$

$$F(s) = \mu_1 s^2 + (2\lambda_1 \omega_0 \zeta_1 \mu_1 + 2\lambda_2 \omega_0 \zeta_2 \mu_2) s + \mu_1 \lambda_1^2 \omega_0^2 + \mu_2 \lambda_2^2 \omega_0^2$$

$$G(s) = (-2\lambda_2 \omega_0 \zeta_2 \mu_2) s - \mu_2 \lambda_2^2 \omega_0^2$$

$$I(s) = \mu_2 s^2 + (2\lambda_2 \omega_0 \zeta_2 \mu_2) s + \mu_2 \lambda_2^2 + \omega_0^2$$

Transfer Function of the main structure can be found by solving the Eq. (4.33):

$$TF_s(s) = \frac{X_s}{F} = \frac{1}{m_s} \frac{F(s)I(s) - G(s)G(s)}{A(s)F(s)I(s) - A(s)G(s)G(s) - B(s)B(s)I(s)} \tag{4.34}$$

Once the Transfer Function is obtained Dynamic Amplification Factor can be calculated through setting s=iω in the Transfer Function and computing $k_s \left| TF_s(i\omega) \right|$. Then optimum values are calculated using the minimum-maximum amplitude procedure. If damping ratio ζ_s of the structure and mass ratio μ of the TMD is known, the optimization procedure is analogous to TMD case but this time there is four parameters to be optimized. The damping ratios ζ_1, ζ_2 and frequency ratios λ_1, λ_2 for the first and second masses respectively will be calculated by:

- The damping ratio ζ_1, ζ_2 and frequency ratio of the first mass λ_1 of the DTMD is fixed to zero; within the range of 0.8-1.2 control parameter λ_2 is increased with an increment of 0.01. In each increment maximum amplitude of Dynamic Amplification Factor (DAF_{max}) is determined. The optimum value in this step is the one which minimize the maximum response amplitude, min (DAF_{max}).
- The frequency ratio of the first mass λ_1 of the DTMD is increased by an increment of 0.01 and the rest of the procedure in Step 1 is repeated thus another minimum for the maximum response amplitude is calculated. By comparing all the minimum values that have been computed, the minimum [min (DAF_{max})], for the range of $0.8 < \lambda_1 < 1.2$ is determined.
- The damping ratio of the second mass ζ_2 of the DTMD is increased by an increment of 0.01 and Step 1 and Step 2 are repeated to obtain minimum [min [min (DAF_{max})]] for the range of $0 < \zeta_2 < 0.20$.
- The damping ratio of the first mass ζ_1 of the DTMD is increased by an increment of 0.01 and Steps 1-3 are repeated to obtain minimum [min [min [min (DAF_{max})]]] for the range of $0 < \zeta_2 < 0.20$.
- The corresponding parameters which make min. [min [min [min (DAF_{max})]]] are the optimum parameters for the DTMD system.

An equivalent single-degree-of-freedom system with following parameters is considered to be equipped with DTMD. The equivalent stiffness, k_s=1.10^5 kN/m; the equivalent mass, m_s=1.10^4 tons; and damping coefficient, c_s=3,16.10^3 N/s which corresponds to a %5 structural damping. The mass ratio, μ_1, of the large TMD unit is %4.5 and mass ratio, μ_2, of the small TMD unit is %0.5. Following aforementioned procedures the optimum parameters are obtained as 1.01 for frequency ratio of the large TMD to primary structure, λ_1, and 0.92 for frequency ratio of the small TMD to primary structure, λ_2. The optimum damping ratio of the smaller TMD unit,ζ_2, is 0.19, and there is no damping requirement for the large TMD unit.

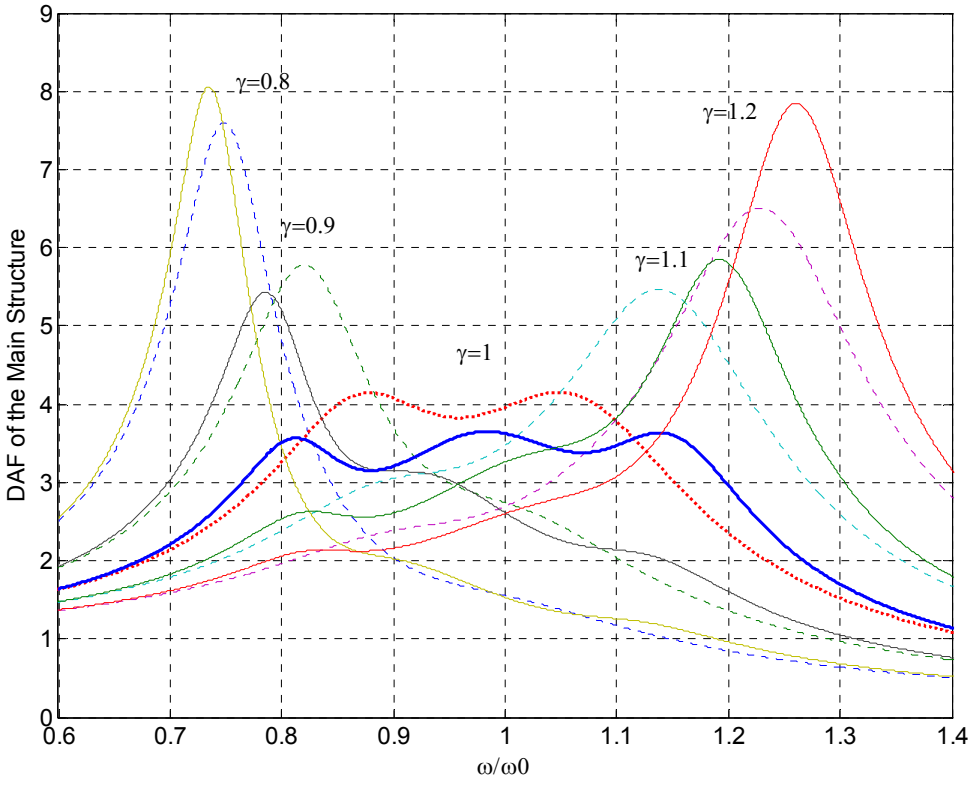

Figure 4.9. DAF of the main structure with respect to TMD and DTMD: TMD (----), DTMD (——)

It is evident from Figure 4.9 and Table 4.2 that, DTMD is more effective and robust to the changes of forced frequency ratio than TMD in reducing the DAF of the main structure when mistuning factor, γ, is 1. The DAF is 4.15 in TMD case where as DAF is

3.65 in DTMD case. On the other hand sensitivity to miscalculation of actual building frequency is not improved. Once we introduce a mistuning factor of 0.8 the DAF becomes 7.59 in the TMD case which corresponds to a % 83 increase in DAF, on the other hand DAF in DTMD case is 8.06 which is a % 94 increase in DAF. Also, for a mistuning factor of 1.2 in TMD case DAF is 6.51 and in DTMD case DAF is 7.85. These values corresponds to % 57 increase in TMD case and % 89 increase in DTMD case.

Table 4.2. The maximum DAF of the main structure respectively with the TMD and DTMD cases

DAF,γ	0.8	0.9	1.0	1.1	1.2
Max. DAF of the main structure with TMD	7.592	5.781	4.151	5.472	6.509
Max. DAF of the main structure with DTMD	8.056	5.433	3.652	5.851	7.846

For further study, multiple tuned mass dampers (MTMD) will be investigated for its performance and robustness

4.4. Multiple Tuned Mass Damper (MTMD)

The equation of motion of the MTMD structure system can be written as follows:

$$m_s\ddot{x}_s + \left[(c_s + \sum_{n=1}^{N} c_n)\dot{x}_s - c_n\dot{x}_n)\right] + \left[(k_s + \sum_{n=1}^{N} k_n)x_s - k_n x_n\right] = F(t) \tag{4.35}$$

$$m_n\ddot{x}_n + \left[k_n(x_n - x_s)\right] + \left[c_n(x_n - x_s)\right] = 0 \qquad \text{n=1,2…N} \tag{4.36}$$

Where, subscript s donates for the main structure, subscript n donates for the n^{th} TMD in the MTMD. F(t) is the input excitation; m, k, c are respectively the mass, stiffness, and damping coefficients; x_s is the displacement of the main structure with respect to the ground, x_n represents the displacement of the n^{th} TMD with respect to the ground.

Let's denote:

$$\mu_n = \frac{m_n}{m_s}; \lambda_n = \frac{\omega_n}{\omega_0}$$
$$\zeta_s = \frac{c_s}{2m_s\omega_0}; \zeta_n = \frac{c_n}{2m_n\omega_n} \qquad \text{n=1, 2… N}$$
$$\omega_0 = \sqrt{k_s / m_s}; \omega_n = \sqrt{k_n / m_n}$$

Transferring Equations (4.35) and (4.36) into frequency domain by Laplace transform which is defined as Z(s) = L[z(t)] and introducing the above parameters gives:

$$X_s s^2 + \left[(2\omega_0\zeta_s + \sum_{n=1}^{N} 2\lambda_n\omega_0\zeta_n\mu_n)X_s - (2\lambda_n\omega_0\zeta_n\mu_n)X_n \right] s$$
$$+ \left[(\omega_0^2 + \sum_{n=1}^{N} \mu_n\lambda_n^2\omega_0^2)X_s - (\mu_n\lambda_n^2\omega_0^2)X_n \right] = F / m_s \qquad \text{n=1,2…N} \qquad (4.37)$$

$$(\mu_n X_n)s^2 + \left[2\lambda_n\omega_0\zeta_n\mu_n(X_n - X_s)\right]s + \left[\mu_n\lambda_n^2\omega_0^2(X_n - X_s)\right] = 0 \qquad \text{n=1,2…N} \qquad (4.38)$$

In which:

X_s=X_s(s)=L[x_s],
X_n=X_n(s)=L[x_n],
F=F(s)=L[F(t)],

Equations (3.37) and (3.38) can be cast into matrix form as follows:

$$\begin{bmatrix} A(s) & [B(s)]_{1xN} \\ [B(s)]_{Nx1} & diag[G(s)]_{NxN} \end{bmatrix} \begin{bmatrix} X_s \\ [X_n]_{Nx1} \end{bmatrix} = \begin{bmatrix} 1 \\ [0]_{Nx1} \end{bmatrix} F / m_s \qquad (4.39)$$

In which:

$$A(s) = s^2 + (2\omega_0\zeta_s + \sum_{n=1}^{N} 2\lambda_n\omega_0\zeta_n\mu_n)s + \omega_0^2 + \sum_{n=1}^{N} \mu_n\lambda_n^2\omega_0^2$$

$$B_n(s) = -(2\lambda_n\omega_0\zeta_n\mu_n)s - \mu_n\lambda_n^2\omega_0^2 \qquad \text{n=1, 2… N}$$

$$G_n(s) = \mu_n s^2 + (2\lambda_n\omega_0\zeta_n\mu_n)s + \mu_n\lambda_n^2\omega_0^2 \qquad \text{n=1, 2… N}$$

Transfer Function of the main structure can be found by solving the Eq. (4.39).

$$TF_s(s) = \frac{1}{m_s}\frac{G_1(s)G_2(s).....G_N(s)}{A(s)G_1(s)G_2(s).....G_N(s) - \sum_{j=1}^{N} B_j^2(s)G_1(s)..G_{j-1}(s)G_{j+1}(s)....G_N(s)} \tag{4.40}$$

The natural frequency of the j[th] TMD can be expressed as:

$$\omega_j = \omega_C\left[1 + (j - \frac{N+1}{2})\frac{\Delta\omega}{N-1}\right] \tag{4.41}$$

where, ω_C is the central frequency which is the average of the natural frequencies of each TMD unit in the MTMD and $\Delta\omega$ is the frequency range which is defined as:

$$\Delta\omega = \frac{\omega_N - \omega_1}{\omega_C} \tag{4.42}$$

Varying frequencies of each TMD unit is realized by altering the mass while keeping stiffness and damping constants fixed. So if we set a total mass ratio μ for the system, stiffness of TMD units can be calculated from:

$$k_{TMD} = \frac{\mu m_s}{\sum_{i=1}^{N} 1/\omega_i^2} \tag{4.43}$$

Once k_{TMD} is found, mass of each TMD unit can be easily calculated from:

$$m_j = \frac{k_{TMD}}{\omega_j^2} \tag{4.44}$$

Similarly, once m_j is calculated, damping constant of each TMD can be expressed from:

$$c_{TMD} = \zeta_j 2 m_j \omega_j \tag{4.45}$$

By combining Equation (4.44) with Equation (4.45) and defining an average damping ratio ζ_T, which is the average of damping ratios of each TMD unit Equation (4.45) becomes:

$$c_{TMD} = 2\zeta_T k_{TMD} \omega_C \tag{4.46}$$

As described earlier minimum-maximum amplitude procedure is used to find optimum values for controlling parameters $\Delta\omega$ and ζ_T. The ranges $0<\Delta\omega<0.30$ and $0<\zeta_T<0.15$ are adopted for frequency range and average damping ratio respectively.

As can be seen from Table 4.3 max DAF decreases when the total mass ratio μ increases. Also, for a given mass ratio there is an optimum average damping ratio and corresponding optimum frequency range where max DAF is minimum. Furthermore when the number of TMD units increases max DAF keeps decreasing, however it is also noted that the pace of this decrease slows down with the increasing number of TMD units. Furthermore it should be noted that unlike TMD or DTMD cases, requirement for damping ratio is much smaller in MTMD. For larger numbers of N, damping requirement for each TMD unit is lesser but it necessitates a broader frequency range. To evaluate the robustness of MTMD a mistuning factor, γ, is introduced and consequently following results are obtained.

Drawn from Figure 4.10 and Table 4.4, what worth noting is for γ=0.8,0.9 DTMD is more robust than MTMD, on the contrary when γ is greater than 1.0 i.e. γ=1.1,1.2 MTMD is far more robust than DTMD. For γ=1 DTMD is slightly better than MTMD and they are both superior to TMD. It is also seen that the number of TMD units in MTMD has a modest effect on the response but it can be concluded that robustness in N=3 is better than the higher number of TMD units however, compared to higher number of TMD units N=3 gives higher results in terms of DAF when γ=1. In this sense number of TMD units is

like a tradeoff between performance and robustness. All in all N=5 gives the average results and like a trend line between N=3 and N=9.

Table 4.3. The max. DAF of the main structure with the MTMD for various mass ratios

Total number of TMD units N	Total Mass ratio μ=0.03			Total Mass ratio μ=0.05		
	The average damping ratio ζ_T	The frequency range $\Delta\omega$	max DAF	The average damping ratio ζ_T	The frequency range $\Delta\omega$	max DAF
3	0.05	0.19	4.81	0.06	0.25	4.23
	0.06	0.19	4.74	0.07	0.24	4.17
	0.07	0.18	4.71	0.08	0.24	4.11
	0.08	0.17	4.79	0.09	0.23	4.11
	0.09	0.17	4.85	0.10	0.23	4.15
	0.10	0.16	4.96	0.11	0.22	4.18
5	0.02	0.25	5.13	0.04	0.32	4.10
	0.03	0.25	4.72	0.05	0.31	3.96
	0.04	0.25	4.52	0.06	0.30	3.91
	0.05	0.24	4.79	0.07	0.29	3.91
	0.06	0.23	4.56	0.08	0.28	3.96
	0.07	0.22	4.66	0.09	0.27	4.04
9	0.01	0.29	5.33	0.02	0.37	4.14
	0.02	0.29	4.57	0.03	0.36	3.88
	0.03	0.28	4.44	0.04	0.35	3.79
	0.04	0.27	4.45	0.05	0.34	3.81
	0.05	0.25	4.49	0.06	0.33	3.85
	0.06	0.25	4.58	0.07	0.32	3.90
13	0.01	0.29	5.33	0.02	0.39	3.95
	0.02	0.29	4.57	0.03	0.37	3.87
	0.03	0.28	4.44	0.04	0.36	3.80
	0.04	0.27	4.45	0.05	0.35	3.80
	0.05	0.25	4.49	0.06	0.34	3.85
	0.06	0.25	4.58	0.07	0.33	3.89

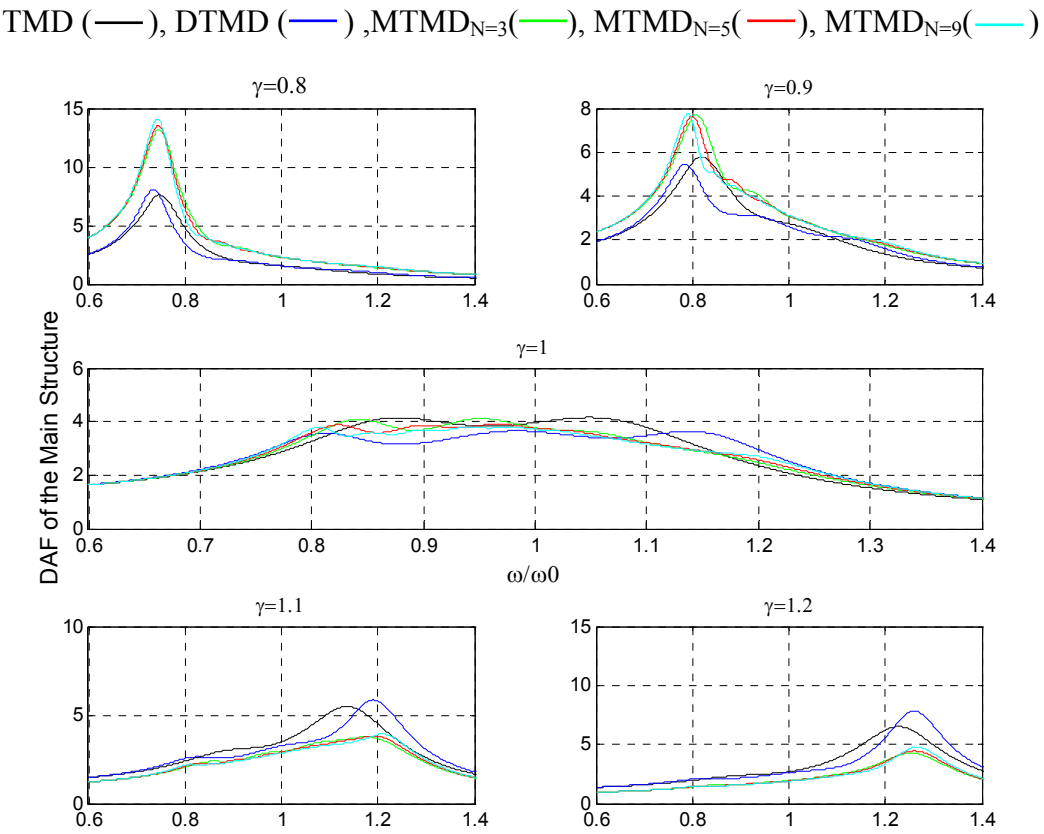

Figure 4.10. DAF of the main structure for TMD, DTMD and MTMD cases

Table 4.4. The max. DAF of the main structure respectively with the TMD, DTMD and MTMD cases

DAF,γ	0.8	0.9	1.0	1.1	1.2
Max. DAF of the main structure with TMD	7.592	5.781	4.151	5.472	6.509
Max. DAF of the main structure with DTMD	8.056	5.433	3.652	5.851	7.846
Max. DAF of the main structure with MTMD N=3	13.203	7.713	4.112	3.752	4.263
Max. DAF of the main structure with MTMD N=5	13.519	7.632	3.908	3.793	4.453
Max. DAF of the main structure with MTMD N=9	14.082	7.756	3.795	3.915	4.764

Table 4.5. The max. DAF of the main structure with the $MTMD_{\gamma}$

Total number of TMD units N	Total Mass ratio μ=0.05 The frequency ratio ω_C / ω_s	The average damping ratio ζ_T	The frequency range $\Delta\omega$	max DAF
3	0.96	0.06	0.22	3.94
		0.07	0.21	3.83
		0.08	0.20	3.80
		0.09	0.20	3.81
		0.10	0.19	3.83
		0.11	0.18	3.86
5	0.97	0.04	0.29	3.80
		0.05	0.28	3.72
		0.06	0.27	3.69
		0.07	0.26	3.72
		0.08	0.25	3.76
		0.09	0.24	3.82
9	0.97	0.02	0.35	3.91
		0.03	0.33	3.71
		0.04	0.32	3.63
		0.05	0.31	3.65
		0.06	0.30	3.69
		0.07	0.28	3.73
13	0.97	0.02	0.36	3.85
		0.03	0.34	3.73
		0.04	0.32	3.69
		0.05	0.31	3.67
		0.06	0.30	3.69
		0.07	0.30	3.73

Table 4.6. The max. DAF of the main structure respectively with the TMD, DTMD and MTMDγ cases

DAF,γ	0.8	0.9	1.0	1.1	1.2
Max. DAF of the main structure with TMD	7.592	5.781	4.151	5.472	6.509
Max. DAF of the main structure with DTMD	8.056	5.433	3.652	5.851	7.846
Max. DAF of the main structure with MTMDγ N=3	12.706	7.177	3.806	4.525	4.776
Max. DAF of the main structure with MTMDγ N=5	13.155	7.219	3.695	4.485	4.893
Max. DAF of the main structure with MTMDγ N=9	13.742	7.325	3.628	4.775	5.237

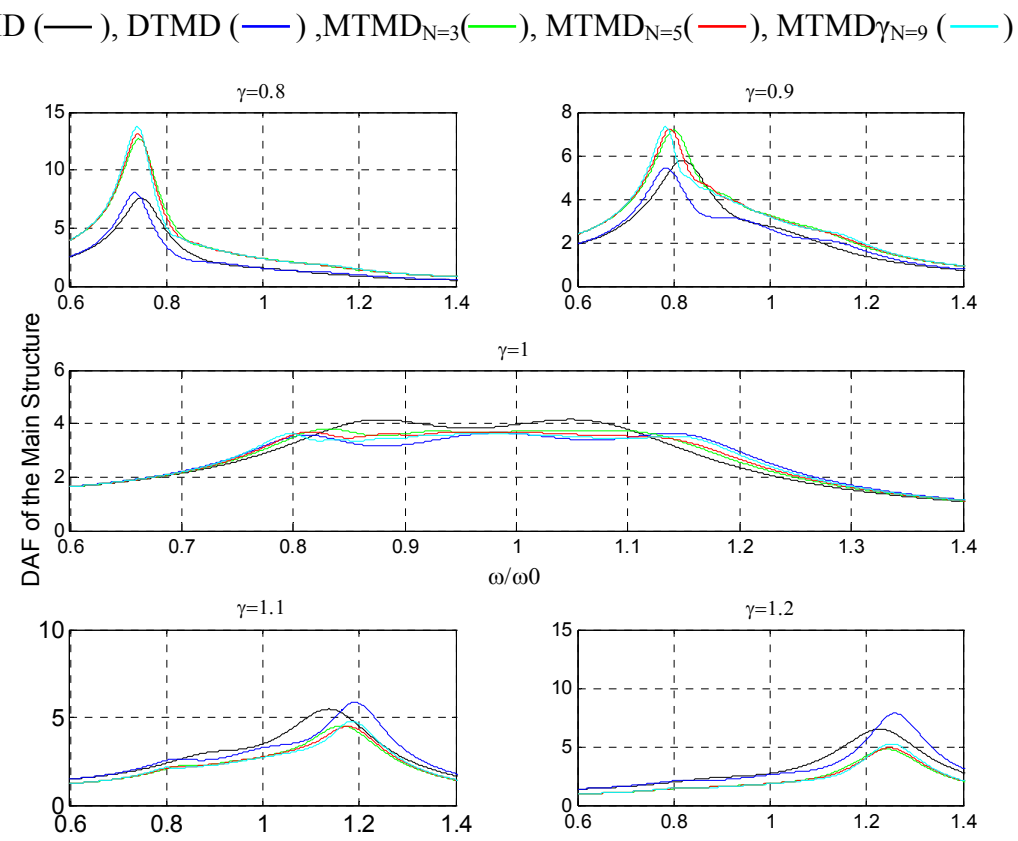

Figure 4.11. DAF of the main structure for TMD, DTMD and MTMDγ cases

Results related to MTMD in Table 4.4 are obtained by setting central frequency, ω_C, to fundamental frequency of the structure, ω_0. However, it is evident that max DAF is not symmetric with respect to mistuning factor, γ. For smaller values of γ DAF is much greater than that of the larger values of γ. It might be an indication of central frequency should be shifted, so we introduce a frequency ratio as a third optimization parameter within the range of $0.9 < \omega_C / \omega_s < 1.1$ and repeat the min max amplitude optimization procedure. Corresponding model is designated as $MTMD_\gamma$ and results can be seen in Table 4.5. It is observed that max DAF is improved in all cases. It is interesting to note that except for N=3, for all cases the frequency ratio is the same, and when compared to MTMD case a narrow frequency range is required for optimum response.

When we look at the robustness of the MTMDγ, the main conclusion from Table 4.6 and Figure 4.11 would be, there is an improvement in robustness since DAF is decreased for γ is different than unity but it is not much pronounced as in the case of $\gamma=1$. All in all, when compared to MTMD, MTMDγ gives better performance in all aspects but improvement is minor especially when robustness is considered. It is interesting to note that sensitivity to mistuning factor γ is more when $\gamma<1$, whereas when $\gamma>1$ MTMD is more robust than DTMD and TMD cases. Though, MTMD has a clear advantage for it necessitates small damping ratios in TMD units which render it a perfect solution when small damping units like tuned liquid dampers (TLD) are concerned.

4.5. Tuned Liquid Damper (TLD)

Lateral sloshing is the wave formation on the surface of a liquid when a tank partially filled with liquid is oscillated. When fluid container is subjected to horizontal accelerations, free liquid surface moves up at one side of the container and moves down at the other forming a wave; then the up half-wave moves down and the down half-wave moves up, and so on. The wave motion has a natural frequency which depends on the container geometry and dimensions, liquid depth and the acceleration of the gravity. During back and forth motion of the container, a fraction of liquid oscillates relative to container and this dynamic effect can be represented by an equivalent mechanical model where the oscillating liquid is represented by a mass spring model and the stationary liquid

is represented with a mass rigidly attached to the container. Figure 4.12 is a graphical representation of the equivalent mechanical model.

The solution of the sloshing problem necessitates solving of some partial differential equations satisfying boundary conditions however; in 1954 Housner [136] presented an approximate method which avoids partial differential equations and series and presents solutions for a number of cases in simple closed form. The essence of the method is the estimation of a simple type of flow which is similar to the actual fluid movement and this is simple flow is used to determine the pressure. The method is analogous to the Rayleigh-Ritz method used in the theory of elasticity and it always overestimates the forces.

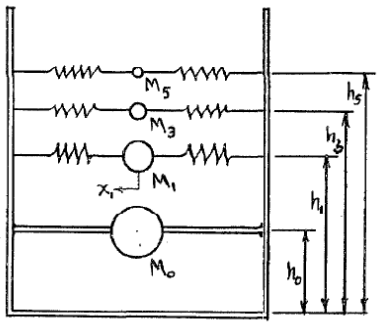

Figure 4.12. Mechanical Model of Sloshing [136]

For a circular container with a radius R, fluid depth h and acceleration of the gravity g; stationary fluid mass M_0, oscillating fluid mass M_1 and natural sloshing frequency ω is given by the following equations:

$$M_0 = M \frac{\tanh\left(\sqrt{3}R/h\right)}{\sqrt{3}R/h} \tag{4.47}$$

$$M_1 = M \frac{1}{4}\sqrt{\frac{27}{8}}\frac{R}{h}\tanh\left(\sqrt{\frac{27}{8}}\frac{h}{R}\right) \tag{4.48}$$

$$\omega^2 = \frac{g}{R}\sqrt{\frac{27}{8}}\tanh\left(\sqrt{\frac{27}{8}}\frac{h}{R}\right) \tag{4.49}$$

Once the above equations are obtained, equivalent spring stiffness K can be computed from:

$$K = \omega^2 M_1 \tag{4.50}$$

It should be noted that, Equations (4.48) and (4.49) are valid when h ≤ 1.6 R. As the container becomes tall and narrow the fluid below depth h=1.6R should be considered to move with the container as a rigid body.

Once TLD is resembled by an equivalent mechanical model, optimization solutions to TMD systems are also valid for TLD systems.

5. PROPOSED CONTROL STRATEGY

5.1. Introduction

The influence of environmental forces to civil engineering structures can be related to the height of the structure. For short and midrise buildings for example the earthquake plays an important role. The traditional approach to seismic design is to provide a combination of strength and ductility to resist the imposed loads. Actually the equation is simple. If we regard the earthquake as an energy input to the structure, some portion of the energy is used by kinetic energy which is in turn related to the displacement of the structure and the rest is dissipated by hysteretic energy i.e. rotation of structural members such as beams, columns, braces and structural walls, also by damaging of nonstructural elements, mostly infill walls. The proportion of how input energy is dissipated relies on the capabilities of the building. If it is strong enough to withstand the seismic forces, than the building will remain in elastic range and all the input energy will be used as kinetic energy, however in economical point of view this approach is not efficient since civil engineering structures possess some inherent ductility, in other words capacity to make some plastic deformation. Thus, identification of this inherent ductility or in energy terms the dissipated energy by plastic rotations will reveal the necessary stain energy or in force terms necessary strength of the primary structural members. This is the underlying concept of seismic design codes although there might be some exceptions. In fact a certain level of structural and nonstructural damage is accepted by using the inherent ductility of the structure, and the desired performance level in this case is the life safety of the occupants. However there might be alternative performance levels such as immediate occupancy and/or operational level for critical structures such as hospitals, police stations, communication centers and major highway bridges in which the operation of the structure is desired to maintain after a major earthquake. This is only possible if we increase the strength of the structure or finding alternative ways of energy dissipation.

Supplemental damping systems can be substitute for hysteretic damping and eliminate the need for additional strength for higher performance levels. Supplemental dampers dissipate the energy mechanically and activated through movements of main

structural system. According to the component of movement, these dissipating systems can be divided into three different categories: displacement-activated devices, velocity-activated devices and motion-activated devices [138].

Displacement-activated devices dissipate energy through the relative displacements that occur between their connecting points. These dampers are usually independent of the frequency of the motion. Also, the forces generated by these devices are usually in-phase with the internal forces resulting from vibration. Displacement-activated devices include metallic dampers, friction dampers and self-centering dampers.

Velocity-activated devices dissipate energy through the relative displacements that occur between their connecting points. The force-displacement response of these dampers usually depends on the frequency of the motion. Also, the forces generated by these devices are usually out-of-phase with the internal forces resulting from vibration. Velocity-activated devices include purely viscous and visco-elastic dampers.

Tuned Mass Dampers are examples of motion-activated devices in which flow of energy in the structure is disturbed through the vibration of a secondary system. In the essence tuned-mass dampers (TMDs) or vibration absorbers are mass-spring-dashpot systems that are tuned to a particular vibration mode of the structure on which they are installed. Under a dynamic excitation, the TMD resonates at the same frequency as the main structure but out-of-phase from it, thereby diverting the input energy from the main structure into itself.

All in all, supplemental damping systems can be considered as a substitute to inherent structural energy dissipation mechanisms either kinetic or hysteretic. Another solution would be to reduce the input energy rather than dissipating it. It is well known from earthquake design spectrums that when the period is increased the transmitted energy from earthquake to structure decreases. The seismic isolation systems lengthen the vibrational period of the structure due to the high flexibility of the isolation system that is usually located between the foundation and superstructure. The isolators designed to have a much lower stiffness than the structure they are installed. From energy point of view, a seismic isolation system limits the transfer of seismic energy to the superstructure. This is

naturally accomplished for high rise structures since they have inherently long vibrational periods. So, importance of environmental influence shifted from earthquakes to winds for high rise buildings. The nature of the problem is also changed. For earthquake cases, seismic safety or operational integrity of the building is important and accordingly based on performance criterion degree of plastic deformations are decided, however for wind cases no plastic deformation is allowed and all the vibration energy is dissipated by kinetic energy. This is understandable since earthquake motion is reversible there are no permanent displacements or if any they are in tolerable limits although plastic deformations take place. However, for wind cases input excitation is one sided and plastic deformations may lead to progressive failure. Since all the wind induced deformation should take in elastic range, the problem is no more structural integrity but occupancy comfort and/or integrity of nonstructural elements such as cladding. The kinetic damping is very low in high-rise buildings so the main aim of the supplementary dampers is to increase the damping to alleviate the resonance vibrational peaks and/or to maintain the floor accelerations below a certain threshold which is human perception. To summarize, for short and mid-rise buildings earthquake influence is more prominent than wind, and structural safety is in question. The input is the ground acceleration and considered response quantity is the inter-story floor displacements since it can be directly related to rate of plastic deformations, thus performance levels. For high-rise buildings however, the input is wind force and the response quantity in question is either total displacement for the integrity of the secondary elements or floor accelerations for human comfort or both simultaneously.

As can be recalled from Chapter 4 that tuned mass damper is most effective when it is tuned to the frequency of the input excitation. However environmental loads, such as wind and earthquake loads, possess many frequency components. Therefore, tuned mass dampers are optimized to render them effective for such large bandwidth inputs. Generally optimization target is to minimize the frequency response peaks of a structure/TMD system. For a selected mass ratio μ, that is the ratio of TMD mass to structure mass, frequency ratio λ, which is the ratio of the frequency of the TMD to frequency of the structure, and damping ratio ζ of the TMD are optimized by resorting to a numerical search procedure called minimum-maximum amplitude procedure. The example structure defined in Section 3.6 is equipped with TMD of mass ratio μ=0.01. The calculated optimum

parameters in this case would be 0.98 for frequency ratio λ and %7 for damping ratio ζ. In Figure 5.1 Bode magnitude plots of the plant, combined non-optimum TMD/plant and finally combined optimum TMD/plant systems are plotted for displacement response. As can be observed, the sharp peak of the plant at resonance frequency is smoothed by the attachment of the optimum TMD. The reduction in peak response is about %40 even though for a small mass ratio μ=0.01. On the other hand when we look at the non-optimized TMD/plant system the great reduction in response can be observed around tuning frequency, however there are now two resonance peaks since the combined system is a two-degree-of-freedom system. These two new resonance peaks are the sole reason why we have to resort to optimal TMD since we can not guarantee to have a disturbance which's driving frequency falls into the operating range, which is defined as the narrow zone between the two resonance peaks where non-optimal TMD is most effective.

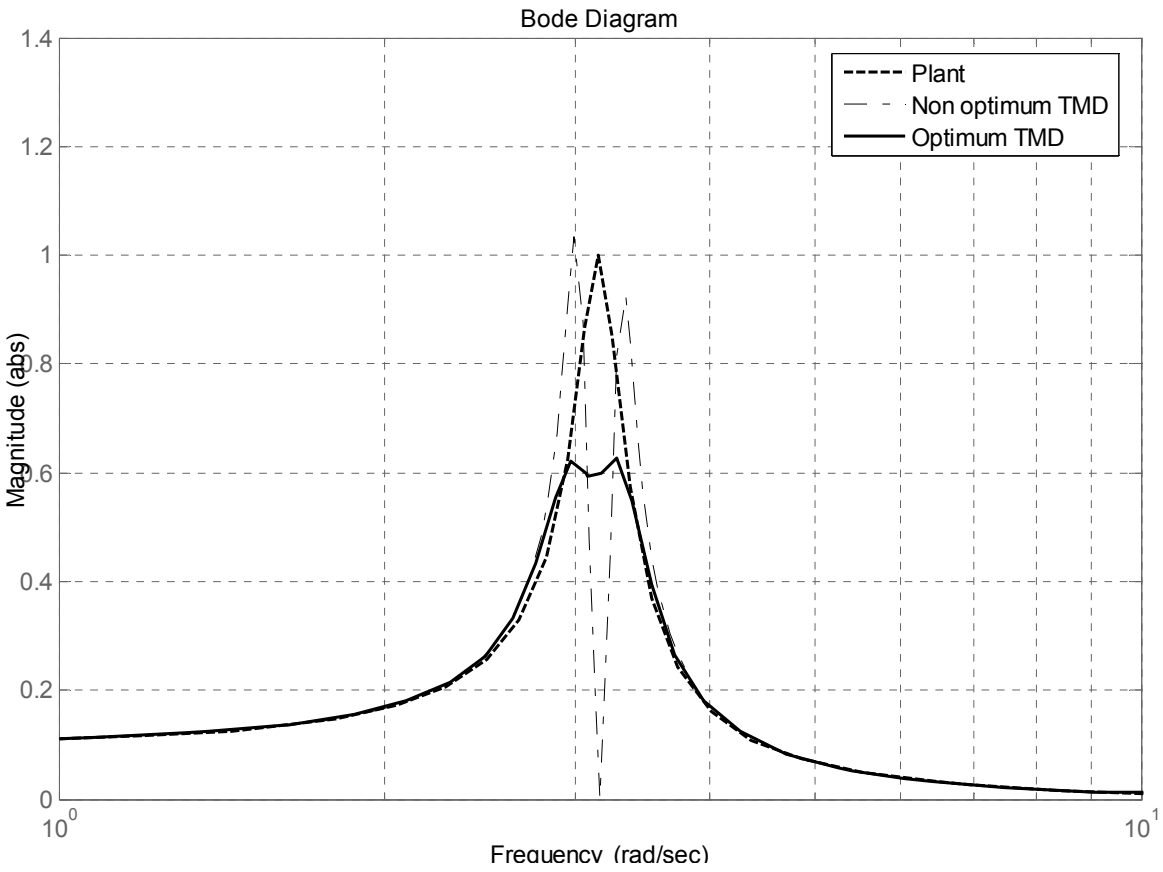

Figure 5.1. Bode magnitude plots of plant, non-optimal TMD and optimal TMD

It can be recalled from Section 2.1.2 that when a system is excited by a harmonic input, the steady state system response is also harmonic with the same frequency of the input. That is to say output frequency of the system matches the input frequency of the system in steady sate, and since the TMD is tuned to the frequency of the structure it is also tuned to the input excitation where TMD is most effective. So what if we might able to force the structure to mimic a steady state response to a single frequency harmonic excitation. Then what ever the actual frequency content of the excitation, the shaped structure will response as if it is excited by a single frequency harmonic input. Two questions arise in this stage:

- Will non-optimized TMD be effective as indicated in Figure 5.1, when it is tuned to the frequency of the shaped response of the structure?
- Can we shape a response of a structure to behave as if it is the response of a single frequency harmonic excitation whether the actual excitation has a wide band frequency content?

The answer to the first question will be investigated in the subsequent sections but the answer to the second question is already given in Section 3. In a tracking system, if a reference signal is chosen to be a harmonic function, than the response of the controlled system will try to track the reference command. This is illustrated in Figures 5.2 and 5.3. A single-degree-of-freedom system described in Section 3.6 is excited with a white noise input shown in Figure 5.2 and the response of the controlled system is monitored when a reference signal is a sinusoidal command with frequency 2 rad/sec. It can be seen from the following figures that the controlled system is successfully tracking the reference signal; consequently the frequency of the response is 2 rad/sec.

Since we are able to alter the frequency of the response in a tracking system, next step will be to attach a TMD to the controlled system and monitor the effectiveness of this new hybrid system. When compared to a standard regulator problem, for the same level displacement response smaller control forces are expected since, in the hybrid system states are not regulated to zero. Instead controller tries to help TMD to suppress vibration effectively.

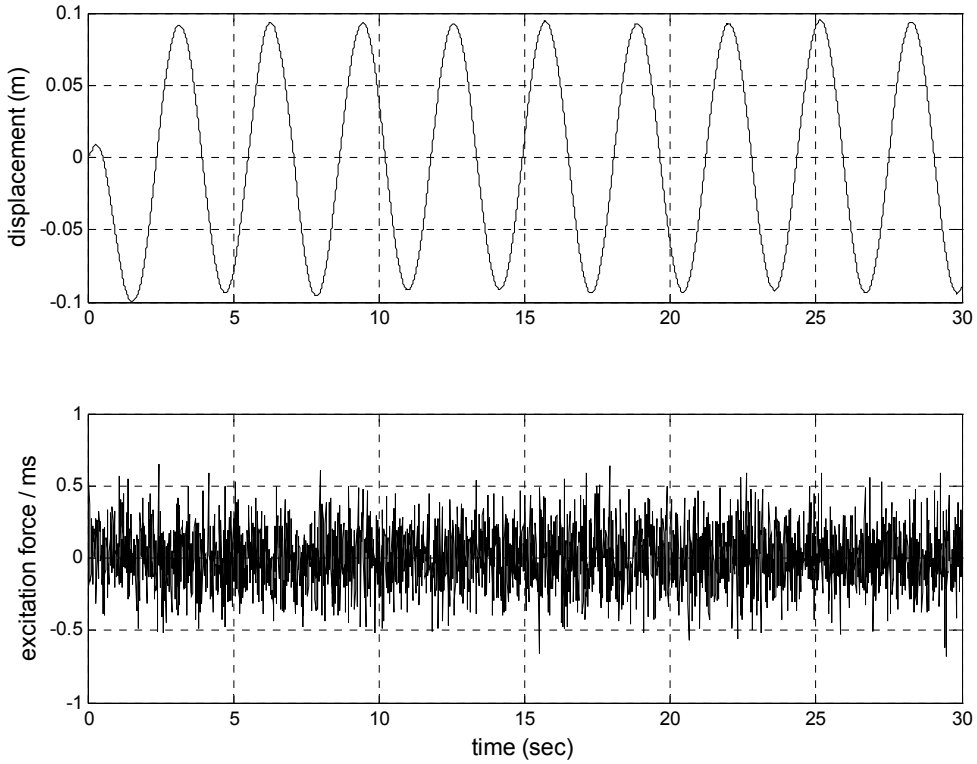

Figure 5.2. Tracking performance of an LQR controller to white noise disturbance

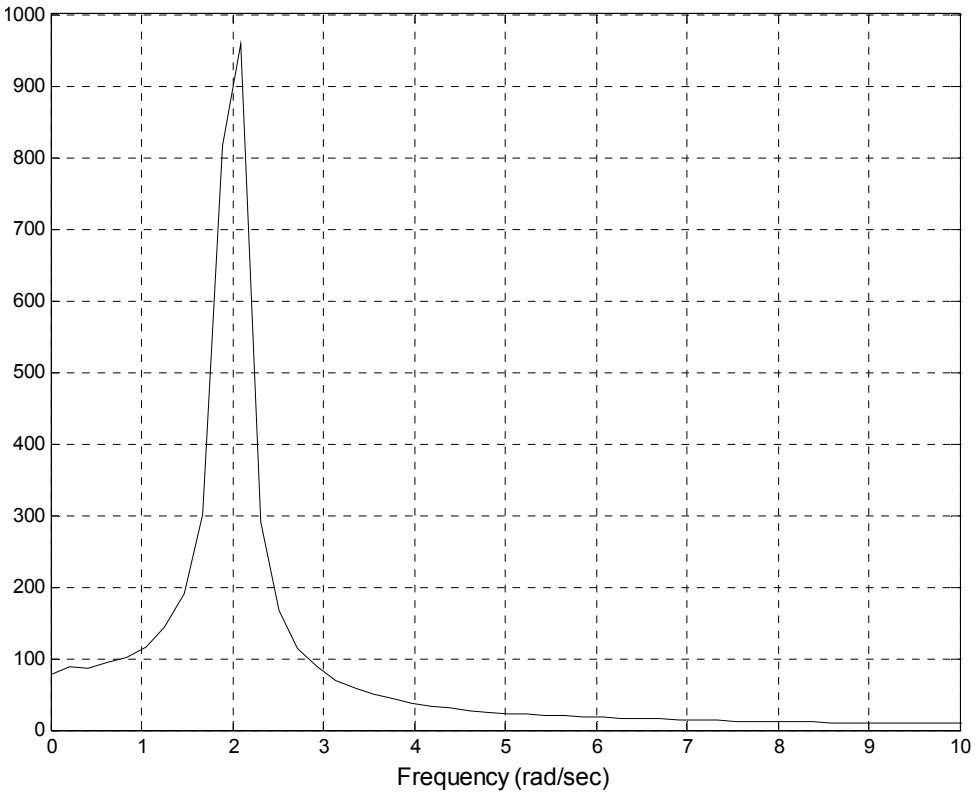

Figure 5.3. FFT of the tracking system response

5.2. Tracking Type LQR Control System with Attached TMD

5.2.1. State Equations of the Combined TMD/Structure System

Single-degree-of-freedom (SDOF) system given in Section 3.6 and non-optimized TMD with mass ratio μ=0.01 has following structural parameters:

k_s = 1.10^5 kN/m
c_s = $3{,}16.10^3$ kN/s (%5 damping)
m_s = 1.10^4 tons
k_{TMD} = 1000 kN/m
m_{TMD} = 100 tons
c_{TMD} = 0 N/s (%0 damping)

Equations of motion for the two-degree-of-freedom system is given by

$$m_s \ddot{y}_s(t) + (c_s + c_{TMD})\dot{y}_s(t) + (k_s + k_{TMD})y_s(t) = k_{TMD}y_{TMD} + c_{TMD}\dot{y}_{TMD} + u(t) + w(t) \quad (5.1)$$

$$m_{TMD}\ddot{y}_{TMD}(t) + c_{TMD}\dot{y}_{TMD}(t) + k_{TMD}y_{TMD}(t) = k_{TMD}y_s + c_{TMD}\dot{y}_s \quad (5.2)$$

If we define the states $x_1 = y_s, x_2 = y_{TMD}$, $x_3 = \dot{y}_s$ and $x_4 = \dot{y}_{TMD}$ the state equations of the plant can be written as:

$$\begin{bmatrix} \dot{x}_1 \\ \dot{x}_2 \\ \dot{x}_3 \\ \dot{x}_4 \end{bmatrix} = \begin{bmatrix} 0 & 0 & 1 & 0 \\ 0 & 0 & 0 & 1 \\ -10.1 & 0.1 & -0.3316 & 0 \\ 10 & -10 & 0 & 0 \end{bmatrix} \begin{bmatrix} x_1 \\ x_2 \\ x_3 \\ x_4 \end{bmatrix} + \begin{bmatrix} 0 & 0 \\ 0 & 0 \\ 1 & -1 \\ 0 & 0 \end{bmatrix} \begin{bmatrix} w(t) \\ u(t) \end{bmatrix} \quad (5.3)$$

$$\begin{bmatrix} y_1 \\ y_2 \\ y_3 \\ y_4 \end{bmatrix} = \begin{bmatrix} 1 & 0 & 0 & 0 \\ 0 & 1 & 0 & 0 \\ 0 & 0 & 1 & 0 \\ 0 & 0 & 0 & 1 \end{bmatrix} \begin{bmatrix} x_1 \\ x_2 \\ x_3 \\ x_4 \end{bmatrix} \quad (5.4)$$

In Equation (5.4) the excitation and control forces entered to system are normalized with the mass of the plant. The plant has four outputs. First and second outputs are the displacement of the structure and TMD respectively, third and the fourth outputs are the velocities of the structure and TMD respectively.

5.2.2. Tracking a reference sinusoidal signal

Performance index in quadratic form is written as:

$$J = \frac{1}{2}\int_0^{t_f} x^T(t)Q(t)x(t) + u^T(t)R(t)u(t)dt \tag{5.5}$$

The frequency of the plant is calculated as 3.16 rad/sec. When the plant is equipped with TMD the frequencies of the combined 2-DOF system are 3.03 rad/sec and 3.30 rad/sec. The TMD is tuned to the frequency of the plant, thus operating frequency is also 3.16 rad/sec. Therefore the displacement output of the plant is desired to track a sinusoidal signal with frequency 3.16 rad/sec and amplitude of 0.1m which is the static deflection of the plant to a unit step disturbance. In state space form linear reference model for the sinusoidal signal can be written as:

$$\begin{bmatrix} \dot{z}_1 \\ \dot{z}_2 \end{bmatrix} = \begin{bmatrix} 0 & 1 \\ -9.986 & 0 \end{bmatrix} \begin{bmatrix} z_1 \\ z_2 \end{bmatrix} \tag{5.6}$$

$$\tilde{y} = \begin{bmatrix} 1 & 0 \end{bmatrix} \tag{5.7}$$

where z and $\tilde{y}$ are the states and the output of the reference model. If we combine the states of the plant and the reference model the augmented plant is then:

$$\begin{bmatrix} \dot{x}_1 \\ \dot{x}_2 \\ \dot{x}_3 \\ \dot{x}_4 \\ \dot{z}_1 \\ \dot{z}_2 \end{bmatrix} = \begin{bmatrix} 0 & 0 & 1 & 0 & 0 & 0 \\ 0 & 0 & 0 & 1 & 0 & 0 \\ -10.1 & 0.1 & -0.3316 & 0 & 0 & 0 \\ 10 & -10 & 0 & 0 & 0 & 0 \\ 0 & 0 & 0 & 0 & 0 & 1 \\ 0 & 0 & 0 & 0 & -9.9856 & 0 \end{bmatrix} \begin{bmatrix} x_1 \\ x_2 \\ x_3 \\ x_4 \\ z_1 \\ z_2 \end{bmatrix} + \begin{bmatrix} 0 \\ 0 \\ 1 \\ 0 \\ 0 \\ 0 \end{bmatrix} u(t) \tag{5.8}$$

the state weighting matrix, Q, and the control force weighting matrix, R, are selected as:

$$Q = \begin{bmatrix} 1 & 0 & 0 & 0 \\ 0 & 0 & 0 & 0 \\ 0 & 0 & 1 & 0 \\ 0 & 0 & 0 & 0 \end{bmatrix}, R = 0.1 \tag{5.9}$$

In the state weighting matrix emphasis is given to displacement and velocity components of the plant. Then the state weighting matrix for the augmented plant is calculated according to Equation (3.42) as:

$$\hat{Q} = \begin{bmatrix} 1 & 0 & 0 & 0 & -1 & 0 \\ 0 & 0 & 0 & 0 & 0 & 0 \\ 0 & 0 & 1 & 0 & 0 & -1 \\ 0 & 0 & 0 & 0 & 0 & 0 \\ -1 & 0 & 0 & 0 & -1 & 0 \\ 0 & 0 & -1 & 0 & 0 & -1 \end{bmatrix} \tag{5.10}$$

By utilizing $\hat{Q}$ the calculated LQR gain is as the following:

$$K = \begin{bmatrix} 0.48798 & 0.0001 & 3.0118 & 0.00146 & 1.5363 & -0.0097 \end{bmatrix} \tag{5.11}$$

The first four terms of the gain matrix K are associated with the states of the plant, and last two terms are associated with the states of the reference model. As can be viewed from the elements of controller gain, K, the second and fourth terms which are related to

TMD displacement and velocity are near zero which suggests that the motion of the TMD unit is not controlled. The controlling terms are associated with the plant displacement and velocity.

The control input to the plant can be written as:

$$u(t) = K_1 m(t) + K_2 r(t) \tag{5.12}$$

and in matrix form:

$$u = \begin{bmatrix} 0.48798 & 0.0001 & 3.0118 & 0.00146 \end{bmatrix} \begin{bmatrix} x_1 \\ x_2 \\ x_3 \\ x_4 \end{bmatrix} + \begin{bmatrix} 1.5363 & -0.0097 \end{bmatrix} \begin{bmatrix} r_1 \\ r_2 \end{bmatrix} \tag{5.13}$$

The output of the controller is the input to the plant, so the state equation can be rewritten as:

$$\begin{bmatrix} \dot{x}_1 \\ \dot{x}_2 \\ \dot{x}_3 \\ \dot{x}_4 \end{bmatrix} = \begin{bmatrix} 0 & 0 & 1 & 0 \\ 0 & 0 & 0 & 1 \\ -10.588 & 0.01 & -3.3281 & -0.0015 \\ 10 & -10 & 0 & 0 \end{bmatrix} \begin{bmatrix} x_1 \\ x_2 \\ x_3 \\ x_4 \end{bmatrix} + \begin{bmatrix} 0 & 0 & 0 \\ 0 & 0 & 0 \\ 1 & 1.5363 & 0.0971 \\ 0 & 0 & 0 \end{bmatrix} \begin{bmatrix} w \\ r_1 \\ r_2 \end{bmatrix} \tag{5.14}$$

Together with the system states we also desire to see the control forces, so the output equation becomes:

$$\begin{bmatrix} y_1 \\ y_2 \\ y_3 \\ y_4 \\ u \end{bmatrix} = \begin{bmatrix} 1 & 0 & 0 & 0 \\ 0 & 1 & 0 & 0 \\ 0 & 0 & 1 & 0 \\ 0 & 0 & 0 & 1 \\ 0.488 & 0.0001 & 3.012 & 0.0015 \end{bmatrix} \begin{bmatrix} x_1 \\ x_2 \\ x_3 \\ x_4 \end{bmatrix} + \begin{bmatrix} 0 & 0 & 0 \\ 0 & 0 & 0 \\ 0 & 0 & 0 \\ 0 & 0 & 0 \\ 0 & -1.5363 & -0.0097 \end{bmatrix} \begin{bmatrix} w \\ r_1 \\ r_2 \end{bmatrix} \tag{5.15}$$

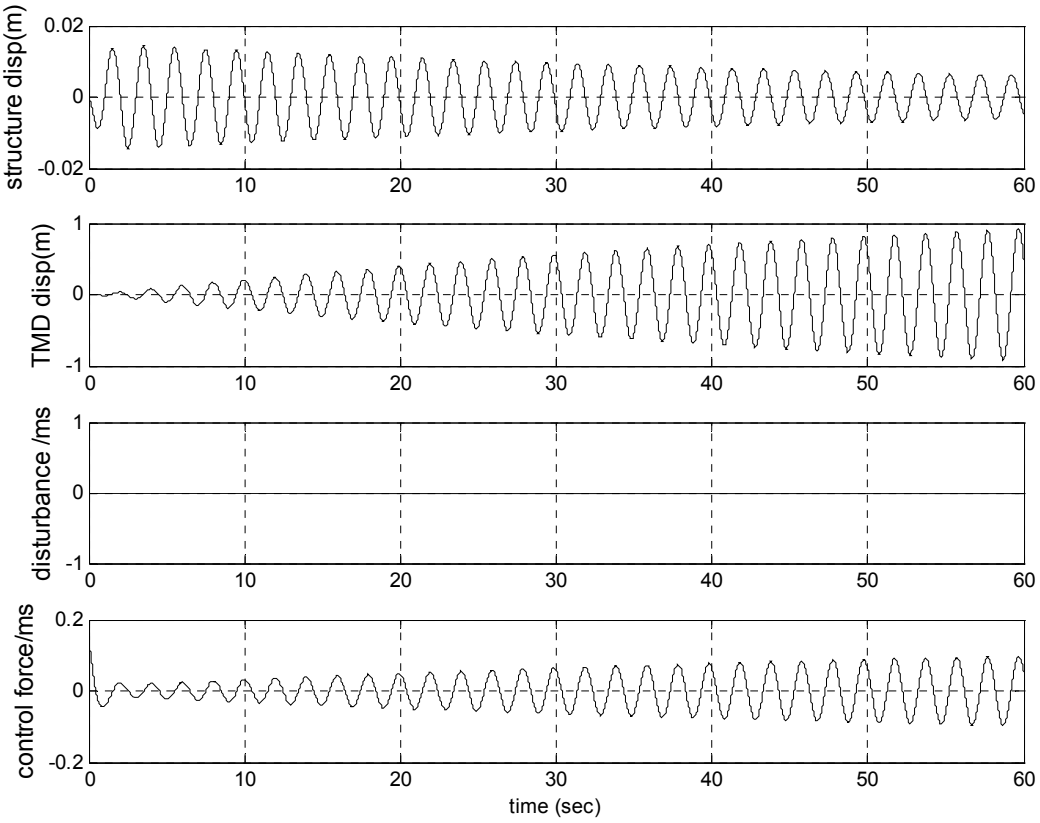

Figure 5.4. LQR tracking performance (R=0.1, w=0)

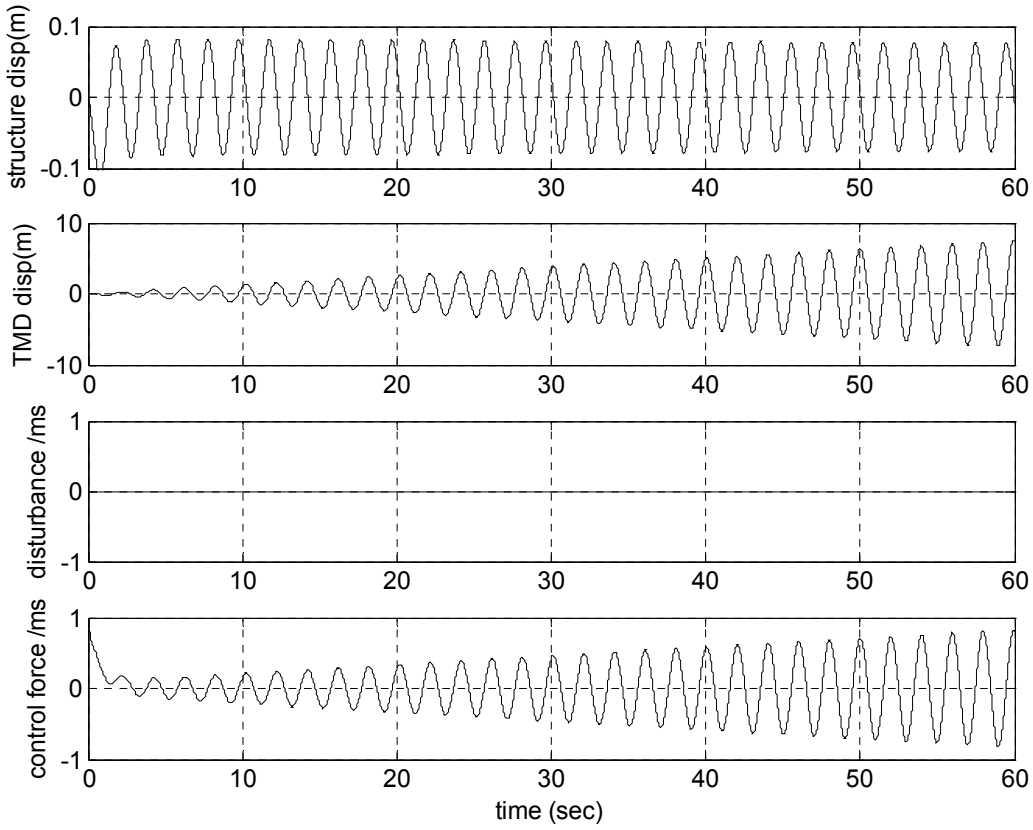

Figure 5.5. LQR tracking performance (R=0.001, w=0)

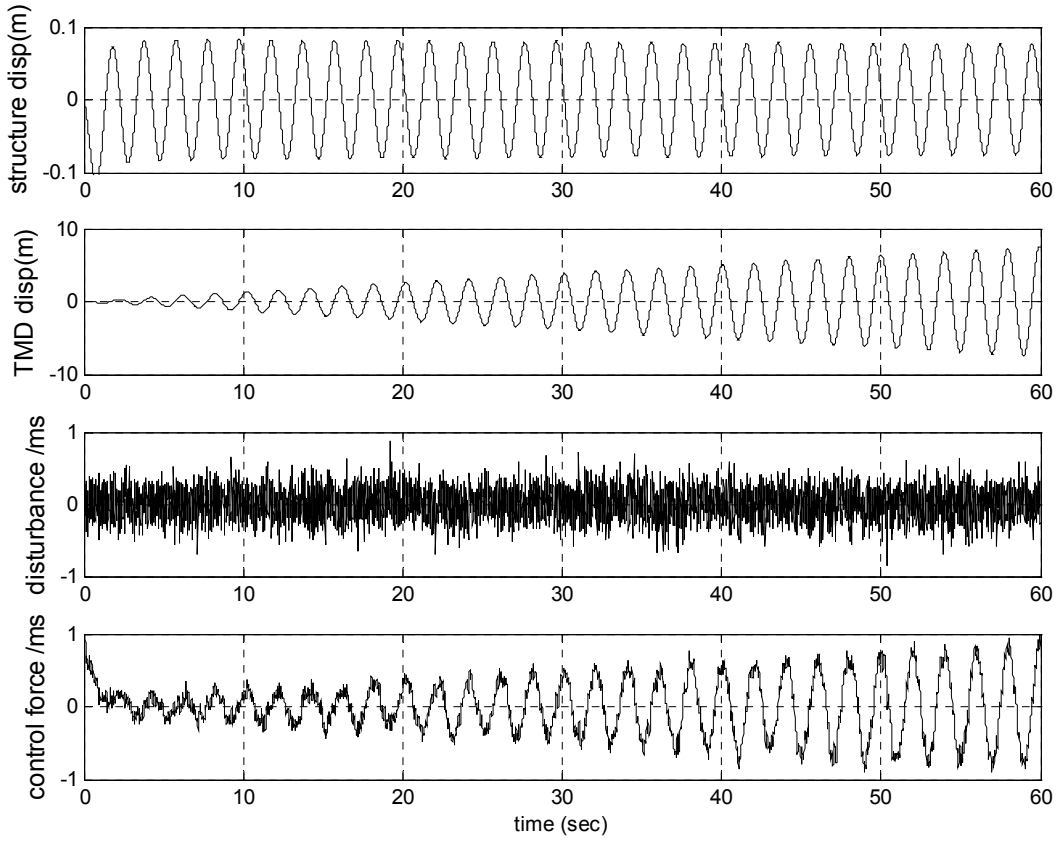

Figure 5.6. LQR tracking performance (R=0.001, w=white noise of 0 dBW power)

In Figures 5.4 and 5.5 tracking system response to a sinusoidal reference signal is shown. In this case external disturbance is set to zero so the problem is pure tracking problem. When there is no tight control as in Figure 5.4 controller could not able to track reference amplitude, displacement of the structure is gradually decreasing due to the damping effect of TMD. It can be further observed that displacement of the TMD unit is gradually increasing suggesting that counter forces inflicted by TMD unit to structure is increasing hence effectiveness of TMD is enhanced. On the other hand, control forces are also gradually increasing in time since controller try to cope with the damping effect of TMD to maintain the response in constant amplitude. This is more pronounced when the emphasis is given to response by setting R=0.001. In this case Figure 5.5 suggest that controller is able to track the reference amplitude but at the expense of very high control forces. In the case of an external disturbance, a white noise disturbance with a power of 0 dBW is entered to the plant. In Figure 5.6 it is demonstrated that tracking performance is not affected from the external output and effectiveness of TMD is not compromised.

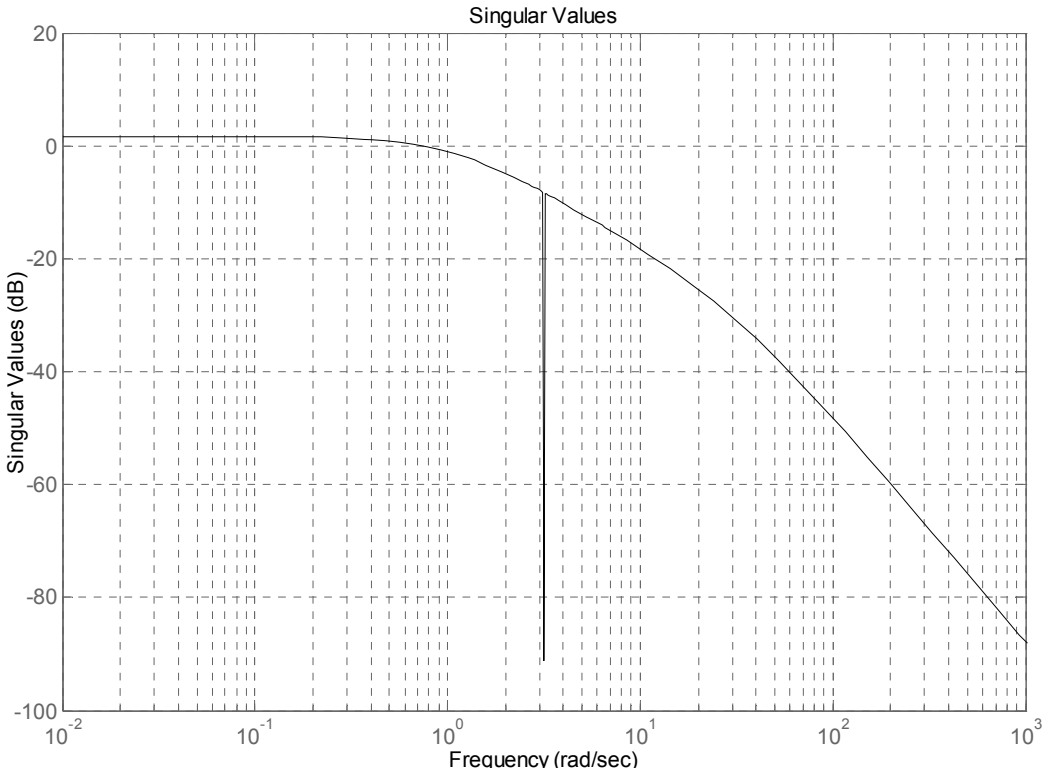

Figure 5.7. Singular values of the LQR closed loop system from input to plant disp.

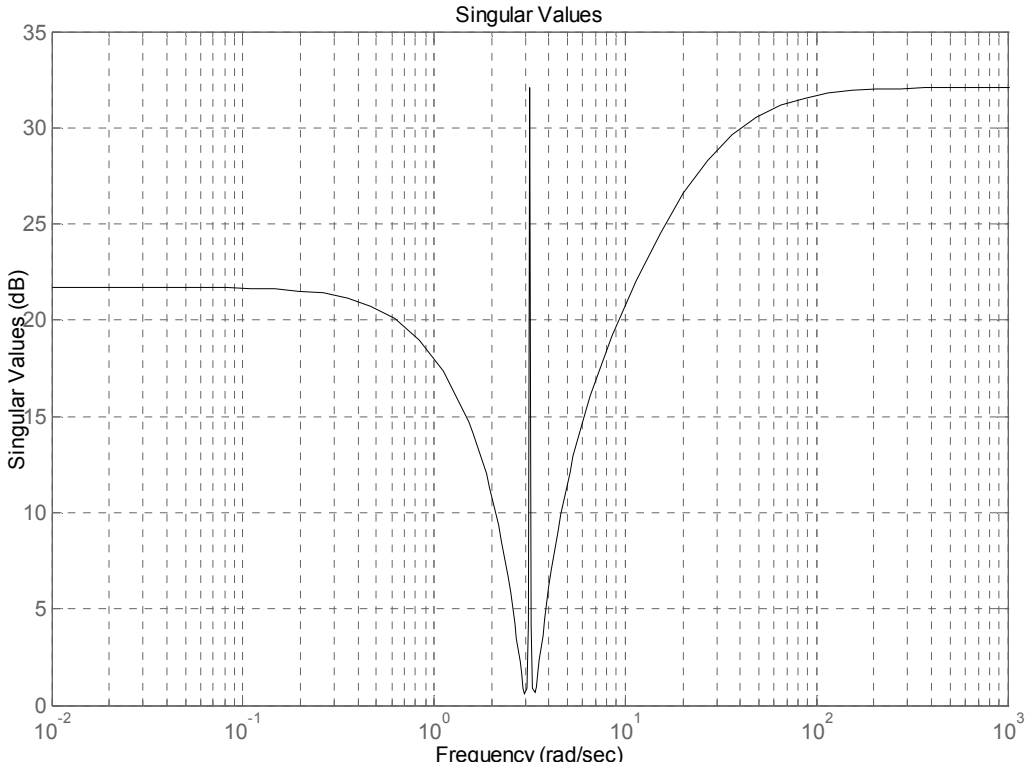

Figure 5.8. Singular values of the LQR closed loop system from input to cont. force

When it comes to singular value plots of the closed-loop system, verification of time response can be observed. At frequency 3.16 rad/sec the displacement response of the plant drops suddenly. This is an indication that TMD is operating in its full performance when the controlled system tracks a harmonic reference command which's frequency is set to the operating frequency of undamped TMD. However, when we inspect Figure 5.8 it is seen that at operating frequency controller forces increase sharply. This is due to constant amplitude tracking. TMD is trying to suppress the response on the other hand controller is trying to maintain displacement response at constant level. Thus, there is a conflict with TMD objectives and controller objectives. At this point a new question arises:

- Is there a way a controller tracks the frequency of a reference signal but not its amplitude?

The answer of the above question is not easy. In literature tracking systems are defined to track the trajectory of a reference signal. Thus error functions are defined in time domain and frequency domain error definitions are not present. However, some how if we can manage to render the reference command in harmony with the closed-loop system output in terms of amplitude than it is possible to alleviate the problem. In this case when TMD is suppressing the response, the controller will follow the updated amplitudes and any conflicts should be resolved. However this is not an easy task either. The first thing that comes in mind is too feed back the plant output as a reference signal. However, if we monitor the plant output in Figure 5.1, we see two dominant amplitudes that correspond to natural frequencies of the combined TMD/structure system. It might have been a good idea to filter out this frequency content and pass only the desired tracking frequency however, the desired tracking frequency is in the operating range of TMD unit. Therefore, that signal is suppressed by the TMD and there is left no signal to feedback. An alternative approach would be to pass the strong signals, i.e. the signal corresponding to natural frequency of the combined TMD/structure system and filter out the remaining signals. Then the frequency of the filtered response could be frequency shifted to desired frequency utilizing techniques frequently used by communication engineers [139]. However this approach requires successive filtering of the signal, which increases the order of the closed-loop system too much and may cause instability due to filter dynamics. Secondly, such an approach is successful only in early steps when the plant response is

dominated by amplitudes that correspond to natural frequencies of the combined TMD/structure system. Then controller forces the system to track the frequency shifted desired signal and the frequency of the closed-loop response matches the desired frequency. However controller still thinks the reference signal corresponds to natural frequency of the combined TMD/structure system and tries to shift the frequency of the signal once more to a new undesired value. Maybe, problem can be solved by monitoring the frequency content of the reference signal and using this information to implement a decision process whether the frequency of the reference is shifted or not. Nonetheless it will complicate the controller to much.

A simpler solution will be to track a reference model instead of a reference signal. This is called model matching problem and controller tries to match the states of the plant with the states of an idealized mathematical model. If we chose a simple oscillator as a reference model and set the natural frequency of the reference model as the operating frequency of the TMD, under same disturbance the response levels of the actual system and idealized mathematical system will be more or less the same. Thus by tracking the response of an idealized model two aspects are accomplished. First, frequency of the reference signal is the desired frequency which is the operating frequency of the TMD and second, the amplitude of the reference signal is more or less in harmony with the closed-loop response.

5.3. LQR as a Model Matching Problem

5.3.1. Model Matching Problem Formulation in LQR Setting

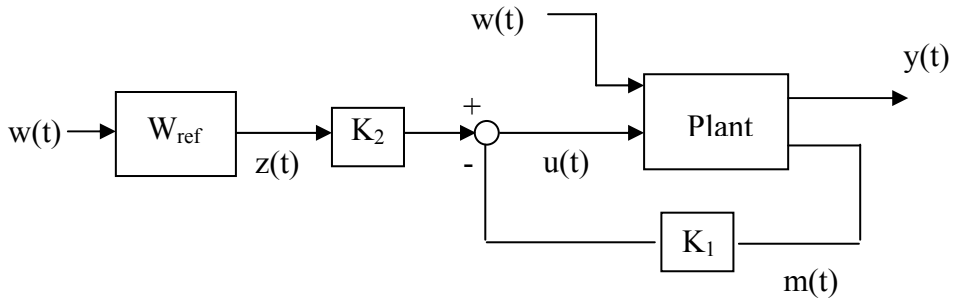

Figure 5.9. Closed-loop system for Model Matching Problem

As can be observed from Figure 5.9 model matching problem is very similar to reference signal tracking in LQR setting. K_1 is the feedback gain to meet the requirement of disturbance rejection and K_2 is the feedforward term applied to the reference signal, which optimizes the response of the overall system to the disturbance input such that the output of the system would be near to that of the chosen ideal system W_{ref}.

If we write the state equations for the plant as:

$$\dot{x} = Ax + \begin{bmatrix} B_w & B_u \end{bmatrix} \begin{bmatrix} w \\ u \end{bmatrix} \tag{5.16}$$

$$m = C_y x \tag{5.17}$$

by defining the desired linear reference model such as:

$$\dot{z} = Fz + Gw \tag{5.18}$$

$$\tilde{y} = Hz \tag{5.19}$$

also by defining the new state as the combination of plant states and reference model states as

$$\hat{x} = \begin{bmatrix} x \\ z \end{bmatrix} \tag{5.20}$$

Then the state equations of the augmented plant can be written as:

$$\begin{bmatrix} \dot{x} \\ \dot{z} \end{bmatrix} = \begin{bmatrix} A & 0 \\ 0 & F \end{bmatrix} \begin{bmatrix} x \\ z \end{bmatrix} + \begin{bmatrix} B_w & B_u \\ G & 0 \end{bmatrix} \begin{bmatrix} w \\ u \end{bmatrix} \tag{5.21}$$

If we combine the controller output and the state equations of the augmented plant we obtain:

$$\begin{bmatrix} \dot{x} \\ \dot{z} \end{bmatrix} = \begin{bmatrix} A & 0 \\ 0 & F \end{bmatrix} \begin{bmatrix} x \\ z \end{bmatrix} + B_u \begin{bmatrix} -K_1 C_y & -K_2 H \end{bmatrix} \begin{bmatrix} x \\ z \end{bmatrix} + \begin{bmatrix} B_w \\ G \end{bmatrix} w \tag{5.22}$$

or in compact form

$$\begin{bmatrix} \dot{x} \\ \dot{z} \end{bmatrix} = \begin{bmatrix} A - B_u K_1 C_y & -B_u K_2 H \\ 0 & F \end{bmatrix} \begin{bmatrix} x \\ z \end{bmatrix} + \begin{bmatrix} B_w \\ G \end{bmatrix} w \tag{5.23}$$

since we desire to see the control forces together with the plant states the output becomes:

$$\begin{bmatrix} y \\ u \end{bmatrix} = \begin{bmatrix} 1 & 0 \\ -K_1 C_y & -K_2 H \end{bmatrix} \begin{bmatrix} x \\ z \end{bmatrix} \tag{5.24}$$

5.3.2. Numerical Illustration

The selected reference model is an oscillator with natural frequency 3.16 rad/sec which is the operating frequency of TMD. If we introduce %5 damping to reference model, the state equations become:

$$\begin{bmatrix} \dot{z}_1 \\ \dot{z}_2 \end{bmatrix} = \begin{bmatrix} 0 & 1 \\ -9.986 & -0.3 \end{bmatrix} \begin{bmatrix} z_1 \\ z_2 \end{bmatrix} \tag{5.25}$$

$$\tilde{y} = \begin{bmatrix} 1 & 0 \end{bmatrix} \tag{5.26}$$

The plant is desired to track the reference model, however if we monitor the response of the reference model to a white noise input the displacement amplitude is beyond our target displacement of 0.005m. Thus in the state equations of the reference

model, mass normalized external disturbance is multiplied by 0.05. In this case maximum displacement amplitude will be less than 0.005m.

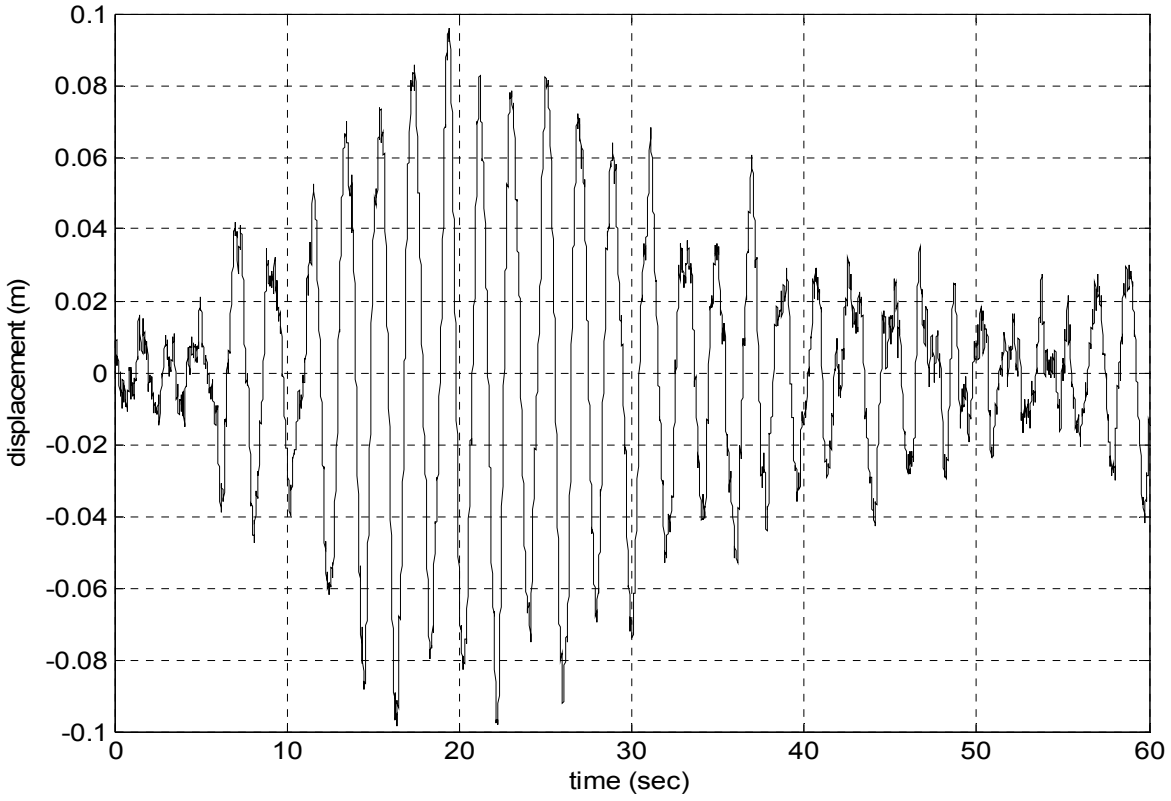

Figure 5.10. Displacement response of reference model

The augmented plant is then:

$$\begin{bmatrix} \dot{x}_1 \\ \dot{x}_2 \\ \dot{x}_3 \\ \dot{x}_4 \\ \dot{z}_1 \\ \dot{z}_2 \end{bmatrix} = \begin{bmatrix} 0 & 0 & 1 & 0 & 0 & 0 \\ 0 & 0 & 0 & 1 & 0 & 0 \\ -10.1 & 0.1 & -0.316 & 0 & 0 & 0 \\ 10 & -10 & 0 & 0 & 0 & 0 \\ 0 & 0 & 0 & 0 & 0 & 1 \\ 0 & 0 & 0 & 0 & -9.986 & -0.3 \end{bmatrix} \begin{bmatrix} x_1 \\ x_2 \\ x_3 \\ x_4 \\ z_1 \\ z_2 \end{bmatrix} + \begin{bmatrix} 0 & 0 \\ 0 & 0 \\ 1 & -1 \\ 0 & 0 \\ 0.05 & 0 \\ 0 & 0 \end{bmatrix} \begin{bmatrix} w \\ u \end{bmatrix} \quad (5.27)$$

For R=0.1 the calculated LQR gain is:

$$K_1 = \begin{bmatrix} 0.4880 & 0.0001 & 3.0118 & 0.0015 & -0.4485 & -2.7712 \end{bmatrix} \quad (5.28)$$

So the close loop state equations become:

$$\begin{bmatrix} \dot{x}_1 \\ \dot{x}_2 \\ \dot{x}_3 \\ \dot{x}_4 \\ \dot{z}_1 \\ \dot{z}_2 \end{bmatrix} = \begin{bmatrix} 0 & 0 & 1 & 0 & 0 & 0 \\ 0 & 0 & 0 & 1 & 0 & 0 \\ -10.59 & 0.01 & -3.328 & -0.0015 & 0.4485 & 2.771 \\ 10 & -10 & 0 & 0 & 0 & 0 \\ 0 & 0 & 0 & 0 & 0 & 1 \\ 0 & 0 & 0 & 0 & -9.986 & -0.3 \end{bmatrix} \begin{bmatrix} x_1 \\ x_2 \\ x_3 \\ x_4 \\ z_1 \\ z_2 \end{bmatrix} + \begin{bmatrix} 0 \\ 0 \\ 1 \\ 0 \\ 0.05 \\ 0 \end{bmatrix} [w] \quad (5.29)$$

$$\begin{bmatrix} y_1 \\ y_2 \\ y_3 \\ y_4 \\ u \end{bmatrix} = \begin{bmatrix} 1 & 0 & 0 & 0 & 0 & 0 \\ 0 & 1 & 0 & 0 & 0 & 0 \\ 0 & 0 & 1 & 0 & 0 & 0 \\ 0 & 0 & 0 & 1 & 0 & 0 \\ -0.488 & -0.0001 & -3.0118 & -0.0015 & -0.4485 & -2.7712 \end{bmatrix} \begin{bmatrix} x_1 \\ x_2 \\ x_3 \\ x_4 \\ z_1 \\ z_2 \end{bmatrix} \quad (5.30)$$

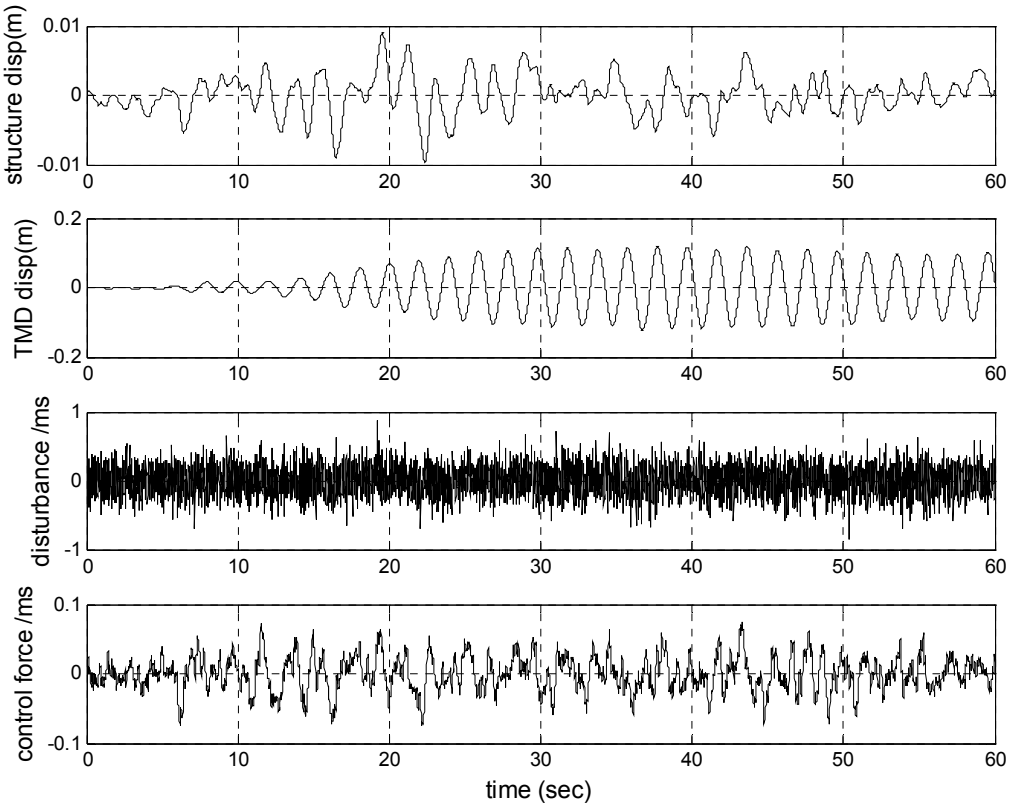

Figure 5.11. Closed-loop system response and control forces – LQR model match

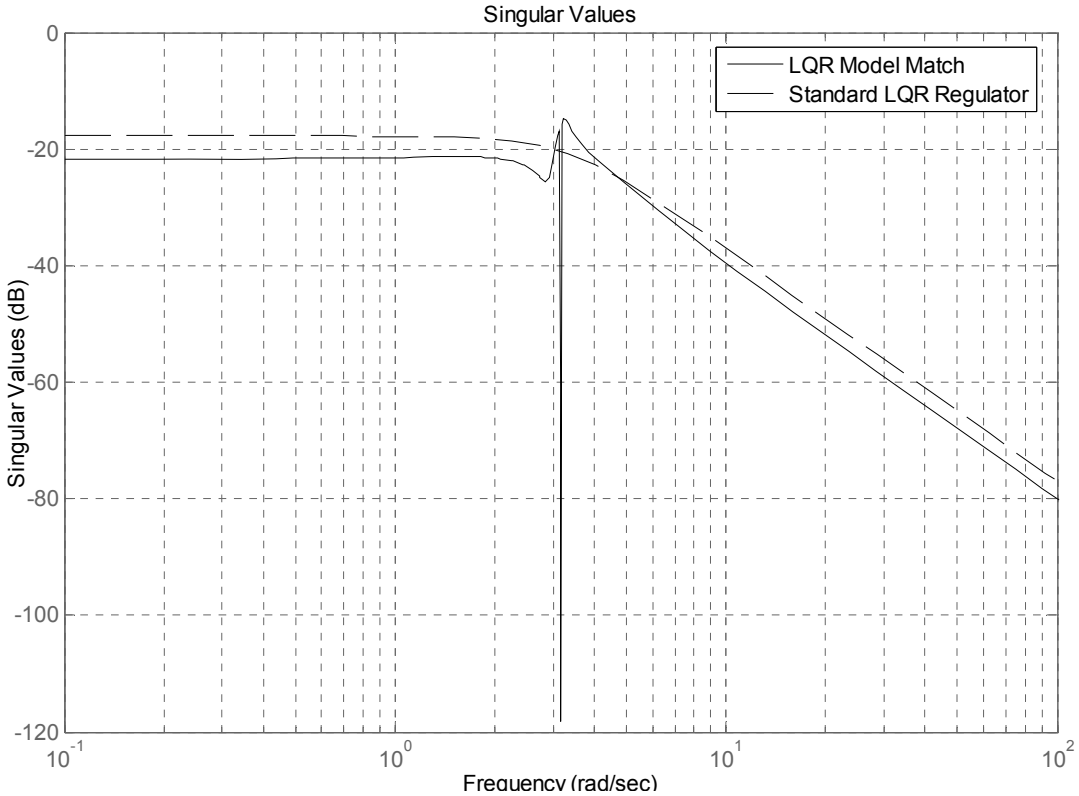

Figure 5.12. LQR closed loop system singular values from input to structure disp.

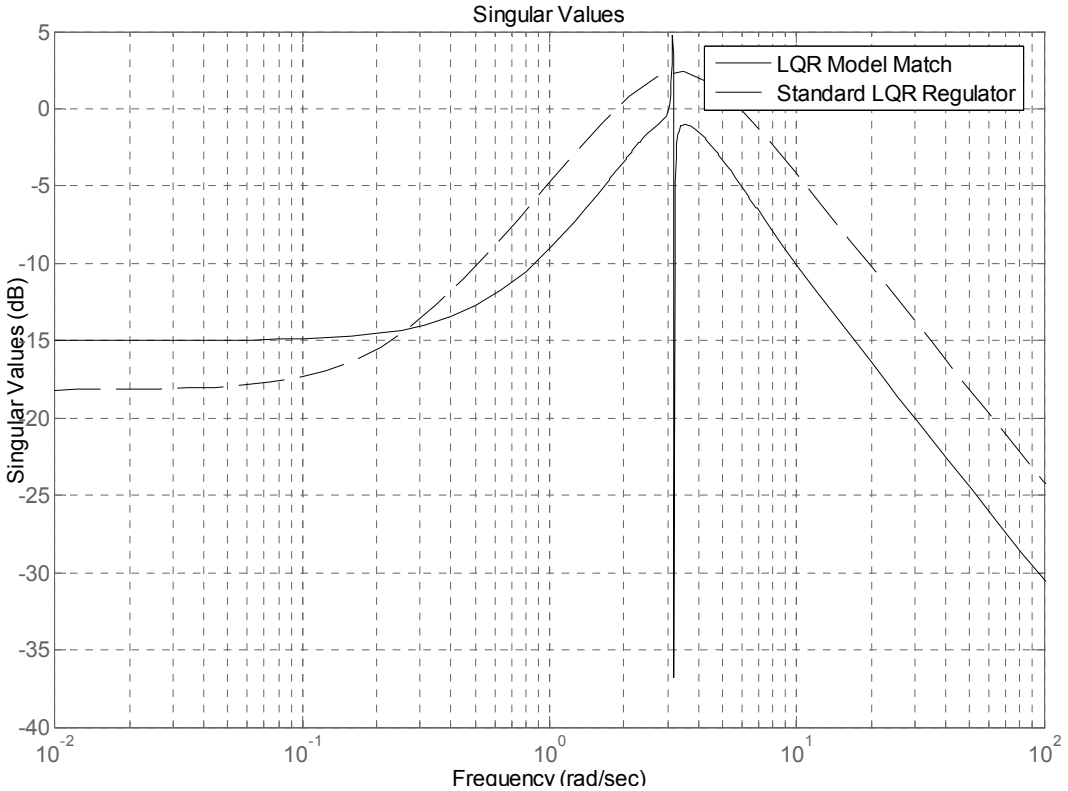

Figure 5.13. LQR closed loop system singular values from input to control force

It is demonstrated in Figure 5.11 that, closed-loop system tracks the displacement of the reference model. Since the natural frequency of the reference model is in the operating range of TMD unit, the displacement of the TMD is increasing within time. On the other hand better insight is obtained when we investigate the singular values of the closed loop transfer functions from input to closed-loop displacement and from input to control force in Figures 5.12 and 5.13 respectively. Figure 5.12 suggest that over all frequency range better response is obtained in general with proposed control approach when compared to standard LQR regulator. Especially at operating frequency of the TMD response drops dramatically, however at resonance frequencies of the closed-loop system there are still some high peaks. When it comes to control forces, proposed control methodology results in lower control forces except for low frequency range. At the operating frequency however there is jump and sudden drop in control forces.

To summarize it is observed that in general the proposed methodology behaves well than the standard LQR regulator, however there high peaks in both closed-loop response and control forces in the vicinity of operating frequency of the TMD. These peaks can be smoothed with H_∞ control, since as defined in Section 3.5 maximum singular values of the weighted outputs are minimized in H_∞ control algorithm.

5.4. H_∞ as a Model Matching Problem

5.4.3. Model Matching Problem Formulation in H_∞ Setting

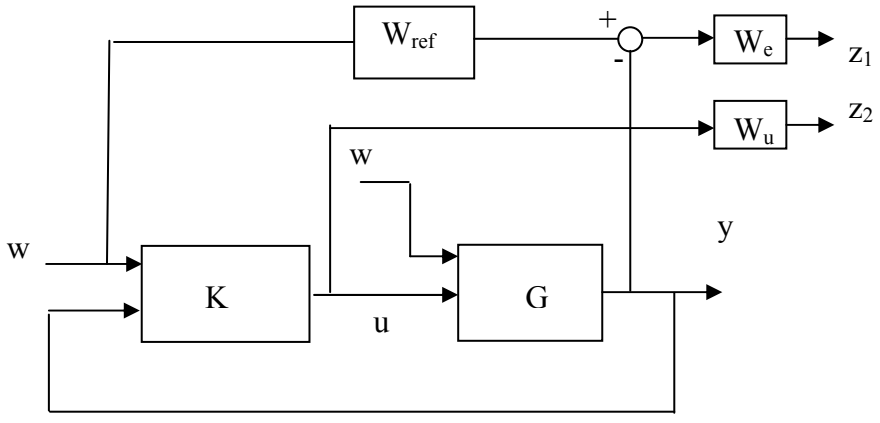

Figure 5.14. Model Matching Configuration in H_∞ setting

Model Matching configuration in Figure 5.14 can be rearranged as the standard configuration of Figure 3.3 by defining

$$w = w\,,\ z = \begin{bmatrix} z_1 \\ z_2 \end{bmatrix},\ y = \begin{bmatrix} w \\ y \end{bmatrix} \text{ and } u = u \tag{5.31}$$

The plant's transfer matrix can be partitioned as follows:

$$\begin{bmatrix} z \\ y \end{bmatrix} = P \begin{bmatrix} w \\ u \end{bmatrix} = \begin{bmatrix} P_{11} & P_{12} \\ P_{21} & P_{22} \end{bmatrix} \begin{bmatrix} w \\ u \end{bmatrix} \tag{5.32}$$

where we may set

$$P_{11} = \begin{bmatrix} W_{ref} W_e - G W_e \\ 0 \end{bmatrix}, P_{12} = \begin{bmatrix} 0 \\ W_u \end{bmatrix}, P_{21} = \begin{bmatrix} I \\ 0 \end{bmatrix}, P_{22} = \begin{bmatrix} G \\ G \end{bmatrix} \tag{5.33}$$

Closed loop relationship between the output vector and the external inputs vector is:

$$z(s) = \left[P_{11}(s) + P_{12}(s) K(s) (I - P_{22}(s) K(s))^{-1} P_{21}(s) \right] w(s) \tag{5.34}$$

5.4.4. Numerical Illustration

In the given case performance weighting function is selected as W_p=1 and the control weighting function W_u=2.6*10^{-1}.

The selected reference model is an oscillator with natural frequency 3.16 rad/sec which is the operating frequency of TMD. If we introduce %5 damping to reference model, the state equations become:

$$\begin{bmatrix} \dot{r}_1 \\ \dot{r}_2 \end{bmatrix} = \begin{bmatrix} 0 & 1 \\ -9.986 & -0.3 \end{bmatrix} \begin{bmatrix} r_1 \\ r_2 \end{bmatrix} \tag{5.35}$$

$$\tilde{y} = \begin{bmatrix} 1 & 0 \end{bmatrix} \tag{5.36}$$

So, the general control configuration given by Equation 5.32 can be constructed by executing following MATLAB statements.

Table 5.1. MATLAB code for generalized plant – Model Matching Problem

```
systemnames = 'G Wr We Wu';
inputvar = '[dist;control]';
outputvar = '[We;Wu;dist;G]';
input_to_G= '[dist;control]';
input_to_Wr= '[dist]';
input_to_We= '[G(1)-Wr(1)]';
input_to_Wu= '[control]';
sysoutname = 'Ggen';
sysic
```

In the model matching problem the output of the generalized plant, *Ggen*, includes weighted control forces, weighted error, disturbance and plant output. Thus we have one disturbance measurement and plant states that go into the controller. The output of the controller and disturbance signal are the inputs of the generalized plant, *Ggen*. The state-space representation of the generalized plant can be written as:

$$\begin{bmatrix} \dot{x}_1 \\ \dot{x}_2 \\ \dot{x}_3 \\ \dot{x}_4 \\ \dot{r}_1 \\ \dot{r}_2 \end{bmatrix} = \begin{bmatrix} 0 & 0 & 1 & 0 & 0 & 0 \\ 0 & 0 & 0 & 1 & 0 & 0 \\ -10.1 & 0.1 & -0.3162 & 0 & 0 & 0 \\ 10 & -10 & 0 & 0 & 0 & 0 \\ 0 & 0 & 0 & 0 & 0 & 1 \\ 0 & 0 & 0 & 0 & -9 & -0.3 \end{bmatrix} \begin{bmatrix} x_1 \\ x_2 \\ x_3 \\ x_4 \\ r_1 \\ r_2 \end{bmatrix} + \begin{bmatrix} 0 & 0 \\ 0 & 0 \\ 0 & 1 \\ 0 & 0 \\ 0.05 & 0 \\ 0 & 0 \end{bmatrix} \begin{bmatrix} w \\ u \end{bmatrix} \tag{5.37}$$

$$\begin{bmatrix} z_1 \\ z_2 \\ w \\ x_1 \\ x_2 \\ x_3 \\ x_4 \end{bmatrix} = \begin{bmatrix} 1 & 0 & 0 & 0 & -1 & 0 \\ 0 & 0 & 0 & 0 & 0 & 0 \\ 0 & 0 & 0 & 0 & 0 & 0 \\ 1 & 0 & 0 & 0 & 0 & 0 \\ 0 & 1 & 0 & 0 & 0 & 0 \\ 0 & 0 & 1 & 0 & 0 & 0 \\ 0 & 0 & 0 & 1 & 0 & 0 \end{bmatrix} \begin{bmatrix} x_1 \\ x_2 \\ x_3 \\ x_4 \\ r_1 \\ r_2 \end{bmatrix} + \begin{bmatrix} 0 & 0 \\ 0 & 0.26 \\ 1 & 0 \\ 0 & 0 \\ 0 & 0 \\ 0 & 0 \\ 0 & 0 \end{bmatrix} \begin{bmatrix} w \\ u \end{bmatrix} \tag{5.38}$$

The design uses the MATLAB command *hinfsyn* that computes a suboptimal H_∞ controller, based on the generalized plant. The input and output arguments of the *hinfsyn* are

[K1,Scl1,gam1] = hinfsyn(P,nm,nc,'gmin',0.1,'gmax',10,'tolgam',0.001);

where number of measurements that are procesed by the controller are the disturbance signal and generalized plant output. The interval for γ iteration is chosen between 0.1 and 10 with tolerance 0.001. The state equations of the controller, *K*, calculated by H_∞ *algorithm* is given by:

$$\begin{bmatrix} \dot{k}_1 \\ \dot{k}_2 \\ \dot{k}_3 \\ \dot{k}_4 \\ \dot{k}_5 \\ \dot{k}_6 \end{bmatrix} = \begin{bmatrix} -0.633 & -0.403 & 0.007 & -0.660 & 0 & 0 \\ -0.403 & -0.557 & 0.004 & 0.727 & 0 & 0 \\ -11.96 & 0.153 & -1003 & -0.073 & 2.239 & 2.5 \\ 9.34 & -10.27 & -0.003 & -2.688 & 0 & 0 \\ 0 & 0 & 0 & 0 & 0 & 1 \\ 0 & 0 & 0 & 0 & -9 & -0.3 \end{bmatrix} \begin{bmatrix} k_1 \\ k_2 \\ k_3 \\ k_4 \\ k_5 \\ k_6 \end{bmatrix}$$
$$+ \begin{bmatrix} 0 & 9.099 & 5.79 & 14.26 & 9.486 \\ 0 & 5.79 & 7.994 & -0.063 & 3.929 \\ 0 & 14.26 & -0.063 & 14360 & 0.038 \\ 0 & 9.486 & 3.929 & 0.038 & 38.61 \\ 0.718 & 0 & 0 & 0 & 0 \\ 0 & 0 & 0 & 0 & 0 \end{bmatrix} \begin{bmatrix} w \\ x_1 \\ x_2 \\ x_3 \\ x_4 \end{bmatrix} \tag{5.39}$$

$$[u] = \begin{bmatrix} -0.061 & 0.0034 & -0.210 & -0.005 & 0.156 & 0.174 \end{bmatrix} \begin{bmatrix} k_1 \\ k_2 \\ k_3 \\ k_4 \\ k_5 \\ k_6 \end{bmatrix} \tag{5.40}$$

As in the case of LQR tracking problem, the H_∞ control has feedback and feedforward terms. The interconnection is given in Table 3.3.

Table 5.2. MATLAB code for plant and controller interconnection – Model Matching Problem

```
systemnames = 'G K1';
inputvar = '[dist]';
outputvar = '[G(1);K1]';
input_to_G= '[dist;K1]';
input_to_K1= '[dist;G]';
sysoutname = 'CL1';
Sysic
```

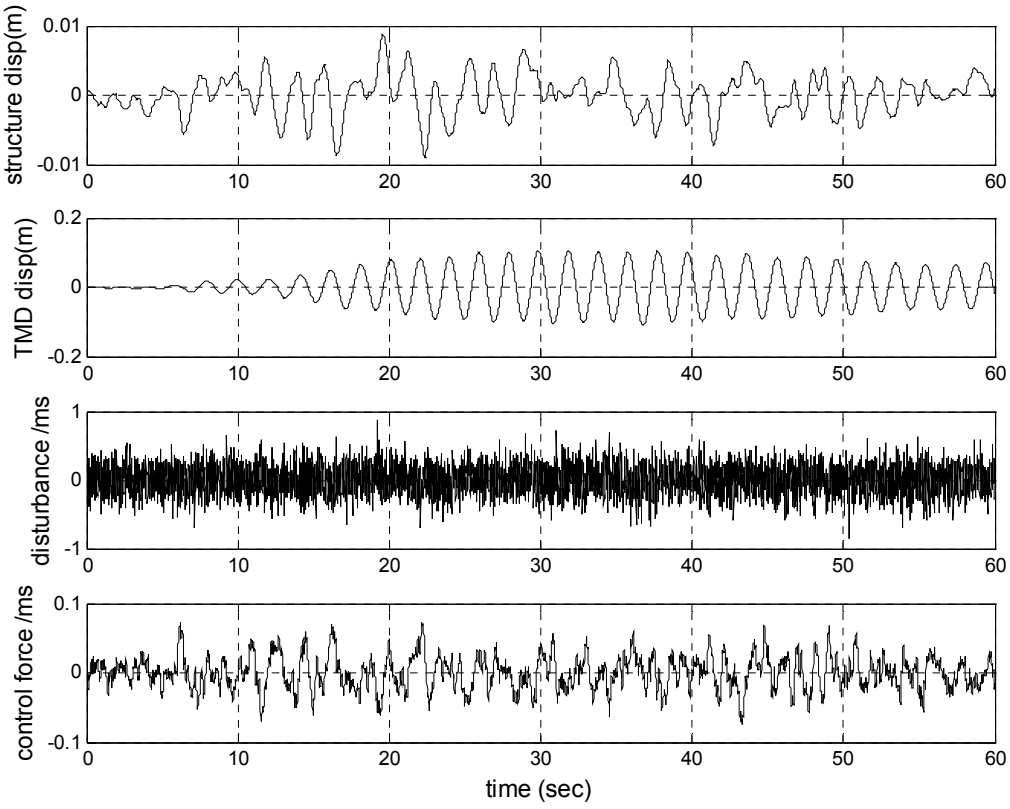

Figure 5.15. Closed-loop system response and control forces – H_∞ model match

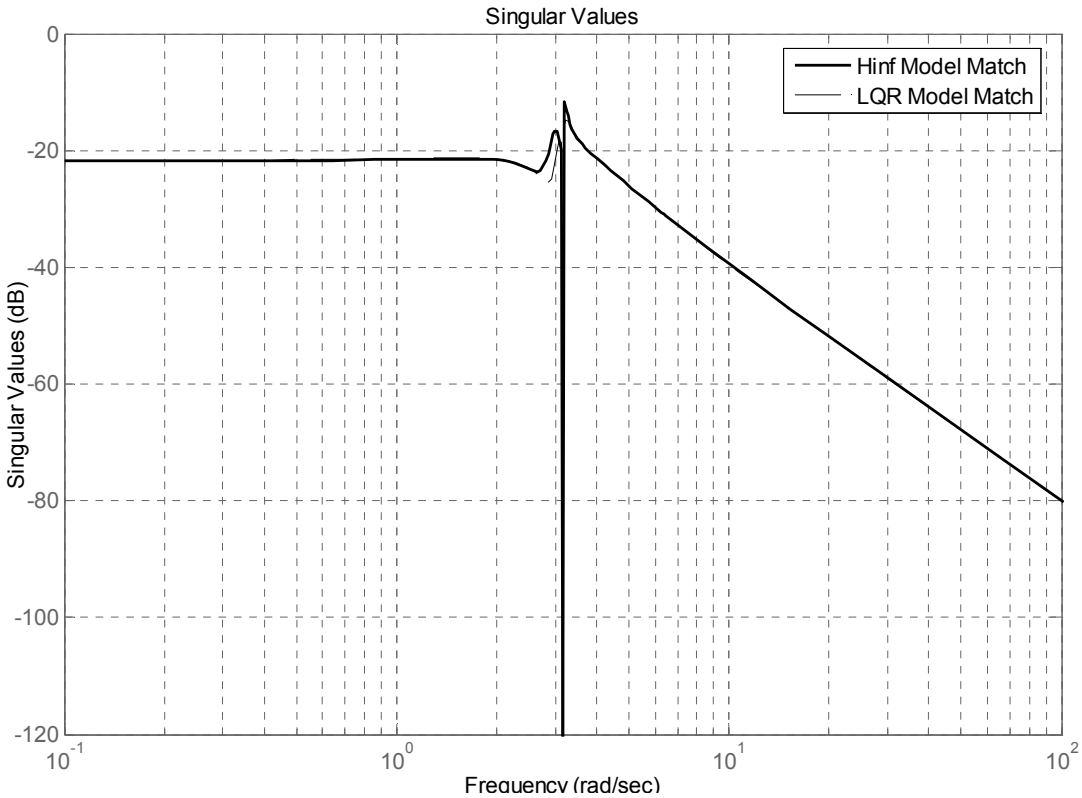

Figure 5.16. H_∞ closed loop system singular values from input to structure disp.

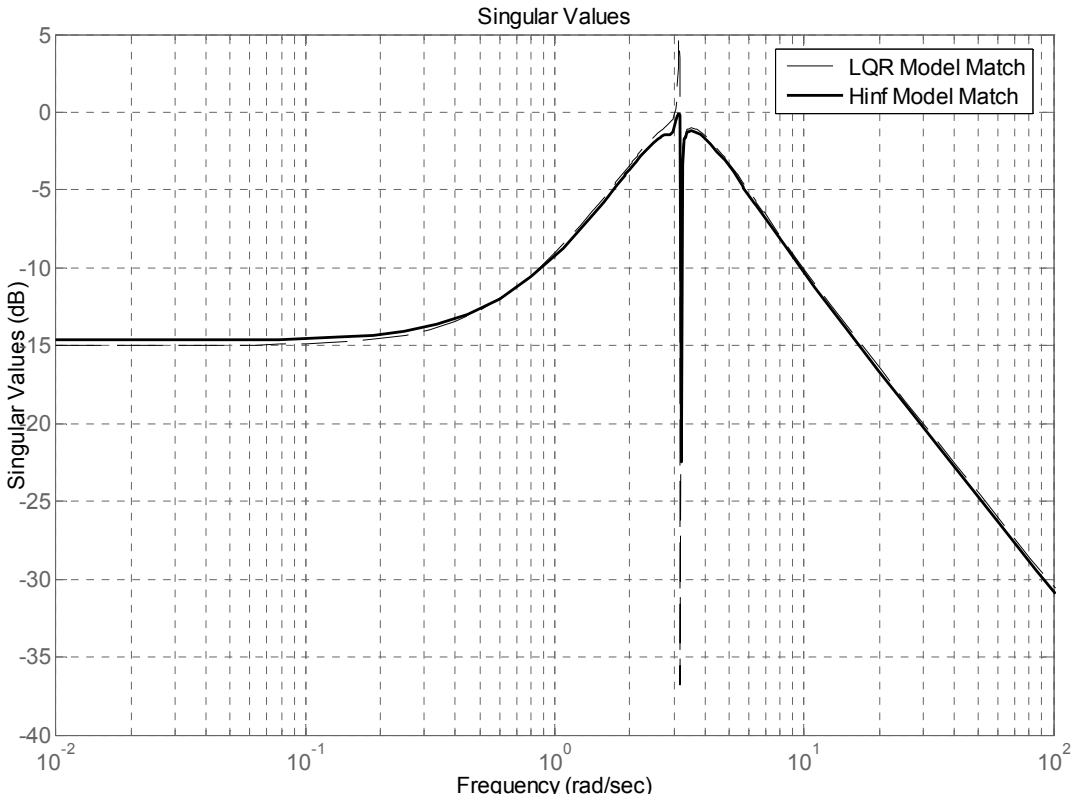

Figure 5.17. H_∞ closed loop system singular values from input to control force

In Figure 5.15 the time response of the closed loop displacement, TMD displacement and control forces are shown. When compared to LQR similar results are obtained. Furthermore singular value plot of the transfer function from disturbance to plant displacement is compared with that of the LQR control in Figure 5.15. The weighting functions are selected such that LQR and H_∞ performances are the same. In this case the singular values of transfer function from disturbance to control forces are also found to be similar except for the sharp peaks that are observed in LQR setting are smoothed in H_∞ synthesis as expected.

To summarize, in this thesis an alternative control approach is proposed where the controller makes the plant track the states of an idealized mathematical model. The selected mathematical model is an oscillator having natural frequency set to the operating frequency of the TMD unit. The objective is to have the controlled response fall into the operating range of TMD unit in frequency domain where the TMD effectiveness is maximized. All in all it can be concluded that, when compared to standard regulator problem where system states are regulated to zero, better control performance in terms of plant displacement can be achieved with the proposed control approach. Also required control forces are found to be lesser than the regulator problem. The sharp peaks in control forces that are observed in LQR setting is further smoothed in H_∞ synthesis.

6. COMPARISON OF PROPOSED CONTROLLERS WITH STANDARD REGULATORS – WIND LOADS

6.1. Plant Dynamics

6.1.1. State Equations of SDOF Plant

Single-degree-of-freedom (SDOF) system has following structural parameters:

$k_s = 1.10^5$ kN/m
$c_s = 3{,}16.10^3$ kN/s (%5 damping)
$m_s = 1.10^4$ tons

Equation of motion for such a system is given by

$$m_s \ddot{y}(t) + c_s \dot{y}(t) + k_s y(t) = u(t) + w(t) \tag{6.1}$$

The state equations of the plant can be written as

$$\begin{bmatrix} \dot{x}_1 \\ \dot{x}_2 \end{bmatrix} = \begin{bmatrix} 0 & 1 \\ -10 & -0.32 \end{bmatrix} \begin{bmatrix} x_1 \\ x_2 \end{bmatrix} + \begin{bmatrix} 0 & 0 \\ 1 & 1 \end{bmatrix} \begin{bmatrix} w \\ u \end{bmatrix} \tag{6.2}$$

$$\begin{bmatrix} y_1 \\ y_2 \end{bmatrix} = \begin{bmatrix} 1 & 0 \\ 0 & 1 \end{bmatrix} \begin{bmatrix} x_1 \\ x_2 \end{bmatrix} \tag{6.3}$$

6.1.2. State Equations of Combined SDOF Plant/non-optimal TMD

Single-degree-of-freedom (SDOF) system given in Section 6.1.1 and non-optimal TMD with mass ratio μ=0.01 has following structural parameters:

k_s = 1.10^5 kN/m

c_s = $3{,}16.10^3$ kN/s (%5 damping)

m_s = 1.10^4 tons

k_{TMD} = 1000 kN/m (λ=1.00)

m_{TMD} = 100 tons (μ=0.01)

c_{TMD} = 0 N/s (%0 damping)

Equations of motion for the two-degree-of-freedom system is given by

$$m_s \ddot{y}_s(t) + (c_s + c_{TMD})\dot{y}_s(t) + (k_s + k_{TMD})y_s(t) = k_{TMD} y_{TMD} + c_{TMD}\dot{y}_{TMD} + u(t) + w(t) \quad (6.4)$$

$$m_{TMD}\ddot{y}_{TMD}(t) + c_{TMD}\dot{y}_{TMD}(t) + k_{TMD} y_{TMD}(t) = k_{TMD} y_s + c_{TMD}\dot{y}_s \quad (6.5)$$

The state equations of the plant can be written as

$$\begin{bmatrix} \dot{x}_1 \\ \dot{x}_2 \\ \dot{x}_3 \\ \dot{x}_4 \end{bmatrix} = \begin{bmatrix} 0 & 0 & 1 & 0 \\ 0 & 0 & 0 & 1 \\ -10.1 & 0.1 & -0.3316 & 0 \\ 10 & -10 & 0 & 0 \end{bmatrix} \begin{bmatrix} x_1 \\ x_2 \\ x_3 \\ x_4 \end{bmatrix} + \begin{bmatrix} 0 & 0 \\ 0 & 0 \\ 1 & 1 \\ 0 & 0 \end{bmatrix} \begin{bmatrix} w(t) \\ u(t) \end{bmatrix} \quad (6.6)$$

$$\begin{bmatrix} y_1 \\ y_2 \\ y_3 \\ y_4 \end{bmatrix} = \begin{bmatrix} 1 & 0 & 0 & 0 \\ 0 & 1 & 0 & 0 \\ 0 & 0 & 1 & 0 \\ 0 & 0 & 0 & 1 \end{bmatrix} \begin{bmatrix} x_1 \\ x_2 \\ x_3 \\ x_4 \end{bmatrix} \quad (6.7)$$

6.1.3. State Equations of Combined SDOF Plant/optimal TMD

Single-degree-of-freedom (SDOF) system given in Section 6.1.1 and optimal TMD with mass ratio μ=0.01 has following structural parameters:

k_s = 1.10^5 kN/m

c_s = $3{,}16.10^3$ kN/s (%5 damping)

m_s = 1.10^4 tons

k_{TMD} = 960.4 kN/m (λ=0.98)

m_{TMD} = 100 tons (μ=0.01)

c_{TMD} = 43386 N/s (%7 damping)

The state equations of the plant can be written as

$$\begin{bmatrix} \dot{x}_1 \\ \dot{x}_2 \\ \dot{x}_3 \\ \dot{x}_4 \end{bmatrix} = \begin{bmatrix} 0 & 0 & 1 & 0 \\ 0 & 0 & 0 & 1 \\ -10.1 & 0.096 & -0.3206 & 0.004 \\ 9.604 & -9.604 & 0.4339 & -0.4339 \end{bmatrix} \begin{bmatrix} x_1 \\ x_2 \\ x_3 \\ x_4 \end{bmatrix} + \begin{bmatrix} 0 & 0 \\ 0 & 0 \\ 1 & 1 \\ 0 & 0 \end{bmatrix} \begin{bmatrix} w(t) \\ u(t) \end{bmatrix} \tag{6.8}$$

$$\begin{bmatrix} y_1 \\ y_2 \\ y_3 \\ y_4 \end{bmatrix} = \begin{bmatrix} 1 & 0 & 0 & 0 \\ 0 & 1 & 0 & 0 \\ 0 & 0 & 1 & 0 \\ 0 & 0 & 0 & 1 \end{bmatrix} \begin{bmatrix} x_1 \\ x_2 \\ x_3 \\ x_4 \end{bmatrix} \tag{6.9}$$

6.2. Controller Dynamics

6.2.1. LQR for SDOF Plant

The state weighting matrix, Q, and the control force weighting matrix, R, are selected as:

$$Q = \begin{bmatrix} 1 & 0 \\ 0 & 1 \end{bmatrix}, R = 0.01 \tag{6.10}$$

The corresponding control gain is calculated to be:

$$K_1 = \begin{bmatrix} 4.1421 & 10.095 \end{bmatrix} \tag{6.11}$$

6.2.2. H_∞ for SDOF Plant

Performance weighting function is selected as W_p=1 and the control weighting function W_u=1*10^{-1}.

The gain matrix *K*, calculated by H_∞ *algorithm* is given by:

$$K = \begin{bmatrix} 4.962 & 10.441 \end{bmatrix} \tag{6.12}$$

6.2.3. LQR for Combined SDOF Plant/optimal TMD

The state weighting matrix, Q, and the control force weighting matrix, R, are selected as:

$$Q = \begin{bmatrix} 1 & 0 & 0 & 0 \\ 0 & 0 & 0 & 0 \\ 0 & 0 & 1 & 0 \\ 0 & 0 & 0 & 0 \end{bmatrix}, R = 0.01 \tag{6.13}$$

The corresponding control gain is calculated to be:

$$K = \begin{bmatrix} 4.2338 & 0.7282 & 9.2267 & 0.047 \end{bmatrix} \tag{6.14}$$

6.2.4. H_∞ for Combined SDOF Plant/optimal TMD

Performance weighting function is selected as W_p=1 and the control weighting function W_u=1*10^{-1}.

The gain matrix *K*, calculated by H_∞ *algorithm* is given by:

$$K = \begin{bmatrix} 4.0537 & 0.088 & 10.082 & 0.004 \end{bmatrix} \tag{6.15}$$

6.2.5. LQR for Combined SDOF Plant/non-optimal TMD

The state weighting matrix, Q, and the control force weighting matrix, R, are selected as:

$$Q = \begin{bmatrix} 1 & 0 & 0 & 0 \\ 0 & 0 & 0 & 0 \\ 0 & 0 & 1 & 0 \\ 0 & 0 & 0 & 0 \end{bmatrix}, R = 0.01 \tag{6.16}$$

The corresponding control gain is calculated to be:

$$K = \begin{bmatrix} 4.1414 & 0.001 & 10.094 & 0.0039 \end{bmatrix} \tag{6.17}$$

6.2.6. H_∞ for Combined SDOF Plant/non-optimal TMD

Performance weighting function is selected as W_p=1 and the control weighting function W_u=1*10^{-1}.

The gain matrix *K*, calculated by H_∞ *algorithm* is given by:

$$K = \begin{bmatrix} 4.9527 & 0.009 & 10.427 & 0.078 \end{bmatrix} \tag{6.18}$$

6.2.7. LQR for Model Matching Problem

The selected reference model is an oscillator with natural frequency 3.16 rad/sec which is the operating frequency of TMD. If we introduce %5 damping to reference model, the state equations become:

$$\begin{bmatrix} \dot{z}_1 \\ \dot{z}_2 \end{bmatrix} = \begin{bmatrix} 0 & 1 \\ -9.986 & -0.3 \end{bmatrix} \begin{bmatrix} z_1 \\ z_2 \end{bmatrix} + \begin{bmatrix} 0. \\ 0.02 \end{bmatrix} w \tag{6.19}$$

$$\tilde{y} = \begin{bmatrix} 1 & 0 \end{bmatrix} \tag{6.20}$$

The state weighting matrix, Q, and the control force weighting matrix, R, are selected as:

$$Q = \begin{bmatrix} 1 & 0 & 0 & 0 \\ 0 & 0 & 0 & 0 \\ 0 & 0 & 1 & 0 \\ 0 & 0 & 0 & 0 \end{bmatrix}, R = 0.012 \tag{6.21}$$

The corresponding control gain is calculated to be:

$$K = \begin{bmatrix} 3.5394 & 0.0001 & 9.1976 & 0.0037 & -3.426 & -8.913 \end{bmatrix} \tag{6.22}$$

6.2.8. H_∞ for Model Matching Problem

Performance weighting function is selected as W_p=1 and the control weighting function W_u=7*10^{-2}.

The selected reference model is an oscillator with natural frequency 3.16 rad/sec which is the operating frequency of TMD. If we introduce %5 damping to reference model, the state equations become:

$$\begin{bmatrix} \dot{z}_1 \\ \dot{z}_2 \end{bmatrix} = \begin{bmatrix} 0 & 1 \\ -9.986 & -0.3 \end{bmatrix} \begin{bmatrix} z_1 \\ z_2 \end{bmatrix} + \begin{bmatrix} 0. \\ 0.01 \end{bmatrix} w \tag{6.23}$$

$$\tilde{y} = \begin{bmatrix} 1 & 0 \end{bmatrix} \tag{6.24}$$

The gain matrix K, calculated by H_∞ *algorithm* is given by:

$$K = \begin{bmatrix} 9.3306 & 0.4214 & 8.2225 & 0.2774 & -1.0536 & -5.5503 \end{bmatrix} \tag{6.25}$$

6.3. Transfer Matrices of the Closed Loop System

6.3.1. Comparison of Closed-loop Systems with LQR

It is demonstrated in Figure 6.1 that the attachment of TMD unit to the plant does not influence the closed loop displacements if TMD is optimized. The response is also same for non-optimal TMD except for the sudden drop at the operating frequency of non-optimal TMD. This is an indication of effectiveness of TMD unit when it is not optimized. The LQR controller also smoothes the two resonance peaks of the combined plant/non-optimal TMD structure. For model matching case on the other hand, the resonance peaks reappear for in this case controller do not try to regulate the response but try to minimize the error between the states of the reference model and actual structure. However, for the frequencies lower than the natural frequency of the plant the displacement response is lesser when compared to regulator cases.

When it comes to control forces, Figure 6.2 suggests that attachment of TMD unit has also no effect again except for the sudden drop at the operating frequency. In the proposed controller however, there is a sharp peak at the operating frequency and the control force requirement is higher for frequencies lower than the natural frequency of the closed-loop system. On the other hand, lesser control effort is needed for frequencies higher than natural frequency. This fact renders proposed control strategy efficient for high frequency noise attenuation.

With H_∞ synthesis there is a slight difference in plant displacements among the plant and optimal TMD equipped plant. This is due to the fact that H_∞ synthesis aims to minimize the largest singular value of the plant which is higher when compared to combined optimal TMD/plant structure. Therefore all response is suppressed a little bit further in the former case. On the other hand there is seen no difference in responses between plant and combined non-optimal TMD/plant structure except for the sudden drop at operating frequency. The model matching case however gives better response for frequencies smaller than the natural frequency and the response is almost the same with the rest of the controllers when frequencies are larger than the natural frequency.

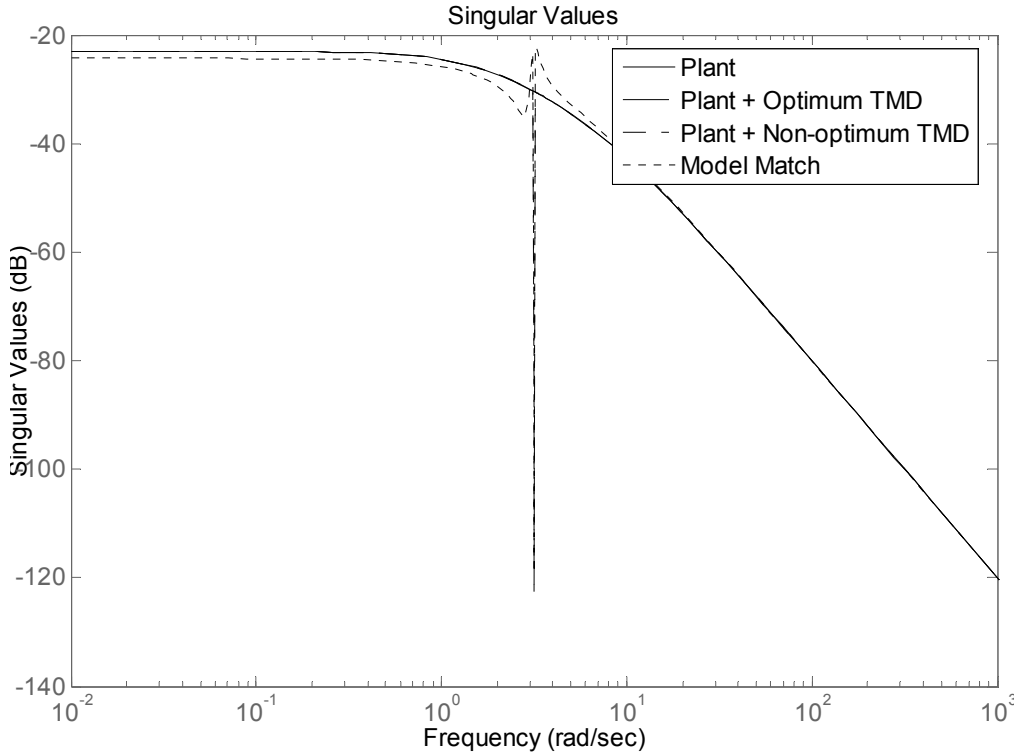

Figure 6.1. Sing. val. of the closed loop systems from input to displacement - LQR

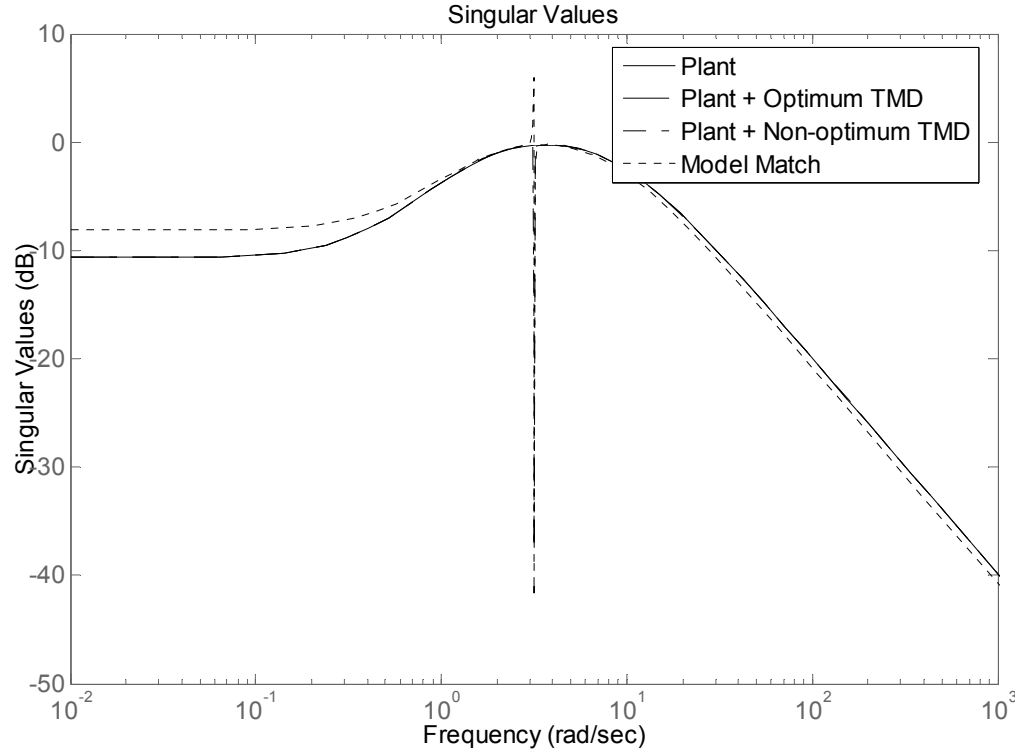

Figure 6.2. Sing. val. of the closed loop systems from input to control force - LQR

6.3.2. Comparison of Closed-loop Systems with H_∞

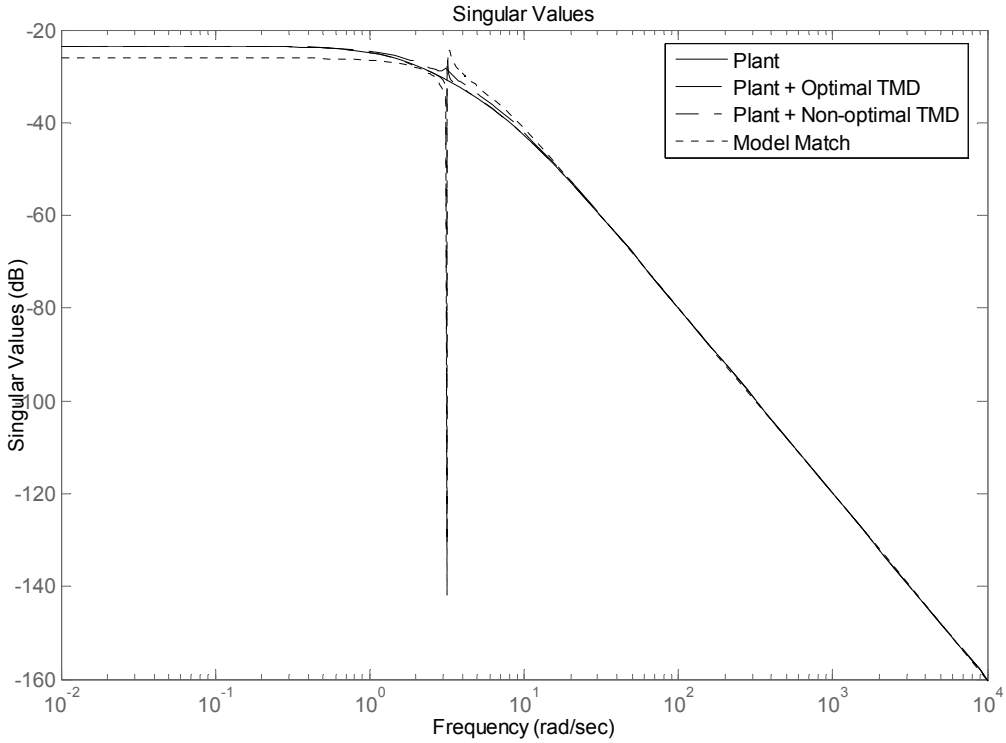

Figure 6.3. Sing. val. of the closed loop systems from input to displacement - H_∞

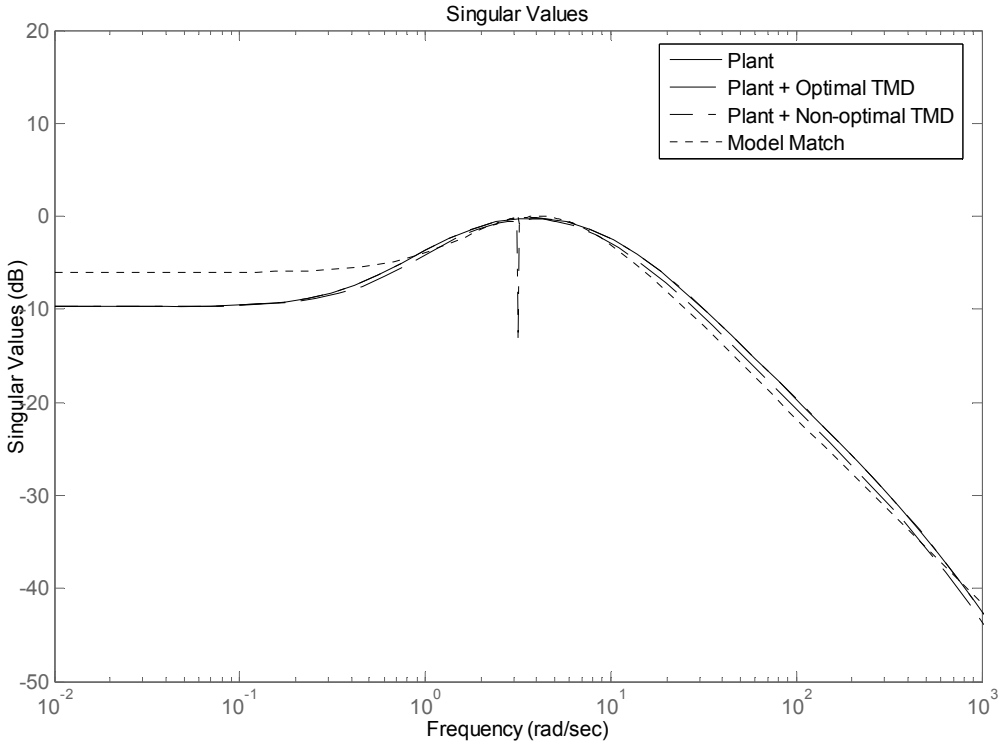

Figure 6.4. Sing. val. of the closed loop systems from input to control force - H_∞

6.3.3. Comparison of H_∞ and LQR Model Matching Problem

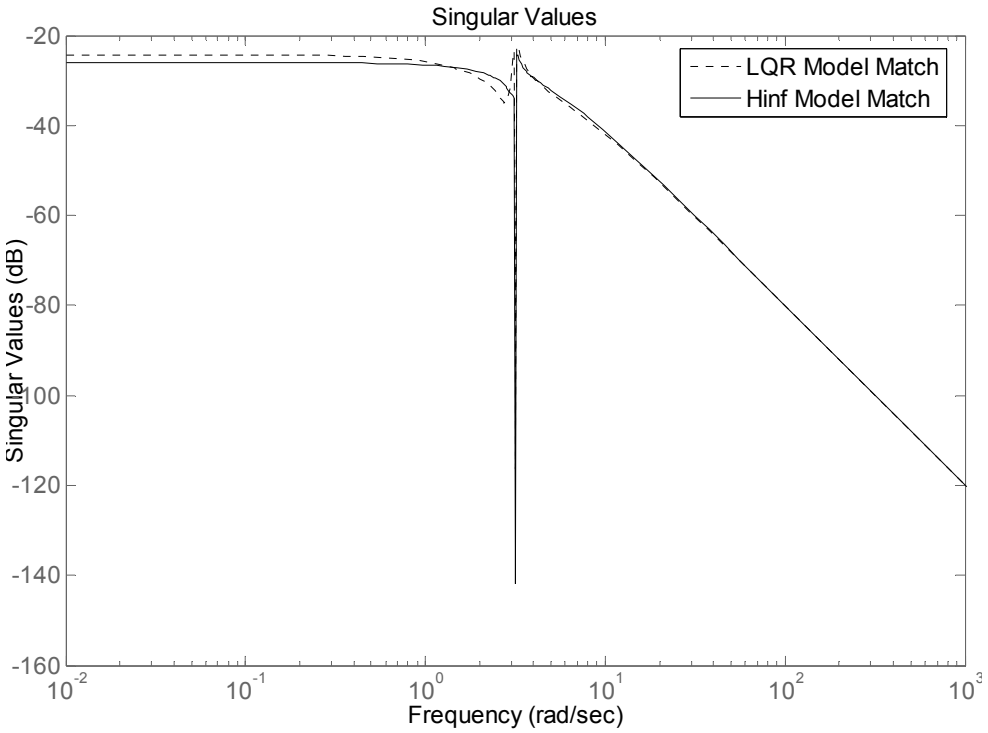

Figure 6.5. H_∞ and LQR closed loop system sing. val. from input to displacement

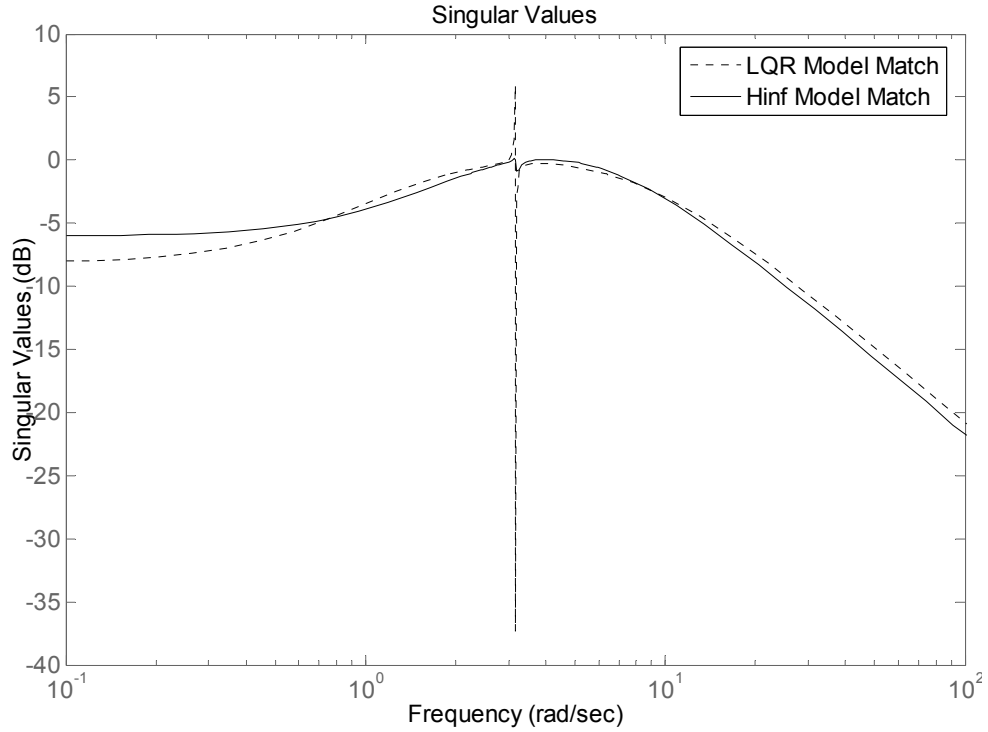

Figure 6.6. H_∞ and LQR closed loop system sing. val. from input to control force

Comparison of proposed controllers in LQR and H_∞ settings reveal that the peaks shown in the vicinity of the tuning frequency in LQR setting is smoothed in H_∞ setting which is expected for H_∞ controllers. The weights of LQR and H_∞ synthesis are chosen such that the time domain response in terms of H_2 norm of the plant displacement is equal for both controllers. That is why apart from the tuning frequency, the displacement response is similar between two controllers as can be observed from Figure 6.5. Still low-frequency response is better in H_∞ controllers. The required control forces however are different between two settings. At low frequencies control energy requirement is less in LQR setting but the situation is reversed at high frequencies. On the other hand the sudden jumps and drops around the tuning frequency in the LQR setting is no more observed in H_∞ synthesis since the maximum singular value of the transfer function from input to control forces is minimized together with the maximum singular value of the transfer function from input to closed-loop disturbance in H_∞ mixed sensitivity optimization problem.

6.4. Time Domain Response of the Closed Loop System

It is demonstrated in Figure 6.7 and further verified in Table 6.1 that the closed-loop performances in terms of H_2 norm of the closed-loop displacement among various configurations are more or less same since performance weights are selected accordingly. So the performance indication will be the control energy requirements. The addition of TMD in both optimal and non-optimal configuration has a marginal effect on control energy when used with standard LQR regulator. On the other hand with the proposed strategy the control energy requirement is %4.5 lesser when compared to standard LQR regulators.

As can be seen from Figure 6.8 and Table 6.2 that, when it comes to maximum control force, best answer is again obtained with the proposed controllers. The improvement in this case is %4.7. It should be noted that control forces are normalized with mass of the plant, thus they indicate control effort in terms of percent weight of the structure.

Figure 6.9 and Table 6.3 suggests that when the H_2 and H_∞ norms of the plant displacement is equated by selecting appropriate performance weights, the control energy requirement is lowest with proposed controller in H_∞ setting. The improvement is %8.7 in this case which is better than LQR setting. As can be inspected from Figure 6.10 and Table 6.4, similar results are obtained in terms of maximum control force. The improvement in this case is %9.

The time domain response of the compared systems reveal that the proposed closed-loop systems both in LQR and H_∞ settings need less control effort for the same closed-loop performance in terms of plant displacement when compared to standard regulators. The improvement is more pronounced in H_∞ which is in agreement with the singular value plots of proposed controllers.

6.4.1. H_2 Norms of Closed-loop Systems with LQR Regulators

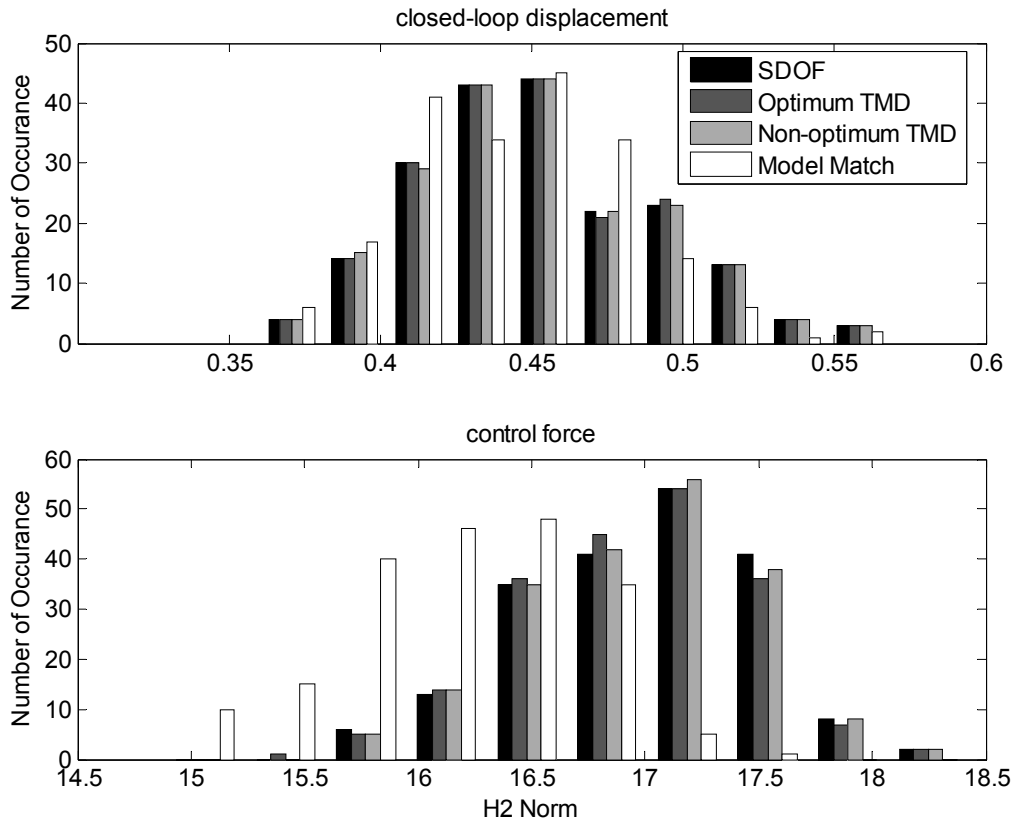

Figure 6.7. H_2 norm of closed-loop disp. and control forces – LQR

Table 6.1. Mean and standard deviation of closed loop response – LQR

(Closed Loop Displacement Energy)$^{1/2}$				
	SDOF	Optimum TMD	Non-optimum TMD	LQR Model Match
μ	0,4486	0,4487	0,4482	0,4431
σ	0,0373	0,0373	0,0372	0,0350
(Normalized Control Force)$^{1/2}$				
	SDOF	Optimum TMD	Non-optimum TMD	LQR Model Match
μ	16,9781	16,9498	16,9705	16,1875
σ	0,5344	0,5329	0,5323	0,5220

6.4.2. H_∞ Norms of Closed-loop Systems with LQR Regulators

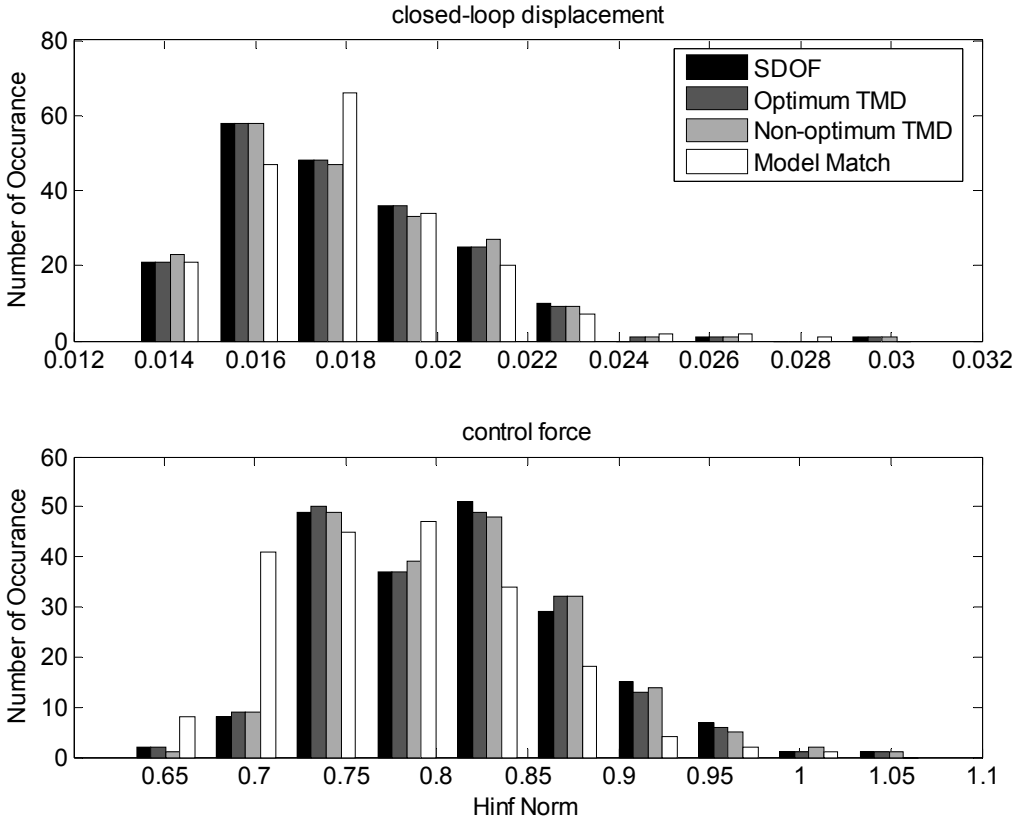

Figure 6.8. H_∞ norm of closed-loop disp. and control forces – LQR

Table 6.2. Mean and standard deviation of closed loop response – LQR

Closed Loop Displacement (m)				
	SDOF	Optimum TMD	Non-optimum TMD	LQR Model Match
μ	0,0178	0,0178	0,0178	0,0179
σ	0,0026	0,0026	0,0026	0,0025
Control Force / m_s				
	SDOF	Optimum TMD	Non-optimum TMD	LQR Model Match
μ	0,8109	0,8095	0,8103	0,7712
σ	0,0694	0,0692	0,0693	0,0671

6.4.3. H_2 Norms of Closed-loop Systems with H∞ Regulators

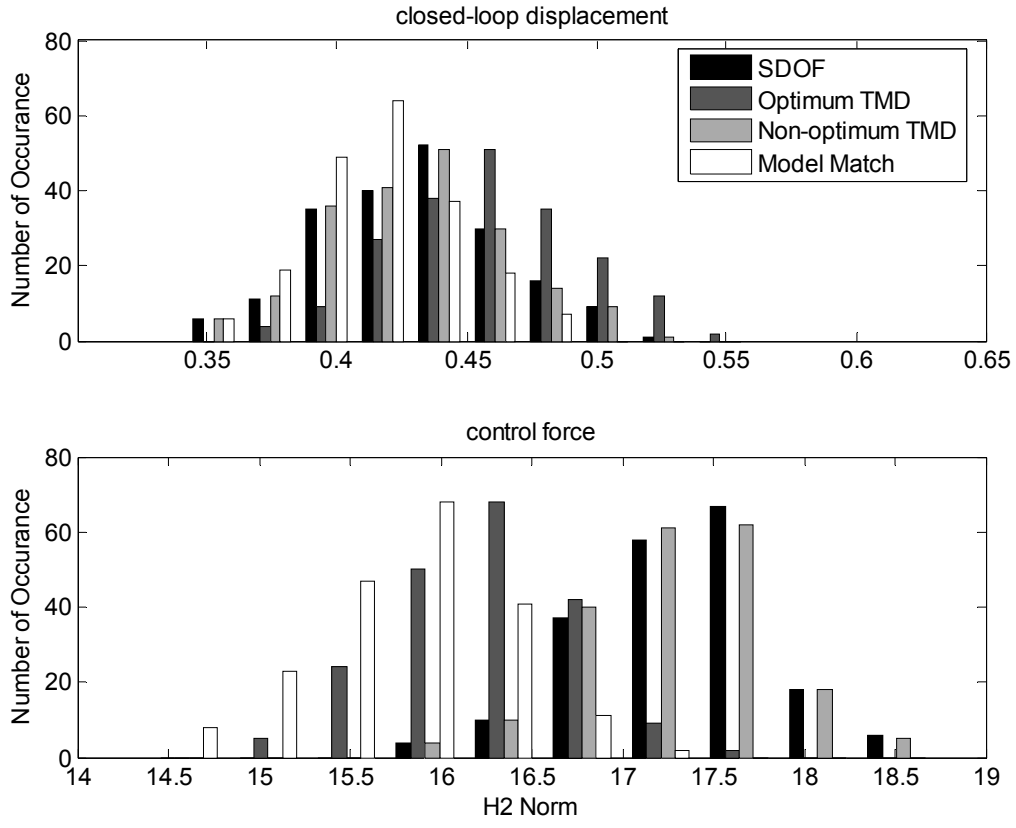

Figure 6.9. H_2 norm of closed-loop disp. and control forces – H_∞

Table 6.3. Mean and standard deviation of closed loop response – H_∞

(Closed Loop Displacement Energy)$^{1/2}$				
	SDOF	Optimum TMD	Non-optimum TMD	H_∞ Model Match
μ	0,4307	0,4591	0,4297	0,4166
σ	0,0354	0,0359	0,0352	0,0278
(Normalized Control Energy)$^{1/2}$				
	SDOF	Optimum TMD	Non-optimum TMD	H_∞ Model Match
μ	17,3174	16,2315	17,2995	15,7950
σ	0,5142	0,5024	0,5123	0,5366

6.4.4. H_∞ Norms of Closed-loop Systems with H∞ Regulators

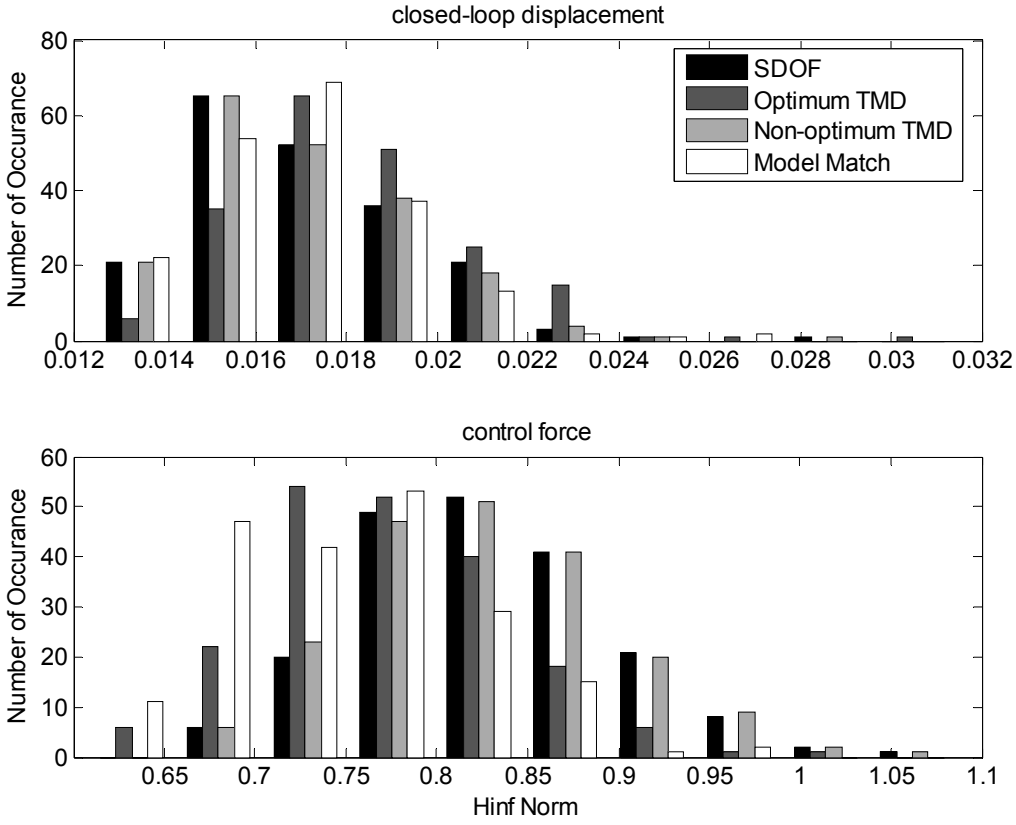

Figure 6.10. H_∞ norm of closed-loop disp. and control forces – H_∞

Table 6.4. Mean and standard deviation of closed loop response – H_∞

Closed Loop Displacement (m)				
	SDOF	Optimum TMD	Non-optimum TMD	H_∞ Model Match
μ	0,0172	0,0183	0,0171	0,0170
σ	0,0025	0,0026	0,0025	0,0023

Control Force / m_s				
	SDOF	Optimum TMD	Non-optimum TMD	H_∞ Model Match
μ	0,8264	0,7733	0,8254	0,7509
σ	0,0698	0,0659	0,0698	0,0671

7. COMPARISON OF PROPOSED CONTROLLERS WITH STANDARD REGULATORS – EARTHQUAKE LOADS

7.1. Plant Dynamics

7.1.1. State Equations of SDOF Plant

Single-degree-of-freedom (SDOF) system has following structural parameters:

$k_s = 1.10^5$ kN/m
$c_s = 3{,}16.10^3$ kN/s (%5 damping)
$m_s = 1.10^4$ tons

Equation of motion for such a system is given by

$$m_s \ddot{y}(t) + c_s \dot{y}(t) + k_s y(t) = u(t) + w(t) \tag{7.1}$$

For earthquake loading, ground motion is expressed by acceleration term, so the forcing term in Equation (7.1) becomes

$$m_s \ddot{y}(t) + c_s \dot{y}(t) + k_s y(t) = u(t) - m_s \ddot{y}_g(t) \tag{7.2}$$

The state equations of the plant can be written as

$$\begin{bmatrix} \dot{x}_1 \\ \dot{x}_2 \end{bmatrix} = \begin{bmatrix} 0 & 1 \\ -10 & -0.32 \end{bmatrix} \begin{bmatrix} x_1 \\ x_2 \end{bmatrix} + \begin{bmatrix} 0 & 0 \\ -1 & 1 \end{bmatrix} \begin{bmatrix} \ddot{y}_g(t) \\ u(t) \end{bmatrix} \tag{7.3}$$

$$\begin{bmatrix} y_1 \\ y_2 \end{bmatrix} = \begin{bmatrix} 1 & 0 \\ 0 & 1 \end{bmatrix} \begin{bmatrix} x_1 \\ x_2 \end{bmatrix} \tag{7.4}$$

7.1.2. State Equations of Combined SDOF Plant/non-optimal TMD

Single-degree-of-freedom (SDOF) system given in Section 7.1.1 and non-optimal TMD with mass ratio μ=0.01 has following structural parameters:

k_s = 1.10^5 kN/m
c_s = $3{,}16.10^3$ kN/s (%5 damping)
m_s = 1.10^4 tons
k_{TMD} = 1000 kN/m (λ=1.00)
m_{TMD} = 100 tons (μ=0.01)
c_{TMD} = 0 N/s (%0 damping)

Equations of motion for the two-degree-of-freedom system subjected to ground motion is expressed by

$$m_s\ddot{y}_s + \left[c_s\dot{y}_s + c_{TMD}(\dot{y}_s - \dot{y}_{TMD})\right] + \left[k_s y_s + k_{TMD}(y_s - y_{TMD})\right] = u(t) - m_s\ddot{y}_g(t) \qquad (7.5)$$

$$m_{TMD}\ddot{y}_{TMD} + c_{TMD}(\dot{y}_{TMD} - \dot{y}_s) + k_{TMD}(y_{TMD} - y_s) = -m_{TMD}\ddot{y}_g(t) \qquad (7.6)$$

As can be seen from Equation (7.6), in earthquake loading TMD unit is also excited by the ground acceleration, however in wind loading external disturbance was only applied to primary structure. In this case the state equations of the plant can be written as

$$\begin{bmatrix}\dot{x}_1\\ \dot{x}_2\\ \dot{x}_3\\ \dot{x}_4\end{bmatrix} = \begin{bmatrix}0 & 0 & 1 & 0\\ 0 & 0 & 0 & 1\\ -10.1 & 0.1 & -0.3316 & 0\\ 10 & -10 & 0 & 0\end{bmatrix}\begin{bmatrix}x_1\\ x_2\\ x_3\\ x_4\end{bmatrix} + \begin{bmatrix}0 & 0\\ 0 & 0\\ -1 & 1\\ -1 & 0\end{bmatrix}\begin{bmatrix}\ddot{y}_g(t)\\ u(t)\end{bmatrix} \qquad (7.7)$$

$$\begin{bmatrix}y_1\\ y_2\\ y_3\\ y_4\end{bmatrix} = \begin{bmatrix}1 & 0 & 0 & 0\\ 0 & 1 & 0 & 0\\ 0 & 0 & 1 & 0\\ 0 & 0 & 0 & 1\end{bmatrix}\begin{bmatrix}x_1\\ x_2\\ x_3\\ x_4\end{bmatrix} \qquad (7.8)$$

7.1.3. State Equations of Combined SDOF Plant/optimal TMD

Let's define:

$$\mu = \frac{m_{TMD}}{m_s}; \lambda = \frac{\omega_1}{\omega_0}; \zeta_s = \frac{c_s}{2m_s\omega_0}; \zeta_1 = \frac{c_{TMD}}{2m_{TMD}\omega_1}; \omega_0 = \sqrt{k_s / m_s}; \omega_1 = \sqrt{k_{TMD} / m_{TMD}}$$

Transferring Equations (7.5) and (7.6) into frequency domain by Laplace transform which is defined as Z(s) = L[z(t)] and introducing the above parameters gives:

$$X_s s^2 + \left[2\omega_0\zeta_s X_s + 2\lambda\omega_0\zeta_1\mu(X_s - X_1)\right]s + \left[\omega_0^2 X_s + \mu\lambda^2\omega_0^2(X_s - X_1)\right] = -\ddot{X}_g \quad (7.9)$$

$$(\mu X_1)s^2 + \left[2\lambda\omega_0\zeta_1\mu(X_1 - X_s)\right]s + \left[\mu\lambda^2\omega_0^2(X_1 - X_s)\right] = -\mu\ddot{X}_g \quad (7.10)$$

In which:

$X_s = X_s(s) = L[x_s]$,
$X_1 = X_1(s) = L[x_1]$,
$\ddot{X}_g = \ddot{X}_g(s) = L\left[\ddot{X}_g(t)\right]$

Equations (7.9) and (7.10) can be written in matrix form as follows:

$$\begin{bmatrix} A(s) & B(s) \\ B(s) & G(s) \end{bmatrix}\begin{bmatrix} X_s \\ X_1 \end{bmatrix} = \begin{bmatrix} -1 \\ -\mu \end{bmatrix}\ddot{X}_g \quad (7.11)$$

In which:

$$A(s) = s^2 + (2\omega_0\zeta_s + 2\lambda\omega_0\zeta_1\mu)s + \omega_0^2 + \mu\lambda^2\omega_0^2$$

$$B(s) = (-2\lambda\omega_0\zeta_1\mu)s - \mu\lambda^2\omega_0^2$$

$$G(s) = \mu s^2 + (2\lambda\omega_0\zeta_1\mu)s + \mu\lambda^2\omega_0^2$$

Transfer Function of the main structure can be found by solving the Eq. (7.11).

$$TF_s(s) = \frac{X_s}{\ddot{X}_g} = \frac{-G(s) + \mu B(s)}{A(s)G(s) - B(s)B(s)} \tag{7.12}$$

Once the Transfer Function is obtained Dynamic Amplification Factor can be calculated through setting s=iω in the Transfer Function and computing $\omega_0^2 \left| [TF_s(i\omega)] \right|$. Then optimum values are calculated using the minimum-maximum amplitude procedure. The calculated optimal TMD parameters corresponding to mass ratio μ=0.01 are given as:

k_s = 1.10^5 kN/m
c_s = $3{,}16.10^3$ kN/s (%5 damping)
m_s = 1.10^4 tons
k_{TMD} = 946.7 kN/m (λ=0.973)
m_{TMD} = 100 tons (μ=0.01)
c_{TMD} = 40000 N/s (%6.5 damping)

The state equations of the plant can be written as

$$\begin{bmatrix} \dot{x}_1 \\ \dot{x}_2 \\ \dot{x}_3 \\ \dot{x}_4 \end{bmatrix} = \begin{bmatrix} 0 & 0 & 1 & 0 \\ 0 & 0 & 0 & 1 \\ -10.09 & 0.095 & -0.3202 & 0.004 \\ 9.467 & -9.467 & 0.4 & -0.4 \end{bmatrix} \begin{bmatrix} x_1 \\ x_2 \\ x_3 \\ x_4 \end{bmatrix} + \begin{bmatrix} 0 & 0 \\ 0 & 0 \\ 1 & 1 \\ 1 & 0 \end{bmatrix} \begin{bmatrix} \ddot{y}_g(t) \\ u(t) \end{bmatrix} \tag{7.13}$$

$$\begin{bmatrix} y_1 \\ y_2 \\ y_3 \\ y_4 \end{bmatrix} = \begin{bmatrix} 1 & 0 & 0 & 0 \\ 0 & 1 & 0 & 0 \\ 0 & 0 & 1 & 0 \\ 0 & 0 & 0 & 1 \end{bmatrix} \begin{bmatrix} x_1 \\ x_2 \\ x_3 \\ x_4 \end{bmatrix} \tag{7.14}$$

7.2. Controller Dynamics

7.2.1. LQR for SDOF Plant

The state weighting matrix, Q, and the control force weighting matrix, R, are selected as:

$$Q = \begin{bmatrix} 1 & 0 \\ 0 & 1 \end{bmatrix}, R = 0.01 \tag{7.15}$$

The corresponding control gain is calculated to be:

$$K = \begin{bmatrix} 4.1421 & 10.095 \end{bmatrix} \tag{7.16}$$

7.2.2. H_∞ for SDOF Plant

Performance weighting function is selected as W_p=1 and the control weighting function W_u=0.9*10^{-1}.

The gain matrix *K*, calculated by H_∞ *algorithm* is given by:

$$K = \begin{bmatrix} 6.0297 & 9.012 \end{bmatrix} \tag{7.17}$$

7.2.3. LQR for Combined SDOF Plant/optimal TMD

The state weighting matrix, Q, and the control force weighting matrix, R, are selected as:

$$Q = \begin{bmatrix} 1 & 0 & 0 & 0 \\ 0 & 0 & 0 & 0 \\ 0 & 0 & 1 & 0 \\ 0 & 0 & 0 & 0 \end{bmatrix}, R = 0.01 \tag{7.18}$$

The corresponding control gain is calculated to be:

$$K = \begin{bmatrix} 4.0548 & 0.087 & 10.082 & 0.0036 \end{bmatrix} \tag{7.19}$$

7.2.4. H_∞ for Combined SDOF Plant/optimal TMD

Performance weighting function is selected as W_p=1 and the control weighting function W_u=0.9*10^{-1}.

The gain matrix K, calculated by H_∞ *algorithm* is given by:

$$K = \begin{bmatrix} 5.1316 & 0.5956 & 8.927 & 0.0977 \end{bmatrix} \tag{7.20}$$

7.2.5. LQR for Combined SDOF Plant/non-optimal TMD

The state weighting matrix, Q, and the control force weighting matrix, R, are selected as:

$$Q = \begin{bmatrix} 1 & 0 & 0 & 0 \\ 0 & 0 & 0 & 0 \\ 0 & 0 & 1 & 0 \\ 0 & 0 & 0 & 0 \end{bmatrix}, R = 0.01 \tag{7.21}$$

The corresponding control gain is calculated to be:

$$K = \begin{bmatrix} 4.1414 & 0.001 & 10.094 & 0.0039 \end{bmatrix} \tag{7.22}$$

7.2.6. H_∞ for Combined SDOF Plant/non-optimal TMD

Performance weighting function is selected as W_p=1 and the control weighting function W_u=0.9*10^{-1}.

The gain matrix K, calculated by H_∞ *algorithm* is given by:

$$K = \begin{bmatrix} 6.0288 & 0.0294 & 8.981 & 0.0857 \end{bmatrix} \tag{7.23}$$

7.2.7. LQR for Model Matching Problem

The selected reference model is an oscillator with natural frequency 3.16 rad/sec which is the operating frequency of TMD. If we introduce %9.5 damping to reference model, the state equations become:

$$\begin{bmatrix} \dot{z}_1 \\ \dot{z}_2 \end{bmatrix} = \begin{bmatrix} 0 & 1 \\ -9.986 & -0.6 \end{bmatrix} \begin{bmatrix} z_1 \\ z_2 \end{bmatrix} + \begin{bmatrix} 0 \\ 0.01 \end{bmatrix} w \tag{7.24}$$

$$\tilde{y} = \begin{bmatrix} 1 & 0 \end{bmatrix} \tag{7.25}$$

The state weighting matrix, Q, and the control force weighting matrix, R, are selected as:

$$Q = \begin{bmatrix} 1 & 0 & 0 & 0 \\ 0 & 0 & 0 & 0 \\ 0 & 0 & 1 & 0 \\ 0 & 0 & 0 & 0 \end{bmatrix}, R = 0.011 \tag{7.26}$$

The corresponding control gain is calculated to be:

$$K = \begin{bmatrix} 3.8163 & 0.0007 & 9.6156 & 0.0038 & -3.779 & -9.212 \end{bmatrix} \tag{7.27}$$

7.2.8. H_∞ for Model Matching Problem

Performance weighting function is selected as W_p=1 and the control weighting function W_u=0.72*10^{-1}.

The selected reference model is an oscillator with natural frequency 3.16 rad/sec which is the operating frequency of TMD. If we introduce %5 damping to reference model, the state equations become:

$$\begin{bmatrix} \dot{z}_1 \\ \dot{z}_2 \end{bmatrix} = \begin{bmatrix} 0 & 1 \\ -9.986 & -0.3 \end{bmatrix} \begin{bmatrix} z_1 \\ z_2 \end{bmatrix} + \begin{bmatrix} 0. \\ 0.01 \end{bmatrix} w \tag{7.28}$$

$$\tilde{y} = \begin{bmatrix} 1 & 0 \end{bmatrix} \tag{7.29}$$

The gain matrix K, calculated by H_∞ *algorithm* is given by:

$$K = \begin{bmatrix} 9.0907 & 0.2912 & 7.666 & 0.2458 & -1.2269 & -5.6874 \end{bmatrix} \tag{7.30}$$

7.3. Transfer Matrices of the Closed Loop System

7.3.1. Comparison of Closed-loop Systems with LQR

As in the case of wind loads, when the input frequency is lower than the natural frequency of the system, the proposed controller gives better results in terms of closed-loop displacement. The sharp peak around the natural frequency is also seen when the system is excited by ground acceleration. On the other hand, the effectiveness of TMD unit at the operating frequency is severely deteriorated. This is due to fact that, wind loads only influence the plant however ground acceleration affects also the TMD unit together with the plant. As can be recalled from Section 4.1 TMD exerts a force to the primary structure which is opposite of the external force. The exerted force is the spring force of TMD and developed through the out-of-phase motion of TMD with the primary structure. However, ground motion accelerates TMD unit in phase with the structure so, out-of-phase displacement is reduced, and therefore exerted force by the TMD unit is decreased.

Figure 7.2 suggests that there is a sudden jump and drop of control forces at the operating frequency which is similar to wind loading. On the other hand reduction in control forces are more pronounced in the low frequency range.

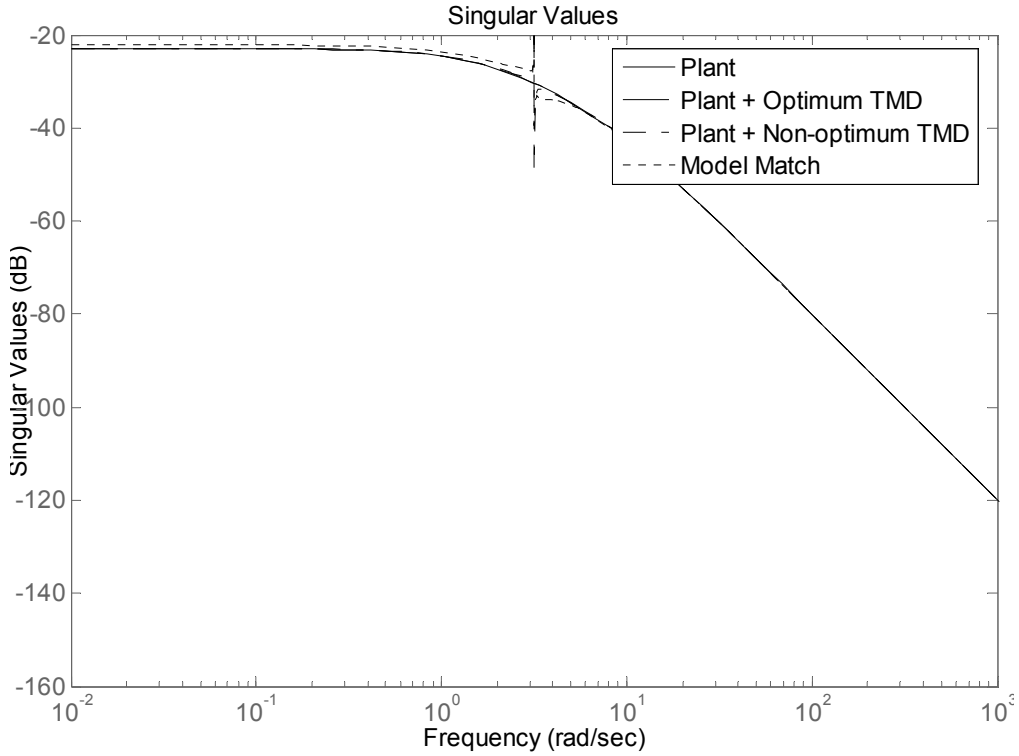

Figure 7.1. Sing. val. of the closed loop systems from input to displacement - LQR

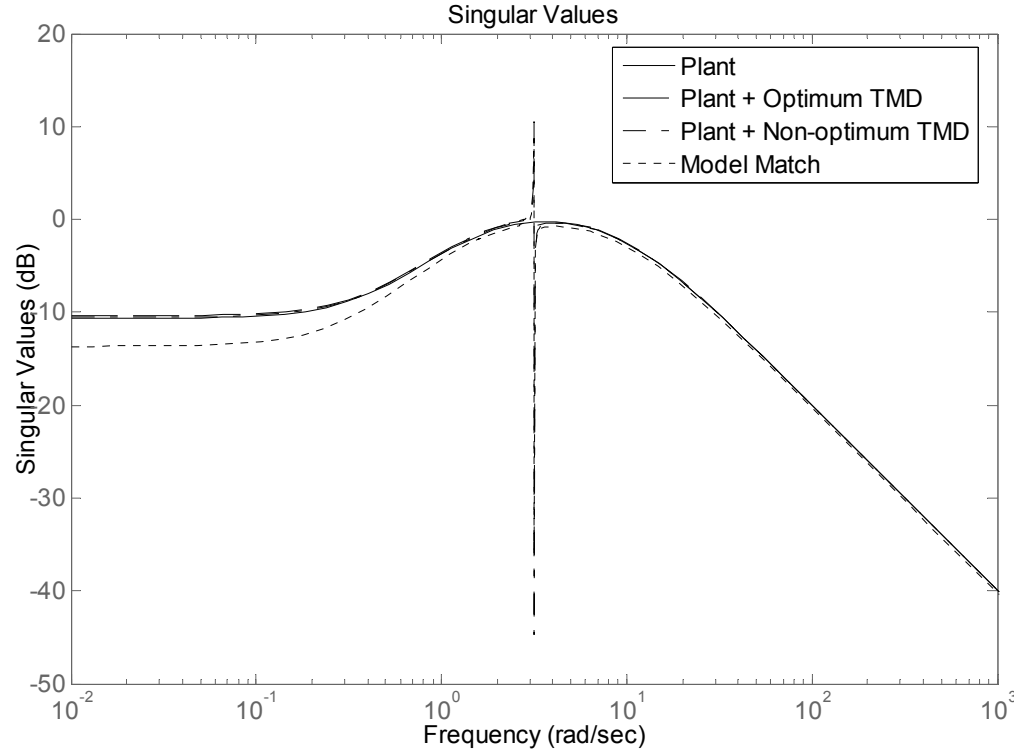

Figure 7.2. Sing. val. of the closed loop systems from input to control force – LQR

7.3.2. Comparison of Closed-loop Systems with H_∞

Similar to wind loading, there is seen no difference in responses between plant and combined optimal TMD/plant structure. On the other hand sudden drop at operating frequency is visible for combined non-optimal TMD/plant structure. Other than that the responses of the three controllers are similar. The proposed controller however gives better response for frequencies smaller than the natural frequency and the response is almost the same with the rest of the controllers when frequencies are larger than the natural frequency

Figure 6.4 suggests that there is a less control demand for frequencies higher than the natural frequency with the proposed controller. Although, for low frequency range more control energy is needed when compared to standard regulators this will not pose a problem since the seismic frequency falls into high frequency range.

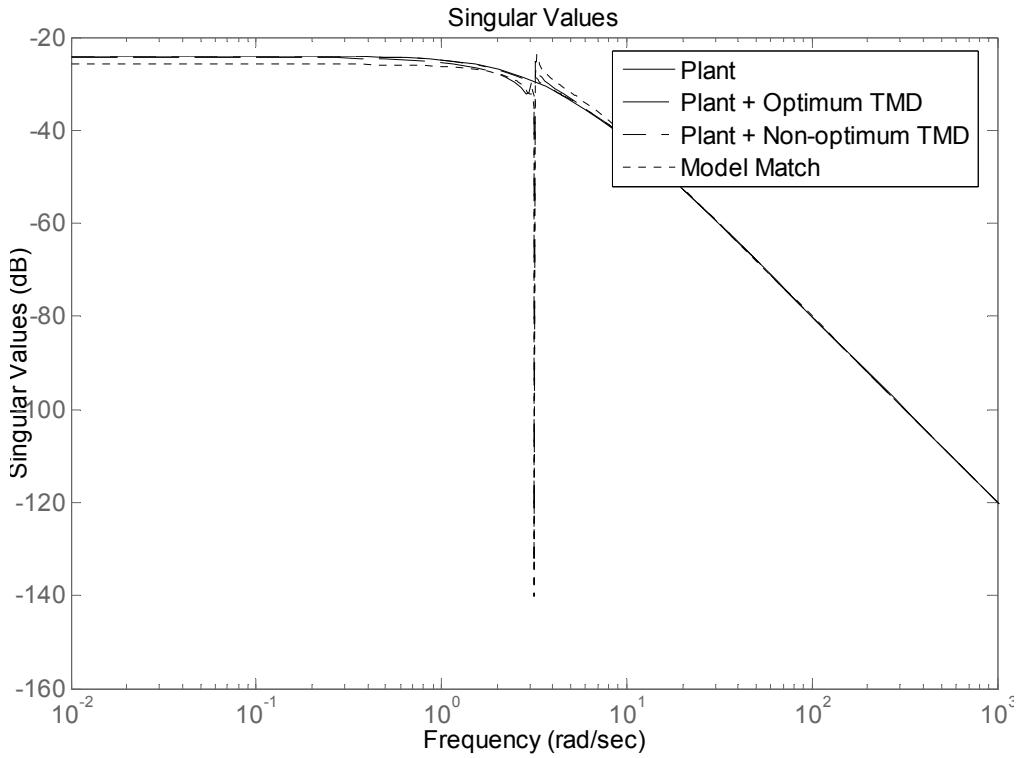

Figure 7.3. Sing. val. of the closed loop systems from input to displacement - H_∞

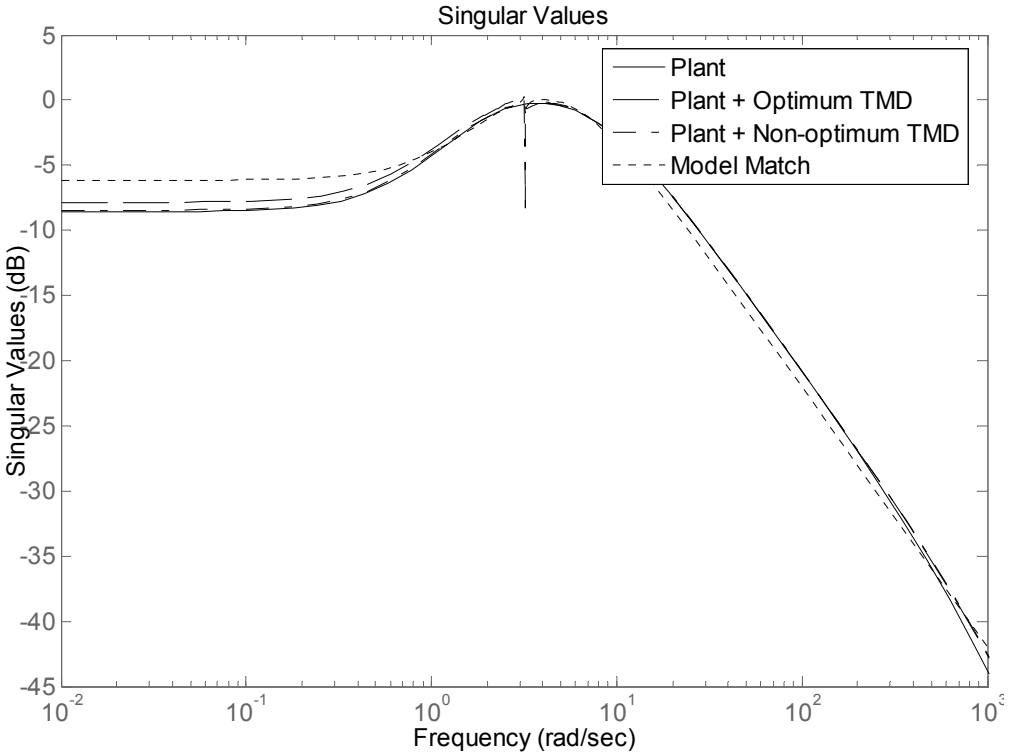

Figure 7.4. Sing. val. of the closed loop systems from input to control force - H_∞

7.3.3. Comparison of H_∞ and LQR Model Matching Problem

When we compare the proposed controllers in LQR and H_∞ settings we see that for high frequency range control performance is identical except for LQR setting is more effective for the frequencies in the vicinity of natural frequency. For low frequencies however H_∞ controller is more effective.

In the LQR setting there is a sharp peak in controller forces corresponding to tuning frequency in order to compensate damping effect of TMD unit. In the H_∞ setting however singular values of the control forces are smoothed. Additionally, control requirement in high frequency range is lesser in H_∞ setting, conversely in low frequency range LQR setting gives less requirement in control forces.

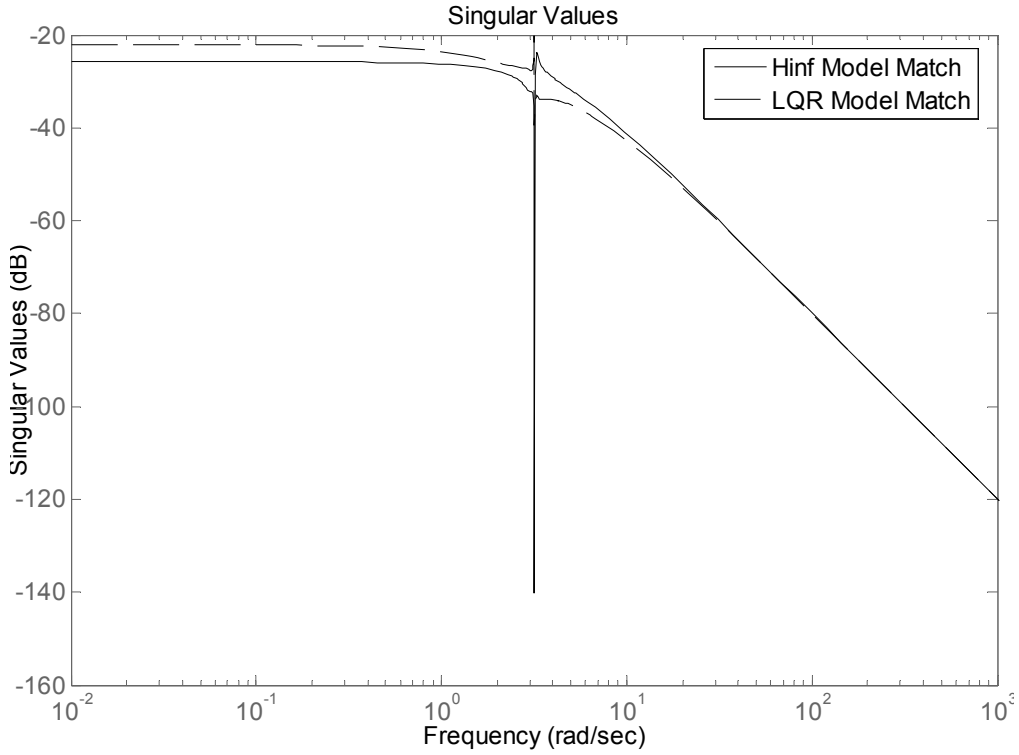

Figure 7.5. H_∞ and LQR closed loop system sing. val. from input to displacement

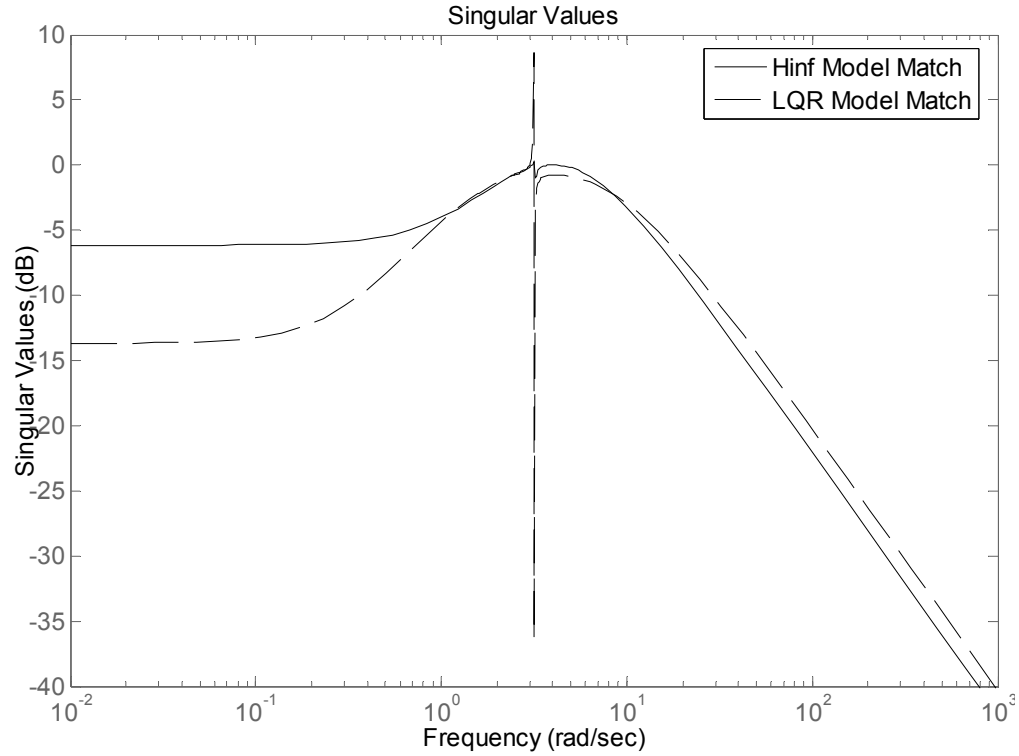

Figure 7.6. H_∞ and LQR closed loop system sing. val. from input to control force

7.4. Time Domain Response of the Closed Loop System to White Noise Input

To demonstrate the effectiveness of proposed strategy in both LQR and H_∞ settings, the performances of various controllers in regulator form in terms of closed-loop displacement and required control force are compared with the proposed tracking type controllers. Compared closed-loop systems include

- SDOF plant controlled with LQR and H∞ regulators
- Combined plant/optimal TMD structure controlled with LQR and H∞ regulators
- Combined plant/non-optimal TMD structure controlled with LQR and H∞ regulators
- Combined plant/non-optimal TMD structure controlled with LQR and H∞ tracking controllers

The last listed systems are the proposed systems in which a LQR/ H_∞ controllers drives the combined plant/non-optimal TMD structure to follow the response of an idealized mathematical model. The selected idealized mathematical model is an oscillator whose natural frequency is set to the operating frequency of non-optimized TMD. The idea was to render the closed-loop response to fall into operating frequency of the TMD unit. To effectiveness of the proposed strategy is assessed through statistical analyses in two parts. In the first part the compared systems are excited with 200 artificially generated white noise inputs. Then the mean values and standard deviations corresponding to each control system is noted and compared to each other. In the second part statistical analyses are rerun with actual seismic records to evaluate the effectiveness in real cases.

As in the case of wind loads, the addition of TMD in optimal configuration has a marginal effect on control energy when used with standard LQR regulator. On the other hand, the effectiveness of TMD is reduced in non-optimal configuration since the ground acceleration has a negative effect on TMD. This also negatively influences the effectiveness of the proposed strategy in LQR setting. As can be seen from Figure 7.7 and Table 7.1 when the structure is subjected to ground acceleration the control energy requirement is %2.4 lesser when compared to standard LQR regulators.

Figure 7.8 and Table 7.2 reveals that when it comes to maximum control force, with the proposed controllers the least control effort in terms of percent weight of the structure is obtained. The improvement in this case is %2.7.

As suggested by Figures 7.9 and 7.10, Tables 7.3 and 7.4, the adverse effect of ground acceleration on TMD unit is also seen in H_∞ setting. Although still better performance is obtained when compared to LQR controllers the improvement in control energy is %4.3 and improvement in maximum control force is %4.7. Nevertheless the best performance is obtained with the proposed controllers.

7.4.1. H_2 Norms of Closed-loop Systems with LQR Regulators

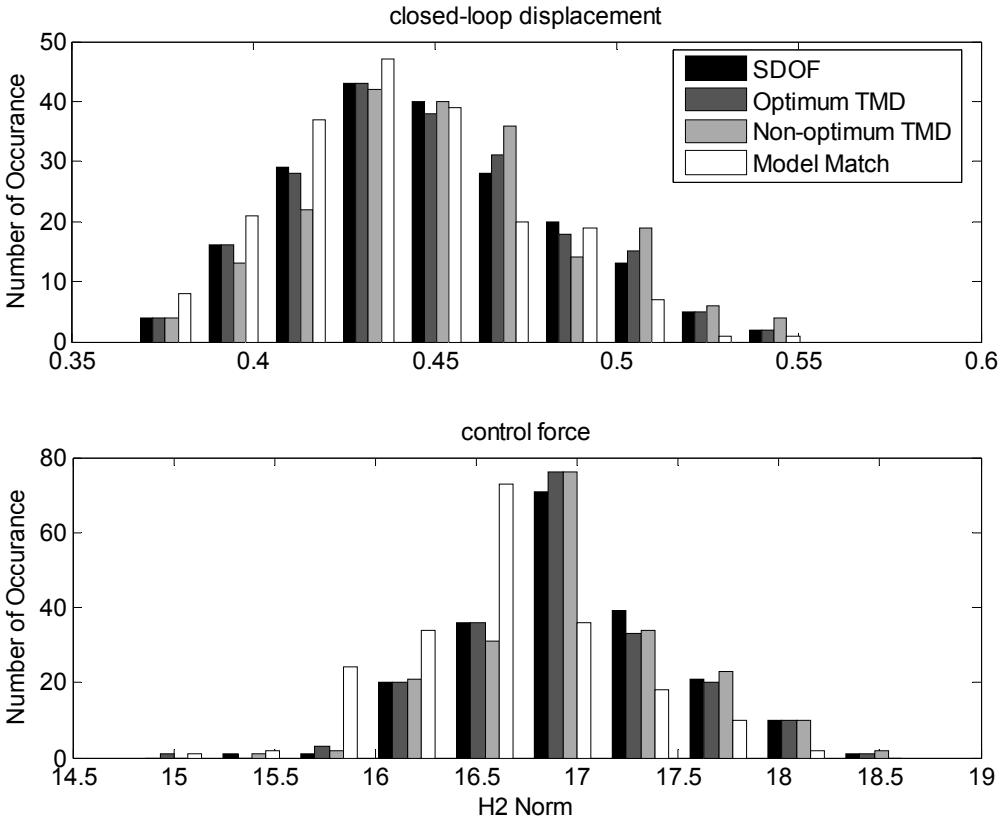

Figure 7.7. H_2 norm of closed-loop disp. and control forces – LQR

Table 7.1. Mean and standard deviation of closed loop response – LQR

(Closed Loop Displacement Energy)$^{1/2}$

	SDOF	Optimum TMD	Non-optimum TMD	LQR Model Match
μ	0,4481	0,4485	0,4523	0,4379
σ	0,0357	0,0357	0,0362	0,0329

(Normalized Control Energy)$^{1/2}$

	SDOF	Optimum TMD	Non-optimum TMD	LQR Model Match
μ	16,9793	16,9640	16,9939	16,5757
σ	0,5344	0,5337	0,5431	0,5392

7.4.2. H_∞ Norms of Closed-loop Systems with LQR Regulators

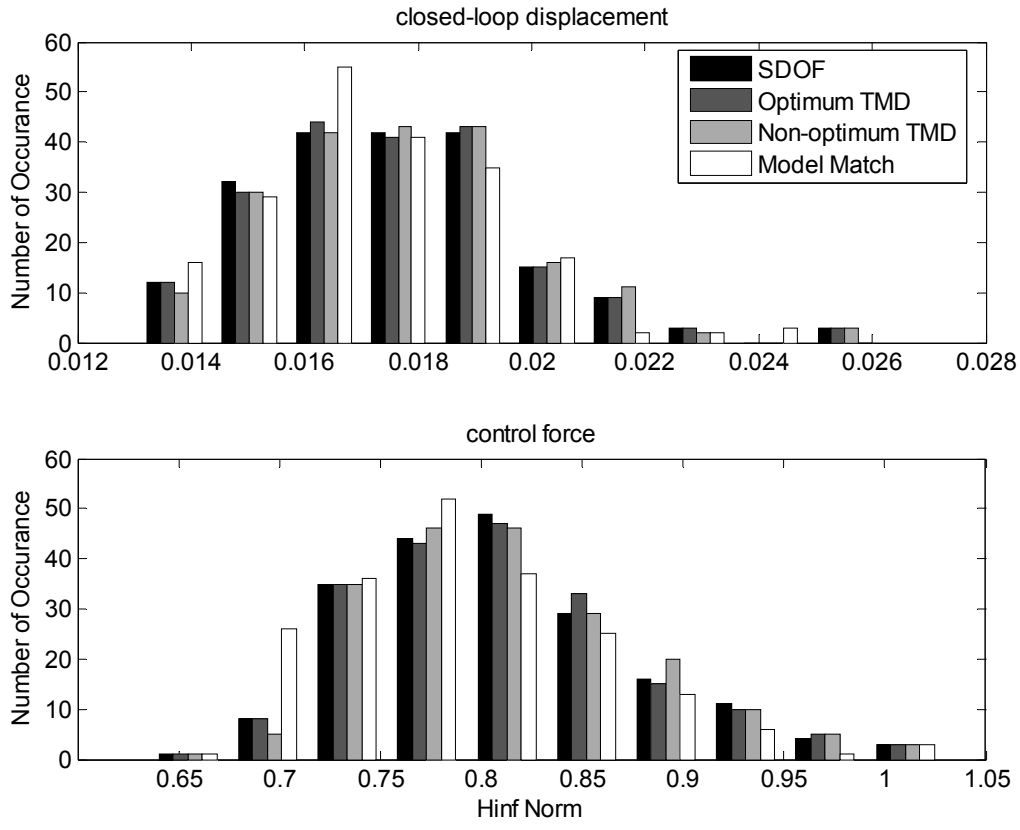

Figure 7.8. H_∞ norm of closed-loop disp. and control forces – LQR

Table 7.2. Mean and standard deviation of closed loop response – LQR

Closed Loop Displacement (m)				
	SDOF	Optimum TMD	Non-optimum TMD	LQR Model Match
μ	0,0176	0,0176	0,0177	0,0173
σ	0,0023	0,0023	0,0023	0,0021
Control Force / m_s				
	SDOF	Optimum TMD	Non-optimum TMD	LQR Model Match
μ	0,8104	0,8099	0,8117	0,7899
σ	0,0697	0,0696	0,0689	0,0673

7.4.3. H_2 Norms of Closed-loop Systems with H∞ Regulators

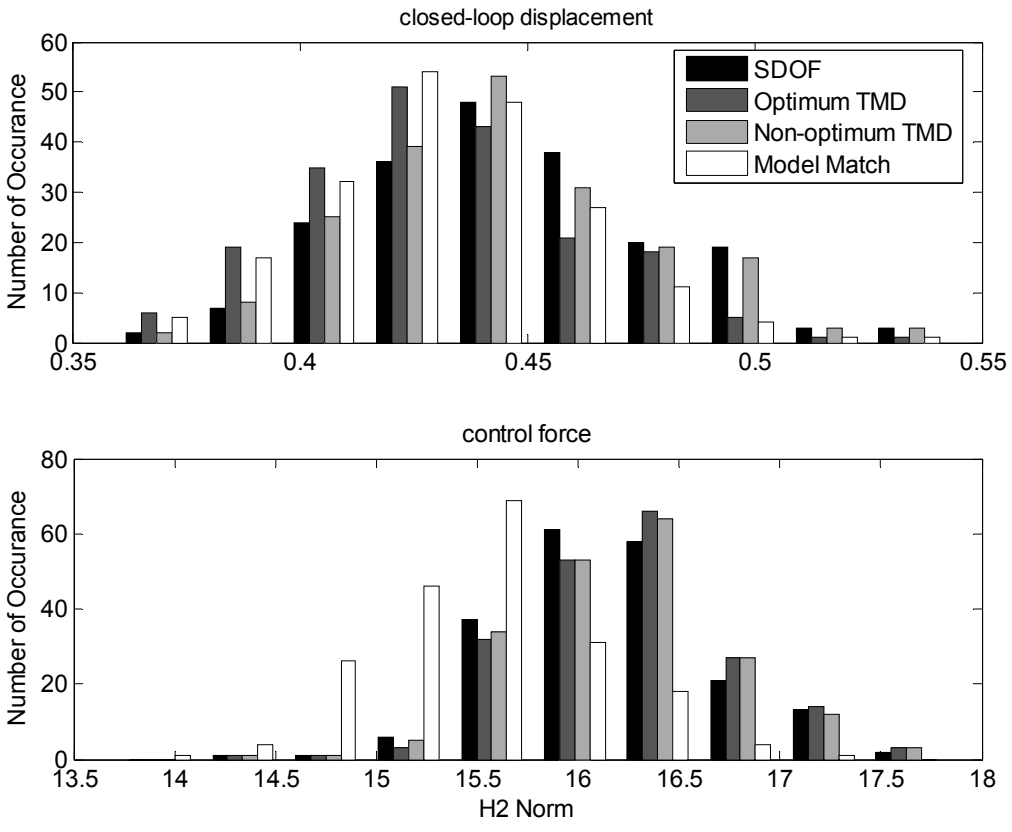

Figure 7.9. H_2 norm of closed-loop disp. and control forces – H_∞

Table 7.3. Mean and standard deviation of closed loop response – H_2

(Closed Loop Displacement Energy)$^{1/2}$				
	SDOF	Optimum TMD	Non-optimum TMD	H_∞ Model Match
μ	0,4467	0,4306	0,4443	0,4312
σ	0,0327	0,0306	0,0326	0,0286
(Normalized Control Energy)$^{1/2}$				
	SDOF	Optimum TMD	Non-optimum TMD	H_∞ Model Match
μ	16,1894	16,2464	16,2298	15,4935
σ	0,5136	0,5190	0,5177	0,5335

7.4.4. H_∞ Norms of Closed-loop Systems with H∞ Regulators

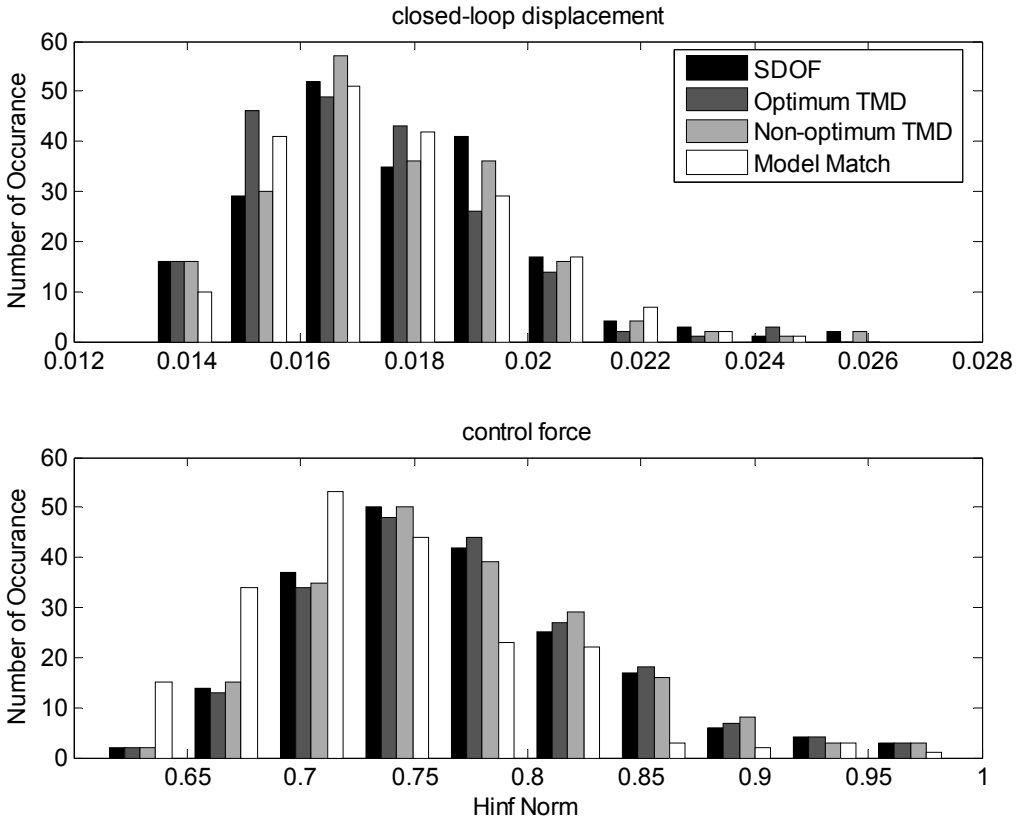

Figure 7.10. H_∞ norm of closed-loop disp. and control forces – H_∞

Table 7.4. Mean and standard deviation of closed loop response – H_∞

Closed Loop Displacement (m)				
	SDOF	Optimum TMD	Non-optimum TMD	H_∞ Model Match
μ	0,0177	0,0171	0,0176	0,0174
σ	0,0022	0,0021	0,0022	0,0020
Control Force / m_s				
	SDOF	Optimum TMD	Non-optimum TMD	H_∞ Model Match
μ	0,7675	0,7708	0,7701	0,7315
σ	0,0665	0,0664	0,0664	0,0631

7.5. Time Domain Response of the Closed Loop System to Seismic Record

With the excitation of actual seismic records, it is seen that proposed controller in LQR setting give the best answer. Appropriate weights are selected in order to equate the displacement energy and max. displacement among the various controllers, thus closed-loop performance is more or less the same as can be observed from Tables 7.6 and 7.7. Then the deciding factor is the control energy and max. control force. Tables 7.8 and 7.9 suggest that the improvement in terms of control energy and maximum control force are %2.1 and %2.7 respectively with the proposed controller when the mean values are considered.

When it comes to H_∞ setting we observe a %4 and %7.2 improvement for control energy and maximum control force respectively. The improvement in maximum control force is more pronounced since the sharp peaks in singular value plot of input to control forces are smoothed in H_∞ setting. On the other hand the displacement energy and maximum displacement of the closed loop system is slightly higher with the proposed controller when mean values are considered.

It is seen that the effectiveness of the proposed strategy depends on the nature of the input force. The proposed controllers render the closed-loop response to fall into operating frequency of the TMD unit. The operating frequency is the resonance frequency of the TMD unit thus effectiveness is gradually increasing with time and closely linked to

the TMD displacement. However, for pulse like inputs as in the case of earthquakes the maximum input acceleration comes so early that TMD unit couldn't find time to operate effectively. On the other hand it is seen that for stations 4,7,11 and 12 the displacement energy and max. displacement is smaller in proposed controllers. Close inspection reveals that the seismic input in station 7 is more uniform in amplitude and the pulses in seismic inputs corresponding to stations 11 and 12 appear later in the record.

All in all, for seismic inputs effectiveness of the proposed controllers are reduced due to the negative effect of the input acceleration on TMD unit and also due to the pulse characteristics of the ground shaking. Thus it renders proposed strategy more effective for wind loads save for still the proposed strategy gives best answer for earthquake loads.

Table 7.5. Seismic records used in the statistical study

Earthquake	Magnitude	Station Name	Station No	Comp.	Peak Acceleration (g)
Imperial Valley 1979	6.6	Calexico Fire Station	1	H315	0,171
			2	H225	0,275
			3	H315	0,187
		Brawley Airport	4	H225	0,160
San Fernando 1971	6.6		5	H172	0,148
		Santa Felicia Dam	6	H262	0,152
		Whittier Narrows Dam	7	H143	0,081
			8	H233	0,107
San Fransisco 1957	5.3		9	H010	0,093
		Golden Gate	10	H100	0,112
Kocaeli 1999	7.4		11	H000	0,150
		Arçelik	12	H090	0,108
			13	H000	0,076
		Botaş	14	H090	0,076
			15	H000	0,074
		Bursa Tofaş	16	H090	0,095
Whittier Narrows 1987	5.9		17	H270	0,374
		Obregon Park	18	H360	0,234
			19	H000	0,158
		MT Wilson	20	H090	0,142

7.5.1. H_2 Displacement Norms of Closed-loop Systems

Table 7.6. Closed loop response of various controllers –Displacement Energy

(Displacement Energy)$^{1/2}$

Station No	SDOF LQR	SDOF H∞	TMDopt LQR	TMDopt H∞	TMD LQR	TMD H∞	Model Match LQR	Model Match H∞
1	0,289	0,304	0,289	0,305	0,288	0,304	0,296	0,333
2	0,264	0,279	0,264	0,278	0,263	0,278	0,268	0,302
3	0,378	0,400	0,379	0,392	0,381	0,398	0,384	0,428
4	0,484	0,498	0,485	0,459	0,492	0,494	0,460	0,467
5	0,205	0,213	0,205	0,204	0,206	0,212	0,199	0,212
6	0,137	0,145	0,137	0,137	0,139	0,144	0,135	0,146
7	0,157	0,162	0,157	0,154	0,159	0,161	0,152	0,157
8	0,179	0,187	0,179	0,176	0,182	0,185	0,174	0,184
9	0,014	0,016	0,014	0,016	0,014	0,015	0,015	0,017
10	0,022	0,024	0,022	0,025	0,022	0,024	0,024	0,027
11	0,180	0,181	0,181	0,173	0,182	0,180	0,174	0,172
12	0,464	0,454	0,464	0,432	0,469	0,452	0,442	0,412
13	0,139	0,147	0,139	0,144	0,140	0,146	0,141	0,158
14	0,160	0,164	0,161	0,159	0,163	0,163	0,160	0,164
15	0,411	0,431	0,411	0,414	0,415	0,429	0,409	0,443
16	0,424	0,455	0,424	0,455	0,424	0,455	0,440	0,506
17	0,057	0,062	0,057	0,063	0,057	0,062	0,060	0,069
18	0,123	0,135	0,123	0,139	0,123	0,135	0,132	0,158
19	0,017	0,019	0,017	0,019	0,017	0,019	0,018	0,020
20	0,014	0,015	0,014	0,015	0,014	0,015	0,015	0,016
μ	0,206	0,215	0,206	0,208	0,207	0,214	0,205	0,220
σ	0,156	0,160	0,156	0,154	0,157	0,160	0,153	0,162

7.5.2. H_∞ Displacement Norms of Closed-loop Systems

Table 7.7. Closed loop response of various controllers – Max. Displacement

	Max. Displacement (m)							
Station No	SDOF LQR	SDOF H∞	TMDopt LQR	TMDopt H∞	TMD LQR	TMD H∞	Model Match LQR	Model Match H∞
1	0,0107	0,0121	0,0107	0,0133	0,0105	0,0122	0,0125	0,0156
2	0,0124	0,0125	0,0124	0,0123	0,0124	0,0125	0,0123	0,0130
3	0,0310	0,0328	0,0310	0,0327	0,0310	0,0327	0,0320	0,0344
4	0,0253	0,0263	0,0253	0,0241	0,0256	0,0257	0,0237	0,0258
5	0,0067	0,0069	0,0068	0,0069	0,0067	0,0069	0,0065	0,0077
6	0,0050	0,0053	0,0050	0,0051	0,0051	0,0052	0,0051	0,0052
7	0,0072	0,0075	0,0072	0,0072	0,0073	0,0075	0,0071	0,0074
8	0,0058	0,0059	0,0058	0,0065	0,0056	0,0059	0,0061	0,0065
9	0,0019	0,0020	0,0019	0,0020	0,0019	0,0020	0,0019	0,0021
10	0,0026	0,0028	0,0026	0,0029	0,0026	0,0028	0,0027	0,0031
11	0,0095	0,0092	0,0095	0,0087	0,0096	0,0091	0,0089	0,0079
12	0,0236	0,0239	0,0236	0,0228	0,0237	0,0238	0,0227	0,0220
13	0,0066	0,0076	0,0066	0,0074	0,0066	0,0075	0,0071	0,0083
14	0,0079	0,0088	0,0079	0,0081	0,0080	0,0087	0,0079	0,0088
15	0,0133	0,0147	0,0133	0,0148	0,0133	0,0150	0,0138	0,0176
16	0,0177	0,0187	0,0177	0,0190	0,0179	0,0187	0,0191	0,0215
17	0,0064	0,0068	0,0064	0,0068	0,0064	0,0068	0,0066	0,0073
18	0,0158	0,0170	0,0158	0,0170	0,0158	0,0169	0,0164	0,0183
19	0,0020	0,0021	0,0020	0,0021	0,0020	0,0021	0,0020	0,0021
20	0,0018	0,0018	0,0018	0,0018	0,0018	0,0018	0,0018	0,0019
μ	0,0107	0,0112	0,0107	0,0111	0,0107	0,0112	0,0108	0,0118
σ	0,0083	0,0087	0,0083	0,0084	0,0083	0,0086	0,0083	0,0090

7.5.3. H_2 Control Force Norms of Closed-loop Systems

Table 7.8. Closed loop response of various controllers – Control Energy

(Normalized Control Energy)$^{1/2}$

Station No	SDOF LQR	SDOF H∞	TMD_{opt} LQR	TMD_{opt} H∞	TMD LQR	TMD H∞	Model Match LQR	Model Match H∞
1	15,56	14,92	15,51	14,90	15,50	14,93	15,10	14,20
2	18,57	17,74	18,54	17,72	18,54	17,76	18,01	16,71
3	15,16	14,75	15,12	14,78	15,13	14,78	14,88	14,42
4	12,56	12,17	12,65	12,39	12,68	12,23	12,54	11,97
5	8,09	7,86	8,08	7,89	8,07	7,86	7,92	7,66
6	6,32	6,11	6,33	6,14	6,34	6,13	6,21	5,92
7	6,30	6,01	6,30	6,03	6,31	6,02	6,15	5,70
8	7,44	7,13	7,44	7,16	7,46	7,15	7,29	6,82
9	2,19	2,04	2,19	2,04	2,19	2,04	2,11	1,85
10	2,82	2,62	2,81	2,62	2,82	2,63	2,71	2,39
11	8,04	7,66	8,04	7,68	8,05	7,68	7,83	7,26
12	9,48	9,10	9,50	9,24	9,49	9,14	9,38	8,92
13	6,72	6,52	6,70	6,52	6,73	6,53	6,60	6,33
14	6,68	6,48	6,67	6,49	6,72	6,49	6,60	6,28
15	15,95	15,61	15,94	15,66	15,98	15,63	15,75	15,34
16	19,71	19,40	19,63	19,39	19,64	19,41	19,37	19,20
17	8,74	8,11	8,73	8,11	8,74	8,14	8,39	7,35
18	10,93	10,45	10,91	10,43	10,92	10,46	10,60	9,87
19	2,91	2,69	2,91	2,69	2,91	2,70	2,79	2,42
20	2,77	2,55	2,77	2,54	2,77	2,56	2,65	2,27
μ	9,35	9,00	9,34	9,02	9,35	9,01	9,14	8,64
σ	5,33	5,21	5,32	5,22	5,32	5,22	5,23	5,12

7.5.4. H_∞ Control Force Norms of Closed-loop Systems

Table 7.9. Closed loop response of various controllers – Max. Control Force

	Max. Control Force /m_s							
Station No	SDOF LQR	SDOF H∞	TMDopt LQR	TMDopt H∞	TMD LQR	TMD H∞	Model Match LQR	Model Match H∞
1	1,233	1,174	1,231	1,173	1,231	1,176	1,196	1,100
2	1,415	1,319	1,415	1,319	1,416	1,323	1,363	1,195
3	1,171	1,141	1,162	1,154	1,166	1,143	1,143	1,163
4	0,844	0,822	0,839	0,816	0,840	0,821	0,821	0,798
5	0,436	0,413	0,435	0,411	0,435	0,413	0,420	0,381
6	0,477	0,451	0,477	0,451	0,477	0,452	0,462	0,416
7	0,422	0,386	0,421	0,384	0,422	0,387	0,400	0,336
8	0,457	0,438	0,456	0,439	0,456	0,438	0,446	0,419
9	0,299	0,273	0,299	0,273	0,299	0,274	0,285	0,246
10	0,346	0,328	0,346	0,328	0,346	0,328	0,335	0,306
11	0,728	0,662	0,729	0,663	0,731	0,666	0,696	0,578
12	0,637	0,607	0,637	0,611	0,637	0,610	0,622	0,581
13	0,481	0,468	0,481	0,469	0,483	0,468	0,473	0,451
14	0,489	0,472	0,485	0,466	0,486	0,471	0,473	0,448
15	0,680	0,663	0,676	0,657	0,675	0,665	0,659	0,639
16	0,751	0,728	0,747	0,723	0,749	0,728	0,729	0,699
17	1,339	1,242	1,337	1,242	1,339	1,246	1,287	1,123
18	1,330	1,278	1,330	1,284	1,330	1,280	1,302	1,228
19	0,533	0,492	0,533	0,492	0,533	0,494	0,511	0,440
20	0,412	0,370	0,412	0,369	0,413	0,371	0,390	0,331
μ	0,72	0,69	0,72	0,69	0,72	0,69	0,70	0,64
σ	0,37	0,35	0,37	0,35	0,37	0,35	0,36	0,34

8. CONCLUSIVE REMARKS

In this study a hybrid system is suggested in which a tracking type controller is used together with a passive undamped TMD unit. When a structure is excited with a single frequency disturbance, it is well known that TMD is most effective when it is tuned to input frequency and no damping is introduced. However, for earthquake loads the input has a broadband frequency range and for wind loads the driving frequency is not known a priori. Therefore some damping is introduced to TMD unit to smoothen the sharp peaks of the frequency response function out of the operating range but in this case the effectiveness of TMD unit in the operating range is adversely affected. The proposed control strategy aims to alter the system response to coincide with the operating frequency of TMD unit. Then the response of the controlled structure matches the desired operating frequency of TMD unit no matter what the frequency content of the input is, hence a passive undamped TMD unit can be utilized in full effectiveness.

It was shown in Chapter 5 that an undamped TMD is operating in its full performance when the controlled system tracks a harmonic reference command which's frequency is set to the operating frequency of undamped TMD. However, it was seen that at operating frequency controller forces increase sharply due to constant amplitude tracking. In that case TMD unit was trying to suppress the response on the other hand controller was trying to maintain displacement response at constant level. Thus, there was a conflict with TMD objectives and controller objectives. Consequently an alternative solution was formulated by tracking a reference model instead of a reference signal. In this so called model matching problem controller tries to match the states of the plant with the states of an idealized mathematical model. A simple oscillator with natural frequency set to the operating frequency of the TMD was selected as a reference model. Thus by tracking the response of an idealized model two aspects are accomplished. Firstly, frequency of the reference signal is the desired frequency, which is the operating frequency of the TMD unit. Secondly, the amplitude of the reference signal is maintained to be more or less in harmony with the closed-loop response.

To verify the effectiveness of the proposed control scheme, the performances of standard regulator controllers are compared with the proposed controllers in terms of

closed-loop displacement and required control force. Compared closed-loop systems include a SDOF plant controlled with LQR and H_∞ regulators, a combined plant/optimal TMD structure controlled with LQR and H_∞ regulators, a combined plant/non-optimal TMD structure controlled with LQR and H_∞ regulators, and proposed hybrid system of combined plant/non-optimal TMD structure controlled with LQR and H_∞ tracking controllers. The comparison is made under both wind loads and earthquake loads. For wind loads effectiveness of the proposed strategy is assessed through statistical analyses in which the compared systems are excited with 200 artificially generated white noise inputs. Then the mean values and standard deviations corresponding to each control system is noted and compared to each other. For earthquake loads in addition to white noise inputs statistical analyses are rerun with actual seismic records to evaluate the effectiveness in real cases. The conclusions of this study can be summarized as follows:

- Under wind loads the time domain response of the compared systems reveal that the proposed closed-loop systems both in LQR and H∞ settings need less control effort for the same closed-loop performance in terms of plant displacement. When compared to standard regulators the improvement in LQR setting is %4.5 in control energy requirement, and %4.7 in maximum control force. On the other hand improvement is more pronounced in H∞ which is in agreement with the singular value plots of proposed controllers. In this case the improvement is %8.7 in control energy requirement and %9.0 in maximum control force.
- Under earthquake loads however, the effectiveness of TMD unit is adversely affected by the ground acceleration. In this case ground motion accelerates TMD unit in phase with the structure so, out-of-phase displacement therefore exerted force by the TMD unit to structure is decreased. The control energy requirement and maximum control force are %2.4 and %2.7 lesser with proposed hybrid control system in LQR setting when compared to standard LQR regulators. On the other hand improvement in H∞ setting is %4.3 in control energy requirement and %4.7 in maximum control force.
- The proposed controllers render the closed-loop response to fall into operating frequency of the TMD unit which is actually the resonance frequency of the TMD unit thus effectiveness is gradually increasing with time and closely linked to the TMD displacement. However, for pulse like inputs as in the case of earthquakes the

maximum input acceleration comes in early stages of the response history so that TMD unit couldn't find time to operate effectively. Close inspection of time history responses reveal that for more uniform amplitude inputs or for inputs that pulses appear later in the record the proposed strategy provides better performance.

- When mean values are considered, under the excitation of actual seismic records, it is seen that proposed controller in LQR setting performs %2.1 and %2.7 improvements in terms of control energy and maximum control force respectively. When it comes to H∞ setting, although it is observed a %4 and %7.2 improvements for control energy and maximum control force respectively the closed-loop performance in terms of displacement energy and max. displacement is higher when compared to standard regulators.

REFERENCES

1. J.P. Den Hartog, *Mechanical Vibrations, 4th ed.,* McGraw-Hill, New York, 1956.

2. McNamara, R. J., "Tuned Mass Damper for Buildings" *Journal of the Structural Division*, ASCE, Vol. 103, No.ST9, pp. 1785-1797, Sep. 1977.

3. Warburton G. B. and E. O. Ayorinde, "Optimum absorber parameters for simple systems", *Earthquake Engineering and Structural Dynamics,* Vol. 8, pp. 197-217, 1980.

4. Warburton G. B., "Optimum absorber parameters for minimizing vibration response", *Earthquake Engineering and Structural Dynamics,* Vol. 9, pp. 251-262, 1981.

5. Warburton G. B., "Optimum absorber parameters for various combination of response and excitation parameters", *Earthquake Engineering and Structural Dynamics,* Vol. 10, pp. 381-401, 1982.

6. Abe M. and T. Igusa, "Tuned mass dampers for structures with closely spaced natural frequencies", *Earthquake Engineering and Structural Dynamics,* Vol. 24, pp. 247-261, 1995.

7. Tsai H.C. and G. C. Lin, "Explicit formulae for optimum absorber parameters for force excited and viscously damped systems", *Journal of Sound and Vibration,* Vol. 176, No. 5, pp. 585-596, 1994.

8. Sadek F., B. Mohraz, A.W. Taylor and R.M. Chung, "A Method of Estimating the Parameters of Tuned Mass Dampers for Seismic Applications", *Earthquake Engineering and Structural Dynamics,* Vol. 26, pp. 617-635, 1997.

9. Hoang N., Y. Fujino and P. Warnitchai, "Optimal tuned mass damper for seismic applications and practical design formulas", *Engineering Structures,* Vol. 30, pp. 707-715, 2008.

10. Rüdinger F., "Tuned Mass Damper With Fractional Derivative Damping", Engineering *Structures,* Vol. 28, pp. 1774-1779, 2006.

11. Rüdinger F., "Tuned Mass Damper wwith Nonlinear Viscous Damping", *Journal of Sound and Vibration,* Vol. 300, pp. 932-948, 2007.

12. Almazan J.L., J.C. De la Llera, J.A.Inaudi, D.L.Garcia and L.E. Izquierdo, "A Bidirectional and Homogeneous Tuned Mass Damper: A New Device for Passive Control of Vibrations", *Engineering Structures,* Vol. 29, pp. 1548-1560, 2007.

13. Wong W.O. and Y.L. Cheung, "Optimal Design of a Damped Dynamic Vibration Absorber for Vibration Control of Structure Excited by Ground Motion", *Engineering Structures.* Vol. 30, pp. 282-286, 2008.

14. Yang J. N., A. Danielians and S. C. Liu, "Aseismic Hybrid Control Systems for Building Structures", *Journal of Engineering Mechanics,* Vol. 117, No. 4, pp. 836-853, April, 1991.

15. Tsai, H. C., "The Effect of Tuned Mass Dampers on the Seismic Response of Base Isolated Structures", *International Journal of Solid Structures,* Vol. 32, No. 8/9, pp. 1195-1210, 1995.

16. Taniguchi T., A.D. Kiureghian and M. Melkumyan, "Effect of Tuned Mass Damper on Displacement Demand of Base-Isolated Structures", *Engineering Structures,* Vol. 30, No. 12, pp. 3478-3488, 2008.

17. Rana R and T.T. Soong, "Parametric study and simplified design of tuned mass dampers", *Engineering Structures,* Vol. 20, No. 3, pp. 193-204, 1998.

18. Marano G.C., R. Greco, F. Trentadue and B. Chiaia, “Constrained reliability-based optimization of linear tuned mass dampers for seismic control”, *International Journal of Solids and Structures*, Vol. 44, pp. 7370-7388, 2007.

19. Marano G.C., S. Sgobba, R. Greco and M. Mezzina, “Robust Optimum Design of Tuned Mass Dampers Devices in Random Vibration Mitigation”, *Journal of Sound and Vibration,* Vol. 313, pp. 472-492, 2008.

20. Xu K and T. Igusa, “Dynamic characteristics of multiple substructures with closely spaced frequencies”, *Earthquake Engineering and Structural Dynamics,* Vol. 21, pp 1059-1070, 1992.

21. Yamaguchi H and N. Harnpornchai, “Fundamental characteristics of multiple tuned mass dampers for suppressing harmonically forced oscillations”, *Earthquake Engineering and Structural Dynamics,* Vol.22, pp. 51-62, 1993.

22. Abe M and Y. Fujino, “Dynamic characteristics of multiple tuned mass dampers and some design formulas”, *Earthquake Engineering and Structural Dynamics,* Vol. 23, pp. 813-835, 1994.

23. Kareem A and S. Kline, “Performance of multiple mass dampers under random loading”, *ASCE Journal of Structural Engineering,* Vol. 121, No. 2, pp. 348-361, 1995.

24. Joshi A.S. and R.S. Jangid, “Optimum Parameters of Multiple Tuned Mass Dampers for Base-Excited Damped Systems” *Journal of Sound and Vibration,* Vol. 202, No. 5, pp. 657-667, 1997.

25. Jangid R.S, “Optimum multiple tuned mass dampers for base excited undamped systems”, *Earthquake Engineering and Structural Dynamics,* Vol. 28, pp. 1041-1049, 1999.

26. Li C, "Performance of multiple tuned mass dampers for attenuating undesirable oscillations of structures under the ground acceleration", *Earthquake Engineering and Structural Dynamics,* Vol. 29, pp.1405-1421, 2000.

27. Park J. and D. Reed, "Analysis of uniformly and linearly distributed mass dampers under harmonic and earthquake excitation", *Engineering Structures,* Vol. 23, pp. 802-814, 2001.

28. Gu M., S.R. Chen and C.C. Chang, "Parametric study on multiple tuned mass dampers for buffeting control of Yangpu Bridge", *Journal of Wind Engineering and Industrial Aerodynamics,* Vol. 89, pp. 987-1000, 2001.

29. Li C, "Optimum multiple tuned mass dampers for structures under the ground acceleration based on DDMF and ADMF", *Earthquake Engineering and Structural Dynamics,* Vol. 31, pp. 897-919, 2002.

30. Li C and Y. Liu, "Further Characteristics for Multiple Tuned Mass Dampers", *Journal of Structural Engineering,* Vol. 128, No. 10, pp. 1362-1365, October, 2002.

31. Li C and Y. Liu, "Optimum multiple tuned mass dampers for structures under the ground acceleration based on the uniform distribution of system parameters", *Earthquake Engineering and Structural Dynamics,* Vol. 32, pp. 671-690, 2003.

32. Chen G. and J. Wu, "Experimental Study on Multiple Tuned Mass Dampers to Reduce Seismic Responses of a Three-Storey Building Structure", Earthquake *Engineering and Structural Dynamics,* Vol. 32, pp. 793-810, 2003.

33. Zuo L. and S. A. Nayfeh, "Minimax optimization of multi-degree-of-freedom tuned-mass dampers", *Journal of Sound and Vibration*, Vol. 272, pp. 893-908, 2004.

34. Yau J and Y. Yang, "A wideband MTMD system for reducing the dynamic response of continuous truss bridges to moving train loads", *Engineering Structures.* Vol. 26, pp. 1795-1807, 2004.

35. Hoang N. and P. Warnitchai, "Design of Multiple Tuned Mass Dampers by Using a Numerical Optimizer", *Earthquake Engineering and Structural Dynamics,* Vol. 34, pp. 125-144, 2005.

36. Du D., X. Gu, D. Chu, and H. Hua, "Performance and Parametric Study of Infinite Multiple TMDs for Structures Under Ground Acceleration by H∞ Optimization", *Journal of Sound and Vibration,* Vol. 305, pp. 843-853, 2007.

37. Li H.N. and X.L. Ni, "Optimization of non-uniformly distributed multiple tuned mass damper", *Journal of Sound and Vibration,* Vol. 308, pp. 80-97, 2007.

38. Li C. and J. Zhang, "Evaluation of Arbitrary Integer Based Multiple Tuned Mass Dampers for Structures", *International Journal of Structural Stability and Dynamics,* Vol. 5, No. 3, pp. 475-488, 2005.

39. Li C., "Performance of Dual-Layer Multiple Tuned Mass Dampers for Structures Under Ground Excitations", *International Journal of Structural Stability and Dynamics,* Vol. 6, No. 4, pp. 541-557, 2006.

40. Li C. and B. Zhu, "Estimating double tuned mass dampers for structures under ground acceleration using a novel optimum criterion", *Journal of Sound and Vibration,* Vol. 298, pp. 280-297, 2006.

41. Ok S.Y., J. Song and K.S. Park, "Development of optimal design formula for bi-tuned mass dampers using multi-objective optimization", *Journal of Sound and Vibration,* Vol. 322, pp. 60-77, 2009.

42. Jangid R.S. and T.K. Datta, "Performance of Multiple Tuned Mass Dampers for Torsionally Coupled System", *Earthquake Engineering and Structural Dynamics,* Vol. 26, pp. 307-317, 1997.

43. Lin C.C., J.M. Ueng and T.C. Huang, "Seismic Response Reduction of Irregular Buildings Using Passive Tuned Mass Dampers", *Engineering Structures.* Vol. 22, pp. 513-524, 1999.

44. Lin Y.Y., C.M. Cheng and C.H. Lee, "A Tuned Mass Damper for Suppressing the Coupled Flexural and Torsional Buffeting Response of Long-Span Bridges", *Engineering Structures.* Vol. 22, pp. 1195-1204, 2000.

45. Singh M.P., S. Singh and L.M. Moreschi, "Tuned Mass Dampers for Response Control of Torsional Buildings", *Earthquake Engineering and Structural Dynamics,* Vol. 31, pp. 749-769, 2002.

46. Ahlawat A.S. and A. Ramaswamy, "Multiobjective Optimal Absorber System for Torsionally Coupled Seismically Excited Structures", *Engineering Structures.* Vol. 25, pp. 941-950, 2003.

47. Li C. and W. Qu, "Optimum Properties of Tuned Mass Dampers for Reduction of Translational and Torsional Response of Structures Subject to Ground Acceleration", *Engineering Structures.* Vol. 28, pp. 472-494, 2006.

48. Yao J. T. P., "Concept of Structural Control", *Journal of the Structural Division, ASCE*, Vol. 98, No.7, pp. 1567-1574, July, 1972.

49. Roorda J., "Tendon Control in Tall Structures", *Journal of the Structural Division, ASCE*, Vol. 101, No.3, pp. 505-521, March, 1975.

50. Yang J. N., "Application of Optimal Control Theory to Civil Engineering Structures", *Journal of the Engineering Mechanics Division, ASCE*, Vol. 101, No.6, pp. 819-838, December, 1975.

51. Martin C. R. and T.T. Soong, "Modal Control of Multistory Structures", *Journal of the Engineering Mechanics Division, ASCE*, Vol. 102, No.4, pp. 613-623, August, 1976.

52. Yang J. N. and F. Giannopoulos, “Active Tendon Control of Structures”, *Journal of the Engineering Mechanics Division, ASCE*, Vol. 104, No.3, pp. 551-568, June, 1978.

53. Rohman M. A. and H. H. Leipholz, “Structural Control by Pole Assignment Method”, *Journal of the Engineering Mechanics Division, ASCE*, Vol. 104, No.5, pp. 1159-1175, October, 1978.

54. Rohman M. A., V. H. Quintana and H. H. Leipholz, “Optimal Control of Civil Engineering Structures”, *Journal of the Engineering Mechanics Division, ASCE*, Vol. 106, No.1, pp. 57-73, February, 1980.

55. Sae-Ung S. and T. P. Yao, “Action Control of Building Structures”, *Journal of the Engineering Mechanics Division, ASCE*, Vol. 104, No.2, pp. 335-350, April, 1978.

56. Udwadia F. E. and S. Tabaie, “Pulse Control of Single Degree-of-Freedom System”, *Journal of the Engineering Mechanics Division, ASCE*, Vol. 107, No.6, pp. 997-1009, December, 1981.

57. Udwadia F. E. and S. Tabaie, “Pulse Control of Structural and Mechanical Systems”, *Journal of the Engineering Mechanics Division, ASCE*, Vol. 107, No.6, pp. 1011-1028, December, 1981.

58. Yang J. N., “Control of Tall Buildings Under Earthquake Excitation”, *Journal of the Engineering Mechanics Division, ASCE*, Vol. 108, No.5, pp. 833-849, September, 1982.

59. Yang J. N. and M. J. Lin, “Optimal Critical-Mode Control of Building under Seismic Load”, *Journal of the Engineering Mechanics Division, ASCE*, Vol. 108, No.6, pp. 1167-1185, November, 1982.

60. Yang J. N. and M. J. Lin, "Building Critical-Mode Control: Nonstationary Earthquake", *Journal of the Engineering Mechanics Division, ASCE*, Vol. 109, No. 6, pp. 1375-1389, November, 1983.

61. Samali B., J. N. Yang and S.C. Liu, "Active Control of Seismic Excited Building", *Journal of Structural Engineering, ASCE,* Vol. 111, No. 10, pp. 2165-2180, October, 1985.

62. Reinhorn A. M., G. D. Manolis and C. Y. Wen, "Active Control of Inelastic Structures", *Journal of Engineering Mechanics, ASCE*, Vol. 113, No. 3, pp. 315-333, March, 1987.

63. Yang J. N., A. Akbarpour and P. Ghaemmaghami, "New Optimal Control Algorithms for Structural Control", *Journal of Engineering Mechanics, ASCE*, Vol. 113, No. 9, pp. 1369-1386, September, 1987.

64. Yang J. N., Z. Li, A. Danielians and S. C. Liu, "Aseismic Hybrid Control of Nonlinear and Hysteretic Structures I", *Journal of Engineering Mechanics, ASCE*, Vol. 118, No. 7, pp. 1423-1440, July, 1992.

65. Yang J. N., Z. Li, A. Danielians and S. C. Liu, "Aseismic Hybrid Control of Nonlinear and Hysteretic Structures II", *Journal of Engineering Mechanics, ASCE*, Vol. 118, No. 7, pp. 1441-1456, July, 1992.

66. Yang J. N., Z. Li and S. C. Liu, "Stable Controllers for Instantaneous Optimal Control", *Journal of Engineering Mechanics, ASCE*, Vol. 118, No. 8, pp. 1612-1630, August, 1992.

67. Yang J. N., Z. Li and S. C. Liu, "Control of Hysteretic System Using Velocity and Acceleration Feedbacks", *Journal of Engineering Mechanics, ASCE*, Vol. 118, No. 11, pp. 2227-2245, November, 1992.

68. U. Aldemir, M. Bakioglu and S. S. Akhiev, "Optimal Control of Buildings under Seismic Excitations", *Earthquake Engineering and Structural Dynamics,* Vol. 30, pp. 835-851, 2001.

69. Akhiev S. S., U. Aldemir and M. Bakioglu, "Multipoint Instantaneous Optimal Control of Structures", *Computers and Structures,* Vol. 80, No. 11, pp. 909-917, 2002.

70. Mei G., A. Kareem and J. C. Kantor, "Real-Time Model Predictive Control of Structures under Earthquakes", *Earthquake Engineering and Structural Dynamics,* Vol. 30, pp. 995-1019, 2001.

71. Pang M. and K. K. F. Wong, "Predictive Instantaneous Optimal Control of Inelastic Structures Based on Ground Velocity", *The Structural Design of Tall and Special Buildings,* Vol. 15, pp. 307-324, 2006.

72. Ho C. C. and C. K. Ma, "Active Vibration Control of Structural Systems by a Combination of the Linear Quadratic Gaussian and Input Estimation Approaches", *Journal of Sound and Vibration,* Vol. 301, pp. 429-449, 2007.

73. Rohman M. A., "Time-Delay Effects on Actively Damped Structures", *Journal of Engineering Mechanics, ASCE*, Vol. 113, No. 11, pp. 1709-1719, November, 1987.

74. Chen B. S., S. S. Wang and H. C. Lu, "Stabilization of time-delay systems containing saturating actuators", *International Journal of Control,* Vol. 47, No. 3, pp. 867-881, 1988.

75. Yang J. N., A. Akbarpour and G. Askar, "Effect of Time Delay on Control of Seismic-Excited Buildings", *Journal of Structural Engineering, ASCE,* Vol. 116, No. 10, pp. 2801-2814, October, 1990.

76. Abdel-Mooty M. and J. Roorda, "Time-Delay Compensation in Active Damping of Structures", *Journal of Engineering Mechanics, ASCE*, Vol. 117, No. 11, pp. 2549-2570, November, 1991.

77. Zhang L., C. Y. Yang, M. J. Chajes and A. H. D. Cheng, "Stability of Active-Tendon Structural Control with Time Delay", *Journal of Engineering Mechanics, ASCE*, Vol. 119, No. 5, pp. 1017-1024, May, 1993.

78. Agrawal A. K., Y. Fujino and B. K. Bhartia, "Instability due to Time Delay and Its Compensation in Active Control of Structures", *Earthquake Engineering and Structural Dynamics,* Vol. 22, No.3, pp. 211-224, 1993.

79. Yang J. N., Z. Li and S. Vongchavalitkul, "Generalization of Optimal Control Theory: Linear and Nonlinear Control", *Journal of Engineering Mechanics, ASCE*, Vol. 120, No. 2, pp. 266-283, February, 1994.

80. Lin C. C, J. F. Sheu and S. Y. Chu, "Time-Delay Effect and Its Solution for Optimal Output Feedback Control of Structures", *Earthquake Engineering and Structural Dynamics,* Vol. 25, pp. 547-559, 1996.

81. Chung L. L., Y. P. Wang and C. C. Tung, "Instantaneous Control of Structures with Time-Delay Consideration", *Engineering Structures,* Vol. 19, No. 6, pp. 465-475, 1997.

82. Huang K. and R. Betti, "Predictive Optimal Control for Seismic Analysis of Non-Linear and Hysteretic Structures", *Earthquake Engineering and Structural Dynamics,* Vol. 28, pp. 585-607, 1999.

83. Pu J. P., "Time-Delay Compensation in Active Control of Structures", Journal *of Engineering Mechanics, ASCE*, Vol. 124, No. 9, pp. 1018-1028, September, 1998.

84. Grigoriu M., "Control of Time Delay Linear Systems with Gaussian White Noise", *Probabilistic Engineering Mechanics,* Vol. 12, No. 2, pp. 89-96, 1997.

85. Paola M. D. and A. Pirrotta, “Time Delay Induced Effects on Control of Linear Systems Under Random Excitation”, *Probabilistic Engineering Mechanics,* Vol. 16, No. 1, pp. 43-51, 2001.

86. Cai G. and J. Huang, “Instantaneous Optimal Method for Vibration Control of Linear Sampled-Data Systems with Time Delay in Control”, *Journal of Sound and Vibration,* Vol. 262, No.5, pp. 1057-1071, May, 2003.

87. Wong K. K. F. and R. Yang, “Predictive Instantaneous Optimal Control of Elastic Structures During Earthquakes”, *Earthquake Engineering and Structural Dynamics,* Vol. 32, pp. 2161-2177, 2003.

88. Wong K. K. F. and R. Yang, “Predictive Instantaneous Optimal Control of Inelastic Structures during Earthquakes”, *Earthquake Engineering and Structural Dynamics,* Vol. 32, pp. 2179-2195, 2003.

89. Yang J. N., J. C. Wu and A. K. Agrawal, “Sliding Mode Control for Nonlinear and Hysteretic Structures”, *Journal of Engineering Mechanics, ASCE*, Vol. 121, No. 12, pp. 1330-1339, December, 1995.

90. Yang J. N., J. C. Wu and A. K. Agrawal, “Sliding Mode Control for Seismically Excited Linear Structures”, *Journal of Engineering Mechanics, ASCE*, Vol. 121, No. 12, pp. 1386-1390, December, 1995.

91. Yang J. N., J. C. Wu, A. K. Agrawal and S. Y. Hsu, “Sliding Mode Control with Compensator for Wind and Seismic Response Control”, *Earthquake Engineering and Structural Dynamics,* Vol. 26, pp. 1137-1156, 1997.

92. Adhikari R., H. Yamaguchi and T. Yamazaki, “Modal Space Sliding-Mode Control of Structures”, *Earthquake Engineering and Structural Dynamics,* Vol. 27, pp. 1303-1314, 1998.

93. Matheu E. E., M.P. Singh and C. Beattie, "Output-Feedback Sliding Mode Control with Generalized Sliding Surface for Civil Structures under Earthquake Excitation", *Earthquake Engineering and Structural Dynamics,* Vol. 27, pp. 259-282, 1998.

94. Zhao B., X. Lu, M. Wu and Z. Mei, "Sliding Mode Control of Buildings with Base-Isolation Hybrid Protective System", *Earthquake Engineering and Structural Dynamics,* Vol. 29, pp. 315-326, 2000.

95. Lee S. H., K.W. Min, Y.C. Lee and L. Chung, "Improved Design of Sliding Mode Control for Civil Structures with Saturation Problem", *Earthquake Engineering and Structural Dynamics,* Vol. 33, pp. 1147-1164, 2004.

96. Lee S. H., K.W. Min and Y.C. Lee, "Modified Sliding Mode Control Using a Target Derivative of the Lyapunov Function", *Engineering Structures,* Vol. 27, No. 1, pp. 49-59, 2005.

97. Schmitendorf W. E., F. Jabbari and J. N. Yang, "Robust Control Techniques for Buildings under Earthquake Excitation", *Earthquake Engineering and Structural Dynamics,* Vol. 23, pp. 539-552, 1994.

98. Jabbari F., W. E. Schmitendorf and J. N. Yang, "H_∞ Control for Seismic Excited Buildings with Acceleration Feedback", *Journal of Engineering Mechanics, ASCE*, Vol. 121, No. 9, pp. 994-1002, September, 1995.

99. Kose İ. E., W. E. Schmitendorf, F. Jabbari and J. N. Yang, "H_∞ Active Seismic Response Control Using Static Output Feedback", *Journal of Engineering Mechanics, ASCE*, Vol. 122, No. 7, pp. 651-659, September, 1996.

100. Yang J. N., J. C. Wu, A. M. Reinhorn, M. Riley, W. E. Schmitendorf and F. Jabbari, "Experimental Verifications of H_∞ and Sliding Mode Control for Seismically Excited Buildings", *Journal of Structural Engineering, ASCE,* Vol. 122, No. 1, pp. 69-75, January, 1996.

101. Chase J. G. and H. A. Smith, "Robust H_∞ Control Considering Actuator Saturation I: Theory", *Journal of Engineering Mechanics, ASCE*, Vol. 122, No. 10, pp. 976-983, October, 1996.

102. Wu J. C., J. N. Yang and W. E. Schmitendorf, "Reduced-order H_∞ and LQR Control for Wind-Excited Tall Buildings", *Engineering Structures*, Vol. 20, No. 3, pp. 222-236, 1998.

103. Yang J. N., S. Lin and F. Jabbari, "H_2-Based Control Strategies for Civil Engineering Structures", *Journal of Structural Control,* Vol. 10, pp. 205-230, 2003.

104. Yang J. N., S. Lin and F. Jabbari, "H_∞-Based Control Strategies for Civil Engineering Structures", *Structural Control and Health Monitoring,* Vol. 11, pp. 223-237, 2004.

105. Wu W. H. and C. C. Lin, "H_∞ Energy Control and Its Stability Analysis for Civil Engineering Structures", *Structural Control and Health Monitoring,* Vol. 11, pp. 161-187, 2004.

106. Lim C. W., Y. J. Park and S. J. Moon, "Robust Saturation Controller for Linear Time-Invariant System with Structured Real Parameter Uncertainities", *Journal of Sound and Vibration*, Vol. 294, pp. 1-14, 2006.

107. Park W., K. S. Park and H. M. Koh, "Active Control of Large Structures Using a Bilinear Pole-Shifting Transform with H∞ Control Method", *Engineering Structures*, Vol. 30, No. 11, pp. 3336-3344, 2008.

108. Ma. T. W., N. S. Xu and Y. Tang, "Decentralized Robust Control of Building Structures under Seismic Excitations", *Earthquake Engineering and Structural Dynamics,* Vol. 37, pp. 121-140, 2008.

109. Du H., N. Zhang and H. Nguyen, "Mixed H_2/ H_∞ Control of Tall Buildings with Reduced-Order Modeling Technique", *Structural Control and Health Monitoring,* Vol. 15, pp. 64-89, 2008.

110. Chang J. C. H and T. T. Soong, "Structural Control Using Active Tuned Mass Dampers", *Journal of the Engineering Mechanics Division, ASCE*, Vol. 106, No.6, pp. 1091-1098, December, 1980.

111. Abdel-Rohman M. and H. H. Leipholz, "Active Control of Tall Buildings", *Journal of Structural Engineering, ASCE,* Vol. 109, No. 3, pp. 628-645, March, 1983.

112. M. Abdel-Rohman, "Optimal Design of Active TMD for Building Control", *Building and Environment,* Vol. 19, No. 3, pp. 191-195, 1984.

113. M. Abdel-Rohman, "Feasibility of Active Control of Tall Buildings against Wind", *Journal of Structural Engineering, ASCE,* Vol. 113, No. 2, pp. 349-362, February, 1987.

114. Suhardjo J., B. F. Spencer Jr. and A. Kareem, "Frequency Domain Optimal Control of Wind-Excited Buildings", *Journal of Engineering Mechanics, ASCE*, Vol. 118, No. 12, pp. 2463-2481, December, 1992.

115. Spencer Jr. B. F., J. Suhardjo and M. K. Sain, "Frequency Domain Optimal Control Strategies for Aseismic Protection", *Journal of Engineering Mechanics, ASCE*, Vol. 120, No. 1, pp. 135-158, January, 1994.

116. Chang C. C. and H. T. Y. Yang, "Control of Buildings Using Active Tuned Mass Dampers", *Journal of Engineering Mechanics, ASCE*, Vol. 121, No. 3, pp. 355-366, March, 1995.

117. Ankireddi S. and H. T. Y. Yang, "Simple ATMD Control Methodology for Tall Buildings Subject to Wind Loads", *Journal of Structural Engineering, ASCE,* Vol. 122, No. 1, pp. 83-91, January, 1996.

118. Mackriell L. E., K. C. S. Kwok and B. Samali, "Critical Mode Control of a Wind Loaded Tall Building Using an Active Tuned Mass Damper", *Engineering Structures.* Vol. 19, No.10, pp. 834-842, 1997.

119. Adhikari R. and H. Yamaguchi, "Sliding Mode Control of Buildings with ATMD", *Earthquake Engineering and Structural Dynamics,* Vol. 26, pp. 409-422, 1997.

120. Yan N., C. M. Wang and T. Balendra, "Optimal Damper Characteristics of ATMD for Buildings under Wind Loads", *Journal of Structural Engineering, ASCE,* Vol. 125, No. 12, pp. 1376-1383, December, 1999.

121. Wang C. M., N. Yan and T. Balendra, "Control on Dynamic Structural Response Using Active-Passive Composite-Tuned Mass Dampers", *Journal of Vibration and Control,* Vol. 5, No. 3, pp. 475-489, 1999.

122. Nagashima I., "Optimal Displacement Feedback Control Law for Active Tuned Mass Damper", *Earthquake Engineering and Structural Dynamics,* Vol. 30, pp. 1221-1242, 2001.

123. Li C. and Y. Liu, "Active Multiple Tuned Mass Dampers for Structures under the Ground Acceleration", *Earthquake Engineering and Structural Dynamics,* Vol. 31, pp. 1041-1052, 2002.

124. Li C., "Multiple Active-Passive Tuned Mass Dampers for Structures under the Ground Acceleration", Earthquake *Engineering and Structural Dynamics,* Vol. 32, pp. 949-964, 2003.

125. Cao H, and Q. S. Li, "New Control Strategies for Active Tuned Mass Damper Systems", *Computers and Structures,* Vol. 82, pp. 2341-2350, 2004.

126. Collins R., B. Basu and B. Broderick, "Control Strategy Using Bang-Bang and Minimax Principle for FRF with ATMDs", *Engineering Structures.* Vol. 28, pp. 349-356, 2006.

127. Li C. and B. Zhu, “Investigation of Response of Systems with Active Multiple Tuned Mass Dampers”, *Structural Control and Health Monitoring,* Vol. 14, pp. 1138-1154, 2007.

128. Bani-Hani K. A., “Vibration Control of Wind-Induced Response of Tall Buildings with an Active Tuned Mass Damper Using Neural Networks”, *Structural Control and Health Monitoring,* Vol. 14, pp. 83-108, 2007.

129. Guclu R. and H. Yazici, “Vibration Control of a Structure with ATMD Against Earthquake Using Fuzzy Logic Controllers”, *Journal of Sound and Vibration,* Vol. 318, pp. 36-49, 2008.

130. G. F. Franklin, J. D. Powell and A. Emami-Naeini, *Feedback Control of Dynamic Systems*, Prentice Hall, New Jersey, 2002.

131. A. Tewari, *Modern Control Design with Matlab and Simulink*, Wiley, West Sussex, 2002.

132. S. Skogestad, I. Postlethwaite , *Multivariable Feedback Control*, Wiley, West Sussex, 2005.

133. J.B. Burl, *Linear Optimal Control*, Addison Wesley Longman, California, 1999.

134. T.T. Soong, *Active Structural Control: Theory & Practice*, Longman Scientific and Technical, New York, 1990.

135. D. W. Gu, P. Hr. Petkov and M. M. Konstantinov, *Robust Control Design with MATLAB*, Springer - Verlag, London, 2005.

136. Housner G. W. “Earthquake pressures on fluid containers”, *EightTechnical Report under Office of Naval Research.*

137. T. T. Soong and G. F. Dargush, *Passive Energy Dissipation Systems in Structural Engineering,* John Wiley&Sons, West Sussex, 1997.

138. C. Chirstopoulos and A. Filiatrault, *Principles of Passive Supplemental Damping and Seismic Isolation*, IUSS Press, Pavia, 2006.

139. R. E. Ziemer and W. H. Tranter, *Principals of Communications*, Wiley, New York, 2002.

REFERENCES NOT CITED

Chopra A. K., *Dynamics of Structures: Theory and Applications to Earthquake Engineering,* Prentice Hall, New Jersey, 2001.

Franklin G. F, J.D. Powell and A. Emami-Naeini, *Feedback Control of Dynamic Systems*, Prentice Hall, New Jersey, 2002.

Inman D. J., *Engineering Vibration,* Prentice Hall, New Jersey, 2001.

Yerlici V. and H. Luş, *Yapı Dinamiğine Giriş,* Boğaziçi Üniversitesi, İstanbul, 2007.